Final Report

Guidance on the Application of CAMx Probing Tools

CRC Project A-37-2

Prepared for

Coordinating Research Council, Inc.
3650 Mansell Rd., Suite 140
Alpharetta, GA 30022

Prepared by

Greg Yarwood, Ralph E. Morris, Steven Lau, Usha Ganesh
ENVIRON International Corporation
101 Rowland Way, Suite 220
Novato, CA 94945

Gail Tonnesen
University of California at Riverside
Riverside, CA.

September 18, 2003

TABLE OF CONTENTS

Page

APPENDICES

TABLES

FIGURES

EXECUTIVE SUMMARY

The Comprehensive Air quality Model with extensions (CAMx) is a publicly available three-dimensional multi-scale photochemical grid model (ENVIRON, 2002a). CAMx is used as the host model for implementing several mass balance and sensitivity analysis techniques including Process Analysis (PA), the Decoupled Direct Method (DDM), and the Ozone Source Apportionment Technology (OSAT). CAMx version 3.1 is described in the User's Guide (ENVIRON, 2002a) which is available online electronically http://www.camx.com.

This report demonstrates the application of the OSAT, DDM and PA probing tools in CAMx and provides guidance on how to set-up and analyze a probing tool model run. The demonstration uses a model application developed by the Ozone Transport Assessment Group (OTAG) for a July 1995 ozone episode period in the eastern US. The analysis focuses on four receptor areas, three major urban areas Atlanta, Chicago and New York and a more rural area in Altoona, PA that also has high 8-hour ozone levels. The probing tool runs described here also were analyzed by Zhang et al. (2002). The probing tools can be used to answer questions such as:

- Which emissions cause high ozone?
- How will ozone levels respond to emission changes?
- How important are the initial and boundary conditions?
- What are the influences of different model processes (chemistry, deposition, etc.) on ozone levels at a specific location?

The probing tools can provide information for ozone precursors as well as ozone. Some of these questions can be answered using traditional diagnostic and sensitivity analysis techniques (i.e., changing a model input and measuring the change in model output) but the probing tools are much more efficient and can provide a more complete picture. However, a traditional "brute force" sensitivity simulation still provides the most accurate measure of model response to a large input perturbation. There are two main applications of the information provided by probing tools:

- Improving model performance. Comprehensive sensitivity and diagnostic information will provide greater understanding of how a model is working, increase the likelihood that model performance problems will be identified, and provide direction for how to correct model performance problems.
- Guiding design of control strategies. Understanding in detail what sources contribute to high ozone and/or how ozone will respond to emission reductions enables the selection of more equitable and efficient control strategies.

The probing tools that are currently available in CAMx have differing capabilities and uses as summarized in Table ES-1. The CAMx probing tools will be extended by the addition of reactive tracers for air toxics capability (RTRAC) and PM source apportionment (PSAT, under current development) and Mercury species (current development).

Table ES-1. Overview and comparison of DDM, OSAT and PA capabilities in CAMx.

	DDM	OSAT	PA
Predict O_3 response to changes in emissions, ICs and BCs	**Yes** Sensitivity coefficients are directly applicable and work well for small to moderate changes. [1]	**Yes** OSAT contributions work quite well for small to large changes, except for NOx inhibited areas. APCA less suitable	**No**
Quantify O_3 contributions from emissions, ICs and BCs	**Yes** Can be used, but there are difficulties with negative sensitivities and higher order terms	**Yes** OSAT and APCA are both directly applicable, but different when biogenics are important	**No**
Relative contribution of local sources vs. transport	**Yes** Can be used, but first-order sensitivities do not sum to total ozone.	**Yes** OSAT and APCA are both directly applicable, but may differ when biogenics are important	**No**
Assess whether O_3 is VOC or NOx limited	**Yes** Sensitivity accurately predicts response to small VOC and NOx change	**Yes** OSAT reflects conditions over which ozone was formed, and may not agree with DDM or PA especially in NOx inhibited areas. APCA not suitable	**Yes** CPA/IRR calculated indicator ratios predict response to small VOC and NOx change
Evaluate VOC reactivity	**Yes** See demonstration of methodology by Carter at al. (2002)	**No** Not recommended	**Yes** CPA/IRR can quantify contributions of individual VOCs
Information for species other than ozone?	**Yes** DDM is equally applicable to all species.	**No** OSAT is oriented toward ozone. Information is available for NOx and VOC, but is not generally used.	**Yes** IPR and IRR are equally applicable to all species. CPA is oriented toward ozone.
Detailed chemical analysis	**No**	**No**	**Yes** CPA/IRR calculates many attributes of the chemistry
Impact of model processes	**No**	**No**	**Yes** IPR quantifies all processes in specific grid cells
Are the results unique?	**Yes** Sensitivity coefficients have a unique mathematical derivation.	**No** Source apportionment is never unique for species like ozone that depends upon non-linear processes.	**Yes** IPR and IRR quantify unique properties of a model simulation. CPA may not be unique since parameters are defined around chemical interpretations.

Note:

1. In this table, and throughout the report, small medium and large perturbations are considered to be less than 20, 20 to 40 and greater than 40 percent changes in input emissions (or initial or boundary conditions), respectively.

This report presents example analyses of CAMx probing tool results but does not interpret the implications of the results for air quality planning. This is because the aim of this report is to demonstrate how the tools can be applied, because the OTAG modeling scenarios are dated, and because the results are open to interpretation. In our experience, different importance can be attached to the relative magnitudes of the source apportionments/sensitivities based on perceptions of what is important or significant.

Several updates to the OSAT algorithms were implemented during this study:

- Accounting for ozone destruction reactions.
- Different scheme for apportioning ozone production to VOCs and NOx.
- Different reactivity weighting scheme for apportioning ozone production among VOC categories.

This report describes testing of the OSAT updates and comparisons of OSAT source apportionments and DDM sensitivity coefficients in a chemistry box model. The major differences between the OSAT and DDM algorithms in CAMx are in the chemistry step (horizontal advection is the other, minor, difference) so box model comparisons can provide insight into the relationship between OSAT source apportionment and DDM source sensitivity for ozone. The influences of non-linear chemistry are likely to be more apparent in a box model than a grid model because of the tendency for non-chemical processes to disperse and attenuate non-linear chemical effects in a grid model. Consequently, non-linear effects are likely to become important at smaller perturbation levels in a box model than a grid model. Second order sensitivity coefficients also were calculated (by brute force) in the box model to illustrate the relationship of first-order to higher order sensitivity coefficients for ozone.

The box model comparison of OSAT and DDM did lead to conclusions about the applicability of these tools and the relationship between source apportionment (OSAT) and source sensitivity (DDM).

Source Sensitivity and Source Apportionment

By definition, ozone sensitivity is the response of total ozone to changing a source of ozone, i.e., the local derivative. All the interactions among different chemical species, different emission sources, etc. are propagated through the model to determine the impact of a change in some input on ozone at a later time. Source apportionment should describe how the ozone that is present was formed. Ozone was formed in reactions that involved VOC and NOx precursors and the source apportionment should reflect how this ozone formation occurred. This implies the need for a memory of all the ozone formation events leading up to the current condition. To accurately retain this memory, source apportionments should behave like conserved properties.

Sensitivity has a rigorous mathematical definition but is more difficult to interpret physically. Source apportionment is a physical concept that does not always have a rigorous mathematical definition. In a linear system (e.g., a primary pollutant such as CO) source apportionment is the same thing as first-order sensitivity and the source apportionment is uniquely defined. The

relationship between source apportionment and sensitivity is less clear for non-linear pollutants, such as ozone, where source apportionment is not uniquely defined.

- The box model comparisons demonstrate the conclusion that first-order sensitivity and source apportionment are different for ozone chemistry because the chemical equations are a non-linear system.

- When first-order sensitivities are attenuated under photochemically reactive conditions they are replaced by higher-order sensitivities. This is why first-order sensitivities typically sum to only about 2/3 of the total ozone in a grid model simulation (Dunker et al., 2002b).

- The rapid attenuation of first-order sensitivities under photochemically reactive conditions suggests limitations to the concept of source apportionment. A chemical interpretation of the rapid attenuation of the sensitivity to initial ozone is that "if the initial ozone were reduced, then the photochemical system would replace it rapidly." The Lagrangian view of ozone transport is that if a background of X ppb is transported into an area, and the total leaving the area is (X + Y) ppb, then local emissions added Y ppb. The sensitivities are saying that if you reduce ozone transport (X), local ozone production (Y) will increase and partially compensate for the reduced transport. This fact should be recognized in ozone transport arguments and observation-based analyses that are used to support the development of ozone control strategies.

Comparing DDM and OSAT in CAMx

- Ozone source apportionments and source sensitivities should be related, but not identical. Dunker et al. (2002b) showed qualitative consistency in that DDM and OSAT consistently identify the same groups of ozone precursors as important, and identify similar areas of influence for groups of ozone precursors.

- Quantitative comparisons between OSAT and DDM are difficult because source apportionment and source sensitivity are not the same thing (discussed above). Nevertheless, useful insight can be gained from quantitative comparisons, e.g., identifying the need to account for ozone destruction in OSAT (Dunker et al., 2002b).

- DDM sensitivities accurately predict the effects of small to moderate[1] precursor changes.

- OSAT apportionments predict the effects of large precursor changes more accurately than first-order DDM sensitivities.

- DDM sensitivities tend to under-estimate the ozone decreases due to precursor reductions because the sum of the first-order sensitivities tends to be less than (typically about 2/3 of) the total ozone. There may be specific exceptions to this general trend.

[1] Throughout the report, small medium and large perturbations are considered to be less than 20, 20 to 40 and greater than 40 percent changes in input emissions (or initial or boundary conditions), respectively.

- DDM tends to under-estimate the effect of precursor reductions because ozone production becomes more efficient (more ozone formed per precursor reacted) as precursors are reduced under most conditions. First-order sensitivities determine ozone production efficiency at the base case condition.

- OSAT apportionments may over or under-estimate the ozone decreases due to precursor reductions, but over-estimate more often than under-estimate.

- OSAT tends to over-estimate the effect of precursor reduction because ozone production becomes more efficient as precursors are reduced under most conditions. OSAT ozone production efficiencies are a weighted average over the conditions that prevailed as the base case ozone was formed.

- OSAT does not allow for negative source contributions and so will not project ozone increases due to NOx emission reductions under NOx inhibited ozone formation conditions.

- Some studies have addressed the difficulty in interpreting the magnitudes of DDM sensitivities because they do not add up to the total ozone by renormalizing the first order sensitivities (e.g, Zhang et al., 2002). We recommend against renormalizing sensitivities, however if renormalization is performed care should be taken in their interpretation.

1. INTRODUCTION

The Comprehensive Air quality Model with extensions (CAMx) is a publicly available three-dimensional multi-scale photochemical grid model (ENVIRON, 2002a). CAMx was used as the host model for the implementation of several mass balance and sensitivity analysis techniques including Process Analysis (PA), the Decoupled Direct Method (DDM), and the Ozone Source Apportionment Technology (OSAT).

OBJECTIVES

The objective of this report is to demonstrate the application of three CAMx probing tools (OSAT, DDM and PA) and provide guidance on how to set-up and analyze a probing tool model run. The probing tool runs described here were also analyzed in a companion project by Zhang et al. (2002). The remainder of Section 1 provides an overview of CAMx, the probing tools and the demonstration database (the OTAG July 1995 episode). Section 2 discusses how to set up probing tool analyses. Sections 3-5 discuss how to analyze OSAT, DDM and PA results, respectively. Section 6 describes updates to the OSAT algorithms for this study and a comparison of OSAT and DDM with discussion of the relationship between source apportionment and source sensitivity

OVERVIEW OF CAMx

The main features of CAMx version 3.1 are:

- Two-way grid nesting that supports multiple levels of fully interactive grid nesting (e.g., 36/12/4-km).
- CB4 or SAPRC99 chemical mechanisms.
- Two chemical solvers, the Chemical Mechanism Compiler (CMC) Fast Solver or the highly accurate Implicit Explicit Hybrid (IEH) solver.
- Multiple numerical algorithms for horizontal transport including the Piecewise Parabolic Method (PPM), Bott, and Smolarkiewicz advection solvers.
- Subgrid-scale Plume-in-Grid (PiG) algorithm to treat the near-source plume dynamics and chemistry of large NOx point sources.
- Ability to interface with a variety of meteorological models including the MM5 and RAMS prognostic hydrostatic meteorological models (others also compatible).
- Mass consistent and mass conservative transport algorithms.
- Flexi-nesting capabilities that allow the specification of nested fine-grids with explicit fine-grid data for none to all of the inputs. Any fine grid data not supplied are interpolated from a "parent" grid.
- Support for multi-processors in shared memory workstations.
- Three types of probing tool, namely OSAT, DDM and PA.

CAMx version 3.1 is completely described in the User's Guide (ENVIRON, 2002a) which is available online electronically http://www.camx.com.

PROBING TOOLS IN CAMx

Several "probing tools" are now available in CAMx to provide additional diagnostic and sensitivity information for an ozone simulation. The probing tools can be used to answer questions such as:

- Which emissions cause high ozone?
- How will ozone levels respond to emission changes?
- How important are the initial and boundary conditions?
- What are the influences of different model processes (chemistry, deposition, etc.) on ozone levels at a specific location?

The probing tools can provide information for ozone precursors as well as ozone. Some of these questions can be answered using traditional diagnostic and sensitivity analysis techniques (i.e., changing a model input and measuring the change in model output) but the probing tools are much more efficient and can provide a more complete picture. There are two main applications of the information provided by probing tools:

- Improving model performance. Comprehensive sensitivity and diagnostic information will provide greater understanding of how a model is working, increase the likelihood that model performance problems will be identified, and provide direction for how to correct model performance problems.
- Guiding design of control strategies. Understanding in detail what sources contribute to high ozone and/or how ozone will respond to emission reductions enables the selection of more equitable and efficient control strategies.

The probing tools that are available have differing capabilities and uses as discussed below.

Ozone Source Apportionment Technology (OSAT)

OSAT provides information about the relationships between ozone concentrations and sources of precursors in the form of ozone source apportionments. Source apportionment means that the sum of the source contributions adds up to exactly 100% of the total ozone and so all of the ozone is accounted for. OSAT attributes ozone among all of the potential sources of ozone in the simulation, namely emissions, boundary conditions (BCs) and initial conditions (ICs). Ozone formation from VOC and NOx precursors is tracked separately. The emissions contributions can be broken down by geographic area and/or source category. The OSAT methods are described in the CAMx User's Guide (ENVIRON, 2002a) and Dunker et al. (2002b).

OSAT apportions ozone formation based solely on what precursors were present when the ozone is formed. OSAT determines whether ozone formation is NOx or VOC limited in each grid cell at each time step, and attributes ozone production according to the relative contributions of the limiting precursor (VOC or NOx) from different sources present at that time. The precursors are tracked using a reactive tracer (tagged species) approach. Likewise,

the ozone contributions are tracked using a reactive tracer approach and separate tracers are used to track ozone formation attributed to NOx (O3N tracers) and VOC (O3V tracers).

Because ozone formation chemistry is a non-linear process, there is no unique way of apportioning ozone back to precursor sources. The OSAT approach to source apportionment is to attribute ozone formation among the precursors that were present when the ozone was formed. There are two schemes for doing this called OSAT and APCA (Anthropogenic Precursor Culpability Assessment). A third scheme, called GOAT (Geographic Ozone Apportionment Technology), does not attempt to relate ozone to precursors, but rather classifies ozone production simply based on the grid cell where it occurred. GOAT was implemented because it corresponded to how process analysis was used in some studies to trace ozone production back to grid cells, but since GOAT has never been used it is not discussed in detail here.

Anthropogenic Precursor Culpability Assessment (APCA)

Applications of OSAT to the Eastern US consistently identify biogenic emissions as a major contributor to ozone formation. This is not surprising as biogenic VOC emissions are very reactive and dominate regional VOC emissions in the Eastern US, but this finding is not "policy relevant" for designing anthropogenic emissions ozone control plans. The APCA methodology was developed from OSAT to address this issue. APCA stands for Anthropogenic Precursor Culpability Assessment, and differs from OSAT in recognizing that certain emission groups are not controllable (i.e., biogenic emissions) and that apportioning ozone production to these emissions does not provide control strategy relevant information. To address this, in situations where OSAT attributes ozone formation to a non-controllable source category when it was due to the interaction of ozone precursors from a non-controllable (i.e., biogenic) and controllable emissions source, APCA re-directs the ozone attribution to the controllable precursor. In practice, biogenic emissions are the uncontrollable source category and APCA only attributes ozone production to biogenic emissions when ozone formation is due to the interaction of biogenic VOC with biogenic NOx. When ozone formation is due to biogenic VOC interacting with anthropogenic NOx under VOC-limited conditions (where OSAT would attribute ozone production to biogenic VOC's), APCA directs the attribution to the anthropogenic NOx precursors present. The result of using APCA instead of OSAT is that more ozone formation is attributed to anthropogenic NOx sources and little ozone formation is attributed to biogenic sources. APCA is not called a "source apportionment" technique because it expresses biases as to which sources should be implicated (i.e., those that are controllable), hence it is referred to as a "culpability assessment."

Decoupled Direct Method (DDM)

The DDM calculates first-order sensitivity coefficients relating concentrations of ozone (and any other species) to pollutant sources, namely emissions, initial conditions (ICs) and boundary conditions (BCs). The emissions sensitivities can be calculated for specific geographic areas and/or source categories. The sensitivity coefficients describe how ozone will change if the pollutant source is changed and thus are directly applicable to predicting the effects of control strategies. CAMx can calculate “first-order” sensitivity coefficients, which

are likely to be the most important sensitivities. The CAMx implementation of DDM is described in Dunker et al. (2002a and b) and the CAMx User's Guide (ENVIRON, 2002a).

First-order DDM sensitivities appear similar to OSAT source apportionments because they appear to describe similar relationships (between precursors and ozone) and often have similar magnitudes. However, source sensitivity is not the same thing as source apportionment as explored in detail in Section 6. Two comparisons between OSAT and DDM illustrate key differences between source sensitivity and OSAT source apportionments: (1) Sensitivity coefficients can be negative, meaning that reducing emissions will increase ozone, whereas OSAT source apportionments are never negative. An example would be an area with high NOx emissions where reducing NOx emissions will increase ozone (for small changes) and DDM will obtain negative ozone sensitivities to local NOx whereas OSAT will have zero or small ozone apportionments to local NOx. (2) Adding up all the first-order sensitivities over all sources of ozone and precursors typically explains only about 60-70% of the total ozone. The modeled ozone that is "unexplained" by the first-order sensitivity coefficients is explained by higher-order sensitivities, but they are more difficult to calculate and difficult to interpret. An advantage of DDM sensitivity coefficients is that they are rigorously defined (mathematically) and so are unique. The value of this uniqueness is weakened if the sensitivities are interpreted as source apportionments because of the significant portion of the ozone that is "unexplained" by the first-order sensitivities.

The DDM was first implemented in a 3-D air-quality model by Dunker (1981). This implementation of DDM in version 2 of the Urban Airshed Model (UAM) demonstrated the concept but was not a practical tool due to the limitations of the computers used for airshed modeling in the early 1980s which could barely accommodate the host UAM model. The DDM implementation in CAMx (Dunker et al., 2002a) calculates sensitivities using numerical methods that exactly correspond to the methods used to advance the concentrations, and solves sensitivities and concentrations at the same timesteps in order to ensure that the sensitivities are accurate.

Process Analysis (PA)

Process analysis (PA) is a method for obtaining more information on how CAMx predicted concentrations at a specific place and time. The CAMx concentrations are determined by numerous model processes (such as emissions, transport, chemistry, deposition) but the separate contribution of each process is hidden within the final concentration output. Process analysis allows the contribution of each process to be output and used in diagnostic analyses. This is useful for explaining "how the model got the answer it got" and thus understanding model performance issues. Process analysis is less well suited to understanding source contributions to ozone or predicting responses to emissions changes. Further information on process analysis is provided in the CAMx User's Guide (ENVIRON, 2002a) and references therein.

Air quality model (AQM) simulations are usually evaluated primarily in terms of their ability to simulate observed O_3 data. There is an increasing awareness that chemical mechanisms, and AQMs must also be evaluated in terms of their ability to simulate the fundamental chemical processes that control O_3 formation and the sensitivity of O_3 to emissions reductions. Process

Analysis is a method for explaining model simulations by adding algorithms to the AQM to store the integrated rates of species changes due to individual chemical reactions and other sink and source processes (Tonnesen and Jeffries , 1994; Tonnesen, 1995). By integrating these rates over time and outputting them at hourly intervals, PA provides diagnostic outputs that can be used to explain a model simulation in terms of the budgets of free radicals, production and loss of odd oxygen (Ox) and O_3, conversion of NOx to inert forms, as well as the effects of transport and other sink and source terms.

PA is especially useful for quality assurance when developing new model scenarios because it provides rapid, efficient methods to assess the contribution of various chemical reactions and transport processes to O_3 production. This approach can also be applied to inter-comparisons of models, e.g., Tonnesen (2001). The process analysis can also improve model validation by suggesting how ambient data can be used to evaluate model accuracy for key terms in the chemical processing of VOC and NOx (e.g., Imre et al., 1998).

A comprehensive process analysis should include two components:

- A chemical budget analysis using integrated reaction rates (IRR) and/or chemical process analysis (CPA) to analyze the budgets of radicals, NOy, Ox, and O_3.
- An analysis of other integrated process rates (IPR) including transport, deposition and emissions of key species.

The IRR portion of the analysis is especially useful for characterizing O_3 sensitivity to precursor reductions and for comparing different photochemical mechanisms. Analysis of the raw integrated reaction rate data requires detailed knowledge of the chemical mechanism and atmospheric chemistry. IRR data are generally only useful after the data have been post-processed into chemically meaningful parameters. With CPA, a selection of useful parameters is calculated within CAMx and then output to gridded files that can be visualized directly. The IPR analysis is useful for characterizing dynamics including transport, vertical deposition, mass budget analyses and mass conservation. This project will place focus on the CPA analyses because this is most directly relevant to the issue of O_3 sensitivity to precursors. While the IPR analysis can be used to evaluate source contributions to O_3 in particular grid cells, it is not well suited for attributing O_3 production to particular source categories of VOCs.

COMPARISON OF PROBING TOOL CAPABILITIES

The capabilities of the probing tools implemented in CAMx version 3.1 are compared in Table 1-1. DDM and OSAT generally have similar capabilities with the comments in Table 1-1 reflecting the differences between source sensitivity and source apportionment, discussed in Section 6. Process Analysis does not overlap much with DDM or OSAT and provides a complementary set of abilities.

Table 1-1. Overview and comparison of DDM, OSAT and PA capabilities in CAMx.

	DDM	OSAT	PA
Predict O_3 response to changes in emissions, ICs and BCs	**Yes** Sensitivity coefficients are directly applicable and work well for small to moderate changes. [1]	**Yes** OSAT contributions work quite well for small to large changes, except for NOx inhibited areas. APCA less suitable	**No**
Quantify O_3 contributions from emissions, ICs and BCs	**Yes** Can be used, but there are difficulties with negative sensitivities and higher order terms	**Yes** OSAT and APCA are both directly applicable, but different when biogenics are important	**No**
Relative contribution of local sources vs. transport	**Yes** Can be used, but first-order sensitivities do not sum to total ozone.	**Yes** OSAT and APCA are both directly applicable, but may differ when biogenics are important	**No**
Assess whether O_3 is VOC or NOx limited	**Yes** Sensitivity accurately predicts response to small VOC and NOx change	**Yes** OSAT reflects conditions over which ozone was formed, and may not agree with DDM or PA. APCA not suitable	**Yes** CPA/IRR calculated indicator ratios predict response to small VOC and NOx change
Evaluate VOC reactivity	**Yes** See demonstration of methodology by Carter at al. (2002)	**No** Not recommended	**Yes** CPA/IRR can quantify contributions of individual VOCs
Informatuon for species other than ozone?	**Yes** DDM is equally applicable to all species.	**No** OSAT is oriented toward ozone. Information is available for NOx and VOC, but is not generally used.	**Yes** IPR and IRR are equally applicable to all species. CPA is oriented toward ozone.
Detailed chemical analysis	**No**	**No**	**Yes** CPA/IRR calculates many attributes of the chemistry
Impact of model processes	**No**	**No**	**Yes** IPR quantifies all processes in specific grid cells
Are the results unique?	**Yes** Sensitivity coefficients have a unique mathematical derivation.	**No** Source apportionment is never unique for species like ozone that depends upon non-linear processes.	**Yes** IPR and IRR quantify unique properties of a model simulation. CPA may not be unique since parameters are defined around chemical interpretations.

Note:

1. In this table, and throughout the report, small medium and large perturbations are considered to be less than 20, 20 to 40 and greater than 40 percent changes in input emissions (or initial or boundary conditions), respectively.

OTAG MODELING DATABASE

A modeling database for demonstrating the probing tools was developed from EPA's Ozone Transport Assessment Group (OTAG) modeling for a July 1995 episode (OTAG, 1997). The OTAG modeling covered the Eastern US with a 36 km coarse grid and a 12 km fine grid, as shown in Figure 1-1. (The 36 km and 12 km grid resolutions are nominal values because the grids are actually defined in latitude/longitude coordinates and so the physical grid size varies.) The OTAG modeling has relatively coarse vertical resolution with a model top at about 4 km, 7 vertical layers in the fine grid and 5 vertical layers in the coarse grid. The vertical nesting in CAMx allows different numbers of vertical layers in the coarse and fine grids. ENVIRON does not recommend vertical nesting because it can lead to undesirable artifacts when surface concentrations are displayed, as shown in the section of the CAMx User's Guide dealing with Process Analysis (ENVIRON, 2002a). For OTAG, coarse grid layer 1 was split to fine grid layers 1 and 2, and coarse grid layer 2 was split to fine grid layers 3 and 4. The coarse grid surface layer was 100 m deep and the fine grid surface layer was 50 m deep. This modeling used version 3.1 of CAMx (ENVIRON, 2002a) with updates to the OSAT algorithms described in Section 6.

The episode period was July 7-15, 1995. The last 3 days modeled by OTAG (July 16-18) were excluded to reduce model run times and because they were after the main high ozone period in the Midwest and Northeast on July 12-15, 1995. A CAMx nesting feature was employed to further reduce model run times by modeling the spin-up days (July 7-10) with just the coarse grid. Eliminating the fine grid on spin-up days saved over 80% of the CPU time on these days. July 11-15 were run with both coarse and fine grids, and these were the days used in the probing tools analyses.

The emissions were for a 2007 future year base case as used by EPA in developing the "NOx SIP Call" (EPA 1998). The onroad mobile source emissions are based on emission factors from EPA's MOBILE5a model. The OTAG onroad mobile source emission inventories accounted for Tier 1 vehicles, I/M programs as planned by the states, reformulated gasoline in mandated and opt-in areas, Phase II RVP limits in non-reformulated gasoline areas, and clean fuel fleet programs in the mandated areas as these programs were envisioned around 1996/1997 (OTAG, 2002). The NOx SIP Call 2007 emissions did not account for the effects of Tier 2 vehicles and gasoline sulfur control requirements upon onroad vehicle emissions. The NOx emissions for major electricity generating units (EGUs) were based on continuous emissions monitoring (CEM) data and include EPA's estimated reductions due to the NOx SIP Call strategy. The biogenic emissions were prepared using EPA's BEIS2 model. Other emissions were based on an early version of EPA's National emissions trends inventory for 1996 (NET96) adjusted to 2007 to account for the effect of activity growth and controls.

The initial and boundary conditions were the same as in the OTAG modeling. OTAG selected values representing clean background air, namely 40 ppb of ozone, 100 ppb of CO, less than 0.1 ppb of NOx and about 4.4 ppbC of VOC.

Receptor Areas

Four receptor areas were selected for the probing tool analyses: Atlanta, Chicago, New York and Altoona, PA. Atlanta, Chicago and New York were selected as major urban areas that were projected to still have high ozone levels in the OTAG 2007 modeling. They are all in the fine grid, and were expected to cover a range of emission characteristics (VOC/NOx ratio, source category contributions). Altoona, Pennsylvania was selected as a contrasting area with relatively high 8-hour ozone levels but relatively low local emissions where ozone transport is clearly important. Each receptor was defined by a 3 by 3 block of coarse grid cells (9 by 9 fine grid cells) centered over the area, as shown in Figure 1-1.

Source Areas

OSAT and DDM can relate ozone concentrations to emissions from specific geographic source areas. The modeling domain was divided into 17 geographic source areas as shown in Figure 1-1 and described in Table 1-2. This is fewer source regions than used in some previous OSAT analyses for the OTAG domain where source regions were individual states (e.g., EPA, 1998) because of the greater computational burden of DDM compared to OSAT. The source areas were defined around the four receptor areas Atlanta, Chicago, New York and Altoona.

Table 1-2. Source area definitions for OSAT and DDM.

Number	Definition
1	Central and Northern Plains
2	Texas and nearby areas
3	Northern Great Lakes
4	Surrounding Chicago
5	Ohio and Mississippi rivers
6	Gulf Coast
7	Ohio and nearby areas
8	Surrounding Atlanta
9	Florida and nearby areas
10	Northern New England and Eastern Canada
11	Surrounding Altoona
12	Carolina Coast and nearby areas
13	Surrounding New York
14	Chicago area
15	Atlanta area
16	New York area
17	Altoona area

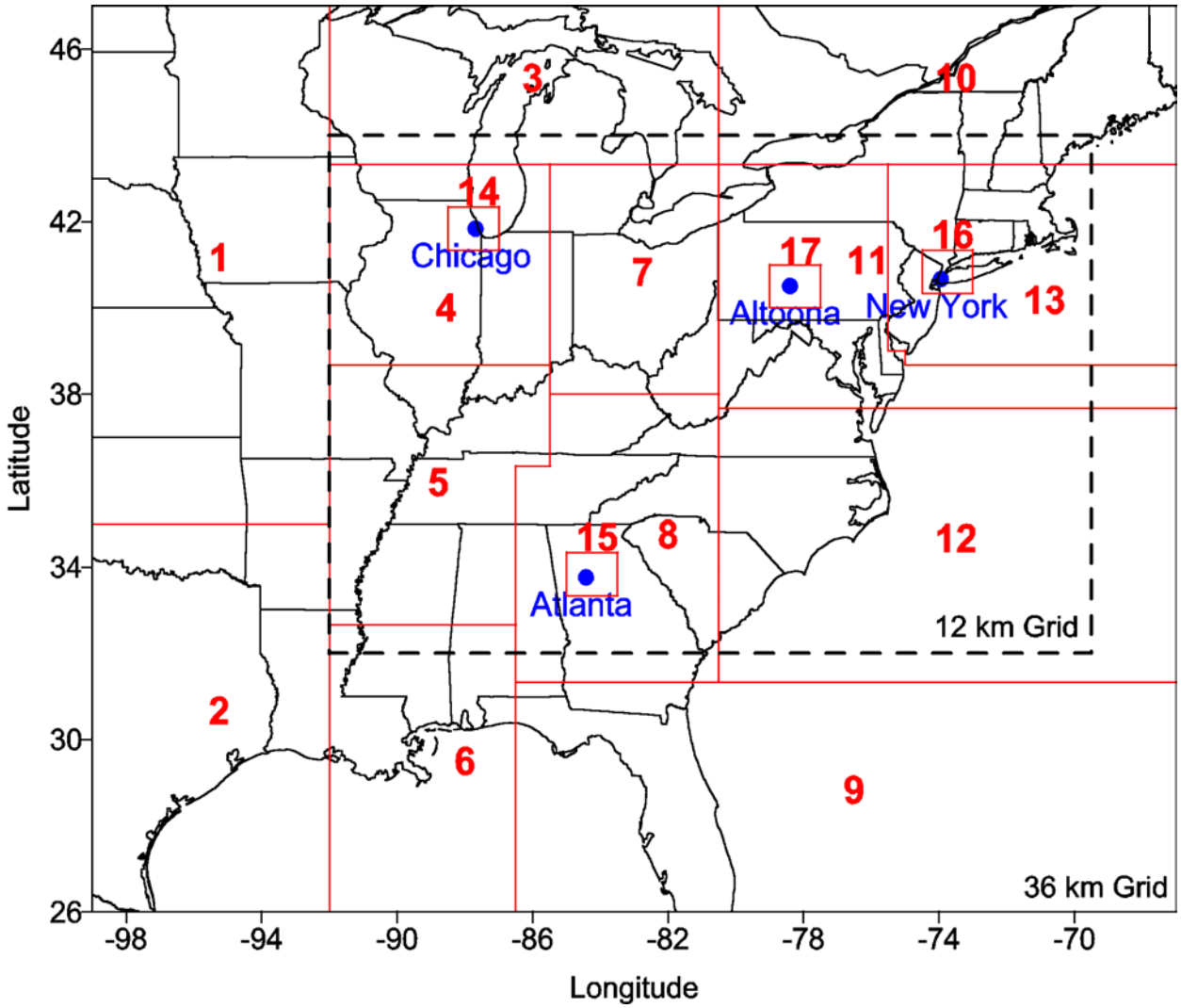

Figure 1-1. OTAG modeling domain showing the 36 and 12 km grids and the 17 source areas used in the probing tool analyses.

Emissions Categories

OSAT and DDM can relate ozone concentrations to emissions from separate source categories. The source categories were defined by the pre-merged emissions files that were available from the EPA as described in Table 1-3.

Table 1-3. Emissions source category definitions.

Source Category	Category Definition
BIO	Biogenic emissions
MV	Motor vehicle emissions
PT	Elevated point source emissions
OAN	Other anthropogenic emissions (i.e., area, offroad mobile and low-level point)

Table Note
1. The MV and OAN categories were combined for all DDM runs except B7, as shown in Table 1-4

Emissions Reductions

Probing tool results were obtained at reduced emission levels to demonstrate and evaluate the use of probing tools in control strategy analysis. Simple "across the board" reductions in anthropogenic emissions (i.e., all categories except biogenic emissions) were sufficient for this purpose. Three scenarios were considered:

- 25% reduction to anthropogenic VOC emissions
- 25% reduction to anthropogenic NOx emissions
- 75% reduction to anthropogenic NOx emissions

The deep NOx emission reduction (75%) level was considered because it will cause urban areas that were VOC-sensitive in the base case, such as Chicago and New York (see below), to become NOx-sensitive. The modeled ozone levels for the base case and emission reduction scenarios are shown for 2 pm (EST) on July 15th in Figure 1-2.

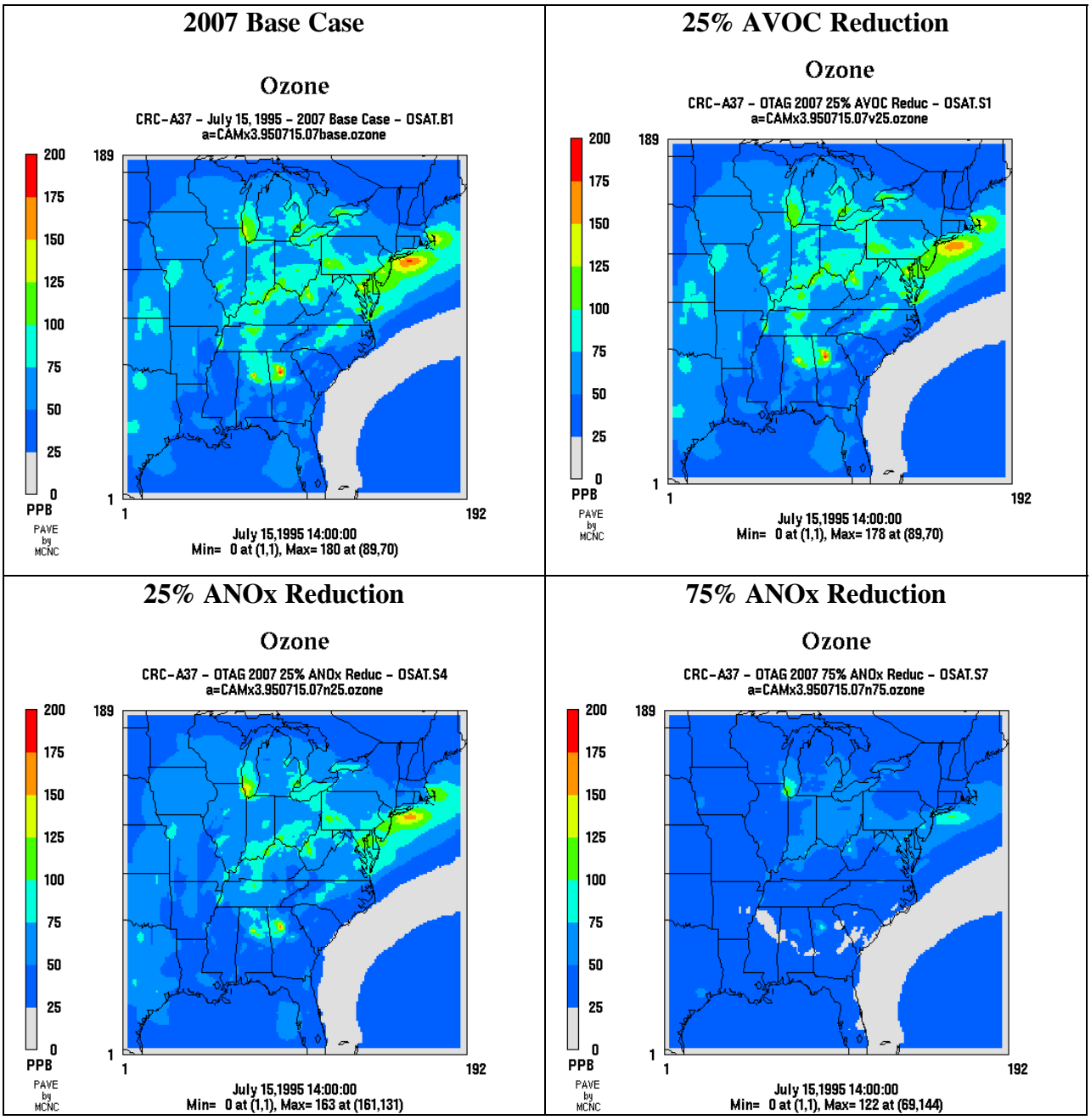

Figure 1-2. Ozone levels (ppb) at 14:00 EST on July 15, 1995 for the 2007 base case and with reductions in anthropogenic VOC (AVOC) and anthropogenic NOx (ANOx).

PROBING TOOL MODEL RUNS

The probing tool model runs are summarized in Table 1-4. Runs were designed to demonstrate and compare the OSAT, DDM and PA tools with the 2007 base case emissions. The OSAT run (B1) simply tracked the contributions of 17 source areas (Table 1-3) times 4 emission categories (Table 1-2) plus the ICs and BCs. Since ozone contributions are tracked from VOC and NOx, obtaining equivalent information by traditional sensitivity analyses (e.g., conducting "zero-out" runs where each source region/category/precursor is independently set

to zero) would require (17 x 4 x 2) + 2 = 138 model runs. Runs with the probing tools related to OSAT (APCA run B5 and GOAT run B6) were configured to match B1. The base case OSAT run B1 was repeated with reduced anthropogenic emission levels in sensitivity runs S1, S4 and S7.

A single CAMx DDM run could be configured with the same source areas and categories as run B1 but the computer requirement would be about 3 gigabytes (GB) of memory (RAM) and over 40 GB of disk storage. The memory size for this project was limited to less than 1 Gbyte.[1] Several DDM runs (B2, B3 and B7) were configured to match most of the information obtained using OSAT in run B1. Run B2 was designed to track sensitivity to VOC and NOx emissions separately in the 11 interior source areas surrounding the receptor areas. The MV and OAN emission categories were combined in runs B2 to reduce the number of emission categories to be tracked from 4 to 3. Run B2 would have required about 1.6 GB of RAM which turned out to be impractical[1] and so the sensitivities to NOx and VOC were calculated separately in two runs called B2N and B2V. Run B3 tracked the sensitivity to VOC and NOx combined in the 6 source areas around the edge of the modeling domain plus the ICs and BCs. Run B7 was designed to provide complete source category resolution without geographic resolution and tracked sensitivity to the VOC and NOx emissions from all four source categories (Table 1-2). Separating the DDM calculations into several runs was necessary in this project, but re-combining sensitivity information across runs complicated the post-processing and should be avoided if possible. The base case DDM runs B2N, B2V and B3 were repeated with reduced anthropogenic emission levels in sensitivity runs (see Table 1-4). Base case run B7 was not repeated in the sensitivity runs with reduced emission levels which, with hindsight, limited the scope of the analysis of the DDM results.

Process analysis runs B4, S3, S6 and S9 were configured to obtain integrated process rate (IPR) and integrated reaction rate (IRR) information for all four receptor areas. In addition, the process analysis runs obtained gridded chemical process analysis (CPA) outputs for the entire coarse and fine grid areas in each run.

[1] ENVIRON had Linux PCs with 2 Gbytes RAM but the Portland Group FORTRAN compiler had an unexpected limitation at 1 Gbyte. The other workstations available to us also had no more than 1 Gbyte RAM.

Table 1-4. Summary of the probing tool simulations and computer resources.

Simulation	Description	Memory Disk Space	CPU Time (Hours)
	2007 Base Case		
B1	OSAT with 17 source areas x 4 source categories plus ICs and BCs. O_3 attributed to VOC and NOx in each source group.	324 MB 4.9 GB	30
B2N	DDM with 11 source areas x 3 source categories. O_3 sensitivity to NOx from each source group.	820 MB 10.9 GB	80
B2V	DDM with 11 source areas x 3 source categories. O_3 sensitivity to VOC from each source group.	820 MB 10.9 GB	80
B3	DDM with 6 source areas x 3 source categories plus ICs and BCs. O_3 sensitivity to all species from each source group (i.e., combined VOC and NOx emissions).	541 MB 6.7 GB	54
B4	PA information extracted for 4 receptor regions (Atlanta, Chicago, New York, and Altoona) plus output of 3-D gridded CPA variables calculated within CAMx.	142 MB 4.4 GB	5.4
B5	APCA - Same configuration as B1	As B1	31
B6	GOAT - with 17 source areas plus ICs and BCs. O_3 attributed to each source area.	178 MB 1.6 GB	15
B7	DDM with 1 source area x 4 source categories. O_3 sensitivity to VOC and NOx from each source group.	284 MB 2.9 GB	25
25% Anthropogenic VOC Emissions Reduction			
S1	OSAT - Same configuration as B1	As B1	30
S2N	DDM - Same configuration as B2N	As B2N	80
S2V	DDM - Same configuration as B2V	As B2V	80
S3	PA - Same configuration as B4	As B4	5.4
25% Anthropogenic NO_x Emissions Reduction			
S4	OSAT - Same configuration as B1	As B1	30
S5N	DDM - Same configuration as B2N	As B2N	80
S5V	DDM - Same configuration as B2V	As B2V	80
S6	PA - Same configuration as B4	As B4	5.4
75% Anthropogenic NO_x Emissions Reduction			
S7	OSAT - Same configuration as B1	As B1	30
S8N	DDM - Same configuration as B2N	As B2N	80
S8V	DDM - Same configuration as B2V	As B2V	80
S9	PA - Same configuration as B4	As B4	5.4

Table Notes:

1. The 4 source categories for B1 and B7 are biogenic, on-road mobile, other surface anthropogenic and elevated point source emissions.
2. Run B2 was split to B2N and B2V to reduce the memory required below 1 GB.
3. The 3 source categories for B2, B3 and B4 are biogenic, surface anthropogenic, and elevated point source emissions.
4. The 17 source areas for B1 are shown in Figure 1-1.
5. The 11 source areas for B2 are 4, 5, 7, 8, 11, 12, 13, 14, 15, 16, and 17 as shown in Figure 1-1.
6. The 6 source areas for B3 are 1, 2, 3, 6, 9, and 10 as shown in Figure 1-1.
7. The 1 source area for B7 is the 36 km grid area shown in Figure 1-1.
8. For DDM, sensitivity to VOC was defined to include CO.
9. Run times are for a single processor 1000 MHz Pentium III PC. For reference, a simulation with no probing tools takes 4.4 hours of CPU time, 85 MBytes of memory (RAM) and 322 MBytes of disk storage.

DETAILED COMPARISON OF RUN TIMES AND EFFICIENCY

Probing tool runs for this project were performed on several workstations in order to evaluate computational efficiency with several operating systems and architectures. Four Linux PC workstations and one Unix workstation were used:

- Pentium III (PIII) 1 GHz
- Pentium 4 (P4) 1.7 GHz
- Athlon 1.2 GHz
- Athlon XP 1600+ (1.4 GHz)
- DEC Alpha 500 MHz

The Portland Group PGF77 compiler was used for the Linux workstations and the DEC FORTRAN77 compiler was used for the DEC Alpha workstation. Run times are summarized in Table 1-5.

Table 1-5. Probing tool run times (hours) on several computers.

Probing Tool	Run	Number of "Species"	Run Time (Hours) PIII 1GHz	P4 1.7 GHz	Athlon 1.2GHz	Athlon 1600+	DEC Alpha
Base			4.4	2.9	3.0	2.6	9.3
PA	B4,S3,S6,S9	35	5.4		3.7	3.1	
OSAT	B1,S1,S4,S7	280	29.3	20.3		17.8	60.7
APCA	B5	280	30.9				
GOAT	B6	76	15.4				
DDM	B7	200	24.8	23.3	20.6		49.2
DDM	B3	500	53.7	61.9	44.1		100.7
DDM	B2N,B2V,S2N S2V,S5N,S5V S8N,S8V	825	79.8	99.9	73		163.1

The run times for the Pentium III workstation are all from complete runs, but for the other computers some times were estimated by running the first six simulation days and extrapolating to get the total run time for nine simulation days.

The most important parameter for run time considerations is the number of "species" added to the simulation to track information, which is given in the third column of Table 1-5. The number of species is the number of OSAT tracers, CPA variables or DDM sensitivities and is the same as the value required for MXTRSP in the CAMx "tracer.com" include file. For the base case OTAG run (July 7-15, 1995 with 36/12 km nested grids) the Linux workstations are very fast, taking as little as 2.6 hours to complete the run.

The efficiency of the probing tool runs is best evaluated as the time for obtaining each "parameter" relative to the time for the base case (Table 1-6). The term parameter is used to refer to a relationship between ozone and a specific set of precursors. Each O3N and O3V tracer is considered a parameter for OSAT and each ozone sensitivity is considered a

parameter for DDM. This calculation was not performed for PA, but Table 1-5 shows that there was very little increase in run time for PA.

Table 1-6. Time per "parameter" for the DDM and OSAT runs.

Probing Tool	Run	Number of Parameters	Time per " parameter " P(III) 1GHz	P4 1.7 GHz	Athlon 1.2GHz	Athlon 1600+	DEC Alpha
OSAT	B1	140	0.040	0.043		0.042	0.039
APCA	B5	140	0.043				
GOAT	B6	19	0.132				
DDM	B7	8	0.580	0.879	0.733		0.536
DDM	B3	20	0.560	1.017	0.685		0.491
DDM	B2N	33	0.519	1.014	0.707		0.501

OSAT is more efficient (smaller time per parameter) than DDM because it uses only two tracer species to obtain each parameter. In comparison, DDM uses one sensitivity coefficient for each gas phase species in the mechanism (25 for CB4) to obtain each parameter. The OSAT efficiency is nearly constant across computer type and the value of about 0.04 means that each parameter was obtained about 25 times faster than would have been the case using a "brute force" method (i.e., conducting separate sensitivity runs for each parameter). APCA is slightly less efficient than OSAT because more calculations are involved at the ozone apportionment step. GOAT is still less efficient because the algorithm provides less information (no attribution to source categories, or to VOC and NOx) but still carries a full set of OSAT tracers. The efficiency of GOAT could be improved with re-coding, but this has never been a priority.

The DDM efficiency is expected to be lower than for OSAT because more "species" must be added to obtain each parameter (25 "species" for the CB4 mechanism). The efficiencies for DDM ranged between about 0.5 and 1, corresponding to between double and the same speed as using the brute force method. The best efficiencies were on PIII and DEC workstations and were about 0.5. This is generally consistent with previous modeling of the Chicago area where the best efficiencies were about 0.55 for a PIII workstation and 0.4 for a Sun Ultra30 workstation.

The efficiency for DDM is expected to improve as more parameters are calculated simultaneously. This generally was the case with the notable exception of the Pentium 4 PC. For the PIII PC, efficiency continually improved from 8 to 20 to 33 parameters. The DEC Alpha and Athlon showed improved efficiency from 8 to 20 parameters but then slowed down slightly for 33 parameters. The P4 was more efficient for 8 parameters than for 20 or 33 parameters.

The anomalous efficiency relationship for DDM on the Pentium 4 processors appears to be related to the chip architecture. Pentium III, Pentium 4 and Athlon chips differ in architectural details such as cache size and instruction pipeline depth. We put some effort into determining which part of the CAMx DDM code runs slowly on P4 PC (chemistry is the dominant effect) and investigated several alternate coding strategies to improve efficiency, but with minimal success. The results obtained here might change for a different modeling grid.

Different FORTRAN compilers, or newer versions of the PGF compiler, also may improve DDM efficiency on P4 PCs. Table 1-6 shows how to evaluate the efficiency of DDM calculations for your application (as does Dunker at al., 2002a) in order to make decisions about the best choice of computing platform.

2. SETTING UP PROBING TOOL ANALYSES

This section discusses considerations in setting up probing tool analyses. We assume that you are familiar with the probing tool descriptions included in the CAMx User's Guide (ENVIRON, 2002a).

DESIGNING OSAT AND APCA APPLICATIONS

The main choices in designing an OSAT (or APCA) application are selecting which source areas and emission groups to track. There is a balance between the desire to have more detailed information (more areas, more groups) and the burden imposed on computer resources and analysis time. Also, remember that as source areas and categories are more finely divided, the contributions tend to decrease and so the results of a highly detailed analysis are likely to show (correctly) that ozone is the sum of many small contributions.

Source Areas. It may be desirable for source areas to follow geo-political boundaries, such as states, counties or non-attainment areas. It can be difficult to follow geo-political boundaries closely (e.g., State boundaries that follow meandering rivers) so there may be limited precision in spatially defining emissions. There are several strategies for addressing this:

- Use fine grid source maps (introduced with CAMx4) to designate source areas at the finest grid resolution available, rather than at the coarse grid level (the only option in CAMx 3.1 and earlier). Quality-assure (QA) the consistency between fine and coarse grid source area maps, if you use them, to avoid confusion.
- Use the "point source override" option to specify the source area number for individual sources overriding the designation that CAMx will calculate based upon which grid cell the source is in. Point source overrides need very careful QA.
- If fine grid source maps do not provide high enough resolution, you could use the emissions preprocessor to make separate emissions files for selected geographic areas (e.g., make an emissions file with just nonattainment area emissions). In other words, geographic areas could be treated as separate emission categories.

The source areas do not have to correspond to receptor analysis areas (e.g., in this study the Atlanta grid cells were both a source area and a receptor area) although this may be useful for defining relative contributions of local emissions and transport. For OSAT and APCA, every grid cell must be assigned to a valid source area.

Point Source Override. CAMx automatically sets the source area for each point source to the source area of the grid cell containing the source. Sometimes it is desirable to override the automatic source area assignment for a point source. The CAMx point source file follows UAM-IV format and includes a 3-D cell index (i, j, k) for each point source. The (i, j) values are not used by CAMx because geographic location is determined from the stack coordinates. The plume injection layer (k-cell) is not used because CAMx internally calculates the plume rise from the stack parameters and meteorological conditions. This means the point source file (i, j, k) values can be used for OSAT specific purposes without changing the regular model

simulation. The OSAT "point source override" feature looks at the k-cell value specified for each point source, and if the value is negative it is interpreted as the source area number for the point source. The point source override feature is useful in situations where source area boundaries are only approximated by the source area map (e.g., for large utility sources located on rivers that are also State boundaries). However, the point source override option also requires careful QA because there is no way for CAMx to check for erroneous overrides. We suggest plotting a map showing both override source area numbers at the point source location and comparing this to the grid source area map for inconsistencies.

Source Categories. We recommend treating major source groups as separate emissions categories. Often, it is convenient to base the source groups on emissions that are preprocessed separately and then merged together (e.g., biogenics, onroad mobile, low-level points, offroad mobile, area source). At the very least, treat biogenic emissions as a separate category to:

- Separate the contributions of anthropogenic and biogenic emissions.
- Better characterize the average reactivity of the anthropogenic and biogenic source groups since biogenics often dominate total VOC emissions and are highly reactive.
- Allow for APCA analysis, which requires that biogenic emissions are separated and are the first source group because APCA assumes the first source group is the "non-controllable group."

Leftover Group. OSAT requires that all emissions must be included in one of the source categories so that the ozone apportionments sum to the total ozone. There are two ways to achieve this. (1) The separate emission files provided for each source category can add up to the same total emissions (temporally and spatially) as the base CAMx emissions. OSAT will check that this is the case and stop if any non-trivial discrepancy exists. This CAMx QA step is summarized in the emissions report provided in the *.diag output file. (2) Emission files can be provided for (n-1) of the emissions categories and the n^{th} category is calculated by CAMx as the "leftover group." This can be convenient, but defeats the QA step built into the first approach. An emissions summary is still printed to the *.diag file if the leftover group is used.

Initial and Boundary Conditions. OSAT and APCA always track contributions from initial and boundary conditions. The split between O3V and O3N is not very meaningful for ICs and BCs, as discussed below under pitfalls. If the contribution of boundary conditions is large, consider using the OSAT/APCA option to stratify the boundary contributions to the north, south, east, west and top boundaries.

Receptor Definitions. OSAT and APCA tracer concentrations for specific receptor locations can be output to a receptor file. It is not essential to define receptors because analyses can be performed using the gridded tracer output files. The OSAT receptor file is compatible with a Microsoft Excel post-processing macro described in the CAMx User's Guide. Receptors have advantages and disadvantages, as follows.

Advantages:

- ASCII file format is easy to read and can be processed using spreadsheet tools.
- Receptors can include multiple cells so that contributions can be spatially averaged.
- Wall-of-cells receptor is the only way to get aloft tracer concentrations.

Disadvantages:

- ASCII file format is bulky.
- Receptor locations must be defined before running CAMx.

Candidates for receptor locations are monitors, nonattainment areas and areas with high basecase ozone levels. The wall-of-cells receptor type can be used to define flux-planes upwind or downwind of key areas. If you have defined more than about 100 receptor locations you should consider analyzing the gridded output files.

Computer Resources. The computer resources for an OSAT analysis increase with the number of grid cells (modeling domain) and the number of tracer species (number of source areas X number of source categories). The CPU time, memory and disk storage for the OSAT/APCA runs completed here were compared to the basecase in Table 1-4, which shows that OSAT is very efficient. The following are considerations:

- The limiting factor for an OSAT run may be the memory (RAM) requirement. The best way to determine this is to calculate the number of tracer species required for your analysis (from the formula in the User's Guide and the tracer.com include file), compile CAMx with this number of tracers, and measure the memory requirement using the Unix size command (syntax: size executable_name).
- The 3-D average file flag has no impact on the size of the OSAT output files because the gridded OSAT files always contain only the surface layer. Adding 3-D gridded OSAT output files would approximately double the memory (RAM) requirement for OSAT runs and increase the likelihood of hitting 2 GB output file size limits present with some operating systems.
- The number of species selected for average output has no impact on OSAT output file sizes.
- The support for shared-memory multi-processor workstations (OMP support) introduced with CAMx version 3.1 also works with OSAT and provides significant speedup in model run time.

OSAT Options and Input Files. The main OSAT options are the selection of the technology type (OSAT/APCA/GOAT) and whether or not to stratify the boundary condition source apportionment. The source area and receptor definition files are in ASCII format and are easily prepared. Complicated source area maps that follow geo-political boundaries may require GIS software. Another option is to prepare the source area map from the gridded surrogates used in the emissions modeling. The OSAT emissions input files should be prepared with the same software and input data as the base CAMx emissions to ensure consistency. It is not necessary for the OSAT emissions files to have the same species list as the base CAMx files (e.g., biogenic emissions files often have fewer species than anthropogenic emissions files). It is absolutely essential that the OSAT and base CAMx point source emissions files have the same number of point sources in exactly the same order. This

will mean including sources with zero emissions (dummy sources) in the OSAT point source files if more than one point source category is being source apportioned (e.g., utility sources separate from other point sources).

OSAT PITFALLS

The following errors may result in apparently successful completion of an OSAT/APCA run (i.e., no model error messages) but meaningless, or misleading results:

- Failing to specify biogenics as the first, separate source category in an APCA analysis.
- Using the point source override feature and making errors in the assignments of source areas to point sources.
- Not using the point source override feature and having point sources that were intended to be in one source area assigned to a neighboring area (because the limited precision in representing geo-political boundaries with a gridded source area map).
- Using inconsistent geo-political boundaries (e.g., State, County) between the source area map and the emissions processing. Boundaries can shift by several km between data from different sources, especially near rivers and coastlines.
- Using the leftover emissions group and failing to detect an error in the processing of emissions for one of the other groups.
- Having different numbers and/or orders of point sources between OSAT and base CAMx files.

In addition, when analyzing OSAT or APCA results, remember that the split between O3V and O3N tracers for the initial and boundary conditions is not very meaningful and so the O3N and O3V tracers should be combined in the analysis of ICs and BCs.

DESIGNING DDM APPLICATIONS

The main choice in designing a DDM application is selecting what sensitivities to calculate. For the type of DDM application demonstrated here, i.e., comparable to OSAT, this comes down to selecting source areas and emission groups. Similar considerations apply for DDM as OSAT, so read the discussions of “Source Areas,” “Source Categories” and “Point Source Overide” given above. Differences for DDM are discussed below. However, DDM is much more flexible than OSAT and there are many other types of DDM analyses that could have different considerations, such as using DDM to calculate VOC reactivity factors in a grid model as described by Carter et al., (2002).

DDM Source Areas and Categories. DDM does not need to account for all sources of ozone (or any other species), which leads to some differences from the OSAT discussions above:

- Parts of the source area map for which sensitivities are not calculated are assigned an area of zero.
- The n source areas being followed must be numbered 1 through n. This complicates analyses where geographic sensitivities are calculated in separate runs (e.g., B2 and B3, in this study) because source areas must be renumbered.
- If point source override is being used, remember to set source areas to zero for sources in areas that are not being followed.
- The sum of the sensitivity emissions does not necessarily equal the base CAMx emissions. Unlike OSAT, DDM has no QA checks on emission totals and there is no leftover group.

Initial and Boundary Conditions. Calculating sensitivities to initial and boundary conditions is optional with DDM. DDM can calculate separate sensitivities to boundary/initial O_3, VOC, NOx, any individual species, or to all BC/IC species combined. It is probably useful to know the sensitivity to ICs and BCs. Calculating the sensitivity to all IC and all BC species is probably adequate initially. Sensitivities can be calculated by species if the IC/BC sensitivities are found to be unexpectedly large. If the sensitivity to boundary conditions is large, consider using the option to stratify the boundary contributions to the north, south, east, west and top boundaries.

Receptor Definitions. An ASCII format DDM receptor was added to CAMx for this project and will be publicly available in CAMx4. The considerations for selecting receptors are similar to OSAT, discussed above. Receptors are not essential because the gridded DDM output files can be analyzed. Unlike OSAT, there is no post-processing software specifically designed for the DDM receptor file (the OSAT Excel browser will not work).

Computer Resources. The computer resources for a DDM analysis can be substantial and should be considered carefully. The computer resources for the runs performed in this study are summarized in Table 1-4. Considerations are:

- The limiting factor for a DDM run is likely to be memory (RAM) requirement. The best way to determine this is to calculate the number of tracer species required for your analysis (from the formula in the User's Guide and the tracer.com include file), compile CAMx with this number of tracers, and measure the memory requirement using the Unix size command (syntax: size executable_name).
- With the Portland Group compiler on Linux we have found that CAMx gets unexpected fatal errors with DDM runs requiring more than about 1 GB of RAM. The reason for this is unclear, but if it happens the workaround is to split the DDM run as, for example, run B2 was split to B2N and B2V in this study.
- It is possible that a large DDM analysis could produce output files that exceed the 2 GB file size limit present on some workstation file systems (the DDM fine grid surface files for runs B2N and B2V were 0.8 GB). If this happens, try to use a file system that does not have this limitation (e.g., Linux ext3) or split the DDM analysis into several runs.
- We have found that CAMx DDM is unexpectedly slow on Pentium 4 chips (with Linux and the Portland Group compiler). This is related to the P4 architecture because DDM performs well with Intel Pentium 3 and AMD Athlon chips.
- The 3-D average file flag has no impact on the size of the DDM output files because the gridded DDM files always contain only the surface layer. Adding 3-D gridded DDM

output files would approximately double the memory (RAM) requirement for DDM runs and increase the likelihood of hitting 2 GB output file size limits.

- The number of species selected for average output does impact DDM output file size because sensitivities are only output for affected species selected for average output. If you are interested only in ozone, selecting just O3 can significantly reduce output file sizes.
- The support for shared-memory multi-processor workstations (OMP support) introduced with CAMx version 3.1 also works with DDM and provides significant speedup in model run time.

DDM Options and Input Files. The main DDM options are for selecting which sensitivities to calculate, as discussed in the CAMx User's Guide. The source area and receptor definition files are in ASCII format and are easily prepared. Complicated source area maps that follow geo-political boundaries may require GIS software. Another option is to prepare the source area map from the gridded surrogates used in the emissions modeling. The DDM emissions input files should be prepared with the same software and input data as the base CAMx emissions to ensure consistency. It is not necessary for the DDM emissions files to have the same number species list as the base CAMx files (e.g., biogenic emissions files often have fewer species than anthropogenic emissions files). It is absolutely essential that the DDM and base CAMx point source emissions files have the same number of point sources in exactly the same order. This will mean including sources with zero emissions (dummy sources) in the DDM point source files if more than one point source category is being source followed (e.g., utility sources separate from other point sources).

Advection Solver. The DDM is only implemented for the Bott advection solver.

Plume in Grid. The DDM cannot be used with the Plume-in-Grid sub-model (PiG). The workaround is to turn off PiG.

DDM PITFALLS

The following errors may result in apparently successful completion of a DDM run (i.e., no model error messages) but meaningless, or misleading results:

- Using the point source override feature and making errors in the assignments of source areas to point sources.

- Not using the point source override feature and having point sources that were intended to be in one source area assigned to a neighboring area (because the limited precision in representing geo-political boundaries with a gridded source area map).

- Using inconsistent geo-political boundaries (e.g., State, County) between the source area map and the emissions processing. Boundaries can shift by several km between data from different sources, especially near rivers and coastlines.

- Having different numbers and/or orders of point sources between DDM and base CAMx files.

DESIGNING PA APPLICATIONS

Designing PA applications is simpler than for OSAT or DDM. The only choices to be made are:

- Selecting the type of PA (IPR, IRR/CPA, all types).
- Selecting receptor areas for IPR or IRR.

Candidate receptor areas are monitor locations, areas with high ozone and areas with model performance issues where PA may provide extra information. CPA is applied domain-wide regardless of the receptor areas selected. There are no extra input files to prepare for PA, all options are specified in the CAMx control file. These options are described in the CAMx User's Guide.

Computer Resources. The computer resources for PA increase with the number of receptor cells selected for IPR and/or IRR analysis. CPA adds little to the computer resource requirements for the base model, about 10% increase in CPU time, 50% increase in memory and 100% increase in disk storage. The computer resources for the PA runs completed here are compared to the base case in Table 1-4 (note that the big increase in disk storage is because 3-D CPA outputs were selected whereas only surface concentrations were output in the base case). The limiting factor for PA is likely to be the disk storage requirement. This is especially true if IPR or IRR is used with a large number of receptor grid cells.

PA PITFALLS

We have not found any errors in PA configuration that may result in apparently successful completion of a PA run (i.e., no model error messages) but meaningless, or misleading results. The PA configuration specified in the CAMx control file is relatively easy to check for inconsistencies and several QA checks are built into CAMx to prevent errors. These checks include:

- Receptor areas must be entirely contained within one grid.

- Receptor areas may not overlap each other.

3. ANALYSIS OF OSAT RESULTS

This section presents several example analyses of CAMx OSAT results to show what the OSAT source apportionments look like and illustrate how they can be summarized and analyzed. We do not interpret the implications of the results for air quality planning because the OTAG modeling scenarios are dated and because the results are open to interpretation. In our experience, different importance can be attached to the relative magnitudes of the source apportionments shown in the example analyses based on perceptions of what is important or significant.

OUTPUT FILES

The CAMx output files that are specific to OSAT are listed in Table 3-1. The file formats are described in the CAMx User's Guide (ENVIRON, 2002a) with the exception of the receptor file, which is new and was added for this project. The receptor file is in a self-describing ASCII format that includes the date/time, list of tracers, list of receptors and tracer data (by time and receptor).

Table 3-1. OSAT output file suffix names.

File Suffix	OSAT file type
.sa.inst.1	Coarse grid binary instantaneous tracer file for last odd simulation hour (used for restart), 3-D, all tracers
.sa.inst.2	Coarse grid binary instantaneous tracer file for last even simulation hour (used for restart), 3-D, all tracers
.sa.finst.1	Fine grid binary instantaneous tracer file for last odd simulation hour (used for restart), 3-D, all tracers
.sa.finst.2	Fine grid binary instantaneous tracer file for last even simulation hour (used for restart), 3-D, all tracers
.sa.surf	Coarse grid binary average tracer file, 2-D, surface layer tracers
.sa.fsurf	Fine grid binary average tracer file, 2-D surface layer tracers
.sa.receptor	Receptor file in ASCII format with average tracers at selected receptor locations

The CAMx diagnostic output file (*.diag) also includes important OSAT information that is needed for quality assurance (QA). The diagnostic output file lists the OSAT options and file names and summarizes the VOC and NOx emissions for each source area and source category. This is important information for QA purposes, as discussed below.

QUALITY ASSURANCE

OSAT configuration errors that might go undetected because they do not cause a CAMx error were discussed under "OSAT pitfalls" in Section 2. Important quality assurance checks for OSAT calculations are:

- Checking the source area map and fine grid source area map(s), if used.
- Checking point source overrides, if used.
- Checking that the correct emissions files are provided for each source category.
- Checking the summarizes of VOC and NOx emissions for each source area and source category reported in the diagnostic output file to ensure that the correct source apportionments are being calculated, and that the emissions are consistent with expectations and (preferably) with summary tables from the emissions processing. Note that the VOC emissions reported in the diagnostic output file are calculated from the moles of VOC times representative molecular weights. For CB4, the molecular weights are the number of carbon atoms times 16, which is a long-standing convention. Different assumptions may have been used in the emissions preprocessor.
- Checking receptor definitions, if used.

An example of the emissions information reported to the diagnostic output file is shown in Table 3-2. The table shows emissions from runs B1 and S1. S1 had a 25% reduction in anthropogenic VOC emissions, which is confirmed by the ratio of VOC emission totals shown in Table 3-2.

Analysis of the OSAT results is an important part of the QA process. Source apportionments that are unexpected may point to errors in setting up the analysis.

Table 3-2. Summary of VOC and NOx emissions (tons/day) for July 13 by source area and source category for runs B1 and S1 based on information reported to the CAMx diagnostic output files.

B1 NOx Emissions (tons)

Source Area	Source Category BIO	MV	EPT	OAN	Total
1	3044	1108	1741	2058	7950
2	540	1099	2322	2686	6647
3	379	261	563	447	1650
4	1519	812	1769	1225	5324
5	684	825	2422	1628	5559
6	135	361	1046	1469	3012
7	555	1096	3198	1434	6283
8	271	1025	1692	823	3811
9	127	702	904	602	2335
10	110	163	156	745	1175
11	307	1004	2102	1119	4532
12	183	574	1138	573	2467
13	83	748	645	807	2282
14	38	260	534	334	1166
15	8	264	307	177	757
16	3	309	202	437	951
17	18	37	23	27	105
Total	8005	10648	20765	16589	56007

B1 VOC Emissions (tons)

Source Area	Source Category BIO	MV	EPT	OAN	Total
1	29324	722	82	3219	33347
2	36022	518	124	2846	39510
3	19679	141	71	1141	21032
4	8704	489	156	2088	11436
5	38167	461	246	1961	40834
6	15643	222	67	1033	16965
7	9183	653	116	2677	12629
8	34705	566	83	2319	37673
9	8509	408	20	1299	10235
10	24573	65	46	2121	26805
11	16061	415	53	2038	18567
12	12946	290	34	1569	14838
13	7400	263	41	1740	9444
14	384	110	46	689	1229
15	1695	109	7	337	2148
16	475	104	7	1096	1681
17	1374	16	2	45	1437
Total	264842	5553	1198	28217	299810

S1 NOx Emissions (tons)

Source Area	Source Category BIO	MV	EPT	OAN	Total
1	3044	1108	1741	2058	7950
2	540	1099	2322	2686	6647
3	379	261	563	447	1650
4	1519	812	1769	1225	5324
5	684	825	2422	1628	5559
6	135	361	1046	1469	3012
7	555	1096	3198	1434	6283
8	271	1025	1692	823	3811
9	127	702	904	602	2335
10	110	163	156	745	1175
11	307	1004	2102	1119	4532
12	183	574	1138	573	2467
13	83	748	645	807	2282
14	38	260	534	334	1166
15	8	264	307	177	757
16	3	309	202	437	951
17	18	37	23	27	105
Total	8005	10648	20765	16589	56007

S1 VOC Emissions (tons)

Source Area	Source Category BIO	MV	EPT	OAN	Total
1	29324	542	61	2415	32341
2	36022	388	93	2134	38638
3	19679	106	54	856	20694
4	8704	367	117	1566	10754
5	38167	345	184	1471	40167
6	15643	167	50	775	16635
7	9183	490	87	2008	11768
8	34705	425	62	1740	36931
9	8509	306	15	974	9803
10	24573	49	34	1591	26247
11	16061	312	40	1529	17941
12	12946	217	25	1177	14365
13	7400	197	31	1305	8933
14	384	83	34	516	1018
15	1695	82	5	253	2035
16	475	78	5	822	1379
17	1374	12	1	34	1421
Total	264842	4164	899	21163	291069

POST-PROCESSING TOOLS

PAVE

The gridded OSAT tracer output files are in same format as the CAMx average concentration files and are directly compatible with post-processing software such as PAVE[1]. Recent distributions of PAVE have been able to handle the large number of species present in OSAT output files. The formula capabilities built into PAVE allow tracers to be combined, but there is a limit on the number of species that can be combined in a formula (about 30). Large numbers of tracers can be combined using the CAMxtrct and RANKTRAC tools below.

CAMxtrct

CAMxtrct (CAM-extract) is a post-processing program available from the CAMx ftp site[2]. CAMxtrct extracts concentrations for single species or combinations of species from CAMx coarse and/or fine grid files in average file format. It writes out either a binary file in coarse grid average file format or in an ASCII file in a format similar to Golden Software Surfer GRD format. The specific capabilities of CAMxtrct are:

- Extract a species for a specific grid and layer.
- Select a specific species or combine several species that match a keyword.
- Combine coarse and fine grids to a coarse grid format file at the resolution of the finest grid.
- Extracting specific time intervals or finding daily maximum values.
- Take ratios of two species. Keyword species combinations are allowed in the numerator and/or denominator.

The keywords for combining OSAT tracers are:

TO3 - sum of all ozone tracers (equals the modeled ozone)
TO3N - sum of all O3N tracers
TO3V - sum of all O3V tracers
TNOx - sum of all NOx tracers (equals the modeled NOx)
TVOC - sum of all VOC tracers (equals the modeled VOC)
TO3I - sum of both ozone tracers for initial conditions
TO3B - sum of all ozone tracers for boundary conditions
O3Rnnn - sum of all ozone tracers for source region nnn
EO3Nnnn - sum of all O3N tracers for emissions source category nnn
EO3Vnnn - sum of all O3V tracers for emissions source category nnn
EO3Tnnn - sum of all ozone tracers for emissions source category nnn
O3RnnnEmmm - sum of both ozone tracers for region nnn category mmm

[1] PAVE is available from http://www.emc.mcnc.org/EDSS/pave_doc/Pave.html
[2] The CAMx ftp site is ftp://ftp.environ.org, username=camxuser, password=pass4camx

CAMxtrct is useful for the following purposes:

- Combining information from coarse and fine grids.
- Combining tracers over geographic areas and/or source categories.
- Preprocessing information for PAVE to overcome limitations in PAVE formulas.

RankTrac and Trac8hr

RankTrac and Trac8hr are post-processing program distributed via the CAMx ftp site. RankTrac extracts tracers for selected grid cells (receptors) from the OSAT surface output files. A concentration threshold can be applied so that tracers are only extracted for receptor grid cell/hours when ozone exceeds the threshold amount. The output file is in a flat ASCII format that is easy to interpret and analyze. RankTrac extracts the hourly tracer data present on the CAMx OSAT output files (assuming CAMx was run with hourly output intervals) whereas as Trac8hr calculates running 8-hour averages of tracer data as they are extracted. Trac8hr avoids the need to pre-process the tracer data to 8-hour averages.

```
#!/bin/csh
#
/models/camx/postproc/ranktrac/ranktrac.linux << ieof
Average file type  : FINE
Contribution type  : ppb
Threshold          : 0.0
Extract Region     :14
Output filename    :./jnkout/Chicago.box.1hr.0ppb.OSAT.B1.tbl
Raw ASCII output   :./outputs/Chicago.box.1hr.0ppb.OSAT.B1.asc
Extract Region     :15
Output filename    :./jnkout/Atlanta.box.1hr.0ppb.OSAT.B1.tbl
Raw ASCII output   :./outputs/Atlanta.box.1hr.0ppb.OSAT.B1.asc
Extract Region     :16
Output filename    :./jnkout/NewYork.box.1hr.0ppb.OSAT.B1.tbl
Raw ASCII output   :./outputs/NewYork.box.1hr.0ppb.OSAT.B1.asc
Extract Region     :17
Output filename    :./jnkout/Altoona.box.1hr.0ppb.OSAT.B1.tbl
Raw ASCII output   :./outputs/Altoona.box.1hr.0ppb.OSAT.B1.asc
                    /END/
Mock-receptor file : recept.out
Source area map    :../../ddm.inputs/source_map/fine.source_map.crc.17area.osat
Source map type    :FINE
Emissions table    :
Coarse grid average:$INFIL/CAMx3.950711.07base.OSAT.B1.sa.surf
Coarse grid average:$INFIL/CAMx3.950712.07base.OSAT.B1.sa.surf
Coarse grid average:$INFIL/CAMx3.950713.07base.OSAT.B1.sa.surf
Coarse grid average:$INFIL/CAMx3.950714.07base.OSAT.B1.sa.surf
Coarse grid average:$INFIL/CAMx3.950715.07base.OSAT.B1.sa.surf
                    /END/
Fine grid average  :$INFIL/CAMx3.950711.07base.OSAT.B1.sa.fsurf
Fine grid average  :$INFIL/CAMx3.950712.07base.OSAT.B1.sa.fsurf
Fine grid average  :$INFIL/CAMx3.950713.07base.OSAT.B1.sa.fsurf
Fine grid average  :$INFIL/CAMx3.950714.07base.OSAT.B1.sa.fsurf
Fine grid average  :$INFIL/CAMx3.950715.07base.OSAT.B1.sa.fsurf
                    /END/
```

Figure 3-1. Example RankTrac application to analyze tracers from OSAT run B1.

```
Boundary filename  :
                   :001  001  BIO_reg1  0         25.0
                   :002  001  BIO_reg2  0         25.0
                   :003  001  BIO_reg3  0         25.0
                   :004  001  BIO_reg4  0         25.0
                   :005  001  BIO_reg5  0         25.0
                   :006  001  BIO_reg6  0         25.0
                   :007  001  BIO_reg7  0         25.0
                   :008  001  BIO_reg8  0         25.0
                   :009  001  BIO_reg9  0         25.0
                   :010  001  BIO_reg10 0         25.0
                   :011  001  BIO_reg11 0         25.0
                   :012  001  BIO_reg12 0         25.0
                   :013  001  BIO_reg13 0         25.0
                   :014  001  BIO_reg14 0         25.0
                   :015  001  BIO_reg15 0         25.0
                   :016  001  BIO_reg16 0         25.0
                   :017  001  BIO_reg17 0         25.0
                   :001  002  MV_reg1   0         25.0
                   :002  002  MV_reg2   0         25.0
                   :003  002  MV_reg3   0         25.0
                   :004  002  MV_reg4   0         25.0
                   :005  002  MV_reg5   0         25.0
                   :006  002  MV_reg6   0         25.0
                   :007  002  MV_reg7   0         25.0
                   :008  002  MV_reg8   0         25.0
                   :009  002  MV_reg9   0         25.0
                   :010  002  MV_reg10  0         25.0
                   :011  002  MV_reg11  0         25.0
                   :012  002  MV_reg12  0         25.0
                   :013  002  MV_reg13  0         25.0
                   :014  002  MV_reg14  0         25.0
                   :015  002  MV_reg15  0         25.0
                   :016  002  MV_reg16  0         25.0
                   :017  002  MV_reg17  0         25.0
                   :001  003  EPT_reg1  0         25.0
                   :002  003  EPT_reg2  0         25.0
                   :003  003  EPT_reg3  0         25.0
                   :004  003  EPT_reg4  0         25.0
                   :005  003  EPT_reg5  0         25.0
                   :006  003  EPT_reg6  0         25.0
                   :007  003  EPT_reg7  0         25.0
                   :008  003  EPT_reg8  0         25.0
                   :009  003  EPT_reg9  0         25.0
                   :010  003  EPT_reg10 0         25.0
                   :011  003  EPT_reg11 0         25.0
                   :012  003  EPT_reg12 0         25.0
                   :013  003  EPT_reg13 0         25.0
                   :014  003  EPT_reg14 0         25.0
                   :015  003  EPT_reg15 0         25.0
                   :016  003  EPT_reg16 0         25.0
                   :017  003  EPT_reg17 0         25.0
                   :001  004  OAN_reg1  0         25.0
                   :002  004  OAN_reg2  0         25.0
                   :003  004  OAN_reg3  0         25.0
                   :004  004  OAN_reg4  0         25.0
                   :005  004  OAN_reg5  0         25.0
                   :006  004  OAN_reg6  0         25.0
                   :007  004  OAN_reg7  0         25.0
                   :008  004  OAN_reg8  0         25.0
                   :009  004  OAN_reg9  0         25.0
                   :010  004  OAN_reg10 0         25.0
                   :011  004  OAN_reg11 0         25.0
                   :012  004  OAN_reg12 0         25.0
                   :013  004  OAN_reg13 0         25.0
                   :014  004  OAN_reg14 0         25.0
                   :015  004  OAN_reg15 0         25.0
                   :016  004  OAN_reg16 0         25.0
                   :017  004  OAN_reg17 0         25.0
                   :IC   ALL  IC        0         25.0
                   :BC   ALL  BC        0         25.0
                    /END/
ieof
```

Figure 3-1. Concluded.

An example RankTrac application to analyze tracers calculated in OSAT run B1 is shown in Figure 3-1. Trac8hr takes the same inputs as RankTrac. The input information required by RankTrac is:

1. Whether the analysis is for coarse or coarse/fine grid files.
2. The value for the concentration threshold (ppb).
3. The numbers of the receptor areas to extract, followed by two output filenames for each receptor. The first file in each case is no longer used and a dummy name is given. The useful output data are in the "raw ASCII output" files. The end of this data block is shown by the /END/ keyword.
4. The mock-receptor file is no longer used and a dummy filename is given.
5. The name of the receptor map file that defines the receptors. In this case, the receptor map is the same as the source area map (Figure 1-1) so that the receptors are areas 14 through 17. The receptor map must be at the finest grid resolution and cover the area of the coarse grid. The end of this data block is shown by the /END/ keyword.
6. The source map file type, coarse or fine. This should match input (1), above.
7. The emissions table file is no longer used and is left blank.
8. The names of the coarse and fine surface tracer files.
9. The boundary filename if the coarse grid has special (irregular) boundaries. If the coarse grid boundaries are the edges of the coarse grid this line can be left blank.
10. A list of definitions for the groups of tracers to be extracted. The group definitions have the following structure:
    a. The region number, or ALL for all regions, or IC or BC.
    b. The emissions group number, or ALL for all groups or all IC/BCs.
    c. A name to describe the group in the RankTrac output file.
    d. Two dummy values that are no longer used and are set to zero and 25.

EXAMPLE ANALYSES

A series of analyses are presented to illustrate how OSAT tracer information can be presented for interpretation. The tables and figures are shown in order at the end of the section. Many of the analyses correspond to analyses of DDM data shown in Section 4.

Figure 3-2 shows plots of ozone attributed to NOx and VOC emissions from biogenic, onroad mobile, elevated point and other anthropogenic emissions at 14:00 EST on July 14, 1999 for the 2007 base emissions scenario. These are displays of OSAT results from run B1. The plots were prepared using PAVE. Figure 3-2 requires calculating sums of ozone tracers over geographic source regions. These tracer sums could be calculated with PAVE formulas, but were calculated more easily using CAMxtrct with "EO3N" and EO3V" keywords, as discussed above. The plots in Figure 3-2 show the coarse grid extent at fine grid resolution, which also was done by CAMxtrct. The western edge of the fine grid is apparent in some of the spatial plots. This is a consequence of the vertical nesting used in the OTAG, which means that coarse grid area represents the first 100 m, whereas the fine grid represents the first 50 m. We do not recommend using vertical nesting.

Figure 3-3 shows time series of OSAT source contributions for single grid cells in each receptor area. The northwest corner grid cell of each receptor (9,9) was chosen because it is

likely to be consistently downwind in all areas with the exception of Atlanta. The sum of the source contributions is the total ozone. The A and B prefixes before NOx and VOC stand for anthropogenic and biogenic. These figures are displays of results from OSAT run B1. The data for each chart were extracted from the OSAT surface output files using RankTrac. A source area map was created to identify the northwest corner grid cells as receptor areas for RankTrac. RankTrac was also able to sum tracers to the six groups shown in the charts. The ASCII output files from RankTrac were plotted using a spreadsheet to produce the charts.

Figure 3-4 illustrates the use of base case tracers to predict ozone levels with reduced emissions, as discussed in Section 2 (see equation 2-7). The figures show time series of ozone for the northwest corner grid cells in each receptor area with reduced emissions. These are the same grid cells that are shown in Figure 3-3. The emission reduction levels are 25% anthropogenic NOx and VOC and 75% anthropogenic NOx. The OSAT estimated ozone levels with reduced emissions were calculated by linearly scaling the base case (run B1) tracer contributions shown in Figure 3-3. The 25% VOC reduction was estimated by multiplying the AVOC contribution by 0.75 and all other contributions by 1. Scaling the base case OSAT apportionments tends to slightly over-predict the ozone reductions for moderate emissions reductions (25% ANOx and 25% AVOC) and underestimate the effect of a large NOx reduction (75% ANOx). This is the expected result, as discussed in Section 2.

Zhang and co-workers (2002) performed a similar analysis for all 81 grid cells in the receptor area (81= 9 x 9) and found poorer agreement in grid cells over the urban core with low ozone where the NOx inhibition effect is greatest. As OSAT does not allow negative ozone source apportionment, it does not project ozone increases due to NOx controls (i.e., NOx disbenefits).

Tables 3-3 to 3-6 show the complete OSAT ozone apportionment for each receptor averaged over all grid cells and hours when total ozone exceeded 80 ppb. Averaging tracer information over all high ozone conditions in a receptor area provides a more representative picture of the source contributions than a single grid cell and hour. Tables like this can be prepared using RankTrac with an ozone threshold (80 ppb, in this case) and summarizing the results using a spreadsheet. The sum of the tracers is the same as the total ozone in the receptor area averaged over the grid cells and hours when total ozone exceeded 80 ppb.

The information shown in Tables 3-3 to 3-6 is condensed in bar charts and compared across receptor areas in Figures 3-5 and 3-6. Figure 3-5 summarizes the ozone contributions by NOx and VOC, whereas Figure 3-6 summarizes the contributions by source category (with NOx and VOC combined). Figures 3-5 and 3-6 also compare tracers for high 1-hour and 8-hour ozone conditions. The summaries for high 8-hour ozone condition were prepared in exactly the same way as for high 1-hour ozone but using Trac8hr rather than RankTrac.
Figures 3-5 and 3-6 also compare the OSAT contributions to high ozone in the base and emission reduction cases. It is important to average tracers over a fixed set of grid cells and hours in the base and emission reduction cases, otherwise the average contributions will not be comparable.

The effect of emission reductions on the OSAT contributions for specific source regions, categories and species (NOx or VOC) is shown in Figure 3-7. All OSAT contribution in Figure 3-7 are averages over the grid cells and hours when 1-hour ozone exceeded 80 ppb in

the basecase. This means that Figure 3-7 shows scatter plots of the emissions contribution reported at the top of Tables 3-3 through 3-6 against corresponding contributions for the emission reduction cases.

The dashed lines in Figure 3-7 show the expected relationship if the contributions scale linearly with emissions reduction. For example, at top left, if the contributions from anthropogenic NOx are unchanged by a 25% reduction in anthropogenic VOC, then the points will fall an a 1:1 line, which they do. At top right in Figure 3-7, if the contributions from anthropogenic VOC are reduced 25% by a 25% reduction in anthropogenic VOC, then the points will fall on a line with slope 0.75. The response of emission tracers to the emission reduction scenarios is summarized below.

Figure 3-7 combines tracers across receptors, source areas and emission categories on the same charts and shows consistency in the responses of the tracers to emission reductions across receptors, source areas and emission categories.

25% reduction in AVOC: The contributions from ANOx are mostly unchanged and the contributions from AVOC are reduced by 25%. Deviations from the linear relationships are small.

25% reduction in ANOx: The contributions from ANOx are reduced by less than 25% with a 25% reduction in ANOx. The less than linear reduction in ANOx contributions can be interpreted as the ozone formation efficiency (ozone formed per NOx) increasing as NOx was reduced. The AVOC contributions are reduced by the 25% reduction in ANOx, which can be interpreted as a shift to more NOx-limited (less VOC sensitive) conditions as NOx is reduced.

75% reduction in ANOx: The contributions from ANOx are reduced by less than 75% with a 75% reduction in ANOx. The less than linear reduction in ANOx tracers can be interpreted as the ozone formation efficiency (ozone formed per NOx) increasing as NOx was reduced. For a few Chicago and New York points (i.e., source regions/categories) the contribution from ANOx is larger in the control case than the basecase, which can be interpreted as a large shift toward NOx-limited conditions in response to the deep NOx emissions reduction. The AVOC contributions are substantially reduced by the 75% reduction in ANOx, which also indicates a large shift to more NOx-limited (less VOC sensitive) conditions when NOx is reduced by 75%.

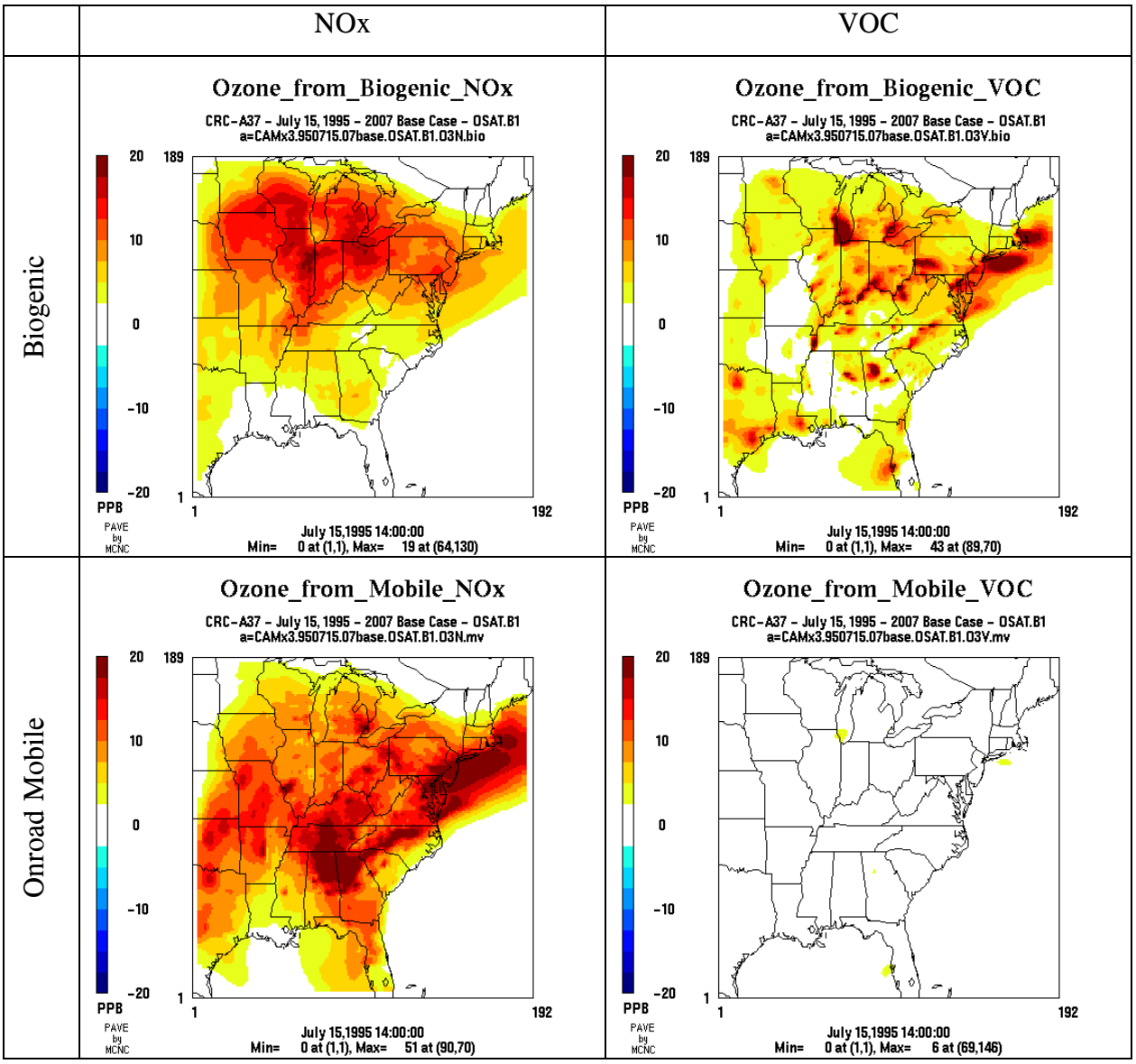

Figure 3-2. Spatial plots of OSAT source apportionments to NOx and VOC emissions from biogenic, onroad mobile, elevated point and other anthropogenic emissions at 14:00 EST on July 14, 1999 for the 2007 base emissions scenario. Results from run B1.

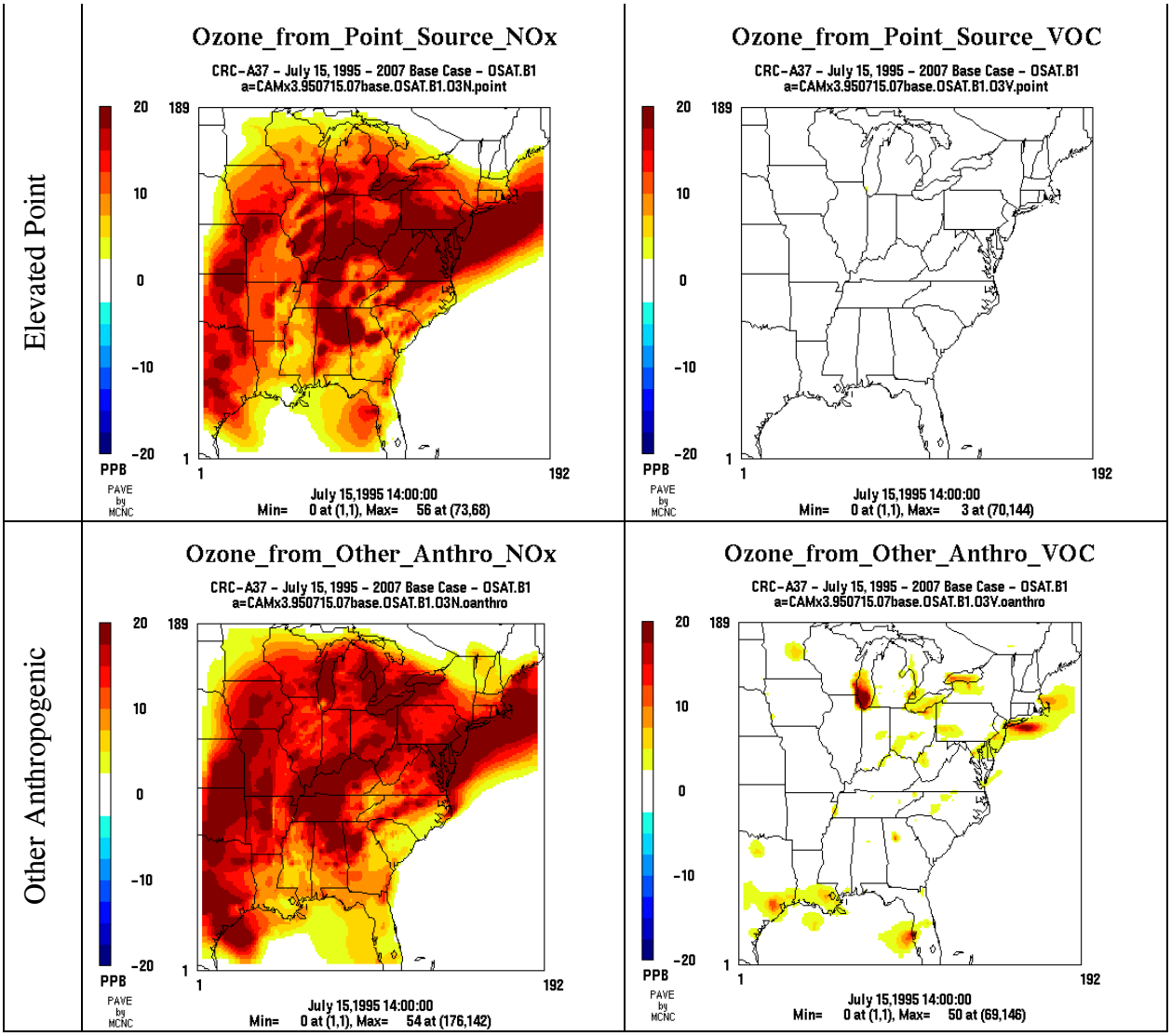

Figure 3-2 (concluded).

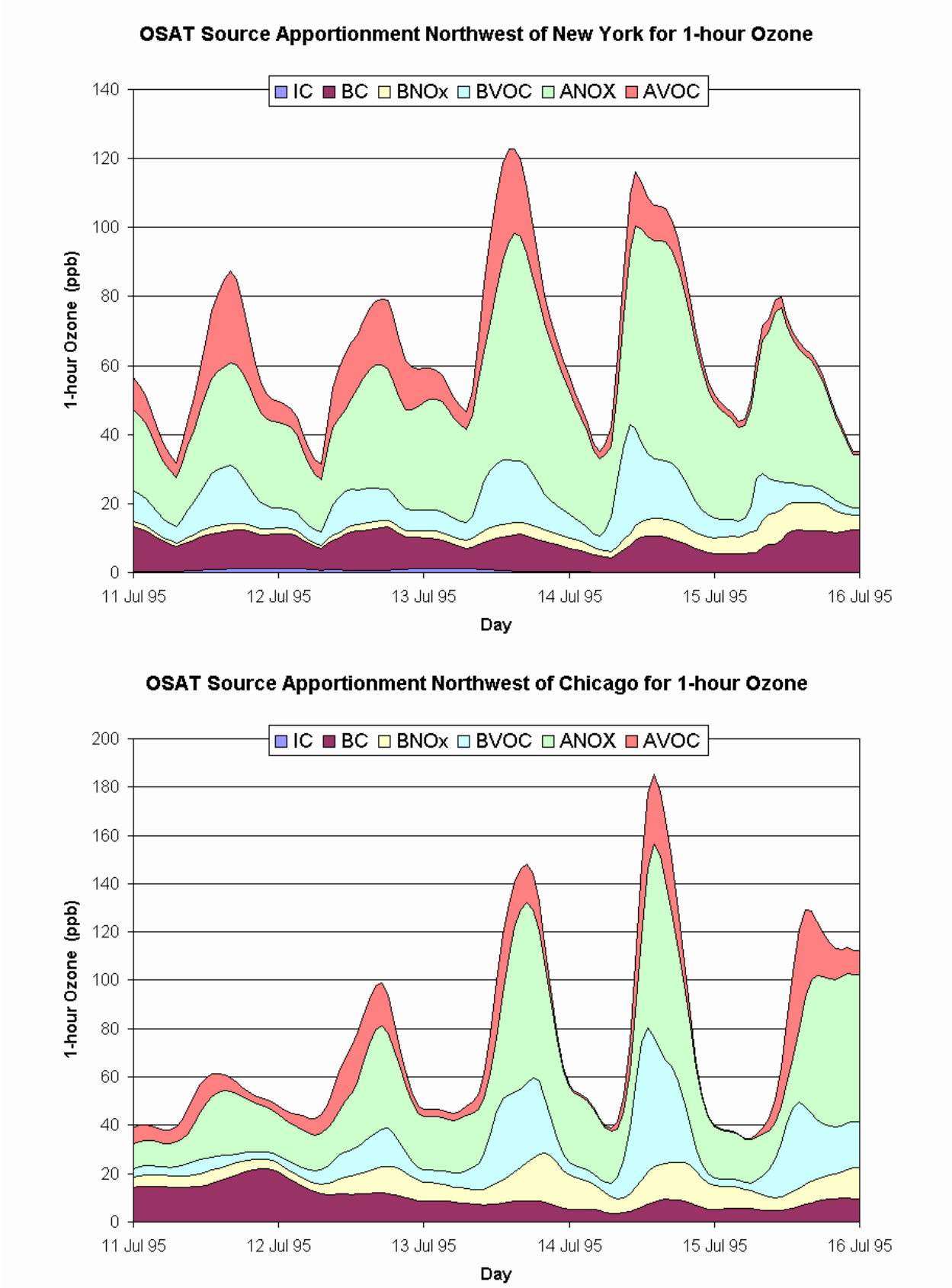

Figure 3-3. Time series of OSAT source apportionments for the northwest corner grid cell in each receptor area. Results from run B1.

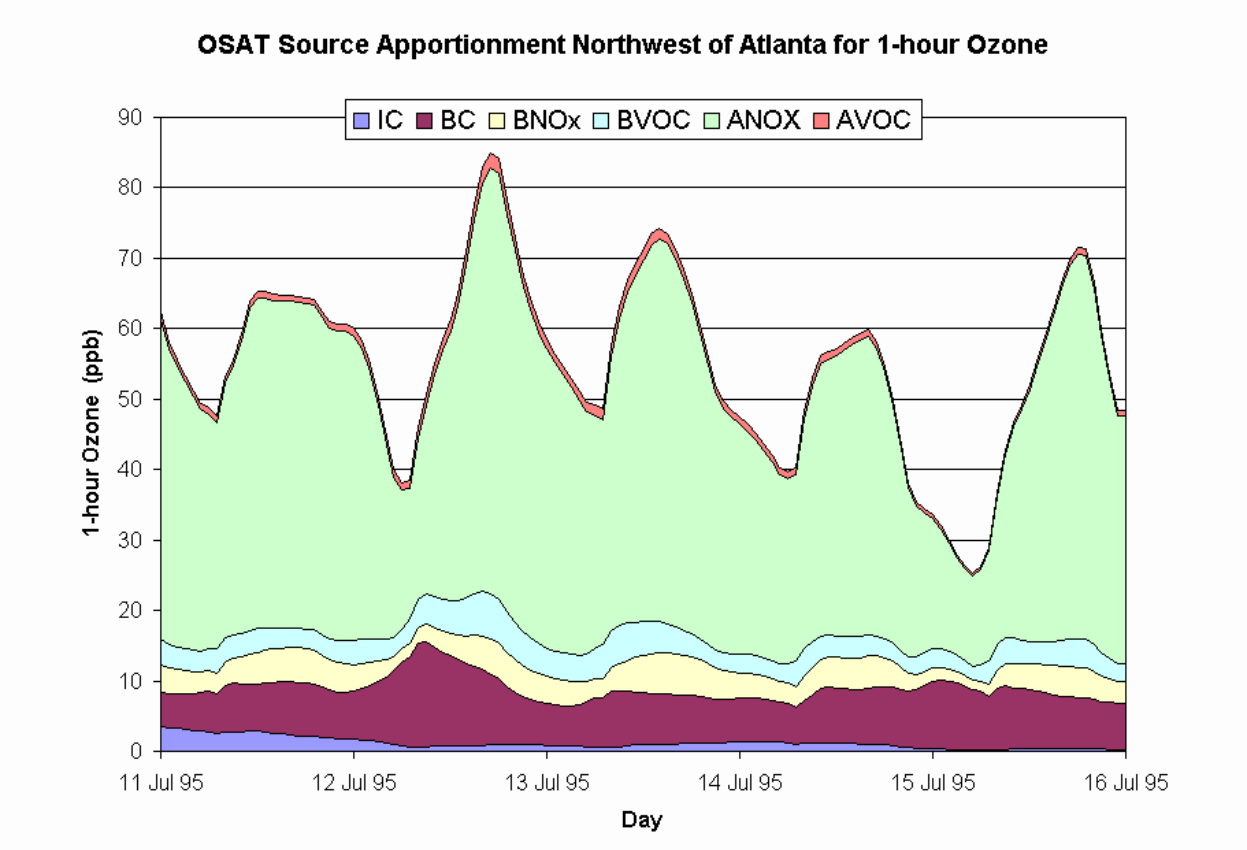

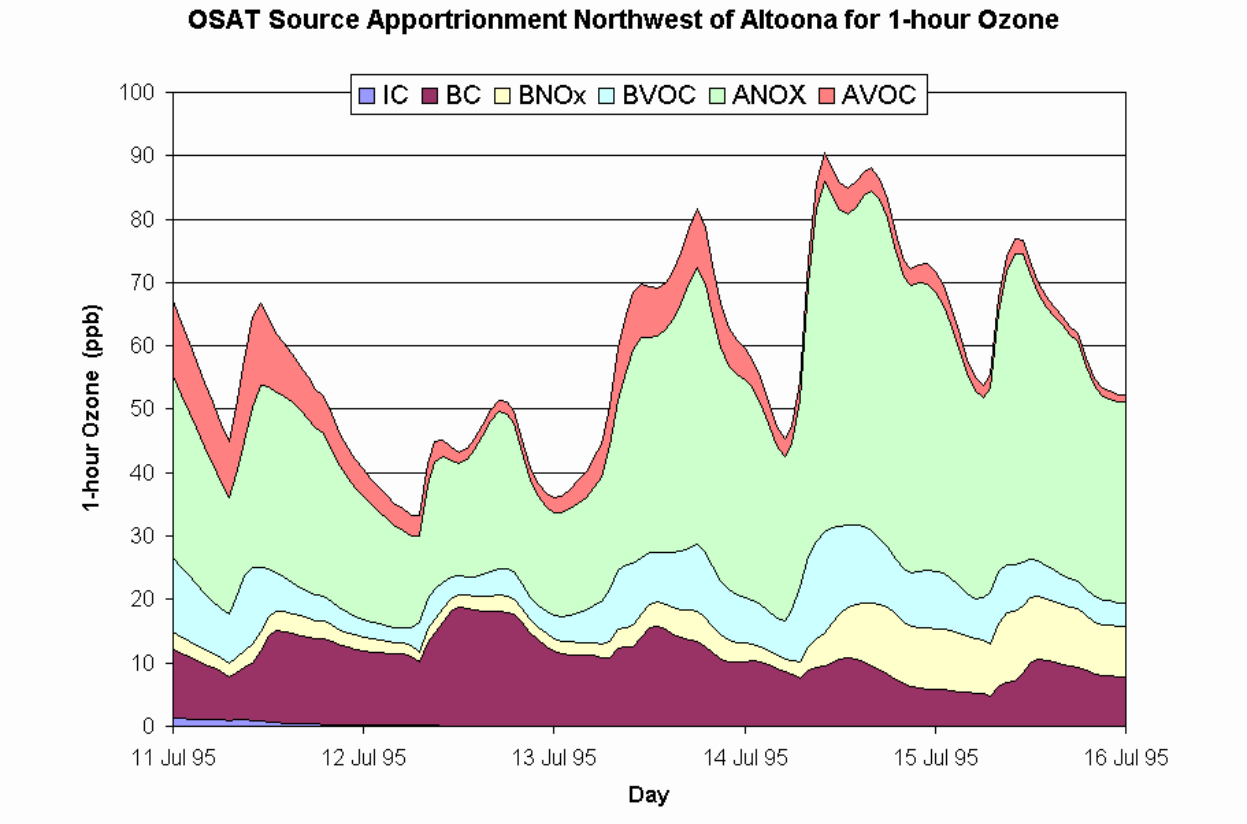

Figure 3-3 (concluded).

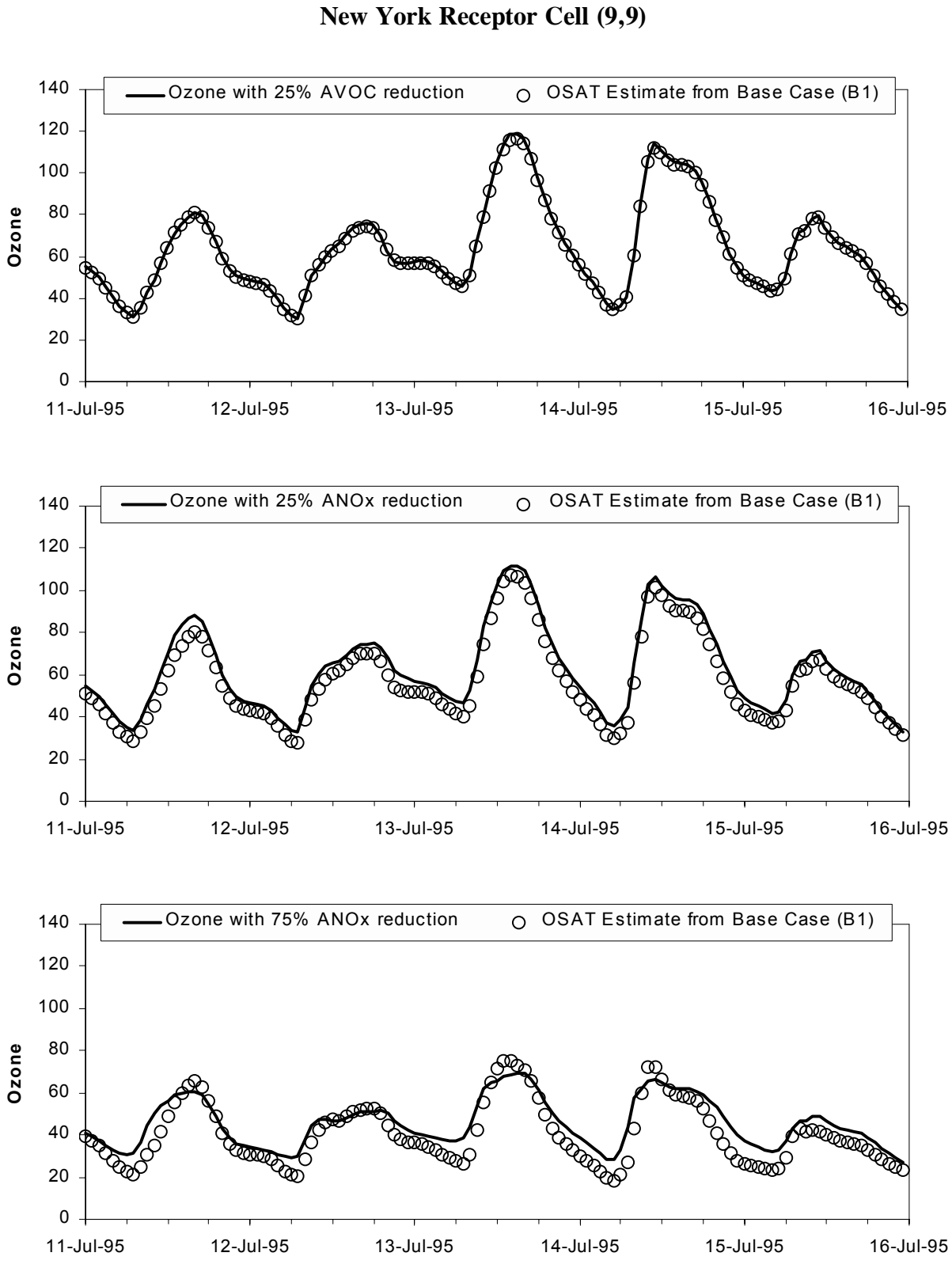

Figure 3-4. Time series of ozone for the northwest corner grid cell in each receptor area with reduced emissions (line) compared to the estimated ozone from the base case concentrations and OSAT source apportionments (circles). OSAT results from run B1.

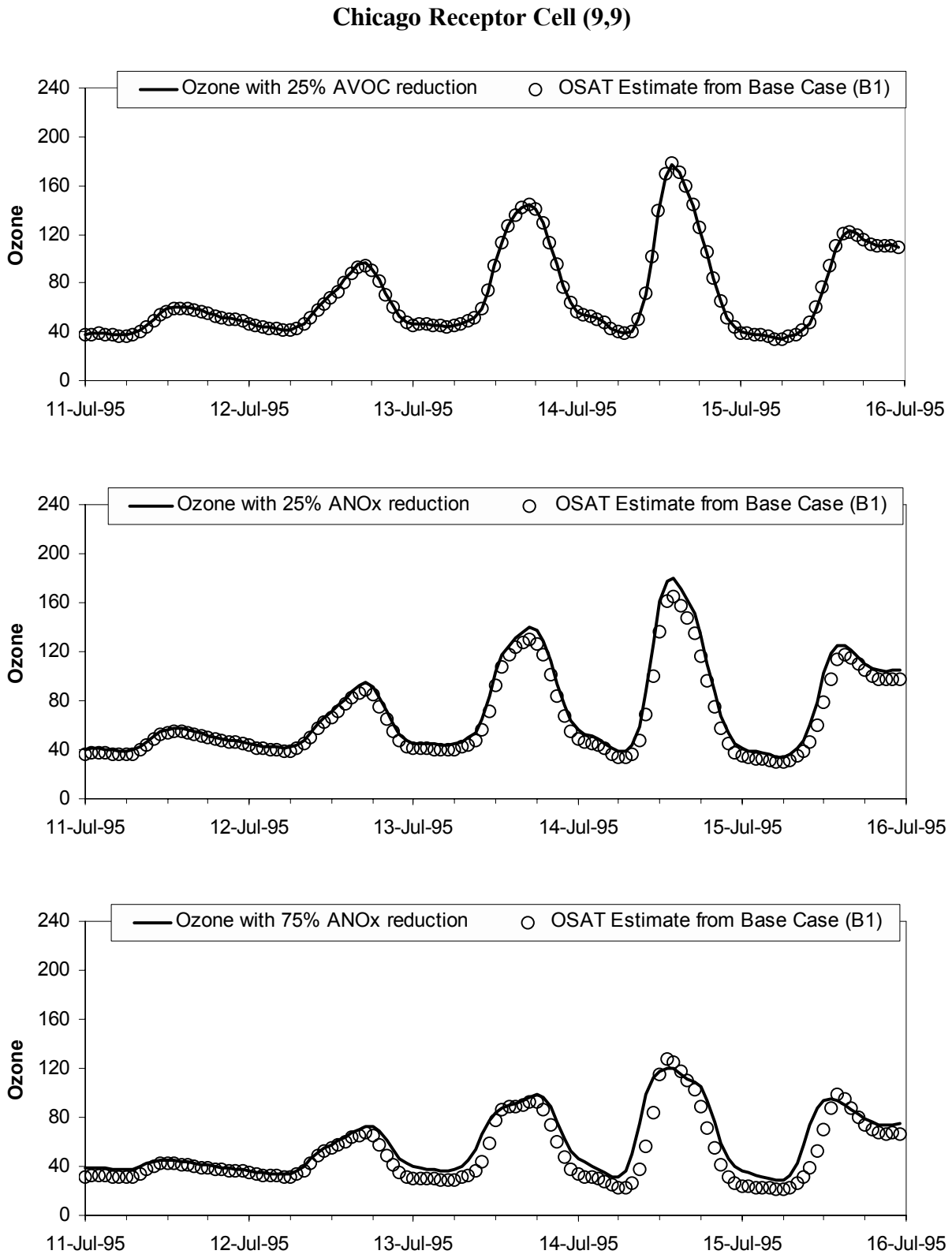

Figure 3-4 (continued).

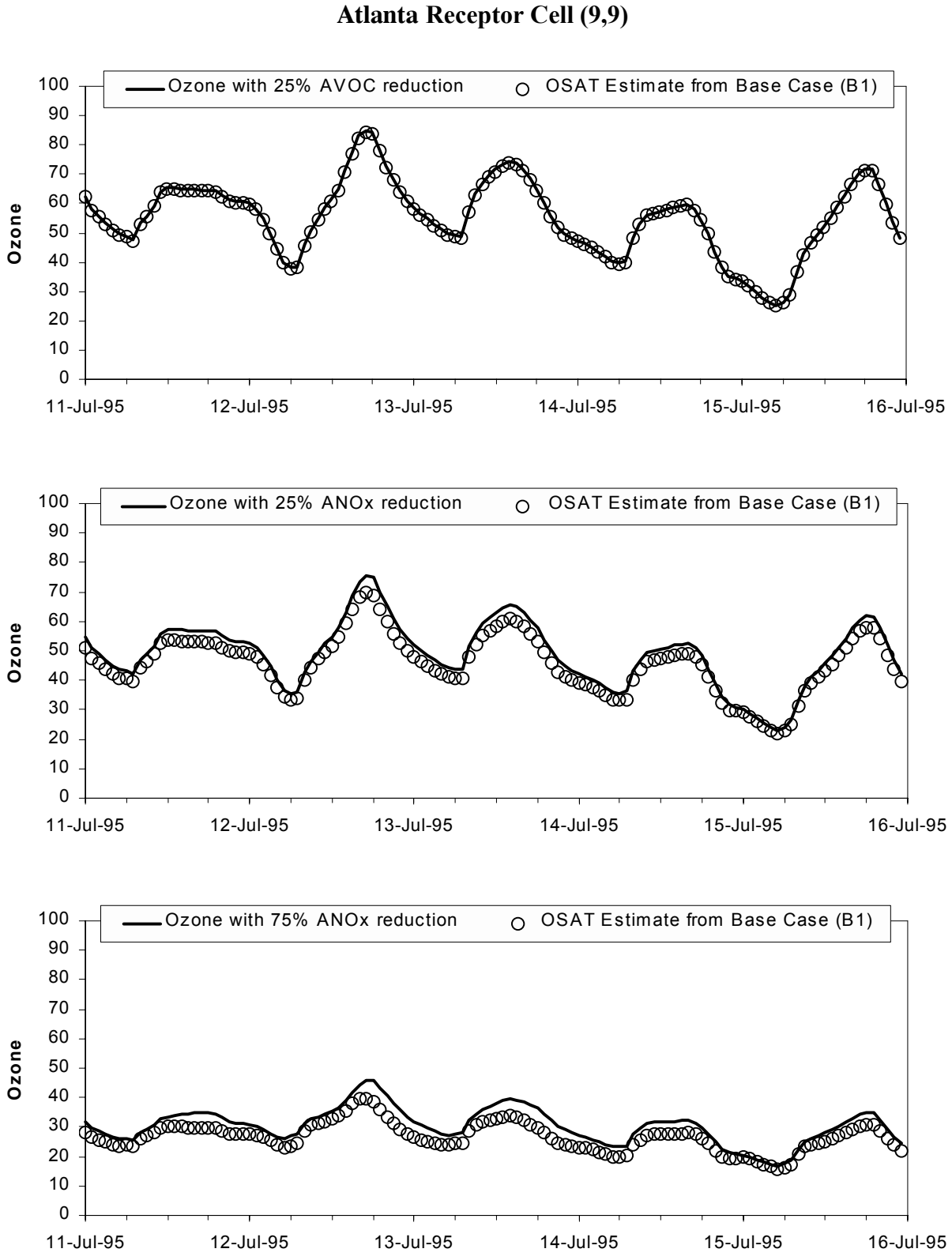

Figure 3-4 (continued).

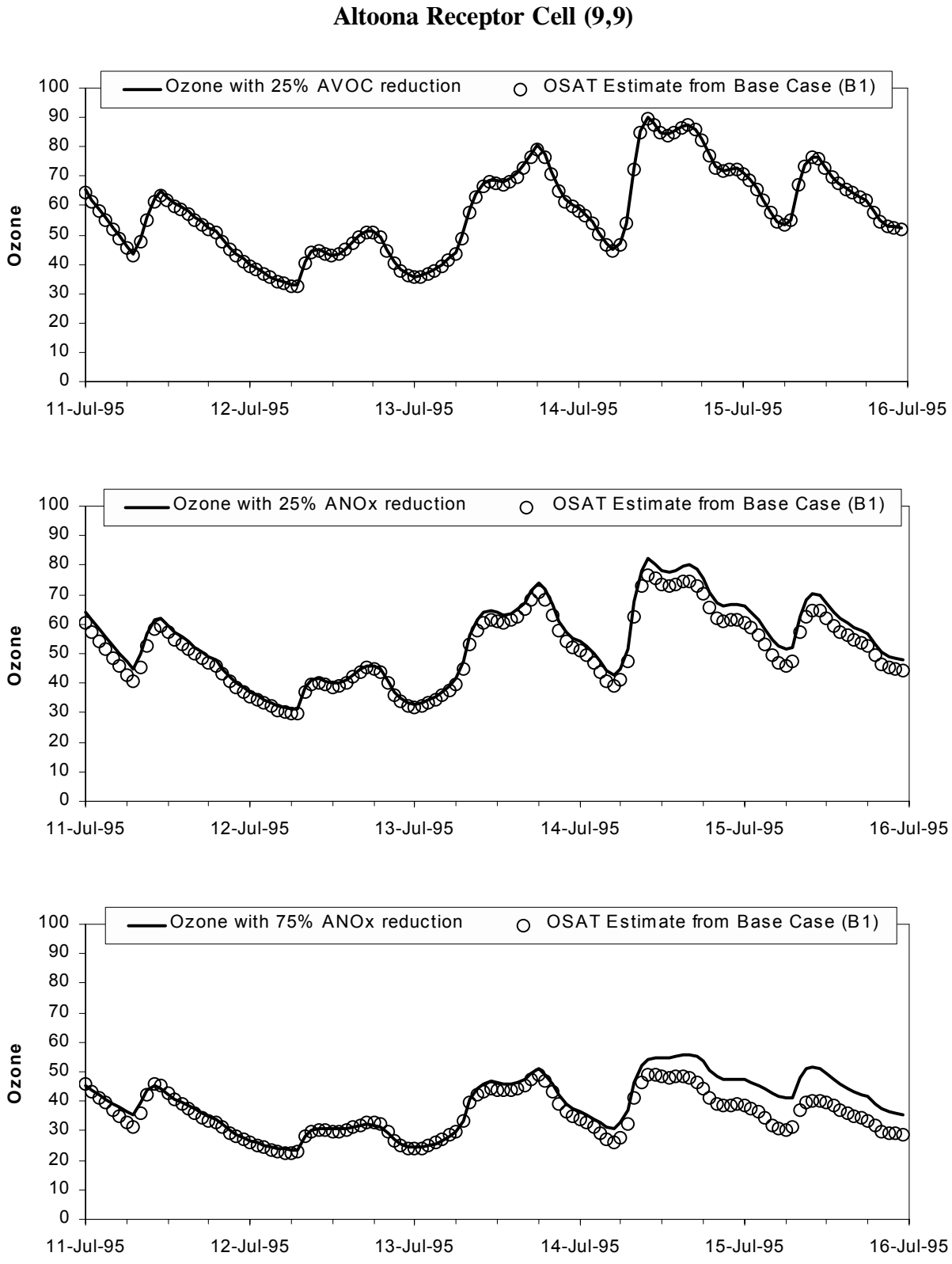

Figure 3-4 (concluded).

Table 3-3. OSAT contributions to 1-hour ozone greater than 80 ppb in the Altoona receptor area in the 2007 base case (run B1).

Ozone Contribution from NOx Emissions (ppb)

Source Area	Source Category PT	MV	OAN	BIO	Total
1	0.8	0.5	0.9	1.0	3.3
2	0.1	0.1	0.1	0.0	0.3
3	0.2	0.1	0.2	0.1	0.5
4	2.7	1.7	2.9	2.8	10.0
5	2.2	0.8	1.6	1.0	5.6
6	0.0	0.0	0.0	0.0	0.0
7	7.7	2.8	3.7	1.6	15.8
8	0.3	0.5	0.4	0.1	1.3
9	0.0	0.0	0.0	0.0	0.0
10	0.0	0.0	0.0	0.0	0.0
11	11.6	3.1	2.6	0.6	18.0
12	0.0	0.0	0.0	0.0	0.0
13	0.0	0.0	0.0	0.0	0.0
14	0.6	0.1	0.2	0.0	1.0
15	0.0	0.0	0.0	0.0	0.0
16	0.6	1.6	1.2	0.7	4.0
17	0.0	0.0	0.0	0.0	0.0
Total	26.8	11.3	13.7	7.9	59.7

Ozone Contribution from VOC Emissions (ppb)

Source Area	Source Category PT	MV	OAN	BIO	Total
1	0.0	0.1	0.4	0.6	1.1
2	0.0	0.0	0.0	0.1	0.2
3	0.0	0.0	0.2	0.2	0.5
4	0.1	0.2	0.9	0.9	2.0
5	0.1	0.1	0.6	2.0	2.8
6	0.0	0.0	0.0	0.0	0.0
7	0.1	0.4	1.6	5.5	7.6
8	0.0	0.1	0.2	1.4	1.7
9	0.0	0.0	0.0	0.0	0.0
10	0.0	0.0	0.0	0.0	0.0
11	0.2	0.3	1.0	3.7	5.0
12	0.0	0.0	0.0	0.0	0.0
13	0.0	0.0	0.0	0.0	0.0
14	0.0	0.0	0.3	0.0	0.4
15	0.0	0.0	0.0	0.0	0.0
16	0.0	0.0	0.0	0.0	0.0
17	0.0	0.0	0.1	1.3	1.4
Total	0.5	1.2	5.1	15.7	22.5

Total Ozone Contribution (ppb)

Source Area	Source Category PT	MV	OAN	BIO	BC	IC	Total
1	0.9	0.6	1.3	1.6			4.4
2	0.1	0.1	0.2	0.2			0.4
3	0.2	0.1	0.4	0.3			1.0
4	2.7	1.9	3.8	3.6			12.0
5	2.3	1.0	2.1	3.0			8.3
6	0.0	0.0	0.0	0.0			0.0
7	7.8	3.2	5.3	7.1			23.5
8	0.3	0.5	0.6	1.5			2.9
9	0.0	0.0	0.0	0.0			0.0
10	0.0	0.0	0.0	0.0			0.0
11	11.8	3.3	3.6	4.3			23.0
12	0.0	0.0	0.0	0.0			0.0
13	0.0	0.0	0.0	0.0			0.0
14	0.6	0.2	0.5	0.1			1.3
15	0.0	0.0	0.0	0.0			0.0
16	0.0	0.0	0.0	0.0			0.0
17	0.6	1.6	1.2	2.0			5.4
N/A					9.8	0.1	9.9
Total	27.3	12.5	18.9	23.6	9.8	0.1	92.2

Table 3-4. OSAT contributions to 1-hour ozone greater than 80 ppb in the Atlanta receptor area in the 2007 base case (run B1).

Ozone Contribution from NOx Emissions (ppb)

Source Area	Source Category PT	MV	OAN	BIO	Total
1	0.1	0.1	0.2	0.1	0.5
2	0.0	0.0	0.1	0.0	0.1
3	0.0	0.0	0.0	0.0	0.1
4	0.2	0.1	0.1	0.1	0.5
5	1.0	0.5	0.8	0.3	2.4
6	0.1	0.0	0.0	0.0	0.1
7	0.3	0.1	0.1	0.0	0.5
8	7.6	10.7	7.4	2.3	28.0
9	0.3	0.3	0.3	0.1	1.0
10	0.0	0.0	0.0	0.0	0.0
11	0.1	0.0	0.0	0.0	0.1
12	1.8	1.3	1.2	0.6	4.9
13	0.0	0.0	0.0	0.0	0.0
14	0.0	0.0	0.0	0.0	0.1
15	9.6	18.0	13.1	0.7	41.3
16	0.0	0.0	0.0	0.0	0.0
17	0.0	0.0	0.0	0.0	0.0
Total	21.2	31.1	23.2	4.2	79.6

Ozone Contribution from VOC Emissions (ppb)

Source Area	Source Category PT	MV	OAN	BIO	Total
1	0.0	0.0	0.1	0.1	0.2
2	0.0	0.0	0.0	0.0	0.1
3	0.0	0.0	0.0	0.0	0.0
4	0.0	0.0	0.1	0.1	0.2
5	0.0	0.0	0.1	0.4	0.6
6	0.0	0.0	0.0	0.0	0.0
7	0.0	0.0	0.1	0.1	0.1
8	0.0	0.2	0.7	7.5	8.4
9	0.0	0.0	0.1	0.2	0.3
10	0.0	0.0	0.0	0.0	0.0
11	0.0	0.0	0.0	0.0	0.0
12	0.0	0.0	0.2	0.9	1.2
13	0.0	0.0	0.0	0.0	0.0
14	0.0	0.0	0.0	0.0	0.0
15	0.0	0.6	1.9	6.1	8.6
16	0.0	0.0	0.0	0.0	0.0
17	0.0	0.0	0.0	0.0	0.0
Total	0.1	0.9	3.4	15.4	19.7

Total Ozone Contribution (ppb)

Source Area	Source Category PT	MV	OAN	BIO	BC	IC	Total
1	0.2	0.1	0.2	0.2			0.7
2	0.0	0.0	0.1	0.1			0.2
3	0.0	0.0	0.0	0.0			0.1
4	0.2	0.1	0.2	0.2			0.7
5	1.0	0.5	0.9	0.7			3.1
6	0.1	0.0	0.0	0.0			0.1
7	0.3	0.1	0.2	0.1			0.6
8	7.7	10.8	8.1	9.8			36.4
9	0.3	0.3	0.4	0.3			1.3
10	0.0	0.0	0.0	0.0			0.0
11	0.1	0.0	0.0	0.0			0.1
12	1.9	1.4	1.4	1.5			6.1
13	0.0	0.0	0.0	0.0			0.0
14	0.0	0.0	0.1	0.0			0.1
15	9.7	18.5	15.0	6.7			49.9
16	0.0	0.0	0.0	0.0			0.0
17	0.0	0.0	0.0	0.0			0.0
N/A					6.0	1.4	7.5
Total	21.3	32.0	26.5	19.6	6.0	1.4	106.9

Table 3-5. OSAT contributions to 1-hour ozone greater than 80 ppb in the Chicago receptor area in the 2007 base case (run B1).

Ozone Contribution from NOx Emissions (ppb)					
	Source Category				
Source Area	PT	MV	OAN	BIO	Total
1	3.1	2.3	3.4	2.8	11.6
2	0.3	0.3	0.5	0.2	1.4
3	0.0	0.0	0.0	0.0	0.0
4	8.3	3.2	6.7	9.7	27.9
5	2.4	1.4	1.7	1.3	6.7
6	0.0	0.0	0.0	0.0	0.1
7	0.0	0.0	0.0	0.0	0.0
8	0.1	0.1	0.0	0.0	0.2
9	0.0	0.0	0.0	0.0	0.0
10	0.0	0.0	0.0	0.0	0.0
11	0.0	0.0	0.0	0.0	0.0
12	0.0	0.0	0.0	0.0	0.0
13	0.0	0.0	0.0	0.0	0.0
14	5.6	2.7	4.5	0.8	13.6
15	0.0	0.0	0.0	0.0	0.0
16	0.0	0.0	0.0	0.0	0.0
17	0.0	0.0	0.0	0.0	0.0
Total	19.8	10.0	16.8	14.8	61.4

Ozone Contribution from VOC Emissions (ppb)					
	Source Category				
Source Area	PT	MV	OAN	BIO	Total
1	0.0	0.2	0.7	4.7	5.6
2	0.0	0.0	0.2	0.9	1.2
3	0.0	0.0	0.0	0.0	0.0
4	0.1	0.2	1.3	4.9	6.6
5	0.2	0.1	0.6	5.8	6.6
6	0.0	0.0	0.0	0.0	0.0
7	0.0	0.0	0.0	0.0	0.0
8	0.0	0.0	0.0	0.0	0.1
9	0.0	0.0	0.0	0.0	0.0
10	0.0	0.0	0.0	0.0	0.0
11	0.0	0.0	0.0	0.0	0.0
12	0.0	0.0	0.0	0.0	0.0
13	0.0	0.0	0.0	0.0	0.0
14	0.4	0.8	6.5	3.4	11.0
15	0.0	0.0	0.0	0.0	0.0
16	0.0	0.0	0.0	0.0	0.0
17	0.0	0.0	0.0	0.0	0.0
Total	0.7	1.4	9.3	19.8	31.1

Total Ozone Contribution (ppb)							
	Source Category						
Source Area	PT	MV	OAN	BIO	BC	IC	Total
1	3.2	2.5	4.1	7.5			17.2
2	0.3	0.4	0.7	1.1			2.5
3	0.0	0.0	0.0	0.0			0.1
4	8.4	3.4	8.0	14.7			34.4
5	2.6	1.5	2.3	7.1			13.4
6	0.0	0.0	0.0	0.0			0.1
7	0.0	0.0	0.0	0.0			0.0
8	0.1	0.1	0.1	0.1			0.2
9	0.0	0.0	0.0	0.0			0.0
10	0.0	0.0	0.0	0.0			0.0
11	0.0	0.0	0.0	0.0			0.0
12	0.0	0.0	0.0	0.0			0.0
13	0.0	0.0	0.0	0.0			0.0
14	5.9	3.5	11.0	4.2			24.6
15	0.0	0.0	0.0	0.0			0.0
16	0.0	0.0	0.0	0.0			0.0
17	0.0	0.0	0.0	0.0			0.0
N/A					8.8	0.1	8.9
Total	20.5	11.4	26.2	34.6	8.8	0.1	101.6

Table 3-6. OSAT contributions to 1-hour ozone greater than 80 ppb in the New York receptor area in the 2007 base case (run B1).

Ozone Contribution from NOx Emissions (ppb)					
	Source Category				
Source Area	PT	MV	OAN	BIO	Total
1	0.4	0.3	0.5	0.6	1.7
2	0.0	0.0	0.0	0.0	0.1
3	0.5	0.2	0.5	0.3	1.5
4	1.0	0.5	0.9	0.9	3.3
5	0.4	0.1	0.3	0.2	0.9
6	0.0	0.0	0.0	0.0	0.0
7	3.9	1.5	2.1	0.7	8.2
8	0.2	0.2	0.2	0.1	0.6
9	0.0	0.0	0.0	0.0	0.0
10	0.0	0.0	0.1	0.0	0.1
11	7.4	4.7	5.1	1.5	18.7
12	1.4	1.1	1.3	0.4	4.1
13	3.6	4.8	5.0	0.5	13.9
14	0.2	0.1	0.1	0.0	0.4
15	0.0	0.0	0.0	0.0	0.0
16	1.3	2.9	4.3	0.1	8.5
17	0.1	0.2	0.1	0.1	0.5
Total	20.4	16.6	20.4	5.2	62.6

Ozone Contribution from VOC Emissions (ppb)					
	Source Category				
Source Area	PT	MV	OAN	BIO	Total
1	0.0	0.1	0.3	0.3	0.7
2	0.0	0.0	0.0	0.1	0.1
3	0.0	0.0	0.3	0.4	0.7
4	0.1	0.1	0.8	0.4	1.3
5	0.0	0.0	0.2	0.4	0.6
6	0.0	0.0	0.0	0.0	0.0
7	0.1	0.3	1.5	1.8	3.7
8	0.0	0.0	0.1	0.4	0.5
9	0.0	0.0	0.0	0.0	0.0
10	0.0	0.0	0.0	0.0	0.1
11	0.1	0.3	1.5	6.2	8.1
12	0.0	0.1	0.5	1.9	2.5
13	0.1	0.2	1.4	3.0	4.8
14	0.0	0.0	0.3	0.0	0.4
15	0.0	0.0	0.0	0.0	0.0
16	0.1	0.4	3.6	2.3	6.3
17	0.0	0.0	0.0	0.6	0.6
Total	0.5	1.6	10.4	17.7	30.3

Total Ozone Contribution (ppb)							
	Source Category						
Source Area	PT	MV	OAN	BIO	BC	IC	Total
1	0.4	0.3	0.8	0.9			2.4
2	0.0	0.0	0.1	0.1			0.2
3	0.5	0.3	0.8	0.6			2.2
4	1.0	0.6	1.6	1.3			4.6
5	0.4	0.2	0.4	0.6			1.5
6	0.0	0.0	0.0	0.0			0.0
7	4.0	1.9	3.6	2.5			11.9
8	0.2	0.3	0.3	0.4			1.1
9	0.0	0.0	0.0	0.0			0.1
10	0.0	0.0	0.1	0.0			0.2
11	7.5	5.0	6.5	7.7			26.8
12	1.4	1.2	1.8	2.3			6.6
13	3.7	5.0	6.5	3.6			18.7
14	0.3	0.1	0.4	0.0			0.8
15	0.0	0.0	0.0	0.0			0.0
16	1.4	3.3	7.8	2.3			14.8
17	0.1	0.2	0.1	0.7			1.1
N/A					9.1	0.3	9.4
Total	20.9	18.2	30.8	23.0	9.1	0.3	102.4

(b) High 1-hour Ozone

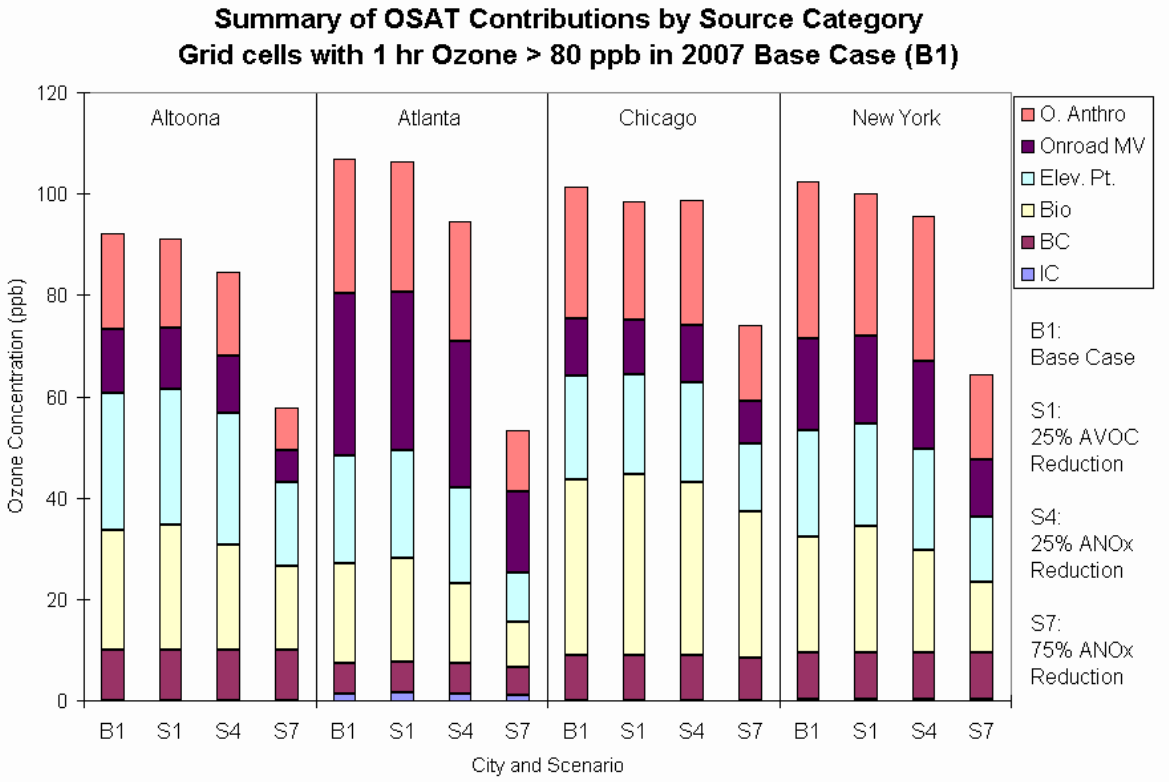

(a) High 8-hour Ozone

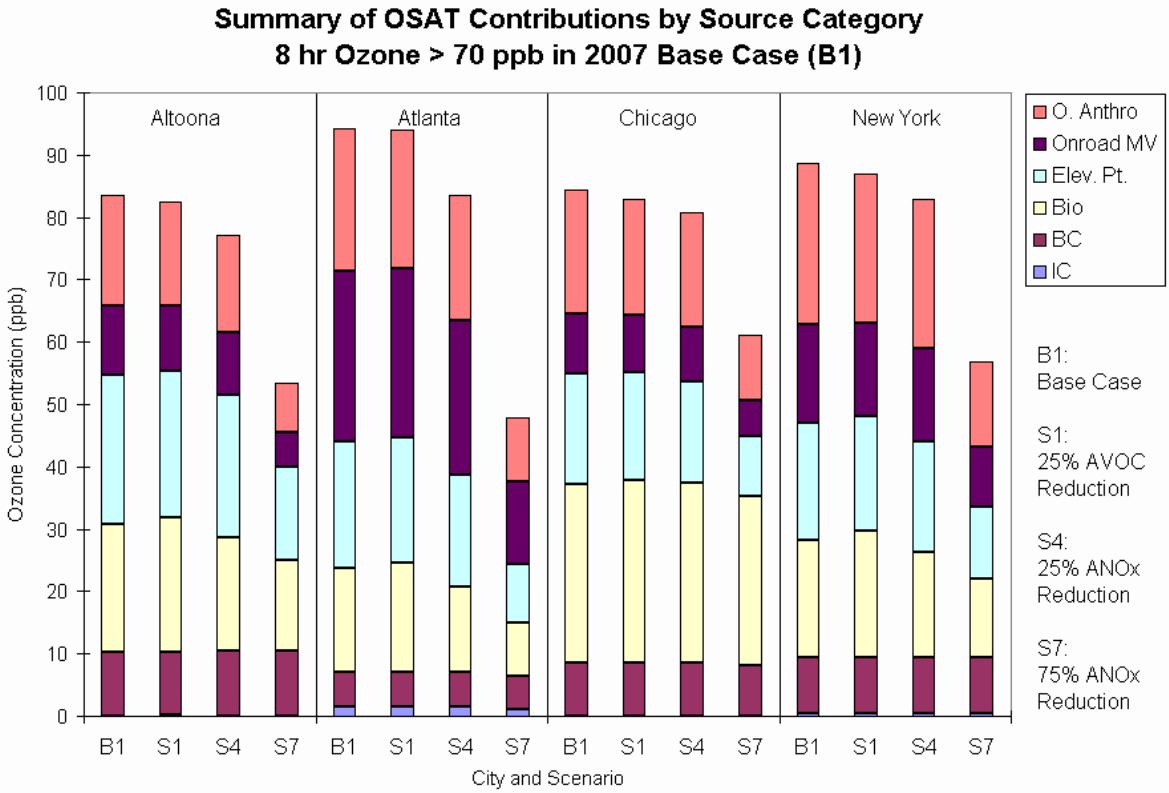

Figure 3-5. Comparison of OSAT contributions by VOC and NOx for high 1-hour and 8-hour ozone levels in each receptor area for the 2007 base case (runs B1, S1, S4 and S7).

(b) High 1-hour Ozone

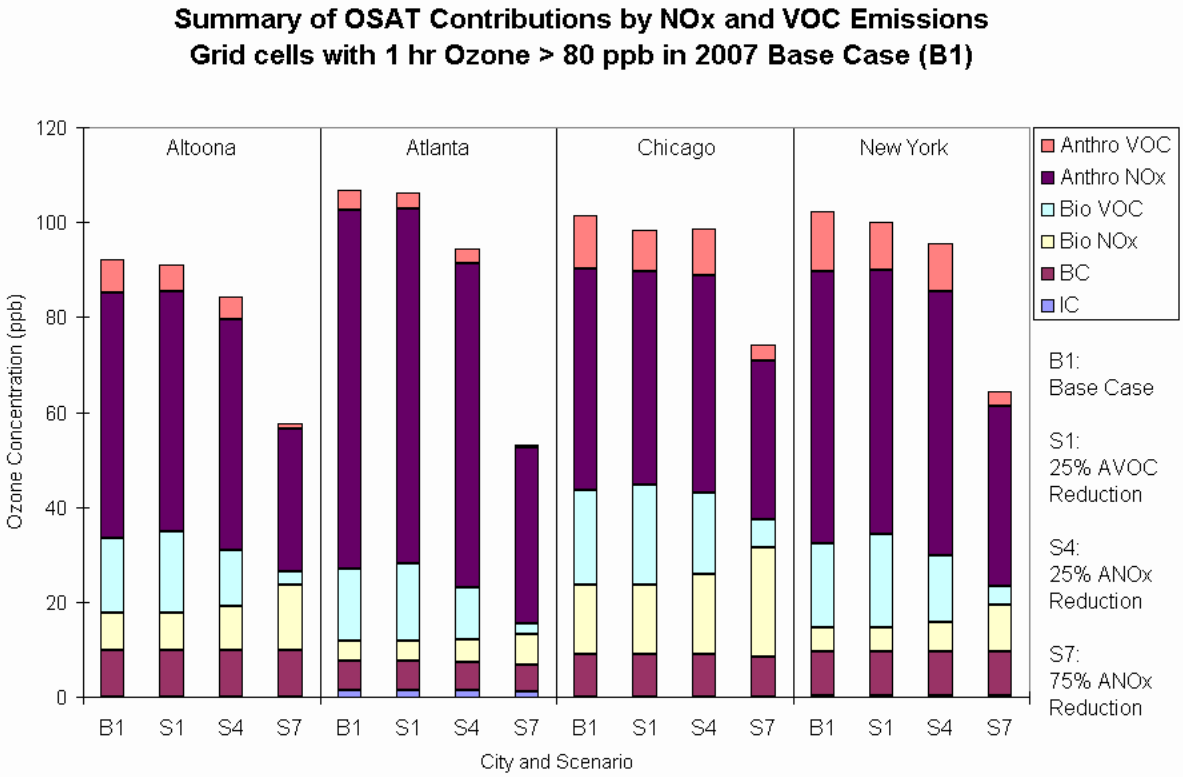

(a) High 8-hour Ozone

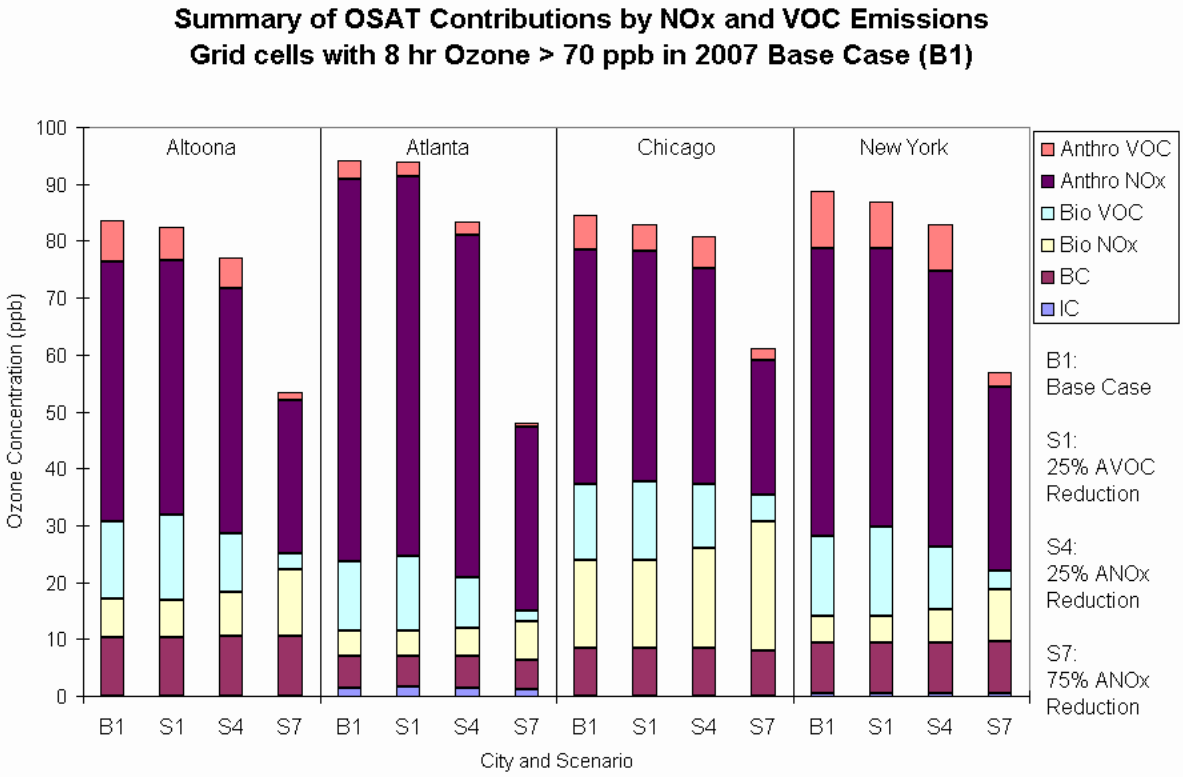

Figure 3-6. Comparison of OSAT contributions by source category for high 1-hour and 8-hour ozone levels in each receptor area for the 2007 base case (runs B1, S1, S4 and S7).

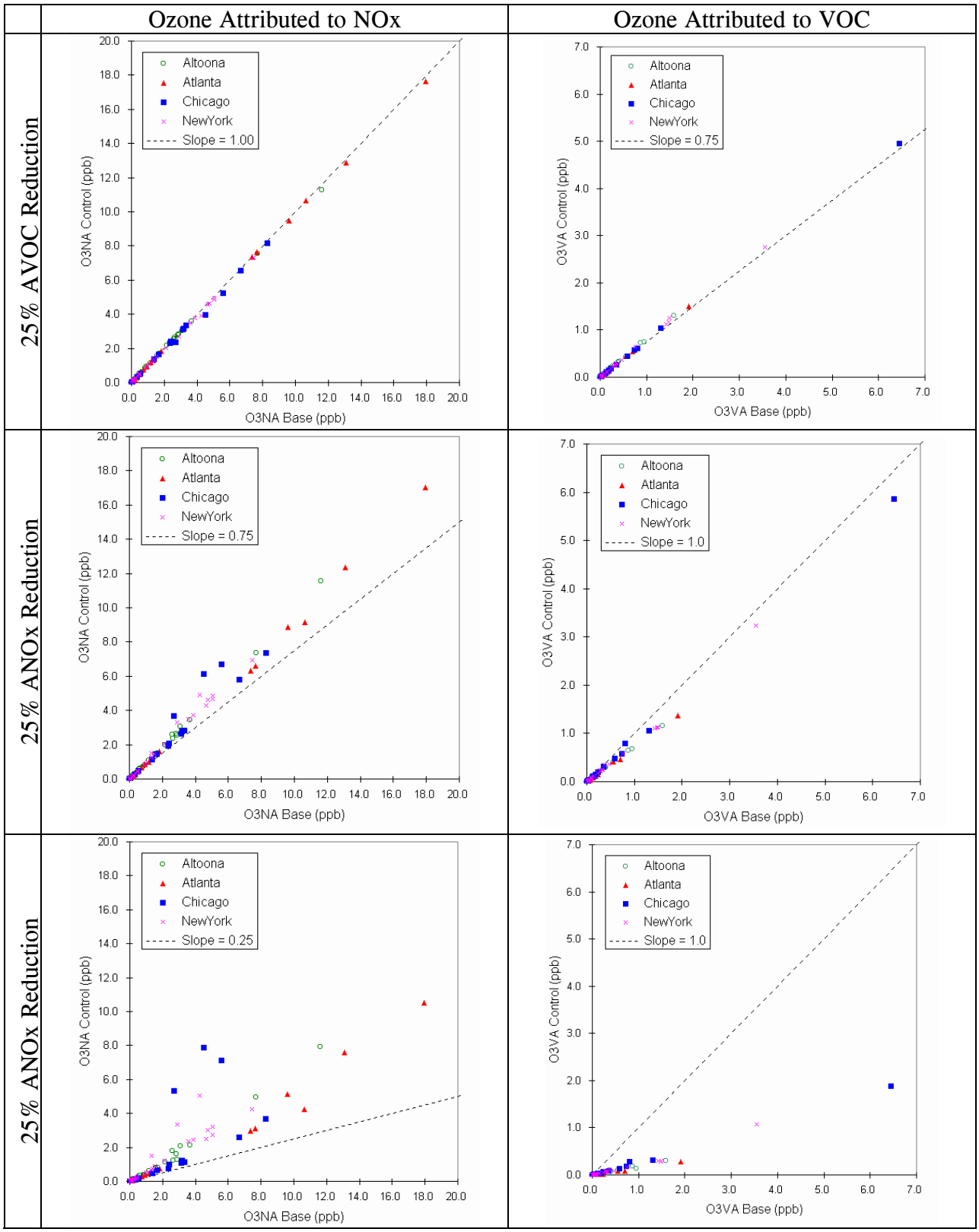

Figure 3-7. Change in OSAT O3N and O3V contributions with emission reductions. Points will fall on the dashed line if contributions scale linearly with emission changes.

4. ANALYSIS OF DDM RESULTS

This section presents several example analyses of CAMx DDM results to show what the DDM sensitivities look like and illustrate how they can be summarized and analyzed. We do not interpret the implications of the results for air quality planning because the OTAG modeling scenarios are dated and because the results are open to interpretation. In our experience, different importance can be attached to the relative magnitudes of the source sensitivities shown in the example analyses based on perceptions of what is important or significant.

OUTPUT FILES

The CAMx output files that are specific to DDM are listed in Table 4-1. The file formats are described in the CAMx User's Guide (ENVIRON, 2002a) with the exception of the receptor file, which is new and was added for this project. The receptor file is in a self-describing ASCII format that includes the date/time, list of sensitivities, list of receptors and sensitivity data (by time and receptor).

Table 4-1. DDM output file suffix names.

File Suffix	DDM file type
.sa.inst.1	Coarse grid binary instantaneous sensitivity file for last odd simulation hour (used for restart), 3-D, all sensitivities
.sa.inst.2	Coarse grid binary instantaneous sensitivity file for last even simulation hour (used for restart), 3-D, all sensitivities
.sa.finst.1	Fine grid binary instantaneous sensitivity file for last odd simulation hour (used for restart), 3-D, all sensitivities
.sa.finst.2	Fine grid binary instantaneous sensitivity file for last even simulation hour (used for restart), 3-D, all sensitivities
.sa.surf	Coarse grid binary average sensitivity file, 2-D, surface layer sensitivities only for affected species requested in the CAMx average file
.sa.fsurf	Fine grid binary average sensitivity file, 2-D surface layer sensitivities only for affected species requested in the CAMx average file
.sa.receptor	Receptor file in ASCII format with average sensitivities at selected receptor locations

The CAMx diagnostic output file (*.diag) also includes important DDM information that is needed for quality assurance (QA). The diagnostic output file lists the definitions of all of the sensitivities being calculated and their names. Sensitivity naming conventions are discussed in the CAMx User's Guide.

QUALITY ASSURANCE

DDM configuration errors that might go undetected because they do not cause a CAMx error were discussed under "DDM pitfalls" in Section 6. Important quality assurance checks for DDM calculations are:

- Checking the source area map and fine grid source area map(s), if used.
- Checking point source overrides, if used.
- Checking that the correct emissions files are provided for each source category.
- Checking the list of sensitivity names in the diagnostic output file to ensure that correct sensitivities are being calculated and that you correctly interpret the sensitivity names.
- Checking receptor definitions, if used.

Analysis of the DDM results is an important part of the QA process. Sensitivities that are unexpected may point to errors in setting up the analysis. The CAMx implementation of DDM has been shown to provide highly accurate first-order sensitivity coefficients (Dunker at al., 2002a).

POST-PROCESSING TOOLS

PAVE

The gridded DDM sensitivity output files are in same format as the CAMx average concentration files and are directly compatible with post-processing software such as PAVE[1]. Recent distributions of PAVE have been able to handle the large number of species present in DDM output files. The formula capabilities built into PAVE allow sensitivities to be combined, but there is a limit on the number of species that can be combined in a formula (about 30). Large numbers of sensitivities can be combined using the CAMxtrct and RANKDDM tools, below. PAVE has no problem displaying negative sensitivities.

CAMxtrct

CAMxtrct (CAM-extract) is a post-processing program available from the CAMx ftp site[2]. CAMxtrct extracts concentrations for single species or combinations of species from CAMx coarse and/or fine grid files in average file format. It writes out either a binary file in coarse grid average file format or in an ASCII file in a format similar to Golden Software Surfer GRD format. The specific capabilities of CAMxtrct are:

- Extract a species for a specific grid and layer.
- Select a specific species or combine several species that match a keyword.
- Combine coarse and fine grids to a coarse grid format file at the resolution of the finest grid.

[1] PAVE is available from http://www.emc.mcnc.org/EDSS/pave_doc/Pave.html
[2] The CAMx ftp site is ftp://ftp.environ.org, username=camxuser, password=pass4camx

- Extracting specific time intervals or finding daily maximum values.
- Take ratios of two species. Keyword species combinations are allowed in the numerator and/or denominator.

There are three keywords for combining DDM sensitivities:

DDMiiIALL – sum of all initial conditions sensitivities for affected species ii
DDMiiBALL – sum of all initial conditions sensitivities for affected species ii
DDMiiRmmmEnnnSjjj – sum of selected emissions sensitivities

Where:

DDM indicates that this is a DDM keyword.
ii is the affected species number.
R precedes the influencing region number mmm (mmm can be ALL, in which case any region matches).
E precedes the influencing emissions group number nnn (nnn can be ALL, in which case any emissions group matches).
S precedes the influencing species number jjj (jjj can be ALL, in which case any species matches).

CAMxtrct is useful for the following purposes:

- Combining information from coarse and fine grids.
- Combining sensitivities over geographic areas and/or source categories.
- Preprocessing information for PAVE to overcome limitations in PAVE formulas.

RankDDM

RankDDM is a post-processing program distributed via the CAMx ftp site. RankDDM extracts sensitivities for selected grid cells (receptors) from the DDM surface output files. A concentration threshold can be applied so that sensitivities are only extracted for receptor grid cell/hours when ozone exceeds the threshold amount. The output file is in a flat ASCII format that is easy to interpret and analyze. RankDDM is not restricted to ozone sensitivities.

```
#!/bin/csh
#
/models/camx/postproc/rankddm/src/rankddm.pgf77.linux << ieof
Average file type  : FINE
Threshold          : 0.0
Extract Region     :14
Raw ASCII output   :./outputs/ascii/Chicago.box.1hr.0ppb.DDM.B3.asc
Extract Region     :15
Raw ASCII output   :./outputs/ascii/Atlanta.box.1hr.0ppb.DDM.B3.asc
Extract Region     :16
Raw ASCII output   :./outputs/ascii/NewYork.box.1hr.0ppb.DDM.B3.asc
Extract Region     :17
Raw ASCII output   :./outputs/ascii/Altoona.box.1hr.0ppb.DDM.B3.asc
                    /END/
Source area map    :../../ddm.inputs/source_map/fine.source_map.crc.17area.osat
Source map type    :FINE
```

Figure 4-1. Example RankDDM application to analyze sensitivities from DDM run B3.

```
Coarse grid surface:../../outputs/CAMx3.950711.07base.DDM.B3.sa.surf
Coarse grid surface:../../outputs/CAMx3.950712.07base.DDM.B3.sa.surf
Coarse grid surface:../../outputs/CAMx3.950713.07base.DDM.B3.sa.surf
Coarse grid surface:../../outputs/CAMx3.950714.07base.DDM.B3.sa.surf
Coarse grid surface:../../outputs/CAMx3.950715.07base.DDM.B3.sa.surf
                    /END/
Fine grid surface  :../../outputs/CAMx3.950711.07base.DDM.B3.sa.fsurf
Fine grid surface  :../../outputs/CAMx3.950712.07base.DDM.B3.sa.fsurf
Fine grid surface  :../../outputs/CAMx3.950713.07base.DDM.B3.sa.fsurf
Fine grid surface  :../../outputs/CAMx3.950714.07base.DDM.B3.sa.fsurf
Fine grid surface  :../../outputs/CAMx3.950715.07base.DDM.B3.sa.fsurf
                    /END/
Coarse grid average:../../outputs/CAMx3.950711.07base.DDM.B3.avrg
Coarse grid average:../../outputs/CAMx3.950712.07base.DDM.B3.avrg
Coarse grid average:../../outputs/CAMx3.950713.07base.DDM.B3.avrg
Coarse grid average:../../outputs/CAMx3.950714.07base.DDM.B3.avrg
Coarse grid average:../../outputs/CAMx3.950715.07base.DDM.B3.avrg
                    /END/
Fine grid average  :../../outputs/CAMx3.950711.07base.DDM.B3.favrg
Fine grid average  :../../outputs/CAMx3.950712.07base.DDM.B3.favrg
Fine grid average  :../../outputs/CAMx3.950713.07base.DDM.B3.favrg
Fine grid average  :../../outputs/CAMx3.950714.07base.DDM.B3.favrg
Fine grid average  :../../outputs/CAMx3.950715.07base.DDM.B3.favrg
                    /END/
Boundary filename  :
Ozone species num  :03
Group Definitions  :01    01  ALL  BIO_reg1
region, emis grp   :02    01  ALL  BIO_reg2
infl spc, decript  :03    01  ALL  BIO_reg3
(A5,A5,A5,A10)     :04    01  ALL  BIO_reg6
                   :05    01  ALL  BIO_reg9
                   :06    01  ALL  BIO_reg10
                   :01    02  ALL  OAN_reg1
                   :02    02  ALL  OAN_reg2
                   :03    02  ALL  OAN_reg3
                   :04    02  ALL  OAN_reg6
                   :05    02  ALL  OAN_reg9
                   :06    02  ALL  OAN_reg10
                   :01    03  ALL  EPT_reg1
                   :02    03  ALL  EPT_reg2
                   :03    03  ALL  EPT_reg3
                   :04    03  ALL  EPT_reg6
                   :05    03  ALL  EPT_reg9
                   :06    03  ALL  EPT_reg10
                   :IC   ALL  ALL  IC
                   :BC   ALL  ALL  BC
                    /END/
ieof
```

Figure 4-1 (concluded).

An example RankDDM application to analyze sensitivities calculated in DDM run B3 is shown in Figure 4-1. The input information required by RankDDM is:

1. Whether the analysis is for coarse or coarse/fine grid files.
2. The value for the concentration threshold (ppb).
3. The numbers of the receptor areas to extract, followed by the output filename for each receptor.
4. The name of the receptor map file that defines the receptors. In this case, the receptor map is the same as the source area map (Figure 1-1) so that the receptors are areas 14 through 17. The receptor map must be at the finest grid resolution and cover the area of the coarse grid. The end of this data block is shown by the /END/ keyword.
5. The names of the coarse and fine sensitivity and concentration files. Concentrations are needed to apply the threshold.

6. The boundary filename if the coarse grid has special (irregular) boundaries. If the coarse grid boundaries are the edges of the coarse grid this line can be left blank.
7. The number of the affected species, in this case 3 for ozone. The number of the affected species can be determined from the list of sensitivity names written by CAMx to the *.diag file for each DDM run.
8. A list of definitions for the groups of sensitivities to be extracted. The group definitions have the following structure:
    a. The region number, or ALL for all regions, or IC or BC.
    b. The emissions group number, or ALL for all groups or all IC/BCs.
    c. The influencing species number, or ALL for all species, or NOx or VOC.
    d. A name to describe the group in the RankDDM output file.

EXAMPLE ANALYSES

A series of analyses are presented to illustrate how DDM sensitivity information can be presented for interpretation. The tables and figures are shown in order at the end of the section. Many of the analyses correspond to analyses of OSAT data shown in Section 3.

Figure 4-2 shows plots of ozone sensitivities to NOx and VOC emissions from biogenic, onroad mobile, elevated point and other anthropogenic emissions at 14:00 EST on July 14, 1999 for the 2007 base emissions scenario. These are displays of DDM results from run B7. The plots were prepared using PAVE. The ozone sensitivities to NOx are the sum of the sensitivities to NO and NO2 calculated using a simple formula in PAVE. The ozone sensitivities to VOC are the sum of the ozone sensitivities to the emitted VOC species (PAR, FORM, MEOH, ETH, OLE, ALD2, ETOH, ISOP, TOL, XYL) calculated with a PAVE formula. The plots in Figure 4-2 show the coarse grid extent at fine grid resolution, which was achieved by using CAMxtrct to combine coarse and fine grid information. The western edge of the fine grid is apparent in some of the spatial plots. This is a consequence of the vertical nesting used in the OTAG, which means that coarse grid area represents the first 100 m whereas the fine grid represents the first 50 m.

Figure 4-3 shows time series of DDM sensitivities for single grid cells in each receptor area. The northwest corner grid cell of each receptor (9,9) was chosen because it is likely to be consistently downwind in all areas with the exception of Atlanta. Sensitivities with negative values are shown against the right axis. Other is the sum of all higher order sensitivities, as discussed in Section 6. The A and B prefixes before NOx and VOC stand for anthropogenic and biogenic. These figures are displays of results from DDM runs B7 (emissions sensitivities) and B3 (IC/BC sensitivities). The data for each chart were extracted from the surface output files using RankDDM. A source area map was created to identify the northwest corner grid cells as receptor areas for Rank DDM. The ASCII output files from RankDDM for B7 and B3 were combined and plotted in a spreadsheet to produce the charts.

Figure 4-4 illustrates the use of base case sensitivities to predict ozone levels with reduced emissions, as discussed in Section 6 (see equation 6-8). The figures show time series of ozone for the northwest corner grid cells in each receptor area with reduced emissions. These are the same grid cells that are shown in Figure 4-3. The emission reduction levels are 25% anthropogenic NOx and VOC and 75% anthropogenic NOx. The DDM estimated ozone

levels with reduced emissions were calculated from the base case (run B7) sensitivities to anthropogenic NOx and VOC (shown in Figure 4-3) and the base case ozone level. The base case sensitivities accurately predict the ozone levels for moderate emissions reductions (25% ANOx and 25% AVOC) but tend to underestimate the effect of a large NOx reduction (75% ANOx). This is the expected result, as discussed in Section 6 and Dunker et al. (2002a).

Zhang and co-workers (2002) performed a similar analysis only for all 81 grid cells in the receptor area and found that DDM could accurately project ozone effects due to small (25%) VOC or NOx emission reductions, but produced larger differences in projected ozone concentrations for a 75% reduction in anthropogenic NOx emissions.

Tables 4-2 to 4-5 summarize all of the sensitivities calculated for each receptor averaged over all grid cells and hours when total ozone exceeded 80 ppb. Averaging sensitivity information over all high ozone conditions in a receptor area provides a more representative picture of the sensitivity characteristics than a single grid cell and hour. Tables like this can be prepared using RankDDM with an ozone threshold (80 ppb, in this case) and summarizing the results using a spreadsheet. Table 4-2 combines results from DDM runs B2N, B2V, B3 and B7. Some sensitivities were not calculated in these runs as shown by N/C in the tables. Other is the sum of all higher order sensitivities, as discussed in Section 6. The sum of the sensitivities is the same as the total ozone in the receptor area averaged over the grid cells and hours when total ozone exceeded 80 ppb. The other sensitivity shown in the table was calculated from the difference between the total ozone and the sum of the first order sensitivities to emissions, BCs and ICs.

The information shown in Tables 4-2 to 4-5 is condensed in bar charts and compared across receptor areas in Figures 4-5 and 4-6. Figure 4-5 compares emissions sensitivities to VOC and NOx whereas Figure 4-6 compares emissions sensitivities by source category (with NOx and VOC combined). Figure 4-5 also compares sensitivities for high 1-hour and 8-hour ozone conditions. The summaries for high 8-hour ozone condition were prepared in exactly the same way as for high 1-hour ozone, except that running 8-hour averages were calculated for the gridded concentration and sensitivity output files before analyzing the data using RankDDM.

Comparing sensitivity information between the base and emissions reduction cases is complicated for this study because fewer sensitivities were calculated for the reduced emissions cases than for the base case. This was because of the high computational requirement for the DDM runs. If the same sensitivity information were available in all cases, preparing comparisons like Tables 4-2 and Figures like 4-5 across emissions scenarios would be straightforward.

For the emission reductions scenarios, sensitivities to VOC and NOx emission categories were calculated for the source areas in and around the receptor areas (i.e., corresponding to runs B2N and B2V). The sensitivities to anthropogenic emissions groups in the base and sensitivity cases are compared in Figure 4-7 for the grid cells and hours when 1-hour ozone exceeded 80 ppb in the basecase. It is important to average sensitivities over a fixed set of grid cells and hours in the base and control cases, otherwise the average sensitivities are not comparable. Figure 4-7 shows scatter plots of the values reported at the top of Tables 4-2 through 4-5 against corresponding information for the emission reduction cases.

The dashed lines in Figure 4-7 show the expected relationship if the sensitivities scale linearly with emissions reduction. For example, at top left, if the sensitivities to anthropogenic NOx are unchanged by a 25% reduction in anthropogenic VOC, then the points will fall an a 1:1 line, which they do. At top right in Figure 4-7, if the sensitivities to anthropogenic VOC are reduced 25% by a 25% reduction in anthropogenic VOC, then the points will fall an a line with slope 0.75. The response of emission sensitivities to the emission reduction scenarios is summarized below. Figure 4-7 combines sensitivities across receptors, source areas and emission categories on the same charts and shows consistency in the responses of the sensitivities to emission reductions across receptors, source areas and emission categories.

25% reduction in AVOC: The sensitivities to ANOx are mostly unchanged and the sensitivities to AVOC are reduced by slightly less than 25%. The slightly less than linear reduction in AVOC sensitivities can be interpreted as the ozone formation efficiency (ozone formed per VOC) increasing slightly as VOCs were reduced.

25% reduction in ANOx: Positive sensitivities to ANOx are reduced by less than 25% with a 25% reduction in ANOx. The less than linear reduction in ANOx sensitivities can be interpreted as the ozone formation efficiency (ozone formed per NOx) increasing as NOx was reduced. The sensitivities to AVOC are mostly reduced by the 25% reduction in ANOx, which can be interpreted as a shift to more NOx-limited (less VOC sensitive) conditions as NOx is reduced.

25% reduction in ANOx: Positive sensitivities to ANOx are reduced by less than 75% with a 75% reduction in ANOx. The less than linear reduction in ANOx sensitivities can be interpreted as the ozone formation efficiency (ozone formed per NOx) increasing as NOx was reduced. The sensitivities to AVOC are substantially reduced by the 75% reduction in ANOx, which can be interpreted as a large shift to more NOx-limited (less VOC sensitive) conditions when NOx is reduced by 75%. ANOx sensitivities that were negative in the basecase become positive in the control case, which is consistent with a shift toward NOx-limited conditions.

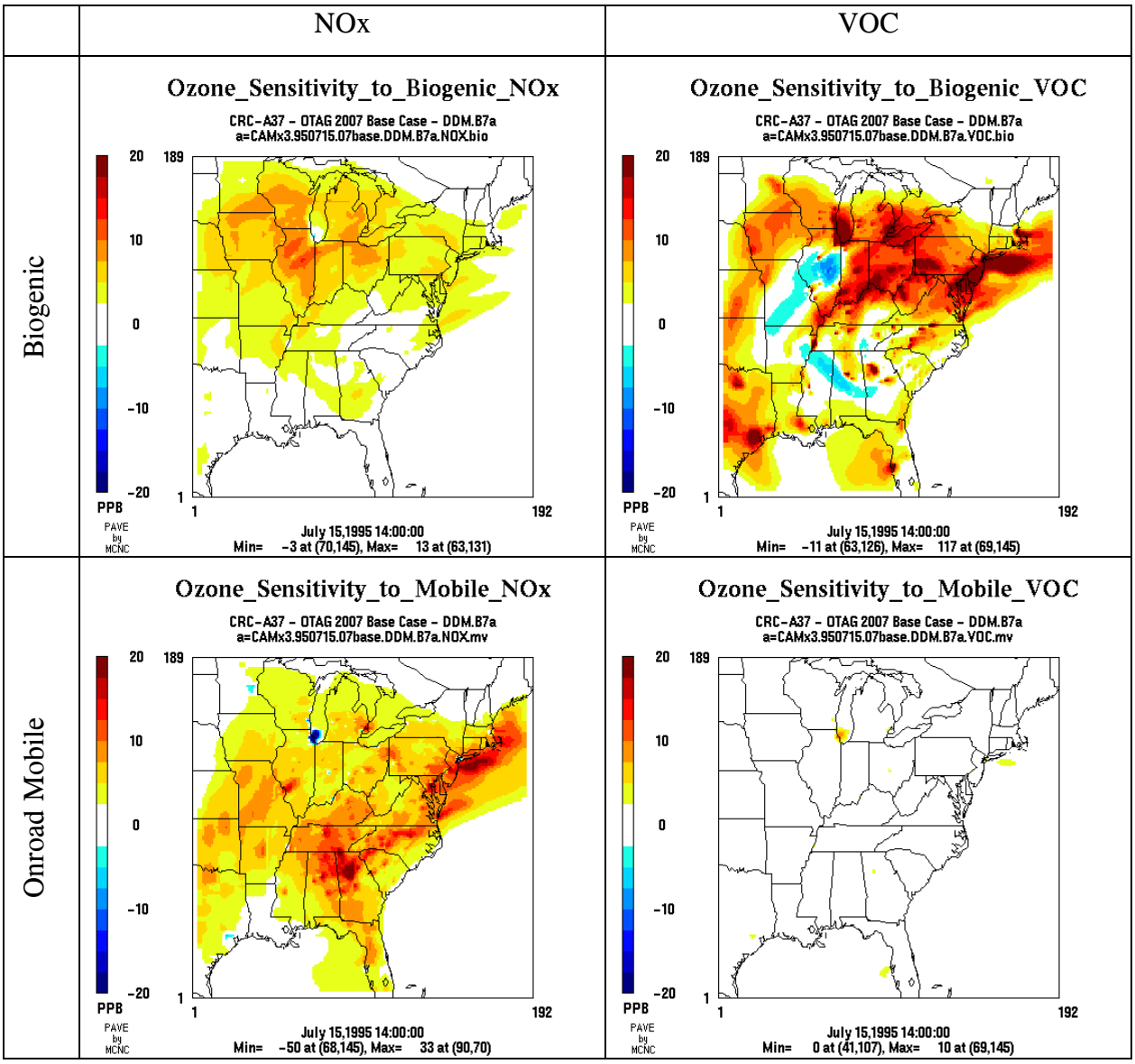

Figure 4-2. Spatial plots of ozone sensitivity to NOx and VOC emissions from biogenic, onroad mobile, elevated point and other anthropogenic emissions at 14:00 EST on July 14, 1999 for the 2007 base emissions scenario. DDM results from run B7.

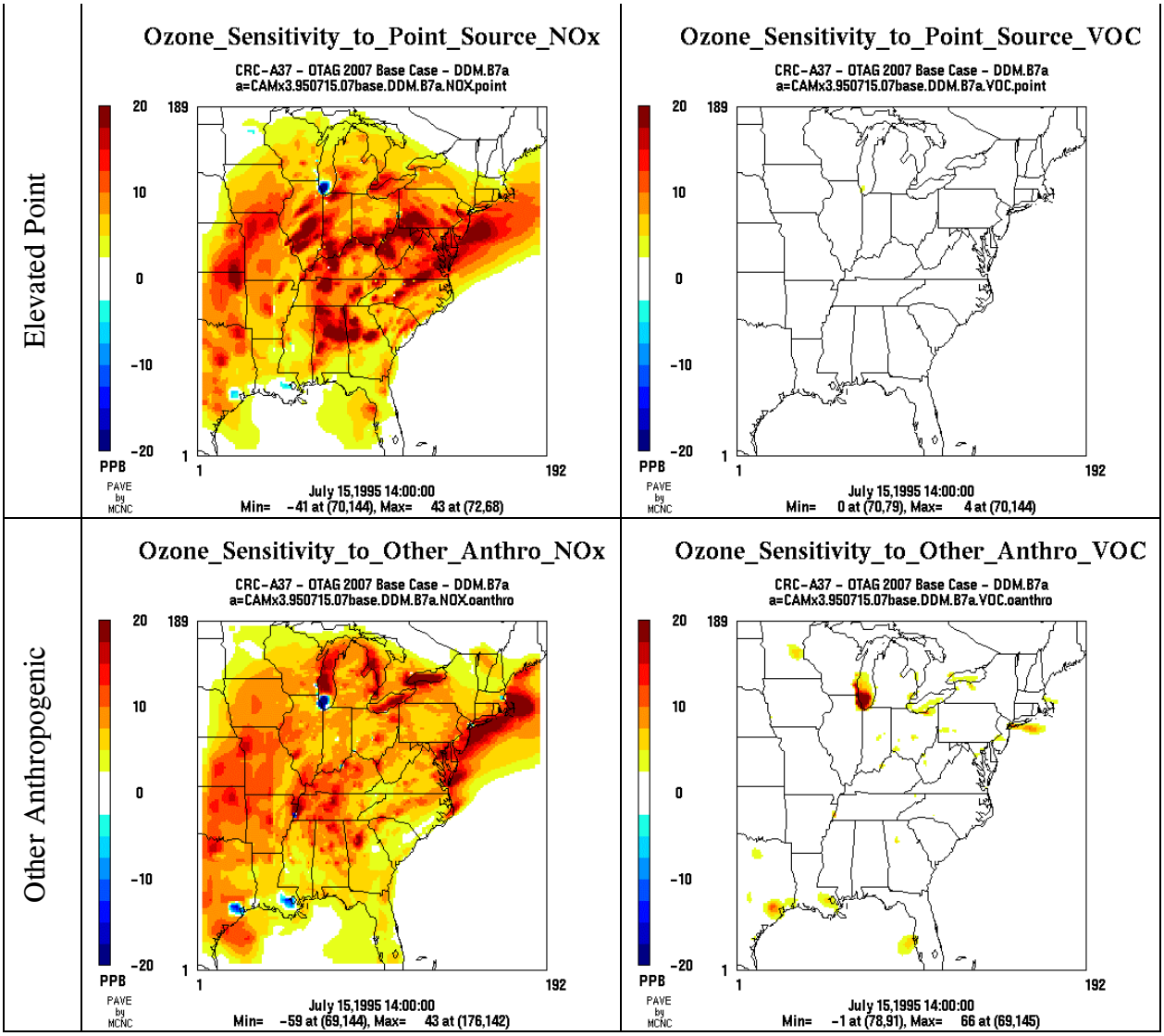

Figure 4-2 (concluded).

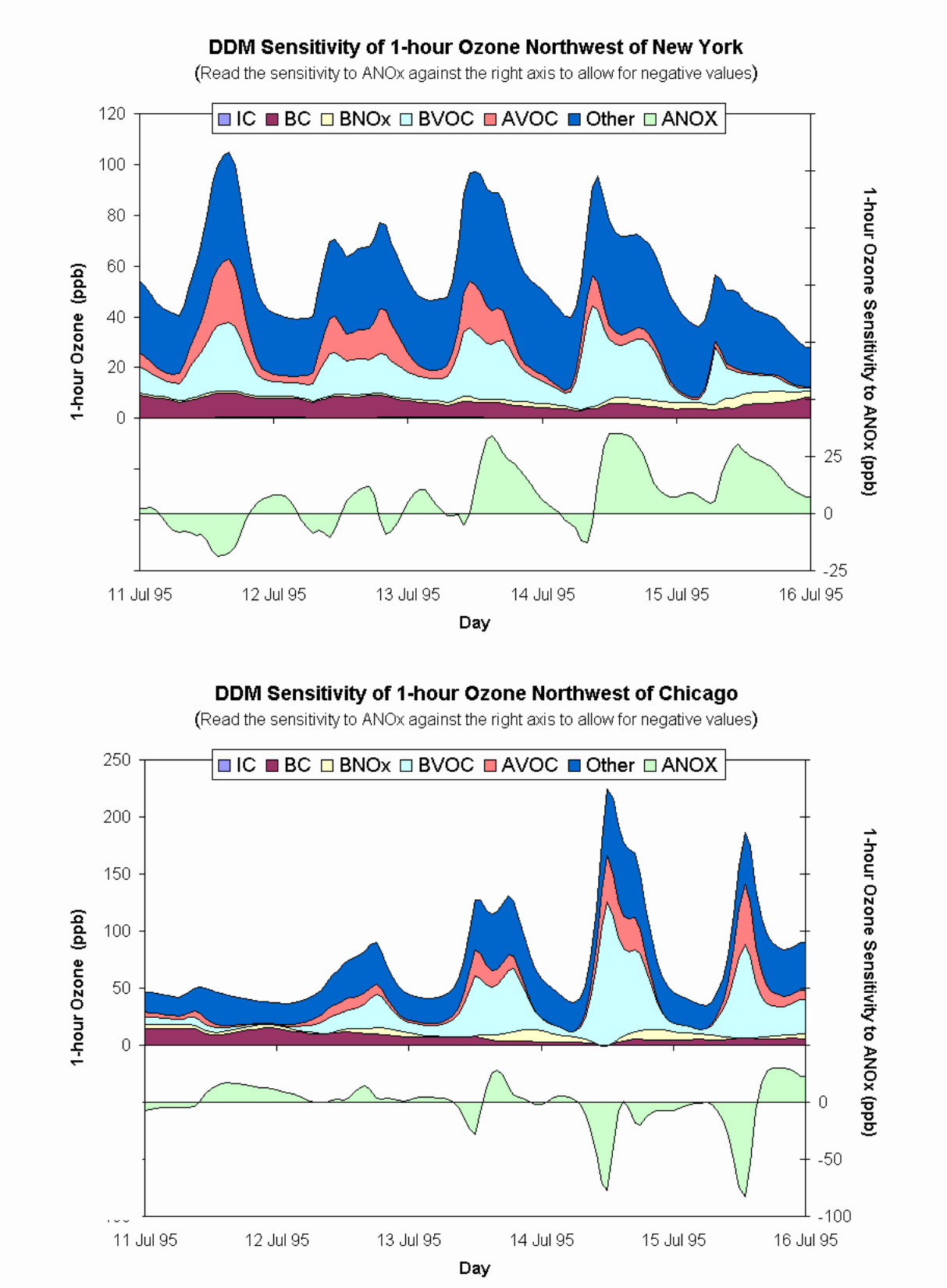

Figure 4-3. Time series of DDM sensitivities for the northwest corner grid cell in each receptor area. Other is the sum of higher order sensitivities. Sensitivities with negative values are shown against the right axis. DDM results from runs B2N, B2V, B3 and B7.

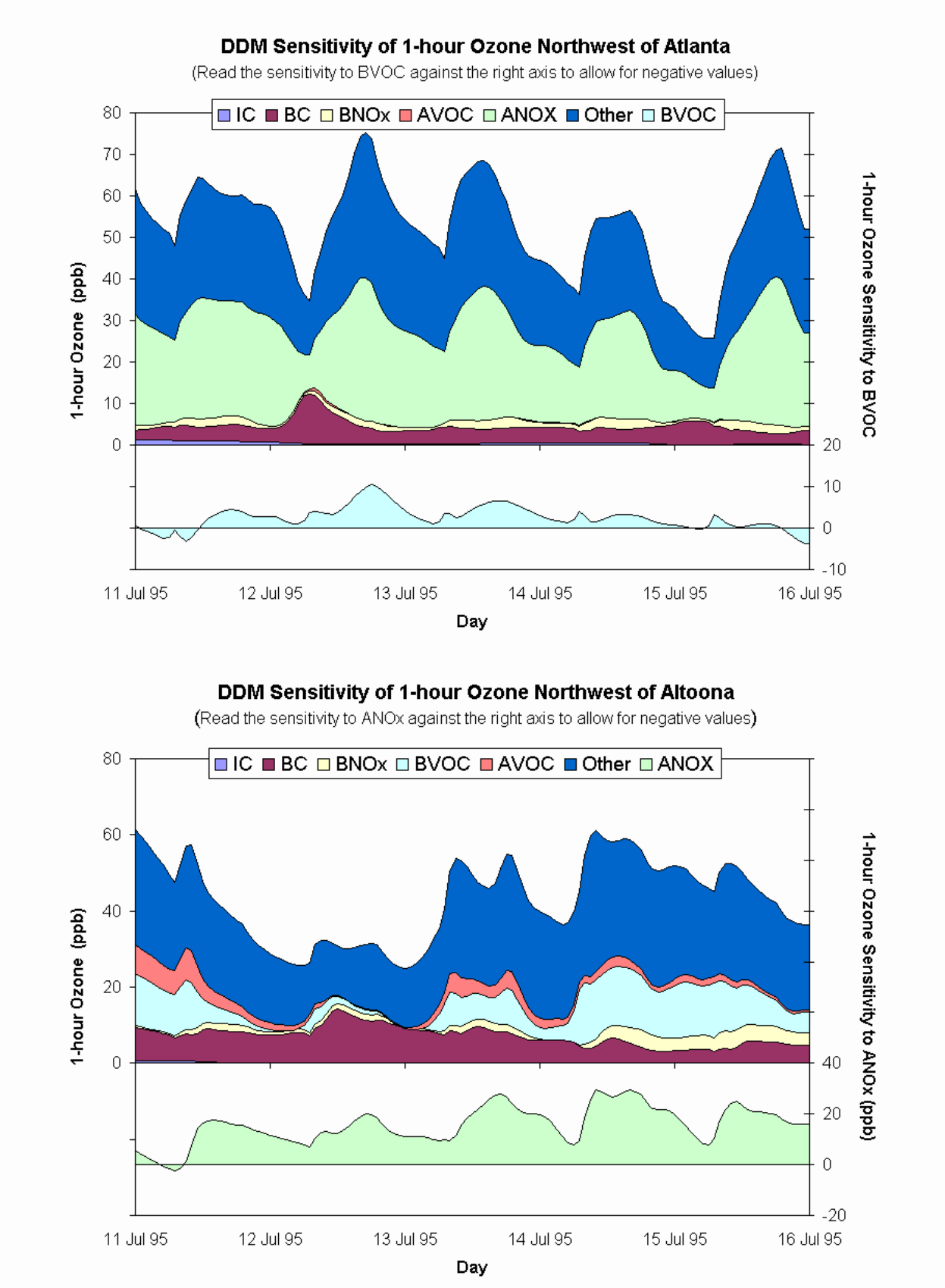

Figure 4-3 (concluded).

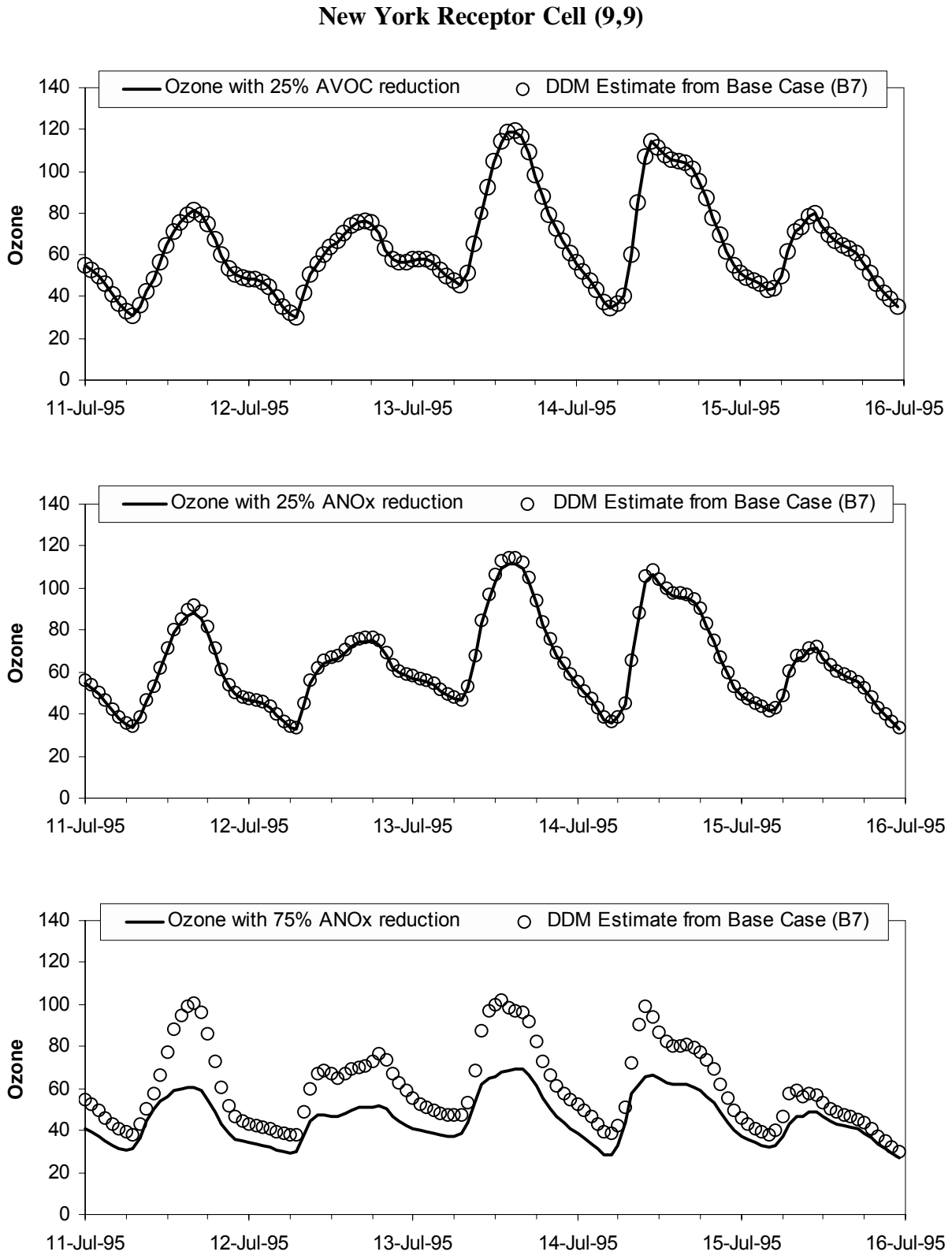

Figure 4-4. Time series of ozone for the northwest corner grid cell in each receptor area with reduced emissions (line) compared to the estimated ozone from the base case concentrations and DDM sensitivities (circles). DDM results from run B7.

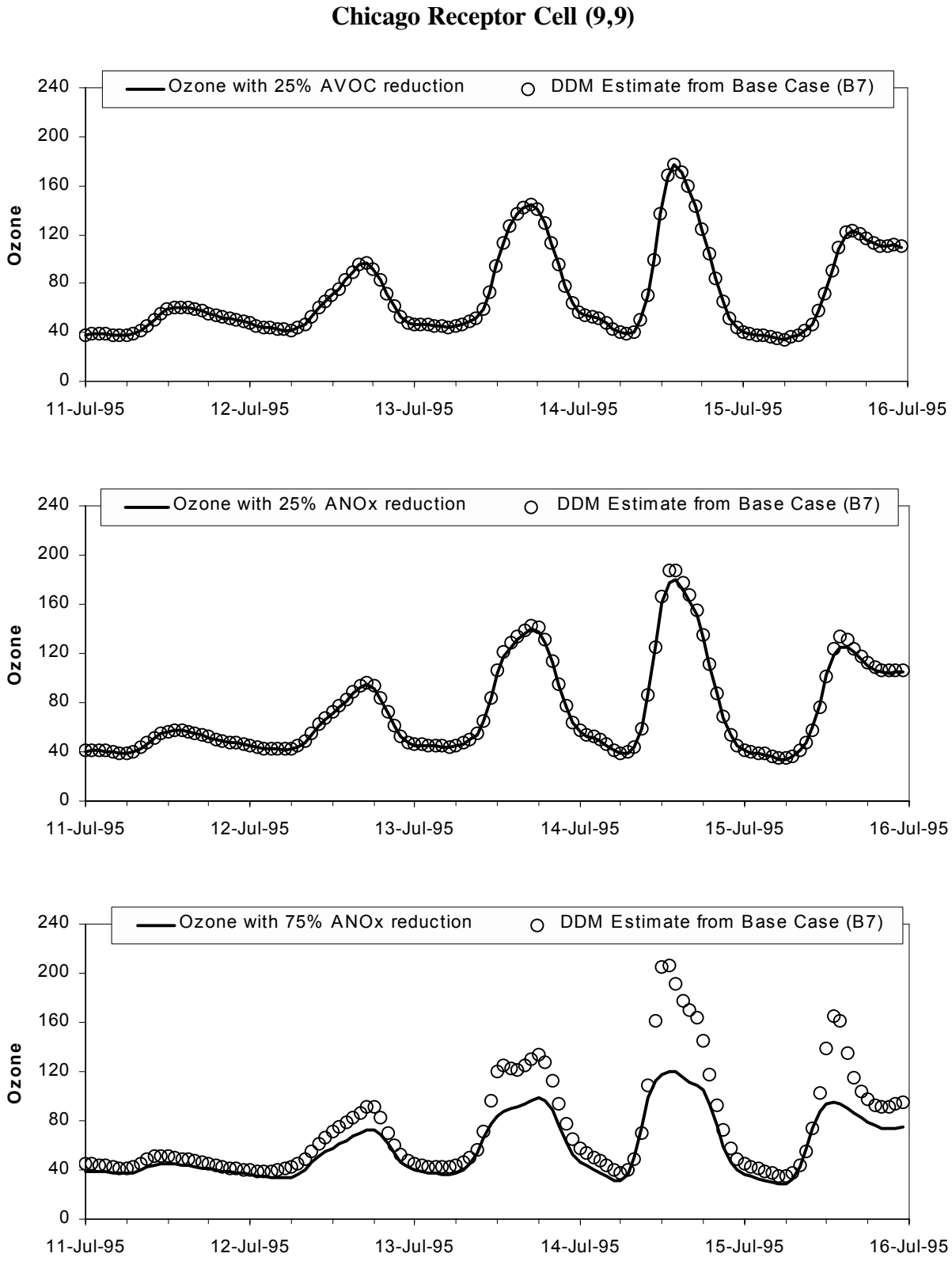

Figure 4-4 (continued).

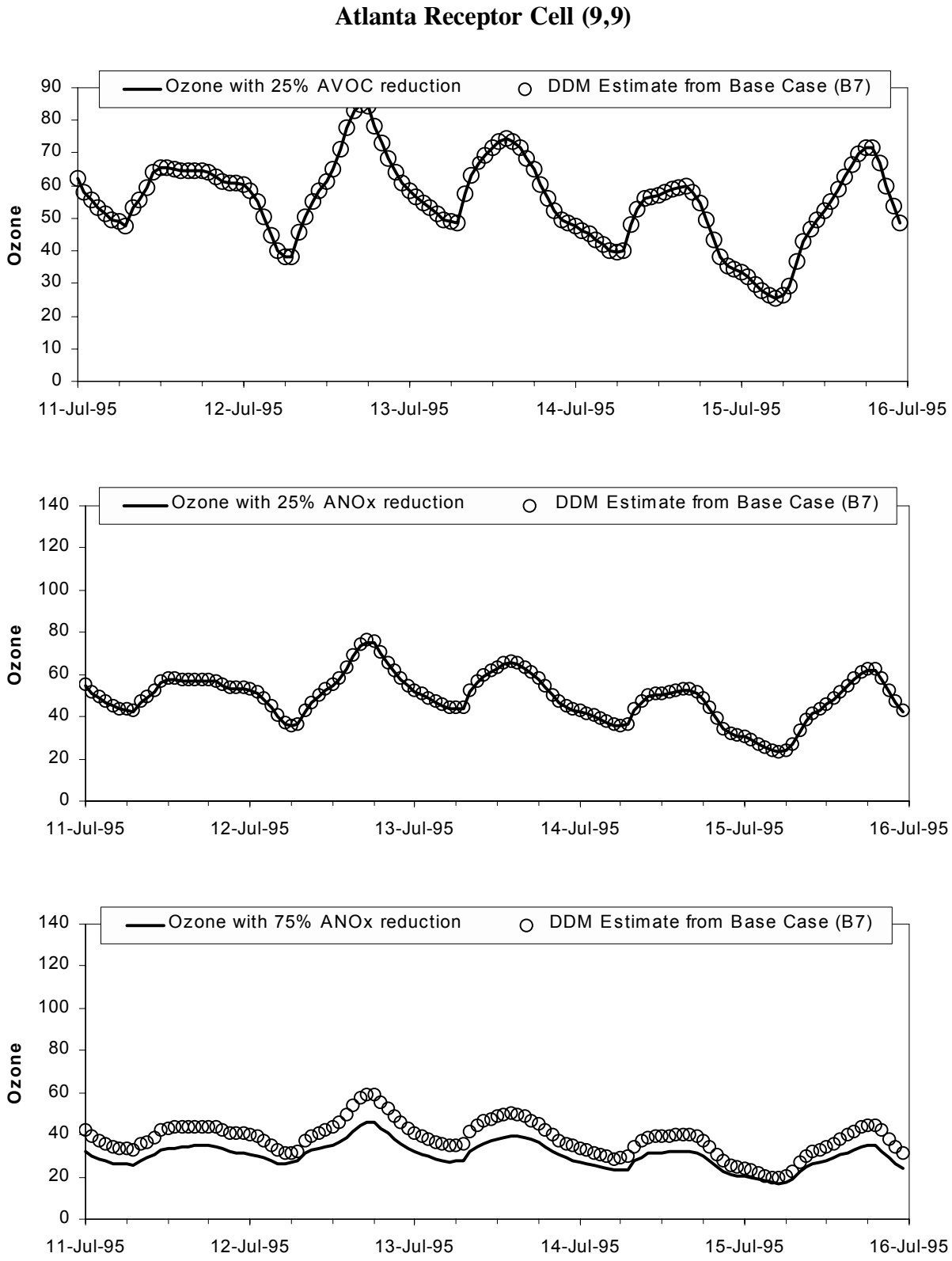

Figure 4-4 (continued).

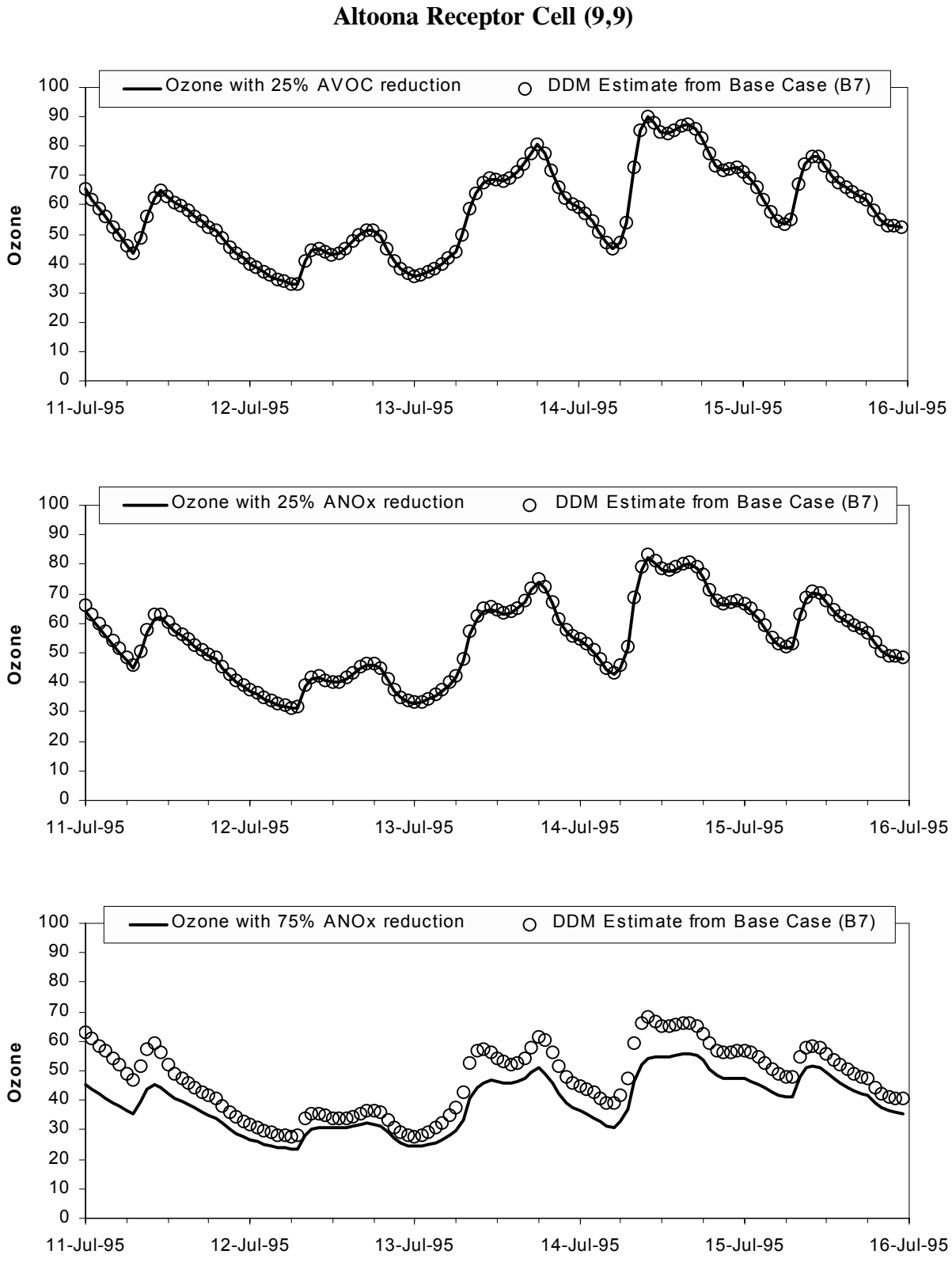

Figure 4-4 (concluded).

Table 4-2. DDM sensitivities when 1-hour ozone exceeds 80 ppb in the Altoona receptor area in the 2007 base case (runs B2N, B2V, B3 and B7).

Ozone Sensitivity from NOx Emissions (ppb)

Source Area	Source Category PT	MV/OAN		BIO	Total
1	N/C	N/C	N/C	N/C	N/C
2	N/C	N/C	N/C	N/C	N/C
3	N/C	N/C	N/C	N/C	N/C
4	1.2	1.9		1.0	4.1
5	1.0	0.7		0.3	2.0
6	N/C	N/C	N/C	N/C	N/C
7	3.8	3.0		0.7	7.6
8	0.1	0.2		0.0	0.3
9	N/C	N/C	N/C	N/C	N/C
10	N/C	N/C	N/C	N/C	N/C
11	7.3	3.8		0.3	11.5
12	0.0	0.0		0.0	0.0
13	0.0	0.0		0.0	0.0
14	0.3	0.1		0.0	0.4
15	0.0	0.0		0.0	0.0
16	0.0	0.0		0.0	0.0
17	0.3	1.3		0.2	1.9
Total	14.4	5.5	6.1	3.0	29.1

Ozone Sensitivity to VOC Emissions (ppb)

Source Area	Source Category PT	MV/OAN		BIO	Total
1	N/C	N/C	N/C	N/C	N/C
2	N/C	N/C	N/C	N/C	N/C
3	N/C	N/C	N/C	N/C	N/C
4	0.0	0.6		1.4	2.0
5	0.0	0.4		4.0	4.4
6	N/C	N/C	N/C	N/C	N/C
7	0.3	1.1		6.1	7.4
8	0.0	0.2		1.9	2.1
9	N/C	N/C	N/C	N/C	N/C
10	N/C	N/C	N/C	N/C	N/C
11	0.3	0.7		0.3	1.3
12	0.0	0.0		0.0	0.0
13	0.0	0.0		0.0	0.0
14	0.0	0.2		0.0	0.2
15	0.0	0.0		0.0	0.0
16	0.0	0.0		0.0	0.0
17	0.0	0.0		0.2	0.2
Total	0.7	1.2	2.3	19.3	23.5

Total Ozone Sensitivity (ppb)

Source Area	Source Category PT	MV/OAN		BIO	BC	IC	Other	Total
1	0.3	0.7		1.3				2.3
2	0.0	0.1		0.2				0.3
3	0.1	0.2		0.3				0.6
4	1.2	2.5		2.4				6.1
5	1.1	1.1		4.2				6.4
6	0.0	0.0		0.0				0.0
7	4.1	4.1		6.8				15.0
8	0.1	0.3		2.0				2.4
9	0.0	0.0		0.0				0.0
10	0.0	0.0		0.0				0.0
11	7.6	4.5		3.9				16.0
12	0.0	0.0		0.0				0.0
13	0.0	0.0		0.0				0.0
14	0.3	0.3		0.1				0.7
15	0.0	0.0		0.0				0.0
16	0.0	0.0		0.0				0.0
17	0.3	1.4		1.1				2.8
N/A					5.8	0.1		5.9
N/A							33.6	33.6
Total	15.1	6.7	8.4	22.3	5.8	0.1	33.6	92.2

Table Notes:

N/C shows sensitivities that were not calculated in runs B2N, B2V, B3 or B7.

N/A source area is not applicable to IC/BCs and the sum of higher sensitivities (Other)

The sensitivities to MV and OAN by geographic area were combined in runs B2N, B2V and B3, but were separated over all areas in run B7.

Table 4-3. DDM sensitivities when 1-hour ozone exceeds 80 ppb in the Atlanta receptor area in the 2007 base case (runs B2N, B2V, B3 and B7).

Ozone Sensitivity to NOx Emissions (ppb)

Source Area	Source Category PT	MV/OAN		BIO	Total
1	N/C	N/C	N/C	N/C	N/C
2	N/C	N/C	N/C	N/C	N/C
3	N/C	N/C	N/C	N/C	N/C
4	0.1	0.1		0.0	0.1
5	0.4	0.4		0.1	0.9
6	N/C	N/C	N/C	N/C	N/C
7	0.1	0.1		0.0	0.2
8	4.7	8.8		1.0	14.5
9	N/C	N/C	N/C	N/C	N/C
10	N/C	N/C	N/C	N/C	N/C
11	0.0	0.0		0.0	0.0
12	0.9	1.1		0.3	2.3
13	0.0	0.0		0.0	0.0
14	0.0	0.0		0.0	0.0
15	6.7	19.3		0.3	26.4
16	0.0	0.0		0.0	0.0
17	0.0	0.0		0.0	0.0
Total	13.0	17.4	12.6	1.8	44.7

Ozone Sensitivity to VOC Emissions (ppb)

Source Area	Source Category PT	MV/OAN		BIO	Total
1	N/C	N/C	N/C	N/C	N/C
2	N/C	N/C	N/C	N/C	N/C
3	N/C	N/C	N/C	N/C	N/C
4	0.0	0.1		0.1	0.2
5	0.0	0.1		1.0	1.1
6	N/C	N/C	N/C	N/C	N/C
7	0.0	0.0		0.1	0.1
8	0.0	0.0		5.8	5.9
9	N/C	N/C	N/C	N/C	N/C
10	N/C	N/C	N/C	N/C	N/C
11	0.0	0.0		0.0	0.0
12	0.0	0.0		1.4	1.4
13	0.0	0.0		0.0	0.0
14	0.0	0.0		0.0	0.0
15	0.0	1.4		6.1	7.5
16	0.0	0.0		0.0	0.0
17	0.0	0.0		0.0	0.0
Total	0.1	0.9	0.9	15.0	16.7

Total Ozone Sensitivity (ppb)

Source Area	Source Category PT	MV/OAN	BIO	BC	IC	Other	Total
1	0.0	0.1	0.2				0.35
2	0.0	0.0	0.0				0.05
3	0.0	0.0	0.0				0.06
4	0.1	0.1	0.1				0.31
5	0.4	0.5	1.0				1.93
6	0.0	0.0	0.0				0.02
7	0.1	0.1	0.1				0.33
8	4.7	8.9	6.8				20.40
9	0.0	0.1	0.2				0.33
10	0.0	0.0	0.0				0.00
11	0.0	0.0	0.0				0.05
12	0.9	1.2	1.6				3.72
13	0.0	0.0	0.0				0.00
14	0.0	0.0	0.0				0.04
15	6.7	20.7	6.5				33.89
16	0.0	0.0	0.0				0.00
17	0.0	0.0	0.0				0.00
N/A				2.3	0.58		2.86
N/A						42.55	42.55
Total	13.0	18.2	13.5	16.7	2.3	0.58	42.55	106.90

Table Notes:

N/C shows sensitivities that were not calculated in runs B2N, B2V, B3 or B7.

N/A source area is not applicable to IC/BCs and the sum of higher sensitivities (Other)

The sensitivities to MV and OAN by geographic area were combined in runs B2N, B2V and B3, but were separated over all areas in run B7.

Table 4-4. DDM sensitivities when 1-hour ozone exceeds 80 ppb in the Chicago receptor area in the 2007 base case (runs B2N, B2V, B3 and B7).

Ozone Sensitivity to NOx Emissions (ppb)

Source Area	Source Category PT	MV/OAN		BIO	Total
1	N/C	N/C	N/C	N/C	N/C
2	N/C	N/C	N/C	N/C	N/C
3	N/C	N/C	N/C	N/C	N/C
4	5.7	5.4		5.1	10.8
5	1.2	0.7		0.3	2.2
6	N/C	N/C	N/C	N/C	N/C
7	0.0	0.0		0.0	0.0
8	0.0	0.0		0.0	0.0
9	N/C	N/C	N/C	N/C	N/C
10	N/C	N/C	N/C	N/C	N/C
11	0.0	0.0		0.0	0.0
12	0.0	0.0		0.0	0.0
13	0.0	0.0		0.0	0.0
14	-2.1	-11.6		0.2	-13.5
15	0.0	0.0		0.0	0.0
16	0.0	0.0		0.0	0.0
17	0.0	0.0		0.0	0.0
Total	6.6	-2.1	-1.0	6.8	10.3

Ozone Sensitivity to VOC Emissions (ppb)

Source Area	Source Category PT	MV/OAN		BIO	Total
1	N/C	N/C	N/C	N/C	N/C
2	N/C	N/C	N/C	N/C	N/C
3	N/C	N/C	N/C	N/C	N/C
4	0.1	1.1		7.8	9.0
5	0.1	0.4		9.7	10.2
6	N/C	N/C	N/C	N/C	N/C
7	0.0	0.0		0.0	0.0
8	0.0	0.0		0.0	0.0
9	N/C	N/C	N/C	N/C	N/C
10	N/C	N/C	N/C	N/C	N/C
11	0.0	0.0		0.0	0.0
12	0.0	0.0		0.0	0.0
13	0.0	0.0		0.0	0.0
14	0.4	8.4		7.7	16.5
15	0.0	0.0		0.0	0.0
16	0.0	0.0		0.0	0.0
17	0.0	0.0		0.0	0.0
Total	0.6	1.9	8.8	34.7	46.0

Total Ozone Sensitivity (ppb)

Source Area	Source Category PT	MV/OAN	BIO	BC	IC	Other	Total
1	1.7	2.8	8.9				13.38
2	0.1	0.3	1.7				2.12
3	0.0	0.0	0.0				0.04
4	5.8	6.4	12.9				25.19
5	1.3	1.2	9.9				12.43
6	0.0	0.0	0.0				0.01
7	0.0	0.0	0.0				0.00
8	0.0	0.0	0.0				0.08
9	0.0	0.0	0.0				0.00
10	0.0	0.0	0.0				0.00
11	0.0	0.0	0.0				0.00
12	0.0	0.0	0.0				0.00
13	0.0	0.0	0.0				0.00
14	-1.7	-3.2	7.9				3.06
15	0.0	0.0	0.0				0.01
16	0.0	0.0	0.0				0.00
17	0.0	0.0	0.0				0.00
N/A				4.9	0.11		5.02
N/A						40.27	40.27
Total	7.2	-0.2	7.8	41.5	4.9	0.11	40.27	101.60

Table Notes:

N/C shows sensitivities that were not calculated in runs B2N, B2V, B3 or B7.

N/A source area is not applicable to IC/BCs and the sum of higher sensitivities (Other)

The sensitivities to MV and OAN by geographic area were combined in runs B2N, B2V and B3, but were separated over all areas in run B7.

Table 4-5. DDM sensitivities when 1-hour ozone exceeds 80 ppb in the New York receptor area in the 2007 base case (runs B2N, B2V, B3 and B7).

Ozone Sensitivity to NOx Emissions (ppb)

Source Area	Source Category PT	MV/OAN		BIO	Total
1	N/C	N/C	N/C	N/C	N/C
2	N/C	N/C	N/C	N/C	N/C
3	N/C	N/C	N/C	N/C	N/C
4	0.4	0.4		0.3	1.1
5	0.1	0.1		0.0	0.2
6	N/C	N/C	N/C	N/C	N/C
7	1.8	1.6		0.3	3.6
8	0.1	0.1		0.0	0.2
9	N/C	N/C	N/C	N/C	N/C
10	N/C	N/C	N/C	N/C	N/C
11	4.2	5.7		0.8	10.7
12	0.6	0.9		0.1	1.6
13	2.1	6.2		0.3	8.6
14	0.1	0.1		0.0	0.1
15	0.0	0.0		0.0	0.0
16	-0.7	-4.2		0.0	-4.9
17	0.0	0.2		0.1	0.3
Total	9.0	5.6	5.8	2.2	22.7

Ozone Sensitivity to VOC Emissions (ppb)

Source Area	Source Category PT	MV/OAN		BIO	Total
1	N/C	N/C	N/C	N/C	N/C
2	N/C	N/C	N/C	N/C	N/C
3	N/C	N/C	N/C	N/C	N/C
4	0.0	0.5		0.6	1.2
5	0.0	0.1		0.8	0.9
6	N/C	N/C	N/C	N/C	N/C
7	0.1	1.1		3.4	4.6
8	0.0	0.1		0.7	0.7
9	N/C	N/C	N/C	N/C	N/C
10	N/C	N/C	N/C	N/C	N/C
11	0.1	1.1		7.0	8.2
12	0.0	0.3		2.8	3.1
13	0.0	1.1		3.4	4.6
14	0.0	0.2		0.1	0.3
15	0.0	0.0		0.0	0.0
16	0.1	3.5		4.0	7.6
17	0.0	0.0		0.9	0.9
Total	0.4	1.8	6.4	24.9	33.6

Total Ozone Sensitivity (ppb)

Source Area	Source Category PT	MV/OAN	BIO	BC	IC	Other	Total
1	0.1	0.4	0.7				1.2
2	0.0	0.0	0.1				0.1
3	0.3	0.5	0.6				1.4
4	0.4	0.9	0.9				2.2
5	0.1	0.2	0.9				1.1
6	0.0	0.0	0.0				0.0
7	1.9	2.6	3.7				8.2
8	0.1	0.2	0.7				0.9
9	0.0	0.0	0.0				0.0
10	0.0	0.0	0.0				0.0
11	4.3	6.8	7.8				18.9
12	0.6	1.2	2.9				4.7
13	2.1	7.3	3.7				13.2
14	0.1	0.2	0.1				0.4
15	0.0	0.0	0.0				0.0
16	-0.6	-0.7	4.0				2.7
17	0.0	0.2	0.9				1.1
N/A				5.1	0.2		5.3
N/A						40.8	40.8
Total	9.4	7.5	12.3	27.1	5.1	0.2	40.8	102.4

Table Notes:

N/C shows sensitivities that were not calculated in runs B2N, B2V, B3 or B7.

N/A source area is not applicable to IC/BCs and the sum of higher sensitivities (Other)

The sensitivities to MV and OAN by geographic area were combined in runs B2N, B2V and B3, but were separated over all areas in run B7.

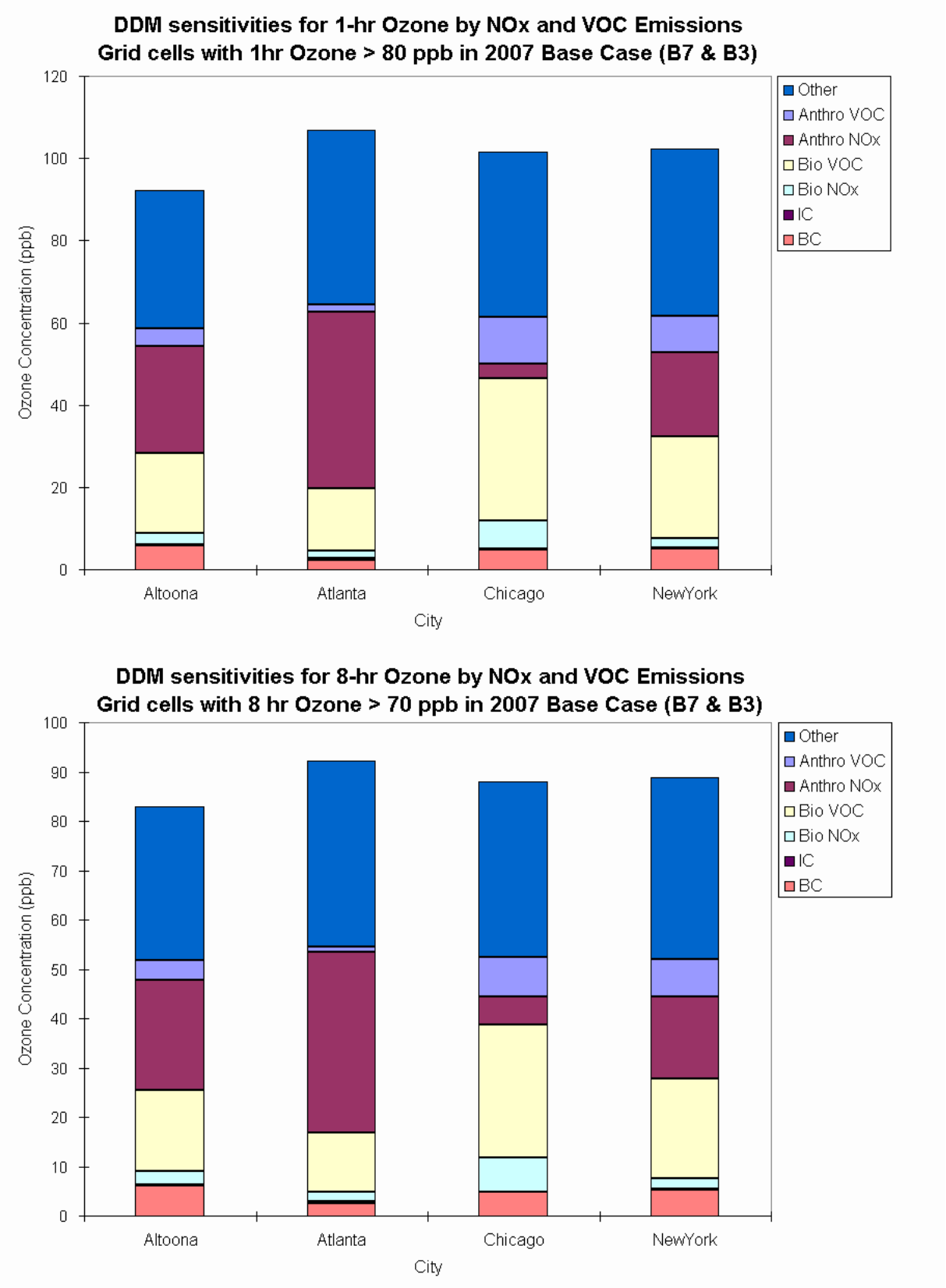

Figure 4-5. Comparison of DDM sensitivities by VOC and NOx for high 1-hour and 8-hour ozone levels in each receptor area for the 2007 base case (runs B3 and B7).

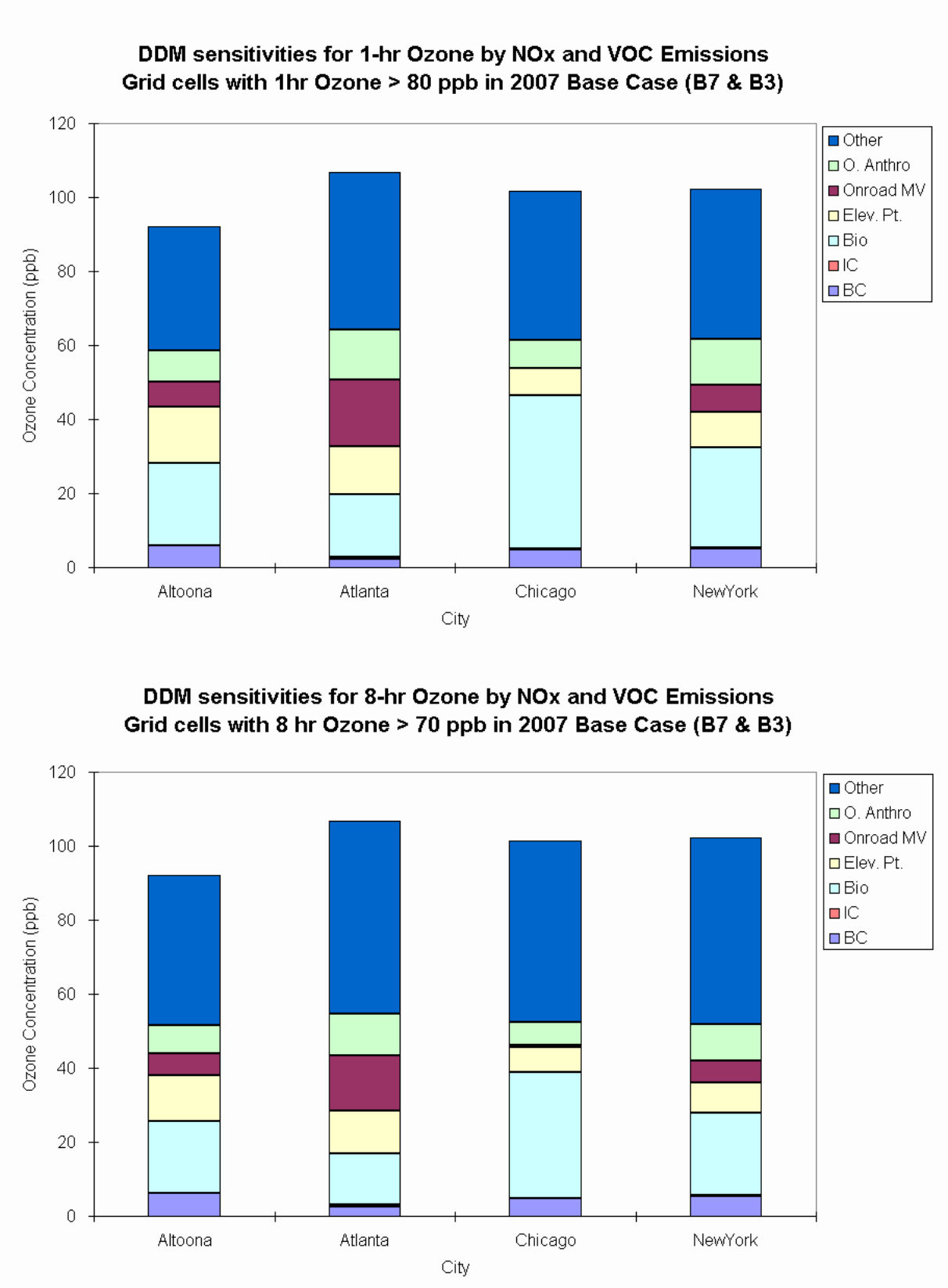

Figure 4-6. Comparison of DDM sensitivities by source category for high 1-hour and 8-hour ozone levels in each receptor area for the 2007 base case (runs B3 and B7).

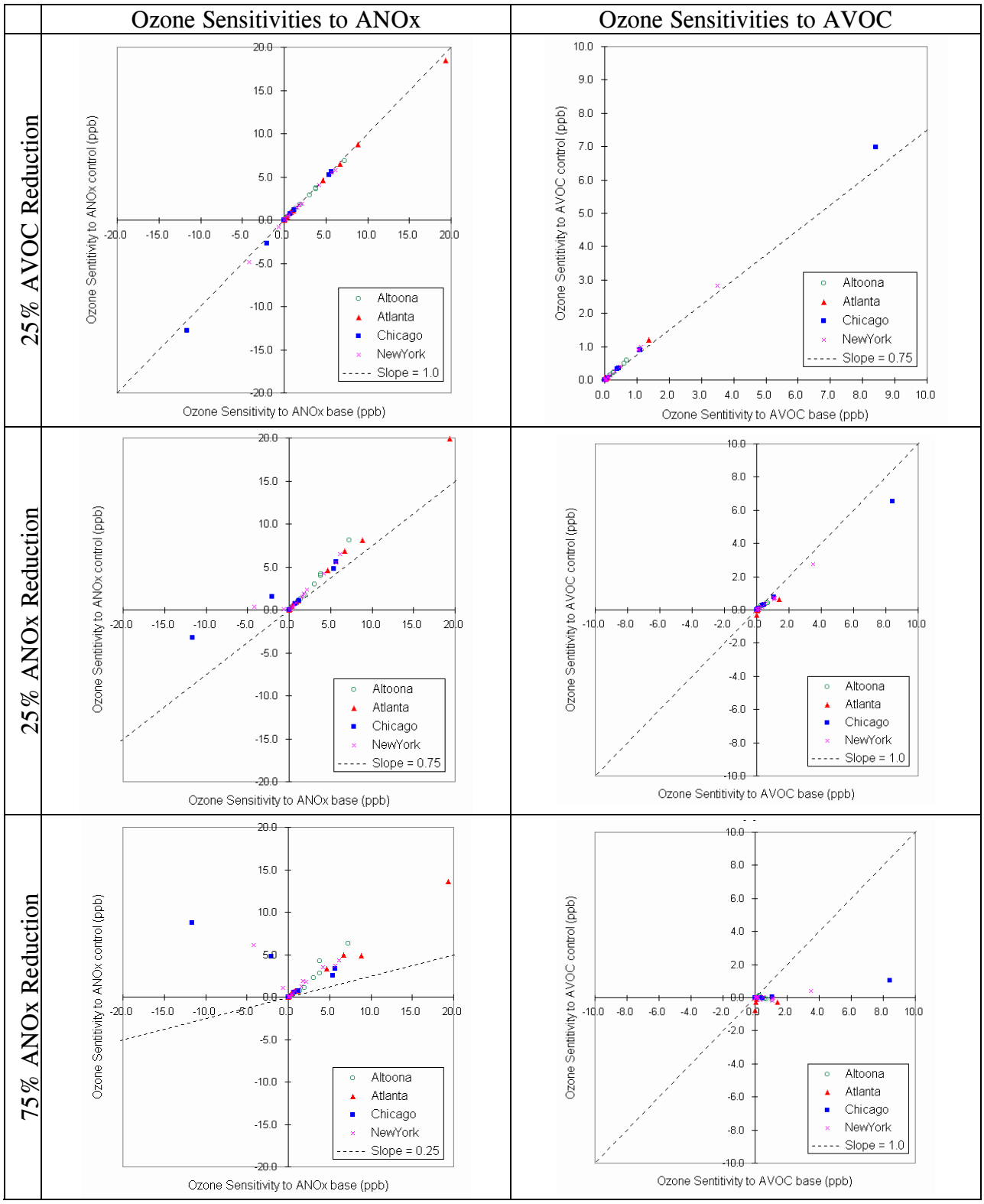

Figure 4-7. Change in DDM sensitivities to anthropogenic NOx and VOC emission groups with emission reductions. Sensitivities are averaged over grid cells and hours when basecase 1-hour ozone exceeded 80 ppb. Points will fall on the dashed line if sensitivities scale linearly with emission changes.

5. ANALYSIS OF PA RESULTS

This section presents several example analyses of CAMx PA results to illustrate how they can be summarized and analyzed. We do not interpret the implications of the results for air quality planning because the OTAG modeling scenarios are dated and because the results are open to interpretation. The PA results are presented in a different way for PA than for OSAT or DDM, in Sections 3 and 4, because the post-processing steps are easier for PA than for OSAT or DDM. However, interpreting the results of Chemical Process Analysis (CPA) is more difficult than for OSAT or DDM because it requires an understanding of atmospheric chemistry and knowledge of the specific chemical mechanism being analyzed. The main part of this section of the report is a demonstration of the CPA results for the OTAG demonstration runs.

OUTPUT FILES

The CAMx output files that are specific to PA are listed in Table 5-1 and the formats are described in the CAMx User's Guide (ENVIRON, 2002a). The PA output files depend upon which PA option is selected, as shown in Table 5-1.

Table 5-1. CAMx output files for Process Analysis.

		CAMx PA Option Selected		
Filename	**Content**	**PA**	**IRR**	**IPR**
*.ipr	Integrated process rate (IPR) information for all selected cells	Yes	No	Yes
*.irr	Integrated reaction rate (IRR) information for all selected cells	Yes	Yes	No
*.grid.cpa *.fgrid.cpa	Chemical process analysis (CPA) parameters for the coarse and (optionally) fine grids	Yes	Yes	No

QUALITY ASSURANCE

CAMx PA runs are relatively easy to QA because there are no input files to create and relatively few choices in options. The only significant QA step is checking the receptor area definitions.

POST-PROCESSING TOOLS

PAVE

The gridded CPA variable output files are in same format as the CAMx average concentration files and are directly compatible with post-processing software such as PAVE[1]. The formula capabilities built into PAVE allow CPA variable to be combined, which is extremely useful, but there is a limit on the number of species that can be combined in a formula (about 30).

CAMxtrct

CAMxtrct (CAM-extract) is a post-processing program available from the CAMx ftp site[2]. CAMxtrct extracts concentrations for single species or combinations of species from CAMx coarse and/or fine grid files in average file format. It writes out either a binary file in coarse grid average file format or in an ASCII file in a format similar to Golden Software Surfer GRD format. The specific capabilities of CAMxtrct are:

- Extract a species for a specific grid and layer.
- Select a specific species or combine several species that match a keyword.
- Combine coarse and fine grids to a coarse grid format file at the resolution of the finest grid.
- Extracting specific time intervals or finding daily maximum values.
- Take ratios of two species.

CAMxtrct is useful for combing CPA variables across coarse and fine grid output files.

FINE2UAM

FINE2UAM is a post-processing program available from the CAMx ftp site[2]. FINE2UAM extracts all of the grids from a CAMx fine grid average format file and writes a coarse grid format file for each nest. This is useful for post-processing fine grid CPA information using tools written for coarse grid (UAM-IV) format files. FINE2UAM also is useful if you have difficulty getting PAVE to directly read fine grid output files – the workaround is to convert the fine grid files to coarse grid format using FINE2UAM and read the coarse grid format files into PAVE.

EXAMPLE ANALYSIS

Process analysis is especially useful for quality assurance when developing new model scenarios because it provides rapid, efficient methods to assess the contribution of various chemical reactions and transport processes to O_3 production. This approach can also be applied to model intercomparison, e.g., Tonnesen (2001). The process analysis can also improve

[1] PAVE is available from http://www.emc.mcnc.org/EDSS/pave_doc/Pave.html
[2] The CAMx ftp site is ftp://ftp.environ.org, username=camxuser, password=pass4camx

model validation by suggesting how ambient data can be used to evaluate model accuracy for key terms in the chemical processing of VOC and NOx (e.g., Imre et al., 1998).

A comprehensive process analysis should include two components:

1. A chemical budget analysis using integrated reaction rates (IRR) to analyze the budgets of radicals, NOy, Ox, and O_3.

2. An analysis of other integrated process rates (IPR) including transport, deposition and emissions of key species.

The IRR portion of the analysis is especially useful for characterizing O_3 sensitivity to precursor reductions and for comparing different photochemical mechanisms. The IPR analysis is useful for characterizing dynamics including transport, vertical deposition, mass budget analyses and mass conservation. This project will place focus on the IRR analyses because this is most directly relevant to the issue of O_3 sensitivity to precursors. While the IPR analysis can be used to evaluate source contributions to O3 in particular grid cells, it is not well suited for attributing O3 production to particular source categories of VOCs.

Figure 5-1 illustrates important components of the chemical processes that control the photochemical formation of O_3. These include the following: photolysis or decomposition reactions that produce new radicals, where the family of radical species is defined as $HOx = OH + HO_2 + RO_2$; a sequence of propagation reaction in which HOx and NOx catalyze the production of O_3; NOx and HOx termination reactions that reduce or stop the production of O_3; and the relationship between production of odd oxygen (Ox) and O_3. Table 5-2 lists the PA outputs that are currently available in the CAMx model and that represent most of the process illustrated in Figure 5-1. The CAMx model can be easily modified to include other model outputs as needed.

One of the strengths of the process analysis outputs is that it provides a wealth of data that can be used to analyze the model performance. However, such analyses are very time intensive in grid models. Moreover, tools and procedures for automating these analyses are not well developed. The typical method is to use a visualization tool such as PAVE and spreadsheets to interactively explore the data. This approach is most useful when there is a particular question about model performance to be investigated, e.g. “Why did an increase in species X cause a decrease in O_3?”. Therefore, the approach used here is to provide a suite of typical output plots that may be suggestive of analyses to be performed. This project does ask the general question of accounting for differences in the predictions of DDM and OSAT. To that end, a post-processing analysis was developed to analyze Ox production that occurs in either VOC sensitive to NOx sensitive regimes, and this is discussed below.

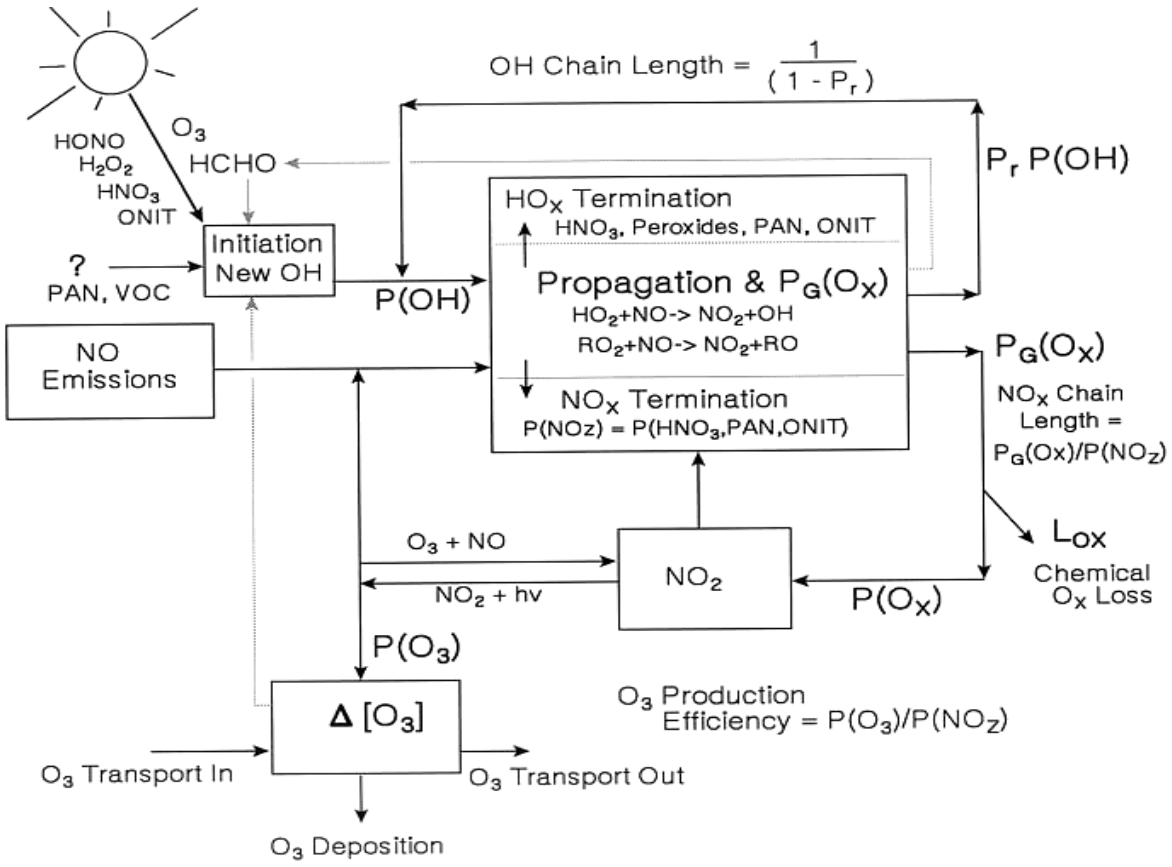

Figure 5-1. Process diagram illustrating important diagnostics for characterizing photochemical production of ozone.

Table 5-2. Chemical Process Analysis variables in CAMx for the CB4 Mechanism.

CPA Variable	Description
Ox Budget	
OxProd	Ox Chemical Production
OxLoss	Ox Chemical Destruction
Radical Initiation	
newOH_O1D	New OH from O1D+H2O
newOHother	New OH from H2O2, HNO3, HONO, PAA, OP1, OP2, O3+HC (except isoprene)
nwHO2_HCHO	New HO2 from HCHO
newHO2tot	New HO2 Production (Total)
newRO2tot	New RO2 Production (Total)
nHOx_isop	New HOx (including OH, HO2 and RO2) from isoprene
Radical Propagation	
OHwCO_CH4	sum of OH+CO and OH+CH4 reactions
ISOPwOH	OH+ISOP
ISOPwOx	isoprene reactions with O3, NO3 and O3P
OHw_all_HC	OH reacted with VOC
OHpropmisc	other OH propagation reactions (e.g.,OH+SO2)
HO2TotProd	Total HO2 Production
RO2TotProd	Total RO2 Production
HO2_to_NO2	NO2 produced from reactions of HO2
HO2_to_OH	OH produced from reactions of HO2
RO2_to_NO2	NO2 produced from reactions of RO2
OH_reacted	Total OH production
Radical Termination	
OHterm	OH termination
HO2term	HO2 termination
RO2term	RO2 termination
Formaldehyde Production	
HCHOp_isop	HCHO produced from isoprene reactions
HCHOp_Tot	HCHO produced from all reactions
NOz Reactions	
HNO3_OHNO2	OH+NO2 $\rightarrow$ HNO3
HNO3_NO3HC	NO3+HC $\rightarrow$ HNO3
HNO3_N2O5	N2O5+H2O $\rightarrow$ 2 HNO3
HNO3reacted	HNO3 reacted (to produce NOx)
PANprodNet	net PAN Prod
PANlossNet	net PAN Loss (source of NOx and a radical)
RNO3_prod	production of organic nitrates
Radical Concentrations	
OH	OH radical concentration
HO2	HO2 radical concentration
NO3	NO3 radical concentration
N2O5	N2O5 radical concentration

Description of PA Results

The description of the results for the process analysis is composed of three topics:

- Description of the chemistry in the 2007 base case for July 11 and 14.
- Analysis of areas in which Ox production is VOC sensitive or NOx sensitive in the base case for July 11 and 14.

The description here is focused primarily on the analysis of the chemistry terms that are provided in the CAMx CPA output files. There is no brief review of the transport terms that are provided in the CAMx IPR files. However, the IPR results are not very useful for providing a detailed source apportionment. The results described here focus on Ox production in VOC sensitive and NOx sensitive regimes for comparison with the DDM and OSAT results.

2007 Base Case CPA Results

A standard set of CPA output plots is included in Figures 5-2 to 5-15. These included a subset of outputs listed in Table 5-2 that are generally useful in characterizing a model simulation. Plots are shown for both July 11 and July 14 to compare and contrast differences in the photochemistry for these two days. Figure 5-2 shows Ox production and confirms that the differences in O_3 on these two days are largely due to differences in photochemical activity. That is, differences in transported O_3 can be ruled out as an alternative explanation for the low large differences in O_3 in the northern part of the domain on July 14 and 15. Figure 5-2 is also useful for identifying the particular grid cells in which Ox production occurred on each day. If these plots are analyzed interactively in PAVE it is also possible to identify the temporal differences in Ox production.

Figure 5-3 shows the destruction of Ox by photochemical reactions for each day, where Ox destruction reactions include, e.g.:

$$NO_3 + hv \rightarrow NO + NO_2$$
$$OH + O_3 \rightarrow HO_2$$
$$O^1D + H_2O \rightarrow 2\ OH$$

The ratio of Figure 5-2 to Figure 5-3 provides a qualitative estimate of the lifetime of Ox and when combined with an analysis of deposition and transport can be used to estimate the influence of regional transport of O_3. The difference of Figure 5-2 and Figure 5-3 is the net production of Ox, and this is equal to the sum of the production of O_3 and the amount of NO emissions oxidized. Typically, the amount of Ox destruction by photochemical reactions is on the order of 10% of the Ox production. The plot is shown here primarily to highlight the difference between production of Ox and production of O_3.

Figure 5-4 shows the sources of OH radical initiation from the reaction of O^1D with H_2O, and Figure 5-5 shows the total initiation of HO_2 from all sources including photolysis of HCHO and aldehydes and decomposition of aromatic decay products. Production of new HO_2 radicals results directly from the VOC emissions, so comparison of new HO_2 initiation versus OH

initiation is useful to quantify the importance of VOC versus O_3 in initiating the chain propagation reactions that produce O_3. The CAMx source code can be easily modified to produce more detailed information on the contribution of individual VOC species to radical initiation. These outputs would not be useful for directly estimating O_3 sensitivity to individual VOC, however, it would be useful for explaining why certain VOC are more reactive than others.

Figure 5-6 shows the amount of OH that reacted with CO and CH_4. Figure 5-7 shows the amount of OH that reacted with all VOC (including CO and CH_4), and Figure 5-8 shows the amount of OH that reacted with isoprene. The plots of OH that reacted with isoprene are an approximate indicator of the contribution of isoprene to O_3 production, and Figure 5-8 shows explicitly the importance of isoprene especially in the southern and northeastern US. Figure 5-8 can be compared with the DDM and OSAT plots which show that O_3 has low sensitivity to isoprene in the rural areas, and that most of the O_3 production in rural areas is attributed to NOx by OSAT. Thus, the CPA results showing the mass of isoprene reacted provides information not available by DDM and OSAT. The DDM sensitivity of O_3 to isoprene for urban areas can be explained by a combination of direct isoprene chemistry (e.g., isoprene reacted southwest of Chicago and New York) and indirect isoprene chemistry that produces HCHO and O_3 in rural areas which are subsequently transported and act as radical precursors in urban areas.

Figure 5-9 shows the amount of NOx converted to HNO_3 by the $OH+NO_2$ reaction. Figure 5-10 shows the amount of NOx converted to HNO_3 by the nighttime N_2O_5 chemistry. Conversion of NOx to inert HNO_3 is a key process in the model because, as discussed below, much of the domain is NOx limited. Conversion of NOx to HNO_3 in the nighttime chemistry can substantially affect the NOx budget and make it unavailable to participate in daytime O_3 production chemistry. This can affect model predicted O_3 concentrations and the sensitivity of O_3 to VOC and NOx. Comparisons of Figures 5-9 and 5-10 show that approximately equal amounts of NOx are being converted to HNO_3 in the nighttime chemistry. This is substantially different from previous simulations of the Regional Acid Deposition Model (RADM) in which approximately 30% of NOx was converted to HNO_3 by nighttime chemistry.

Figures 5-11, 5-12 and 5-13 show indicators of Ox production sensitivity to VOC and NOx (see Tonnesen and Dennis, 2000a for description of indicators based on radical propagation chemistry). In Figure 5-11, areas in red or yellow indicate radical limited conditions in which Ox production is sensitive to VOC and is inhibited by increasing NOx. In Figures 5-12 and 5-13 areas of gray and dark blue indicate these radical limited conditions. Figures 5-11 to 5-13 are useful for assessing the spatial and temporal variability in the sensitivity of Ox and O_3 production to precursors. These indicators will be further evaluated below to assess the sensitivity of O_3 to precursors in the receptor regions.

Figure 5-14 shows the net production efficiency of Ox per NOx converted to HNO_3 ($P(Ox)/P(HNO_3)$). This can be thought of as the NOx chain length and is closely related to the O_3 production efficiency per NOx. Comparisons of $P(Ox)/P(HNO_3)$ in the base case and in the NOx reduction sensitivity cases may be useful for understanding the unresponsiveness of the system to NOx reductions, i.e., the increasing Ox production efficiency at decreasing NOx conditions can provide an explanation for the “piston effect” whereby it becomes increasingly difficult to obtain further O3 reductions. The analysis of $P(Ox)/P(HNO_3)$ and its response to

precursor controls provides fundamental information that can be used to assess the feasibility of attaining an air quality standard using a particular control strategy. This information is probably not accessible from DDM because of non-linearity of the O_3 response to very large precursor changes. Further evaluation may be required to determine if this type of information is accessible in OSAT.

The goal of this section was to provide a somewhat qualitative analysis and comparison of the O_3 production for the model episode and to suggest additional analysis that should be performed. Most likely this analysis will initially be performed interactively working with the model output and with various visualization and analysis tools. Eventually, as more experience is gained in analyzing the CPA, IPR and IRR outputs in grid models, it is expected that tools will be developed to automate these types of analyses.

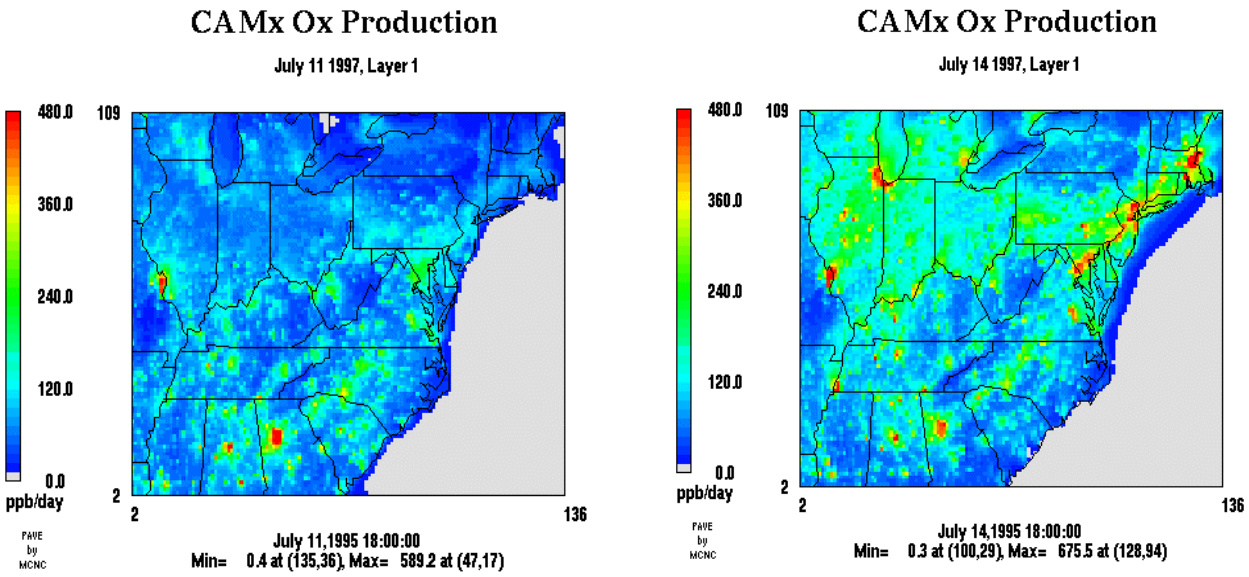

Figure 5-2. Ox production on July 11 (left) and July 14 (right).

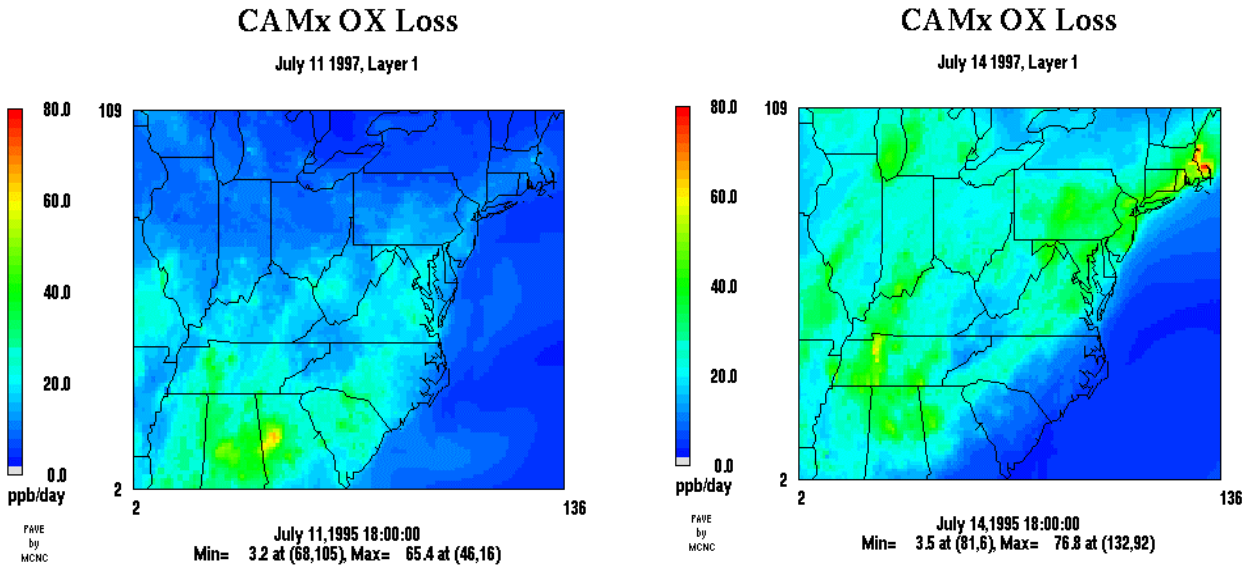

Figure 5-3. Ox photochemical destruction on July 11 (left) and July 14 (right).

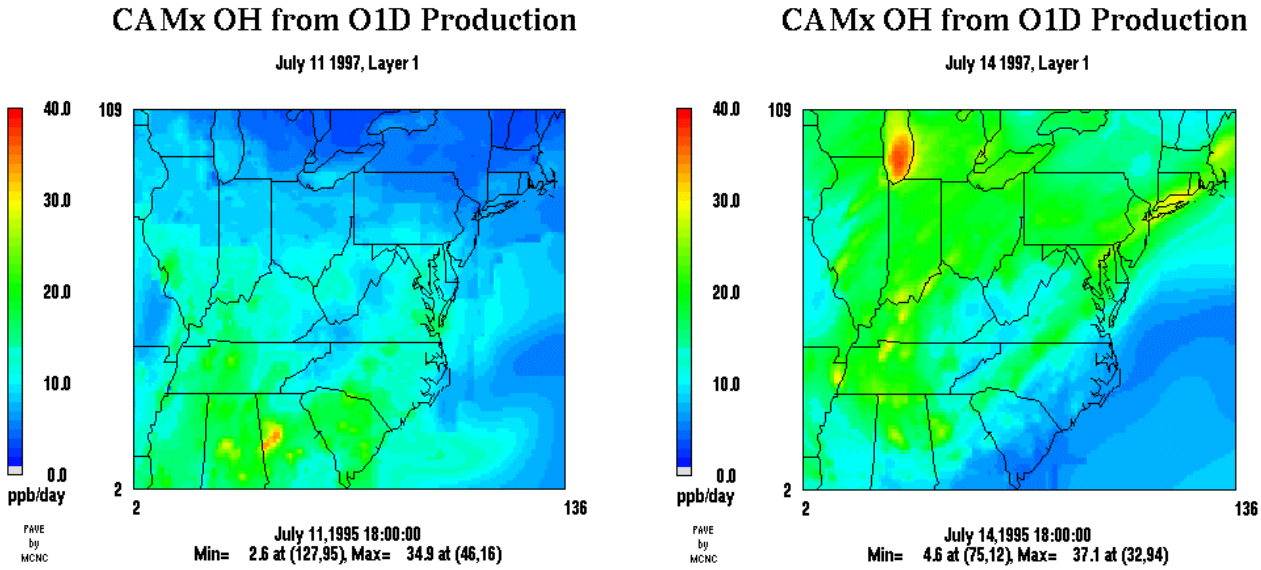

Figure 5-4. OH initiation from O1D on July 11 (left) and July 14 (right).

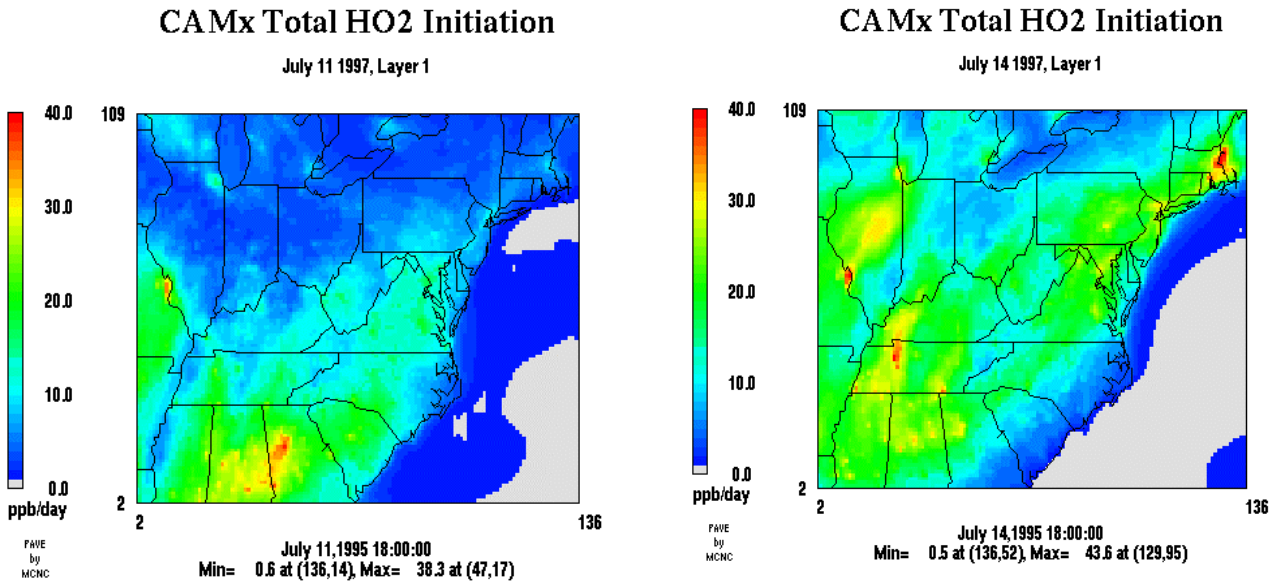

Figure 5-5. HO_2 initiation on July 11 (left) and July 14 (right).

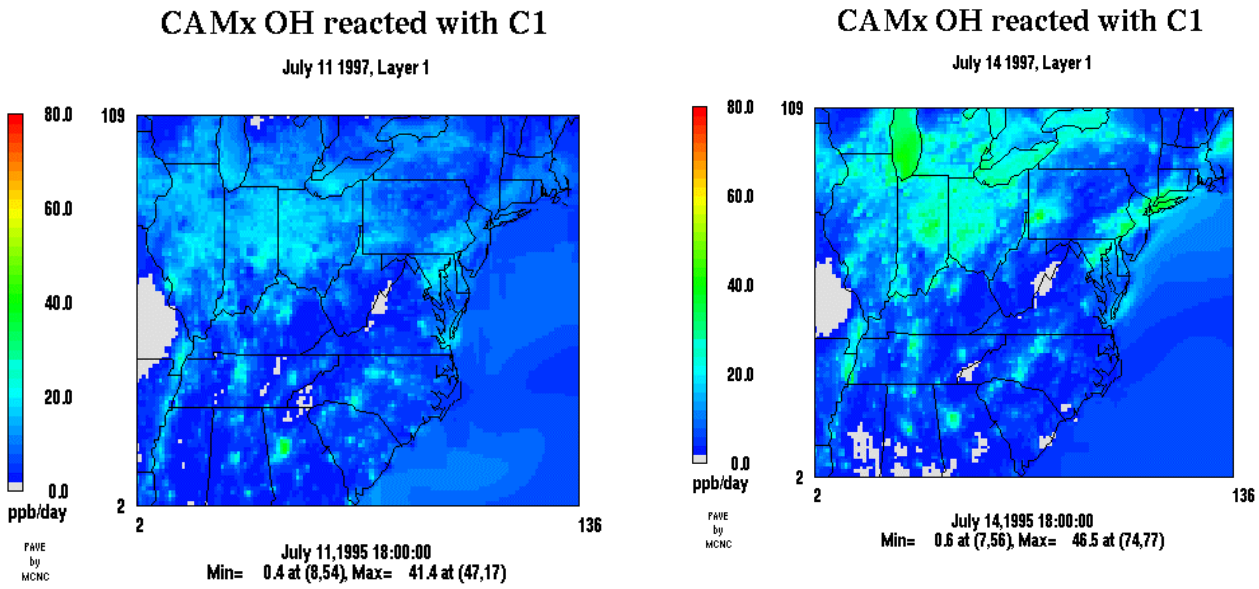

Figure 5-6. OH reacted with CO and methane on July 11 (left) and July 14 (right).

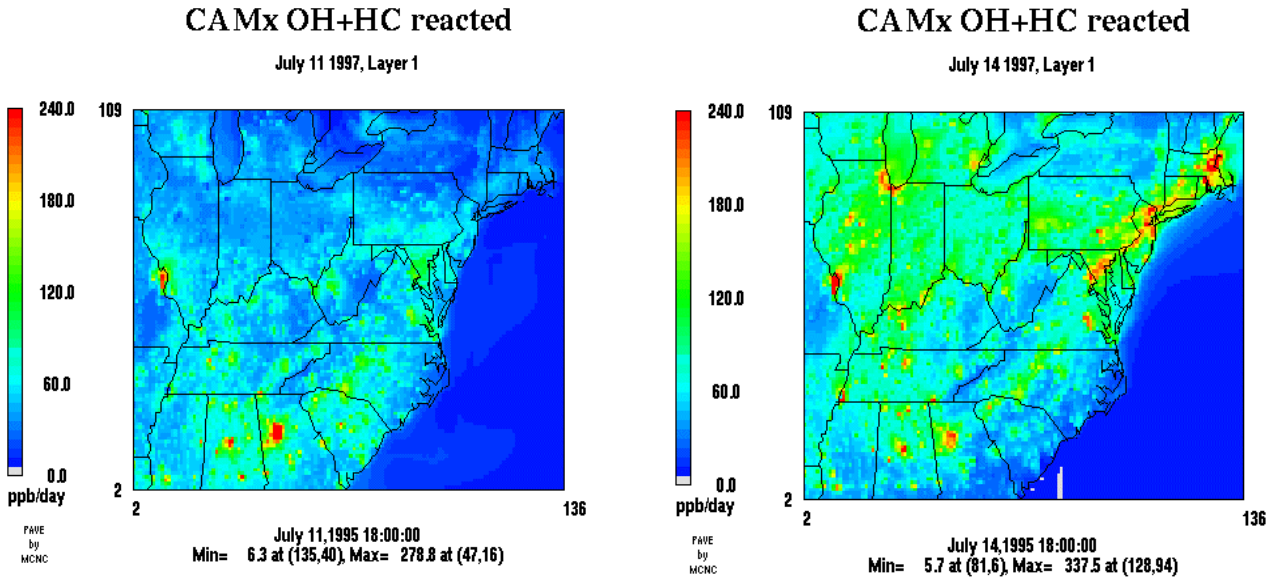

Figure 5-7. OH reacted with all VOC including CO and methane but excluding biogenic VOC on July 11 (left) and July 14 (right).

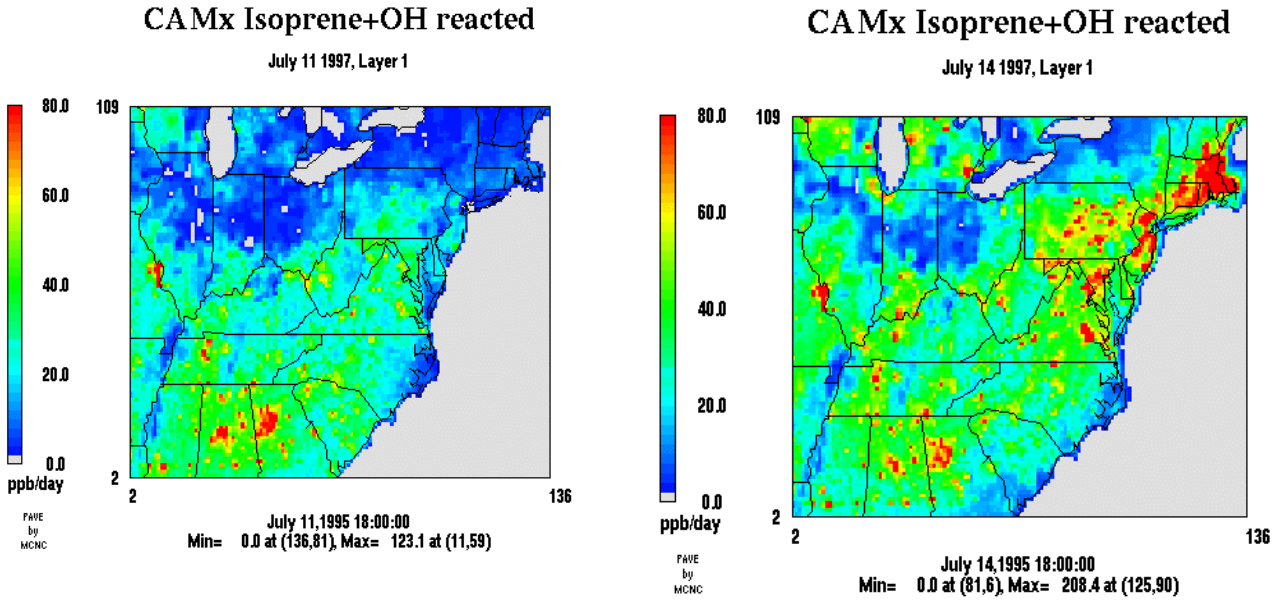

Figure 5-8. OH reacted with isoprene on July 11 (left) and July 14 (right).

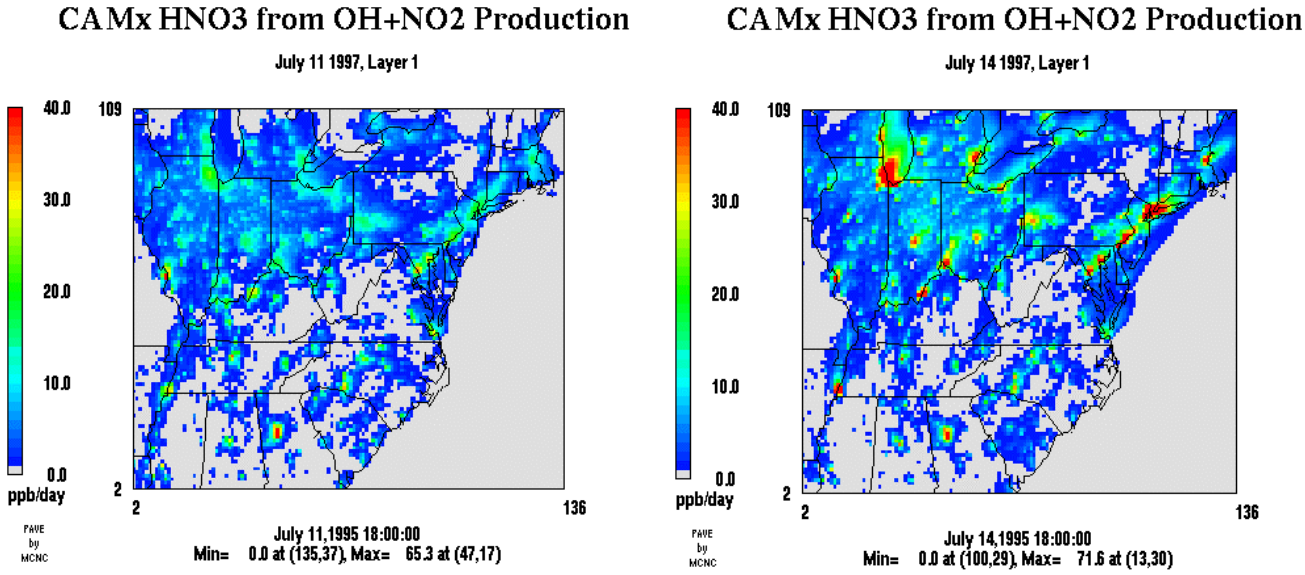

Figure 5-9. HNO3 production from OH+NO2 on July 11 (left) and July 14 (right).

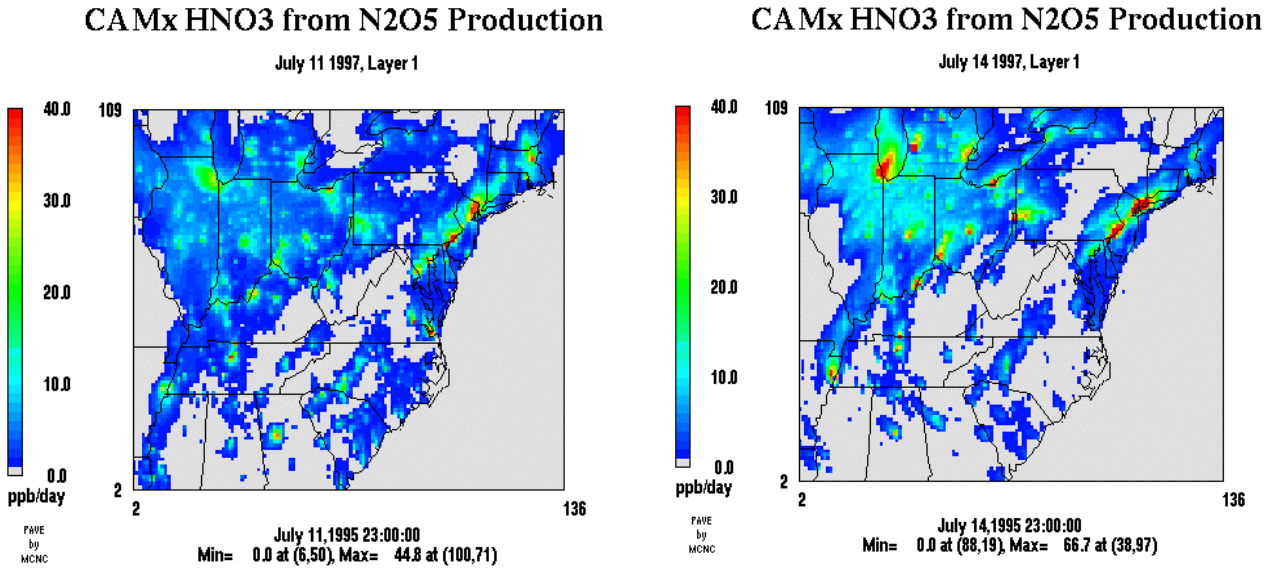

Figure 5-10. HNO3 production from OH+NO2 on July 11 (left) and July 14 (right).

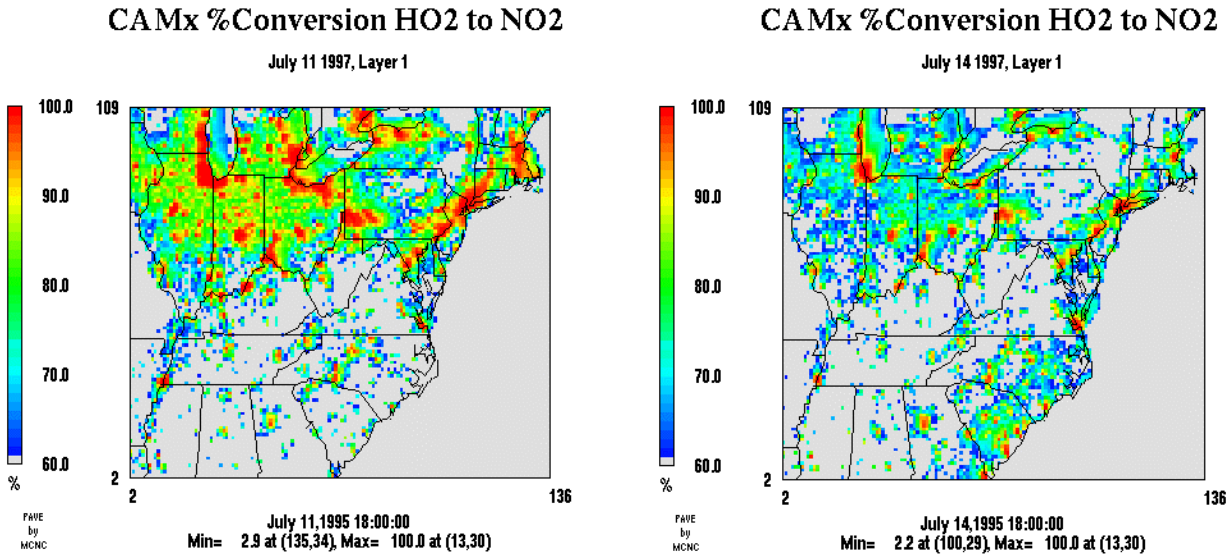

Figure 5-11. Percent conversion of HO_2 to NO on July 11 (left) and July 14 (right).

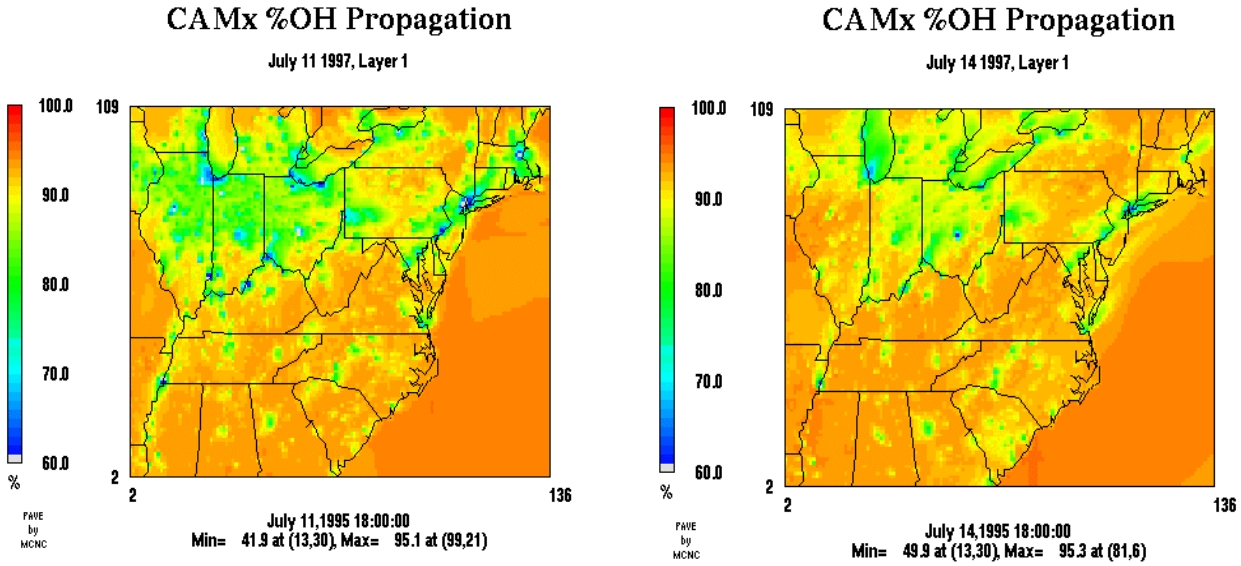

Figure 5-12. Percent of OH reacting in radical propagation reactions on July 11 (left) and July 14 (right).

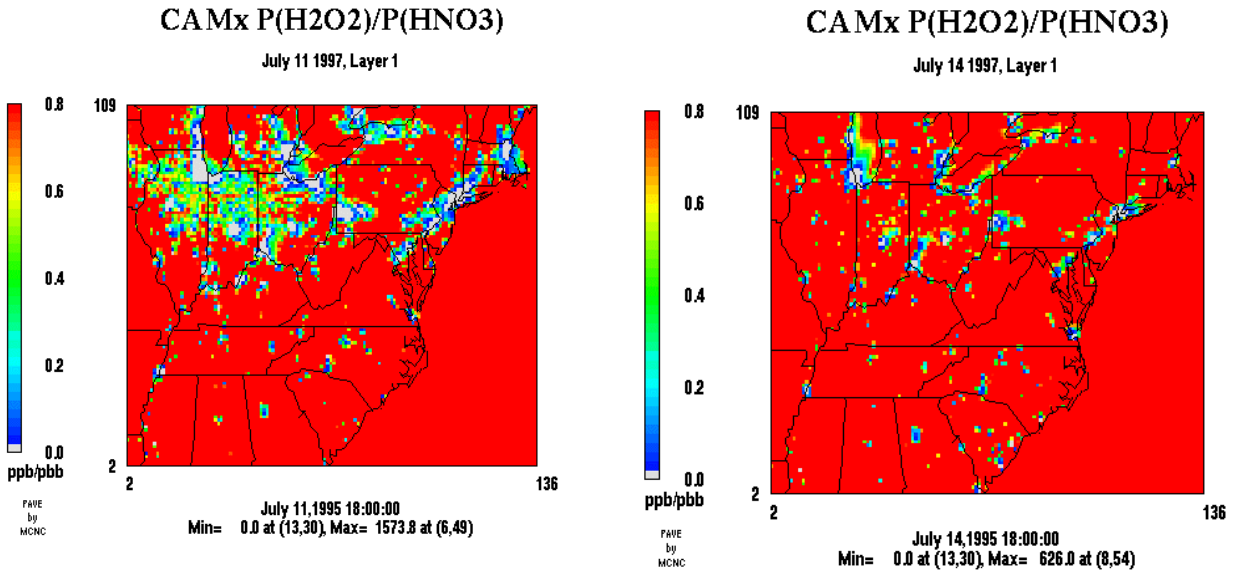

Figure 5-13. Indicator ratio of P(H2O2)/P(HNO3) on July 11 (left) and July 14 (right).

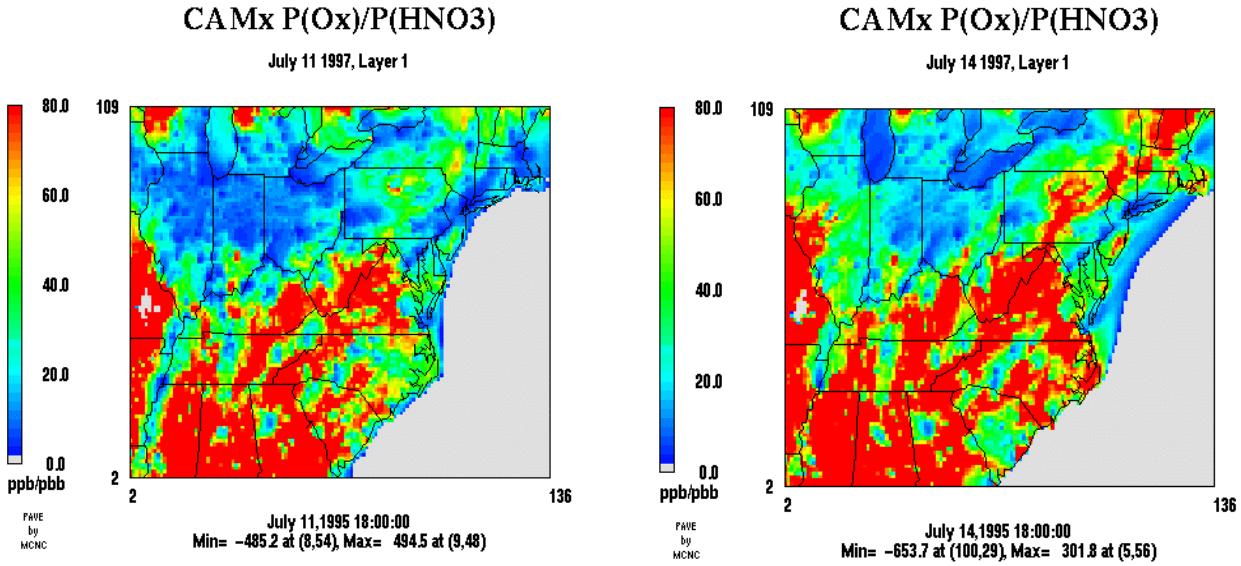

Figure 5-14. Production efficiency of Ox per NOx converted to HNO3 on July 11 (left) and July 14 (right).

Ox production Sensitivity to VOC and NOx

One of the process analysis outputs in the CAMx CPA file is the hourly rate of Ox production. Additional outputs include the rate of termination of HO_2+HO_2 to produce H_2O_2, and the rate of termination of $OH+NO_2$ to produce HNO_3. The ratio of the production rates of $P(H_2O_2)/P(HNO_3)$ is useful as an indicator of $P(O_3)$ and P(Ox) sensitivity to VOC and NOx (Sillman, 1995; Tonnesen and Dennis, 2000a).

There is uncertainty in the particular value of $P(H_2O_2)/P(HNO_3)$ that demarks the transition from VOC sensitive to NOx sensitive conditions. For example, Sillman (1995) found that an ratio of $P(H_2O_2)/P(HNO_3) = 0.35$ indicated conditions of equal O3 concentration sensitivity to VOC and NOx. In later results, Sillman (2000) revised the value to 0.2. Tonnesen and Dennis (2000a) evaluated P(Ox) sensitivity to precursor emissions and found that the value of $P(H_2O_2)/P(HNO_3)$ that demarked the transition was not constant and varied as a function of the O_3 concentration. They found that this ratio ranged between 0.06 to 0.20 for conditions associated with a ridgeline of P(Ox) production defined as:

$$dP(Ox)/dE_{NOx} = 0$$

where E_{NOx} represents emissions of NOx.

Because the CAMx CPA file includes the hourly rates of P(Ox), $P(H_2O_2)$ and $P(HNO_3)$, the ratio of $P(H_2O_2)/P(HNO_3)$ can be used to classify the hourly P(Ox) as either VOC sensitive or NOx sensitive. Because of the uncertainty in the indicator ration, a three-way classification scheme is used here:

- $P(H_2O_2)/P(HNO_3) < 0.06$ implies radical limited (VOC sensitive) conditions.

- $P(H_2O_2)/P(HNO_3)$ between 0.06 to 0.20 implies ridgeline conditions for P(Ox), i.e., approximately equally sensitive to VOC and NOx changes.
- $P(H_2O_2)/P(HNO_3) > 0.20$ implies NOx limited (NOx sensitive) conditions.

A CAMx post processing program (FINE2UAM) can be used to extract nested CPA domains from a single output file that contains the CPA data for all nested grids. For this project, the extraction program was modified to also calculate the P(Ox) sensitivity to VOC and NOx as a separate output. Note that this is one example of post-processing the CPA output, and there may be other post-processing analyses that can provide information about the photochemical system. For example, it may be possible to attribute Ox or O_3 production to the individual VOC species. This calculation was routinely performed using the process analysis output in trajectory models and box models. It has not been performed in a grid model because of the complexity of the bookkeeping required to attribute organic intermediates to their parent species. However, such analyses could be considered in the future, and if feasible this would be a complementary analysis to the DDM and OSAT results that are presented in this report.

Table 5-4(a-d) shows the P(Ox) sensitivity calculated for the S9 sensitivity case. These results are included to show the change in state of O3sensitivity to precursors for the S9 case compared to the base case. For example, comparing Table 5-3(b) to 5-4(b) shows that the Chicago area was more VOC sensitive in the base case with only 47% of the P(Ox) occurring in NOx sensitive conditions while in the S9 case P(Ox) was 89% NOx sensitive. Therefore, the process analysis shows that a deep reduction (75%) in anthropogenic NOx emissions shifted the photochemical regime in the Chicago area from more VOC sensitive conditions in the base case to largely NOx sensitive conditions in the deep NOx reduction case. The analysis of P(Ox) sensitivity in the S9 case would imply that, if additional emissions controls were needed, NOx reductions would be highly effective for reducing O3and VOC controls would be much less effective.

The values in Table 5-3 do not capture the spatial variability in the P(Ox) sensitivity regimes. Figures 5-15 to 5-19 show plots of the Ox production for each of the receptor regions for July 14. (Note that the plot domain for the Chicago area in Figure 5-15 is slightly larger than the receptor domain, and the other plots correspond exactly to the receptor domain.) For convenience, the VOC sensitive and equal sensitivity P(Ox) are included together in the top plots in Figures 6-15 to 6-19.

Figures 5-15 to 5-19 show that there is considerable variability in VOC or NOx sensitive condition among the grid cells in the receptor domains for Chicago, Atlanta and New York. In each case, there are grid cells for which P(Ox) is exclusively VOC sensitive that are adjacent to grid cells in which P(Ox) is largely NOx sensitive. This shows that the values in Table 5-3 do not adequately capture the heterogeneity of VOC and NOx sensitive regimes within the receptor domains. Spatial plots of P(Ox) sensitivity to VOC and NOx are not shown here for the S9 case, but if these plots were evaluated, they could be used to determine whether primarily VOC sensitive areas still existed in Chicago or New York for the S9 case. Thus, it is possible that including the PA outputs in model sensitivity simulations could be used to provide additional information both to understand the O3 formation in the sensitivity case and to suggest additional changes in emissions for subsequent sensitivity simulations. Completing the PA analysis can be time consuming and it may not be a good use of resources to perform

this analysis on all sensitivity cases, but it may be useful in selected cases to fine tune control strategies or explain unexpected results in model sensitivity simulations, for example.

The analysis of P(Ox) represents the grid cells where the chemical production occurred. By contrast, DDM and OSAT represent the O_3 concentration sensitivity. The DDM and OSAT results are therefore more appropriate for assessing the sensitivity of O_3 to precursor reductions. However, the process analysis output may be useful for fine-tuning the control strategy. For example, the process analysis indicates grid cells where control of radical sources would be most effective for reducing P(Ox). The IPR analysis in CAMx could be used to determine which species contribute to radical sources in those grid cells. Considerable work is still required to determine if this would be a fruitful analysis.

Figures 5-15 to 5-18 represent total P(Ox) for July 14 and therefore they do not show the temporal variability in the P(Ox) sensitive during the course of the day. However, this temporal variability can be analyzed using PAVE to visualize the processed CPA output file.

Table 5-3a. Ox production sensitivity to precursors for Atlanta receptor region. Units are ppb of Ox production where the sensitivity was determined using the ratio of P(H2O2)/P(HNO3).

Ox Production Category	**July 11**		**July 12**		**July 13**		**July 14**		**July 15**	
	ppb/day	%	ppb/day	%	ppb/day	%	ppb/day	%	ppb/day	%
VOC Sensitive	23	12	26	14	24	14	30	17	25	12
Equal Sensitivity	12	6	14	8	17	10	17	9	11	5
NOx Sensitive	166	83	144	78	128	76	131	73	165	82
Total	200		184		169		179		201	

Table 5-3b. Ox production sensitivity to precursors for Chicago receptor region. Units are ppb of Ox production where the sensitivity was determined using the ratio of P(H2O2)/P(HNO3).

Chicago Ox Production Category	**July 11**		**July 12**		**July 13**		**July 14**		**July 15**	
	ppb/day	%	ppb/day	%	ppb/day	%	ppb/day	%	ppb/day	%
VOC Sensitive	59	72	64	58	80	40	97	36	87	48
Equal Sensitivity	7	9	11	10	28	14	37	15	23	13
NOx Sensitive	15	18	37	33	92	46	121	47	73	40
Total	82		111		200		255		183	

Table 5-3c. Ox production sensitivity to precursors for New York receptor region. Units are ppb of Ox production where the sensitivity was determined using the ratio of P(H2O2)/P(HNO3).

New York Ox Production Category	**July 11**		**July 12**		**July 13**		**July 14**		**July 15**	
	ppb/day	%	ppb/day	%	ppb/day	%	ppb/day	%	ppb/day	%
VOC Sensitive	47	68	50	57	64	42	90	36	73	28
Equal Sensitivity	8	12	11	13	20	13	27	11	24	9
NOx Sensitive	13	19	25	29	70	45	132	53	161	63
Total	69		87		154		249		257	

Table 5-3d. Ox production sensitivity to precursors for Altoona receptor region. Units are ppb of Ox production where the sensitivity was determined using the ratio of P(H2O2)/P(HNO3).

Altoona Ox Production Category	**July 11**		**July 12**		**July 13**		**July 14**		**July 15**	
	ppb/day	%	ppb/day	%	ppb/day	%	ppb/day	%	ppb/day	%
VOC Sensitive	21	25	9	13	12	13	9	7	8	7
Equal Sensitivity	9	11	5	7	4	4	8	6	6	5
NOx Sensitive	55	65	54	79	78	82	119	88	109	89
Total	84		68		95		136		123	

Table 5-4a. S9 sensitivity run: Ox production sensitivity to precursors for Atlanta receptor region. Units are ppb of Ox production where the sensitivity was determined using the ratio of P(H2O2)/P(HNO3).

Ox Production Category	**July 11**		**July 12**		**July 13**		**July 14**		**July 15**	
	ppb/day	%	ppb/day	%	ppb/day	%	ppb/day	%	ppb/day	%
VOC Sensitive	2	2	2	2	2	2	4	5	3	3
Equal Sensitivity	1	1	1	1	1	1	2	2	2	2
NOx Sensitive	95	97	85	96	79	96	82	93	93	97
Total	98		89		83		88		98	

Table 5-4b. S9 sensitivity run: Ox production sensitivity to precursors for Chicago receptor region. Units are ppb of Ox production where the sensitivity was determined using the ratio of P(H2O2)/P(HNO3).

Chicago Ox Production Category	**July 11**		**July 12**		**July 13**		**July 14**		**July 15**	
	ppb/day	%	ppb/day	%	ppb/day	%	ppb/day	%	ppb/day	%
VOC Sensitive	19	21	17	16	13	8	11	6	13	9
Equal Sensitivity	11	12	11	10	8	5	9	5	9	6
NOx Sensitive	61	66	78	73	133	86	165	89	123	84
Total	92		107		154		185		146	

Table 5-4c. S9 sensitivity run: Ox production sensitivity to precursors for New York receptor region. Units are ppb of Ox production where the sensitivity was determined using the ratio of P(H2O2)/P(HNO3).

New York Ox Production Category	**July 11**		**July 12**		**July 13**		**July 14**		**July 15**	
	Ppb/day	%	ppb/day	%	ppb/day	%	ppb/day	%	ppb/day	%
VOC Sensitive	12	18	13	18	11	10	12	8	6	4
Equal Sensitivity	9	13	6	8	8	7	9	6	3	2
NOx Sensitive	45	67	54	74	86	83	133	86	130	94
Total	67		73		105		155		139	

Table 5-4d. S9 sensitivity run: Ox production sensitivity to precursors for Altoona receptor region. Units are ppb of Ox production where the sensitivity was determined using the ratio of P(H2O2)/P(HNO3).

Altoona Ox Production Category	July 11		July 12		July 13		July 14		July 15	
	Ppb/day	%	ppb/day	%	ppb/day	%	ppb/day	%	ppb/day	%
VOC Sensitive	2	4	0	0	0.4	1	0.0	0	0.1	0
Equal Sensitivity	2	4	1	3	0.3	1	0.1	0	0.3	1
NOx Sensitive	42	91	34	97	48	98	69	100	64	99
Total	46		35		49		69		65	

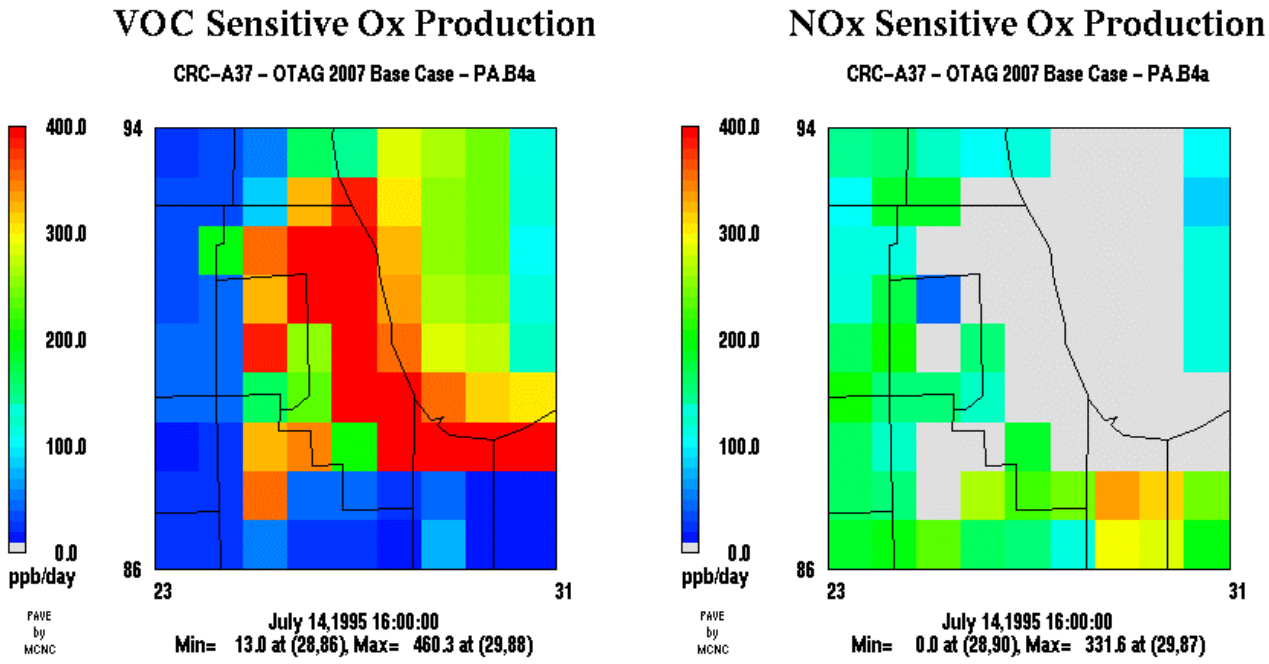

Figure 5-15. Chicago Ox production in VOC sensitive (left) and NOx (right) sensitive regimes for the 2018 base case. The VOC sensitive plot includes Ox produced for equal sensitivity conditions.

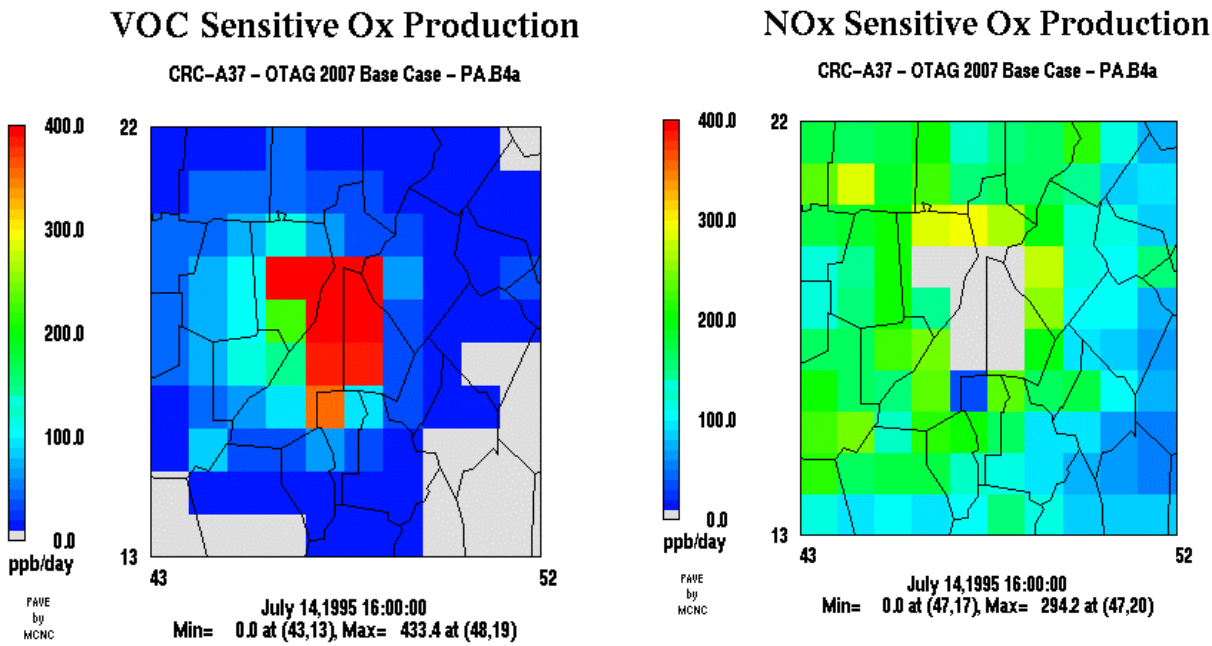

Figure 5-16. Atlanta Ox production in VOC sensitive (left) and NOx (right) sensitive regimes for the 2018 base case. The VOC sensitive plot includes Ox produced for equal sensitivity conditions.

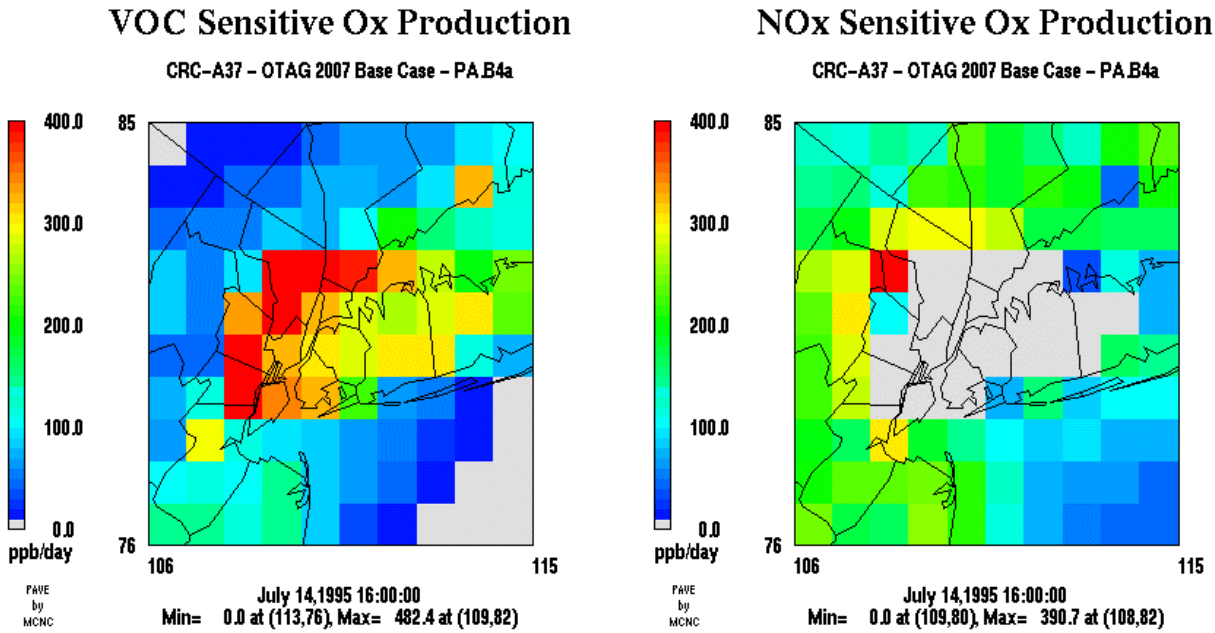

Figure 5-17. New York Ox production in VOC sensitive (left) and NOx (right) sensitive regimes for the 2018 base case. The VOC sensitive plot includes Ox produced for equal sensitivity conditions.

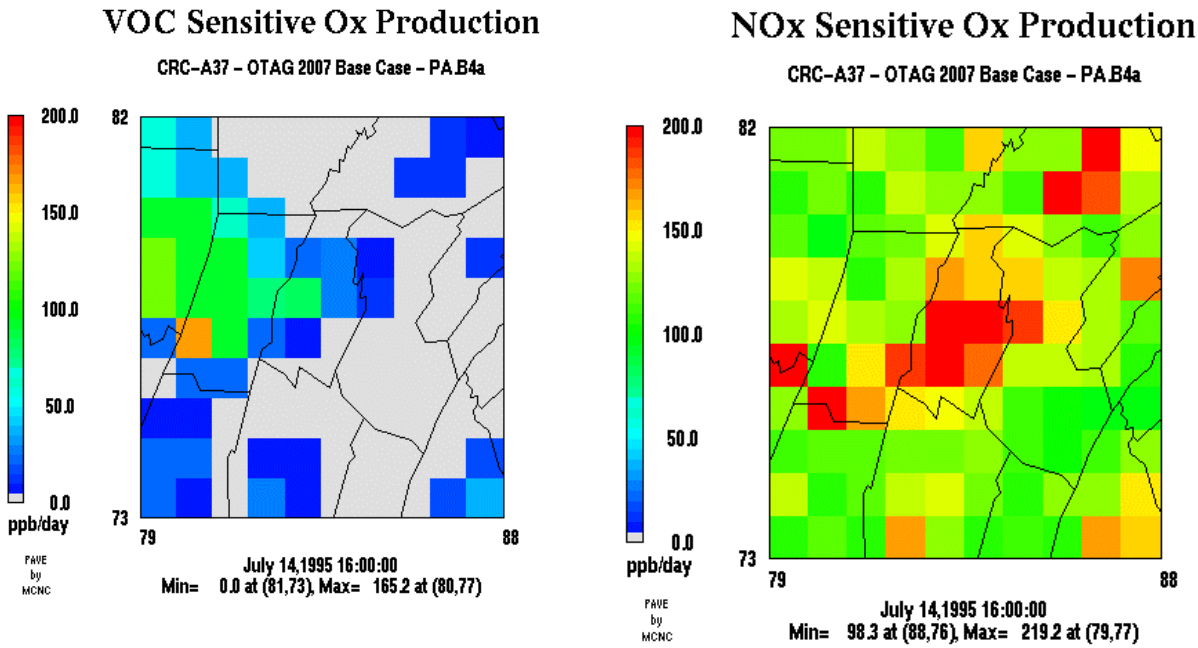

Figure 5-18. Altoona Ox production in VOC sensitive (left) and NOx (right) sensitive regimes for the 2018 base case. The VOC sensitive plot includes Ox produced for equal sensitivity conditions.

IPR TIME SERIES

The integrated process rate (IPR) information output for each receptor area in PA runs P4, S3, S6 and S9 can be extracted and viewed using the post-processing tools described in the CAMx User's Guide. These consist of a FORTRAN program to extract selected information from the binary format *.ipr files produced by CAMx and convert it to a comma-delimited format suitable for spreadsheet analysis, and an Excel macro that prepares three charts from the extracted data.

Time-series of the process contributions (ppb/hr) to the average ozone concentration in each receptor area are shown in Figure 5-19 for the 2007 base case (run B4). The process contributions are averaged over all grid cells in the receptor area for layers 1-5 (surface to 1500m). The contribution of chemistry to ozone formation is generally positive (ozone formation) during the day and negative (ozone destruction) at night. Deposition is always negative because it removes ozone. Transport is resolved by the north, south, east, west and top boundaries of the receptor area and is positive for inflow boundaries and negative for outflow boundaries. The transport terms combine the effects of advection and diffusion. Advection will dominate for the lateral boundaries but diffusion may be important for the top boundary depending upon the depth of the boundary layer. The top of the analysis region for Figure 5-19 was set at 1500 m so that the boundary layer would be mostly contained within the analysis region for more ozone is lost through the top boundary for Atlanta than the other receptor areas, but Figure 5-19 does not show whether this is due to advection or diffusion. Figure 5-20 shows the time averaged process contributions for all model processes in the Atlanta receptor and confirms that ozone is lost through top boundary advection rather than

diffusion. This means that there is frequently a wind convergence zone in the Atlanta receptor that results in upward air movement and loss of ozone from the receptor area through the top of layer 5. Figures 5-19 and 5-20 were produced using the standard IPR post-processing tools described in the CAMx User's Guide (ENVIRON, 2002a).

The total chemical production of ozone in each receptor area through 1500 m is summarized in Table 5-5 for the base case (B4) and the emission reduction cases (runs S3, S6, and S9). This table was prepared by summarizing information in the spreadsheets from Figures 5-19 and 5-20. The table shows how the total ozone production within a receptor volume responded to emission reductions, which is one way of measuring the relative effectiveness of different control strategies. However, it is important to remember that Table 5-5 relates to ozone concentrations in a large volume, which may be different from the response of peak surface ozone concentrations.

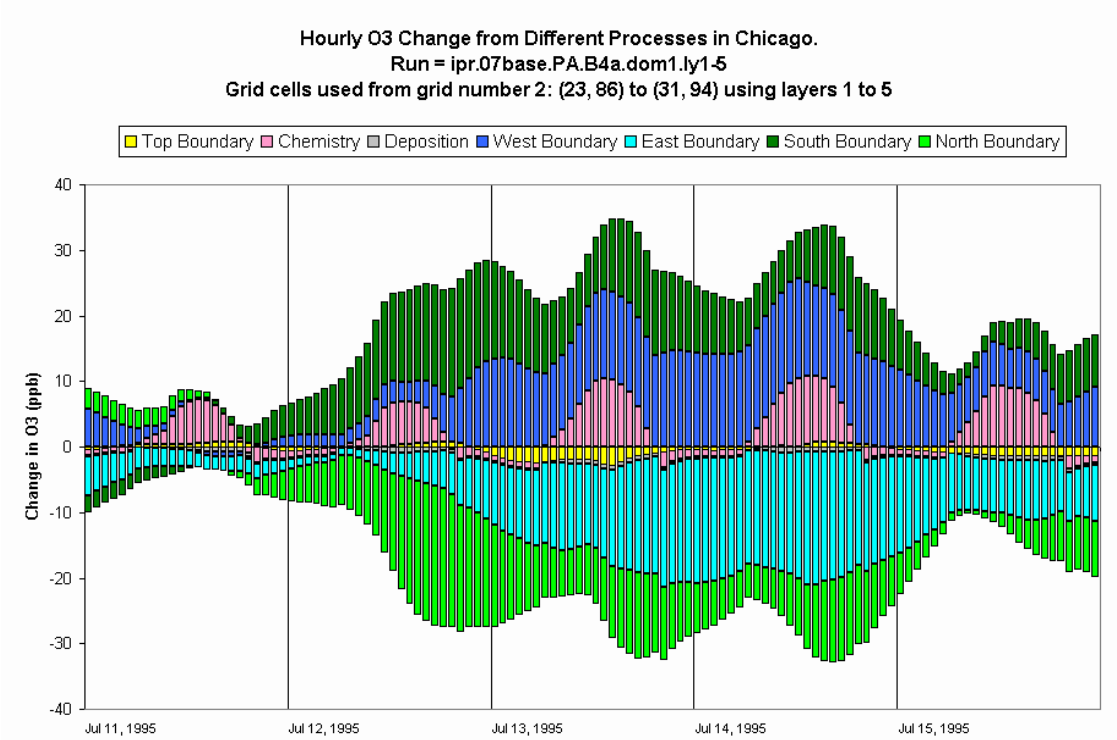

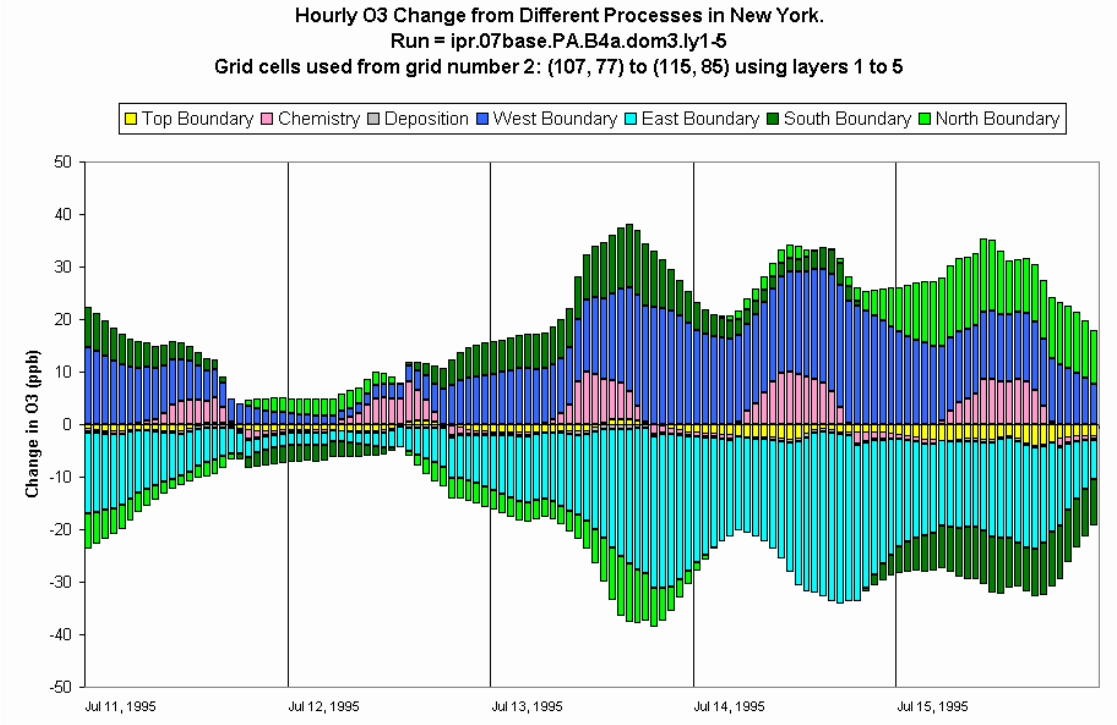

Figure 5-19. Time-series of process contributions (ppb/hr change) to the average ozone concentration in the receptor areas from the surface to 1500m.

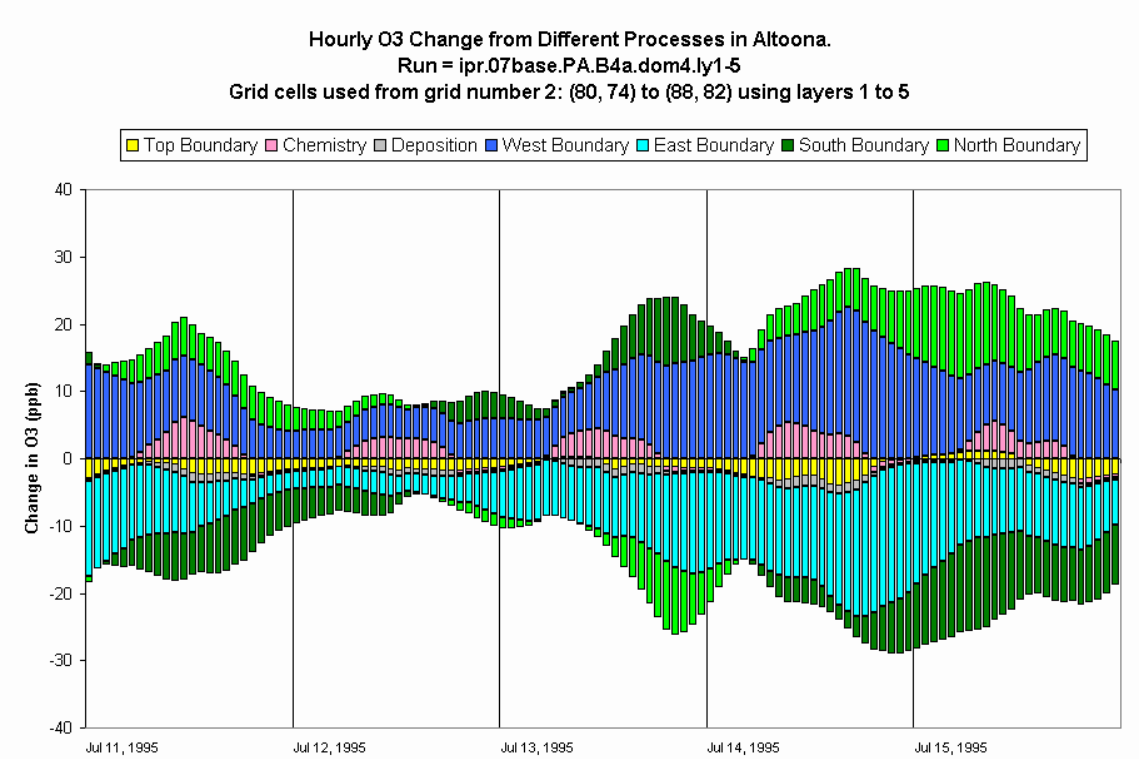

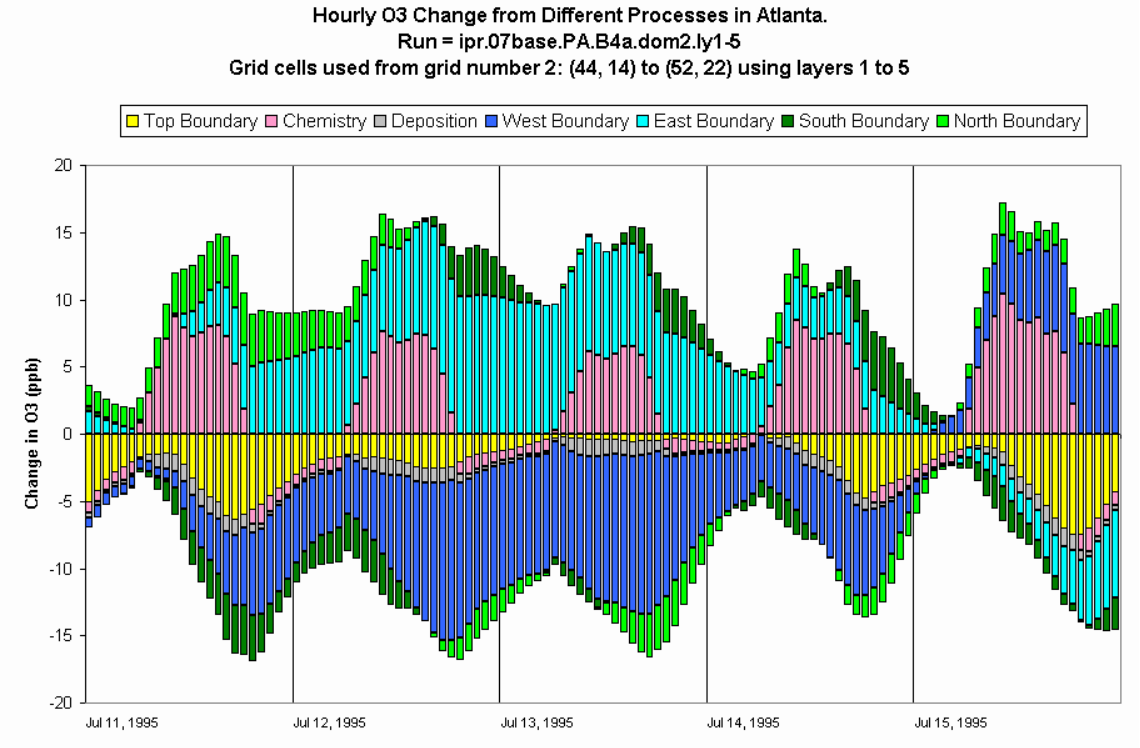

Figure 5-19 (concluded).

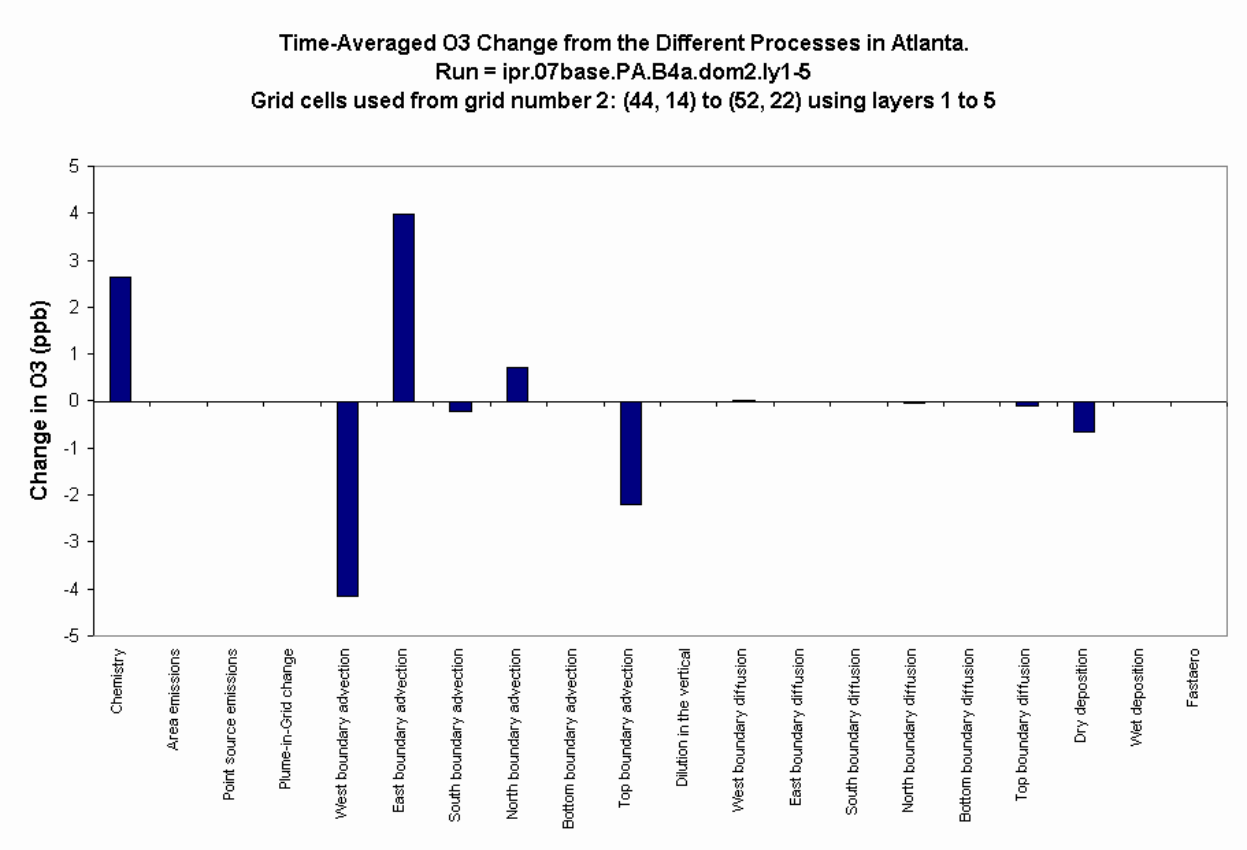

Figure 5-20. Time averaged process contributions (ppb change) to the average ozone concentration in the Atlanta receptor area from the surface to 1500m for July 11-15.

Table 5-5. Total ozone production (ppb/day) in the receptor areas from the surface to 1500m.

	11-Jul	12-Jul	13-Jul	14-Jul	15-Jul
			Total Ozone Production (ppb/day)		
Atlanta					
B4	67.4	58.4	48.5	62.0	80.5
S3	67.1	58.1	48.1	61.4	80.2
S6	59.2	50.9	42.5	54.0	69.7
S9	30.7	24.5	20.9	26.1	34.4
Altoona					
B4	41.4	27.8	34.7	42.5	29.6
S3	40.7	27.5	35.1	42.4	29.6
S6	35.1	23.7	28.1	36.2	24.2
S9	17.5	11.1	13.5	19.2	12.2
Chicago					
B4	36.3	37.2	68.4	77.4	66.6
S3	29.8	34.5	65.9	75.2	63.4
S6	45.3	40.9	70.2	78.1	67.1
S9	37.0	37.9	55.3	58.2	51.1
New York					
B4	25.4	38.1	55.7	74.8	68.7
S3	20.9	32.2	52.9	72.2	67.2
S6	31.3	41.9	51.7	69.6	60.8
S9	24.9	29.5	30.0	40.9	29.5
			Ratio to Base Case (B4)		
Atlanta					
S3	0.99	1.00	0.99	0.99	1.00
S6	0.88	0.87	0.88	0.87	0.87
S9	0.46	0.42	0.43	0.42	0.43
Altoona					
S3	0.98	0.99	1.01	1.00	1.00
S6	0.85	0.85	0.81	0.85	0.82
S9	0.42	0.40	0.39	0.45	0.41
Chicago					
S3	0.82	0.93	0.96	0.97	0.95
S6	1.25	1.10	1.03	1.01	1.01
S9	1.02	1.02	0.81	0.75	0.77
New York					
S3	0.82	0.84	0.95	0.97	0.98
S6	1.23	1.10	0.93	0.93	0.89
S9	0.98	0.78	0.54	0.55	0.43

6. OSAT UPDATES AND COMPARISONS WITH DDM

The Ozone Source Apportionment Technology (OSAT) algorithms implemented in CAMx are described in the CAMx User's Guide (ENVIRON, 2002a) and Dunker et al. (2002b). At the start of this project the OSAT algorithms were updated based on the findings of the OSAT/DDM comparison described in Dunker et al. (2002b). All of the updates relate to the chemistry algorithms, not to the emissions transport or deposition algorithms, which are unchanged. The updates make use of information that is available from the decoupled direct method (DDM) and process analysis (PA) implemented in CAMx by using DDM and PA to gather additional information from the chemistry step in each grid cell at each model time step.

There are three updates to the OSAT chemistry algorithms:

1. Accounting for ozone destruction reactions;
2. Different scheme for apportioning ozone production to VOCs and NOx; and
3. Different reactivity weighting scheme for apportioning ozone production among VOC categories.

All three updates are implemented for OSAT and APCA (Anthropogenic Precursor Culpability Assessment). Only the first update is applicable to GOAT (Geographic Ozone Apportionment Technology) because GOAT does not attempt to assign ozone production to VOCs or NOx, just geographic areas.

ACCOUNTING FOR OZONE DESTRUCTION REACTIONS IN OSAT

The original OSAT algorithm allocated chemical change to ozone tracers based on the total change in ozone (ΔO_3) across a call to the gas-phase chemistry solver. A positive ΔO_3 was equated to ozone production and ozone tracers were incremented according to the OSAT, APCA or GOAT rules for apportioning ozone production. A negative ΔO_3 was equated to ozone destruction and the destruction was applied to all ozone tracers. However, ozone production and destruction mechanisms operate simultaneously within the chemical mechanism (e.g., CB4) and the net change in ozone is the balance of production and destruction. For example, VOC oxidation can be driving photochemical ozone production at the same time as O_3 + VOC reactions are directly consuming ozone, and these processes may lead to a net increase or decrease in ozone depending mainly upon availability of NOx and sunlight. OSAT has been modified to explicitly track several ozone destruction mechanisms as follows:

1. O_3 + VOC reactions since these remove ozone.
2. $O(^3P)$ + VOC reactions since these effectively remove ozone .
3. $O(^1D)$ + H_2O reaction since this effectively removes ozone.
4. HOx + O_3 reactions that do not re-form ozone.

The ozone production is then calculated as ΔO_3 minus the ozone destruction. The OSAT ozone tracers are adjusted first for ozone destruction (applied to all tracers) and second for ozone production (applied using the OSAT, APCA or GOAT rules).

The amount of ozone destruction is calculated using integrated reaction rates obtained using Process Analysis (PA). It is easy to account for processes 1-3 using PA since the ozone destroyed is simply the integrated rates of the reactions involved. Process 4 is less easy to identify but is very important as an ozone destruction mechanism in low NOx (rural) environments. Therefore, accounting for process 4 is important to understanding long range ozone transport.

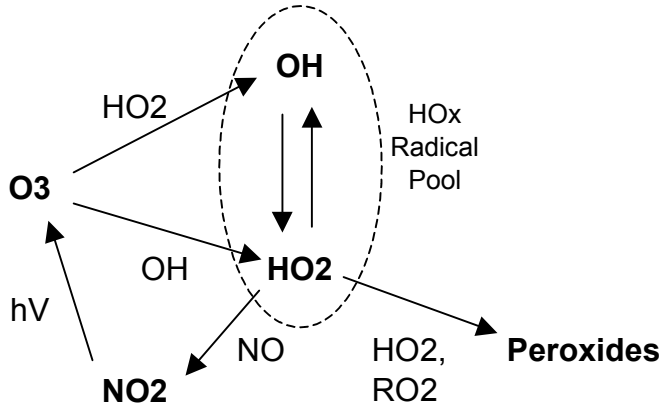

Figure 6-1. Daytime reactions of ozone with HOx (OH and HO_2) showing potential for reformation of ozone or ozone destruction via peroxide formation.

The main reaction pathways between ozone and HOx (OH and HO_2) are shown in Figure 6-1. Ozone reacts directly with both with OH and HO_2:

$$O_3 + OH \rightarrow O_2 + HO_2 \quad (6\text{-}1)$$
$$O_3 + HO_2 \rightarrow 2\ O_2 + OH \quad (6\text{-}2)$$

Since OH and HO_2 radicals inter-convert rapidly during the daytime they can be viewed as a radical pool, called HOx. During the daytime, there are two main sinks for HOx:

(1) *propagation* by reaction with NO, which reforms ozone:

$$NO + HO_2 \rightarrow NO_2 + OH$$
$$NO_2 + h\nu \rightarrow NO + O(^3P)$$
$$O(^3P) + O_2 \rightarrow O_3$$
Net: $$HO_2 + O_2 + h\nu \rightarrow O_3 + OH$$

(2) *termination* by reaction with HO_2 or RO_2 to form peroxides and other organic products, which prevents HOx from propagating to reform ozone:

$HO_2 + HO_2 \rightarrow H_2O_2 + O_2$
$HO_2 + RO_2 \rightarrow ROOH + O_2$
$RO_2 + RO_2 \rightarrow$ organic products $+ O_2$

In the revised OSAT algorithms the ozone destruction rate due to O_3 + HOx reactions is estimated as:

$$Ozone\ Destruction\ Rate = Rate_{(O_3 + HOx)} \times \left(\frac{Rate_{(HO_2\ term)}}{Rate_{(HO_2+NO)} + Rate_{(HO_2\ term)}} \right) \quad (6\text{-}3)$$

This equation is the rate of O_3 + HOx reaction (i.e., the rates of 6-1 plus 6-2) multiplied by a branching ratio that estimates the fraction of O_3 + HOx reactions that result in loss of ozone.

Ozone destruction due to the $O_3 + NO \rightarrow NO_2 + O_2$ titration reaction is explicitly excluded from the accounting of ozone destruction because it is hard to disentangle its role in ozone destruction and production. Under high NOx (ozone titration) conditions and at night this reaction become clearly an ozone destruction pathway, and in these situations ΔO_3 becomes negative and ozone destruction due to the O_3 + NO reaction is accounted for. Under most daytime conditions, this reaction is part of the O_3, NO, NO_2 photo-stationary state and ozone can be reformed again when NO_2 photolyzes so this reaction is not clearly an ozone destruction pathway.

IMPROVED APPORTIONMENT OF OZONE PRODUCTION TO VOCs AND NOx

The original OSAT methods used an indicator ratio (P_{H2O2}/P_{HNO3}) proposed by Sillman to classify grid cells as NOx sensitive or VOC sensitive at each chemistry time step. Limitations of this method include the discrete classification into VOC *or* NOx sensitivity and uncertainty in the value to choose for the indicator ratio cut-point. OSAT has been modified to allocate ozone production in proportion to the local sensitivity of ozone to VOC and NOx in each grid cell at each time step. The required ozone sensitivities are calculated using the DDM implemented in the CAMx CMC chemistry solver. The apportionment of ozone production into VOC-and NOx-sensitive portions is performed by defining:

$$F_{VOC} = \left[\frac{\partial O_3}{\partial VOC} + \left| \frac{\partial O_3}{\partial VOC} \right| \right] \Big/ \left[\frac{\partial O_3}{\partial VOC} + \left| \frac{\partial O_3}{\partial VOC} \right| + \frac{\partial O_3}{\partial NO_x} + \left| \frac{\partial O_3}{\partial NO_x} \right| \right] \quad (6\text{-}4)$$

to be the VOC-sensitive fraction and an analogous ratio to be the NOx-sensitive fraction. Equation (6-4) is used because the sensitivity to NOx (and occasionally to VOC) can be negative, and in such cases all ozone production is allocated to the species with the positive sensitivity. When both sensitivities are positive, ozone production is allocated in proportion to the VOC and NOx sensitivities. Thus, in the old OSAT where ozone production was classified as either VOC-limited or NOx-limited and allocated to either the VOC or NOx tracer precursors present, the new OSAT can allocate ozone formed to both VOC and NOx precursors if the VOC and NOx sensitivities are both positive.

REACTIVITY WEIGHTING FOR VOCs

The original OSAT method quantified the reactivity of VOCs using OH rate constants. The average kOH for VOC emissions from each source group (i.e., emissions from a specific source category/geographic area combination) was calculated as the weighted average kOH over all emissions for the source group for the duration of the model run (usually one day). This average kOH was used both to decay the VOC tracers for each source group (Vi) and to increment the VOC-sensitive ozone tracer for each source group (O3Vi). In the updated OSAT schemes, the decay of VOC tracers is still based on kOH reactivities as follows:

$$V_i = V_i + \Delta VOC \times \left(\frac{V_i \times kOH_i}{\sum (V_i \times kOH_i)} \right) \qquad (6\text{-}5)$$

but the apportionment of VOC sensitive ozone production is based on maximum incremental reactivity (MIR) factors:

$$O3V_i = O3V_i + \Delta O3V \times \left(\frac{V_i \times MIR_i}{\sum (V_i \times MIR_i)} \right) \qquad (6\text{-}6)$$

The MIRs used in equation (6-6) are the weighted average MIRs for the emissions in each source group. The MIR approach was developed by Carter (1994) to approximate the ozone forming potential of VOCs accounting for both kinetic and mechanistic reactivity effects. The MIR represents the ozone formation potential of the VOC mixture accounting for the VOC reactions with OH as well as the effects of all of the VOC products that produce ozone formation. The VOC + OH reaction is still the main VOC destruction mechanism so it is still more appropriate to weight the VOC destruction across the VOC reactive tracers by their composite reaction rate with OH (kOH). The MIR factors for the CAMx CB4 mechanism are shown in Table 6-1 and were calculated in a recent study for the NARSTO Reactivity Research Working Group (Carter, Tonnesen and Yarwood, 2002).

Table 6-1. Reactivity parameters for CB4 species used in the revised OSAT algorithms.

CB4 Species	Number of Carbons	kOH (ppm^{-1} min^{-1})	MIR factor
PAR	1	1203	0.3458
OLE	2	42000	4.831
ETH	2	11920	2.328
TOL	7	9150	0.5139
XYL	8	36200	2.383
FORM	1	15000	5.771
ALD2	2	24000	3.007
ISOP	5	142000	4.375
MEOH	1	1363	0.4101
ETOH	2	4791	0.665

BOX MODEL COMPARISON OF OSAT AND DDM RESULTS

OSAT ozone apportionments were calculated in a box model to test the updates to the OSAT algorithms. DDM sensitivities were calculated at the same time so that the OSAT and DDM results could be compared in a situation where chemistry is the only process taking place. The comparison of OSAT and DDM in a photochemical grid model by Dunker et al. (2002b) found differences in the magnitude of OSAT source apportionments and DDM sensitivities. Some of the differences were explained, such as the lack of decay for OSAT apportionments, leading to the improvements in the OSAT algorithms described above. Other differences were not understood, and comparisons for the simplified conditions of a box model (compared to a grid model) may be informative.

The base case box model scenario was configured with the only source of ozone and precursors being the initial conditions only. There were no emissions, and no dilution (i.e., the volume of the box was constant). The initial conditions were ozone of 40 ppb, VOC of 2 ppmC (urban mix), CO of 1.0 ppm, NO of 167 ppb and NO_2 of 33 ppb. This gives an initial VOC/NOx ratio of 10 (ppmC/ppm), which should be intermediate between VOC and NOx-limited and optimal for high ozone production over the course of a day. The chemical evolution of this mixture was simulated for 12 hours (6 am to 6 pm) with mid-summer, clear sky photolysis conditions. The temperature was a constant 298 K and the humidity was 20,000 ppm of water.

Time Series Analysis

The time evolution of the total ozone, OSAT source apportionments and DDM sensitivities in the base case box model scenario is discussed below. Source apportionments for the old and new OSAT runs are compared to evaluate the effect of the OSAT updates.

Old OSAT

The time series of ozone (at the end of each hour) for the box model test case is shown by the line in Figure 6-2. The starting ozone concentration of 40 ppb is initially reduced by reaction with NO but then rises as ozone is formed from reactions of the initial NOx and VOC. The final ozone concentration is 148 ppb. The box model ozone was apportioned using the old OSAT algorithm as shown by the stacked bars in Figure 6-2. OSAT exactly explains the ozone at all times in terms of the sum of remaining initial ozone, ozone production attributed to VOCs and ozone production attributed to NOx. The initial ozone of 40 ppb is reduced to 28 ppb during the first hour, but then the old OSAT algorithm identified no further ozone destruction because ΔO_3 was always positive. Ozone production was initially attributed to VOCs and then later attributed to NOx. The transition from VOC-limited to NOx-limited ozone formation[1] was diagnosed using the (P_{H2O2}/P_{HNO3}) indicator ratio and occurred between hours 11 and 12. The amount of VOC-limited ozone (80 ppb) produced during the morning

[1] Sometimes the terms VOC-sensitive and NOx-sensitive are used in place of VOC-limited and NOx-limited, but the word "limited" is chosen here to avoid confusion with DDM sensitivity coefficients.

remained constant throughout the afternoon because no ozone destruction was identified. The final ratio of VOC-limited ozone (O3V) to NOx-limited ozone (O3N) was 80:41 (about 2).

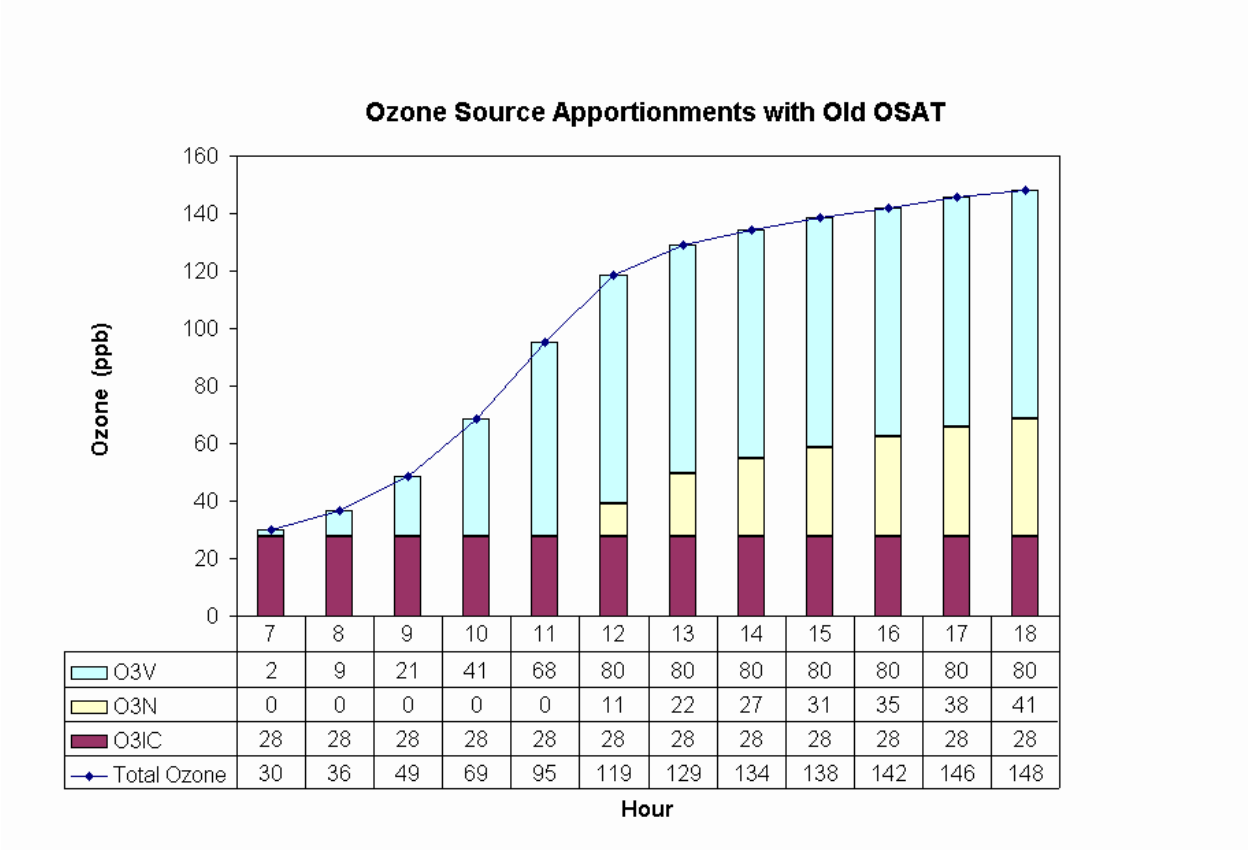

	7	8	9	10	11	12	13	14	15	16	17	18
O3V	2	9	21	41	68	80	80	80	80	80	80	80
O3N	0	0	0	0	0	11	22	27	31	35	38	41
O3IC	28	28	28	28	28	28	28	28	28	28	28	28
Total Ozone	30	36	49	69	95	119	129	134	138	142	146	148

Figure 6-2. Ozone time series for the box model test case with ozone apportioned to initial VOC, NOx and Ozone using the old OSAT algorithm.

DDM

First-order DDM sensitivity coefficients for the box model test case are shown in Figure 6-3. Sensitivities were calculated to the initial VOC, NOx and ozone. CO was classified as a VOC so that the sensitivity to the initial CO is included in the VOC sensitivity. These three sensitivities describe all of the first-order sensitivity to ozone and precursors for this test case. The sum of the first-order sensitivities does not equal the total ozone because there are higher-order sensitivities (quadratic terms, etc.) that are important. The sum of higher-order sensitivities equals the difference between the total ozone and the sum of the first-order sensitivities and is shown by "Other" in Figure 6-3.

The sensitivity to initial ozone decreases more slowly in the early morning than the OSAT contribution of initial ozone. This is because the DDM describes the scavenging of initial ozone by NOx as a negative sensitivity of ozone to NOx, whereas OSAT decreased the initial ozone tracer. The negative sensitivity of ozone to NOx during the morning makes it harder to see that the sum of the stacked bars does equal the total ozone in Figure 6-3. The sensitivity of ozone to NOx grows more negative through hour 11 but then starts to grow less negative and becomes positive by hour 13. The timing of the transition from negative to positive

sensitivity to NOx is consistent with the time at which OSAT starts to attribute ozone formation to NOx. During the morning, large negative sensitivity to NOx is offset by large positive sensitivity to VOC. From hours 7 to 11, the combined sensitivity to initial VOC and ozone exceeds the total amount of ozone present, because of the large negative NOx sensitivity. The transition from negative to positive NOx sensitivity between hours 11 and 13 is accompanied by a rapid decrease in the sensitivity to VOC and initial ozone. The rates of attenuation of DDM sensitivities to initial ozone and VOC between hours 11 and 14 correspond to lifetimes of 4.6 and 3.9 hours, respectively. The final ratio of VOC to NOx sensitivity is 40:42 (about 1). At the end of the day the "other" sensitivities are larger in magnitude than any first-order sensitivity and describe about 35% of the total sensitivity, which is similar to grid model results (Dunker at al., 2002b).

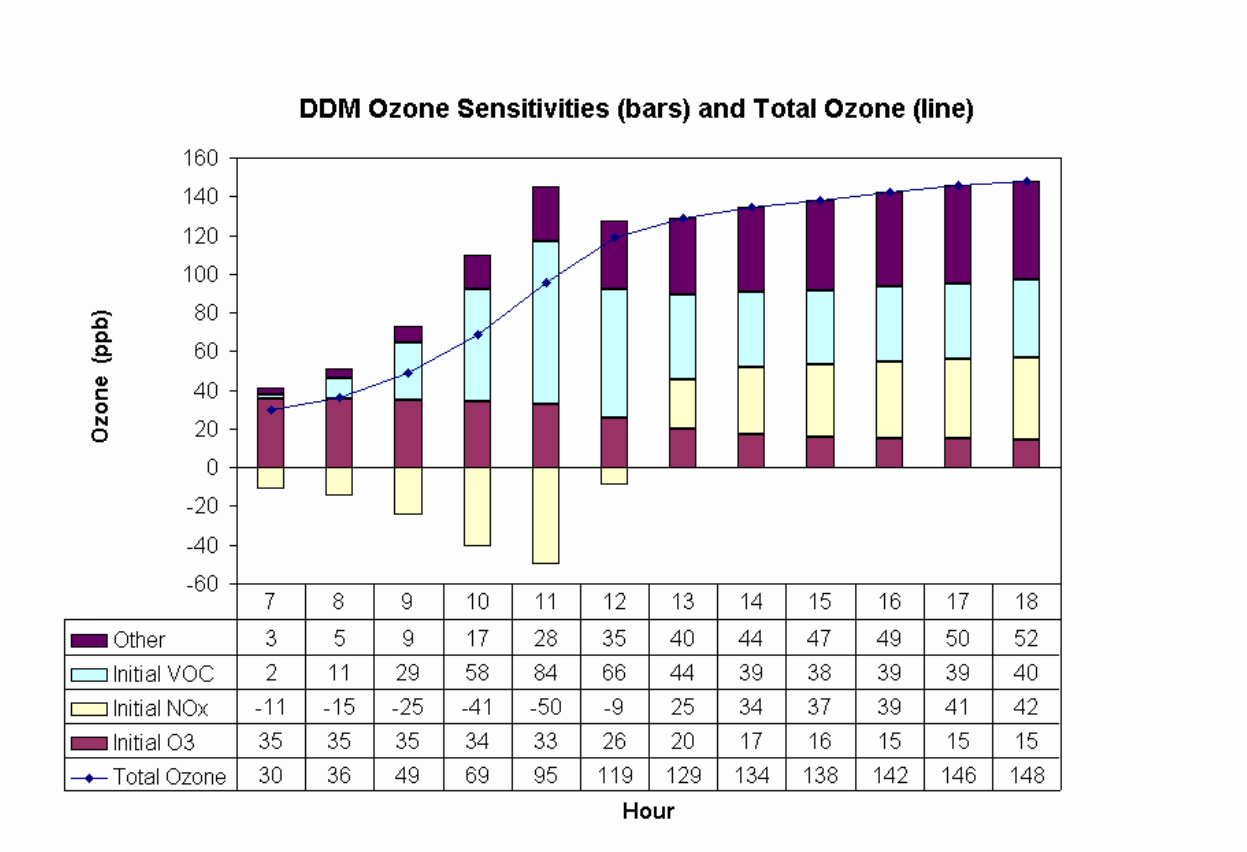

	7	8	9	10	11	12	13	14	15	16	17	18
Other	3	5	9	17	28	35	40	44	47	49	50	52
Initial VOC	2	11	29	58	84	66	44	39	38	39	39	40
Initial NOx	-11	-15	-25	-41	-50	-9	25	34	37	39	41	42
Initial O3	35	35	35	34	33	26	20	17	16	15	15	15
Total Ozone	30	36	49	69	95	119	129	134	138	142	146	148

Figure 6-3. Ozone time series for the box model test case with first-order sensitivities to initial VOC, NOx and Ozone using the DDM. "Other" shows the combined higher-order sensitivities that were not calculated.

Comparing DDM and Old OSAT

- Titration of initial ozone by NOx emissions leads to reduction of the initial ozone tracer from 40 to 28 ppb between hours 6 and 7 in OSAT. The DDM sensitivity to initial ozone is only reduced from 40 to 35 ppb at this time, but a negative sensitivity to NOx emissions of –11 ppb is created by DDM between hours 6 and 7. OSAT responds to titration of ozone by NO by decaying the existing ozone tracers, whereas DDM describes the titration mainly as a negative sensitivity to NO (or NOx, depending upon which sensitivities are calculated).

- Inhibition of ozone formation by NOx between hours 6 and 11 is indicated by a growing negative DDM sensitivity to NOx during this time period, which reaches –50 ppb by hour 11. This growth in negative DDM NOx sensitivity is accompanied by a growth of positive DDM VOC sensitivity because the NOx inhibition period also is the time when ozone formation is strongly VOC-limited. Between 6 and 11, OSAT attributes all of the ozone production to VOC and none to NOx. OSAT and DDM agree that ozone production is VOC-limited between hours 6 and 11, but DDM clearly shows the NOx inhibition effect whereas OSAT does not directly show this effect.

- OSAT sensitivities always add up to the total ozone by definition, DDM (first-order) sensitivities add up to less than the total ozone because of the contribution of higher order sensitivities.

- At times when the sensitivity to NOx is negative, it is possible for the sum of the other first-order sensitivities to be greater than the total ozone.

- With old OSAT, ozone apportionments do not decay chemically unless they encounter net ozone destruction conditions, whereas DDM sensitivities can be attenuated rapidly even as total ozone is increasing. The rates of attenuation of DDM sensitivities to initial ozone and VOC between hours 11 and 14 correspond to lifetimes of 4.6 and 3.9 hours, respectively.

- The rapid attenuation of DDM sensitivity to initial ozone at midday can not be interpreted as chemical decay of the initial ozone. A physical interpretation is that if the initial ozone were reduced by X, the total ozone would decrease by less than X because ozone production from precursors would increase and partially compensate. Radical production from ozone and VOC is a potential mechanism for this effect whereby decreased radical production from ozone could be compensated by more effective use of radicals produced from VOCs, and vice-versa. Therefore, the rapid decline in first-order sensitivity to initial ozone should be associated with a growth in one or more higher-order sensitivities (not calculated here) to initial ozone or interaction(s) between initial ozone and precursors. This interpretation is consistent with the growing size of the “other” bar in Figure 6-3 around midday.

New OSAT

The apportionment of ozone to initial VOC, NOx and ozone using the updated OSAT algorithm is shown in Figure 6-4. The OSAT updates were described above. Because only one VOC apportionment is tracked in this case (initial VOC) the update to VOC reactivity weighting is not relevant. The ozone decay and VOC vs. NOx apportionment updates are probed by this test case. Differences from the old OSAT result are:

- Ozone from initial conditions decays slowly throughout the day rather than remaining constant after the first hour as in old OSAT. The decay is most rapid during the middle of the morning with new OSAT whereas the DDM sensitivity to initial ozone decays most rapidly in the middle of the day. The decay lifetime of initial ozone between hours 8 and 11 is 24 hours with new OSAT compared to 4.6 hours between hours 11 and 14 with

DDM. The final ozone associated with initial ozone is 20 ppb with new OSAT compared to 28 ppb with old OSAT and 15 ppb with DDM.

- The ozone decay scheme in new OSAT also affects the VOC-limited ozone formed during the morning hours. The peak VOC-limited ozone contribution of 77 ppb at hours 12 and 13 decays to 73 ppb at hour 18.

- The change in the scheme used to apportion ozone production between VOCs and NOx (from the (P_{H2O2}/P_{HNO3}) indicator ratio to equation 6-4 using DDM sensitivities) has little impact on the timing of ozone attribution to VOC and/or NOx. The new scheme apportions a small amount of ozone to NOx during the early morning, compared to none with the old scheme. Both schemes attribute the bulk of afternoon ozone production to NOx. The transition from VOC to NOx attribution occurs between hours 11 and 12 with both schemes.

- The final ratio of VOC-limited to NOx-limited ozone is 73/55 (about 1.3) compared to 2 in old OSAT and 1 in DDM. The main reason for the drop from 2 to 1.3 between old and new OSAT is the introduction of ozone decay, not the change in scheme used to apportion ozone production between VOCs and NOx, as shown below.

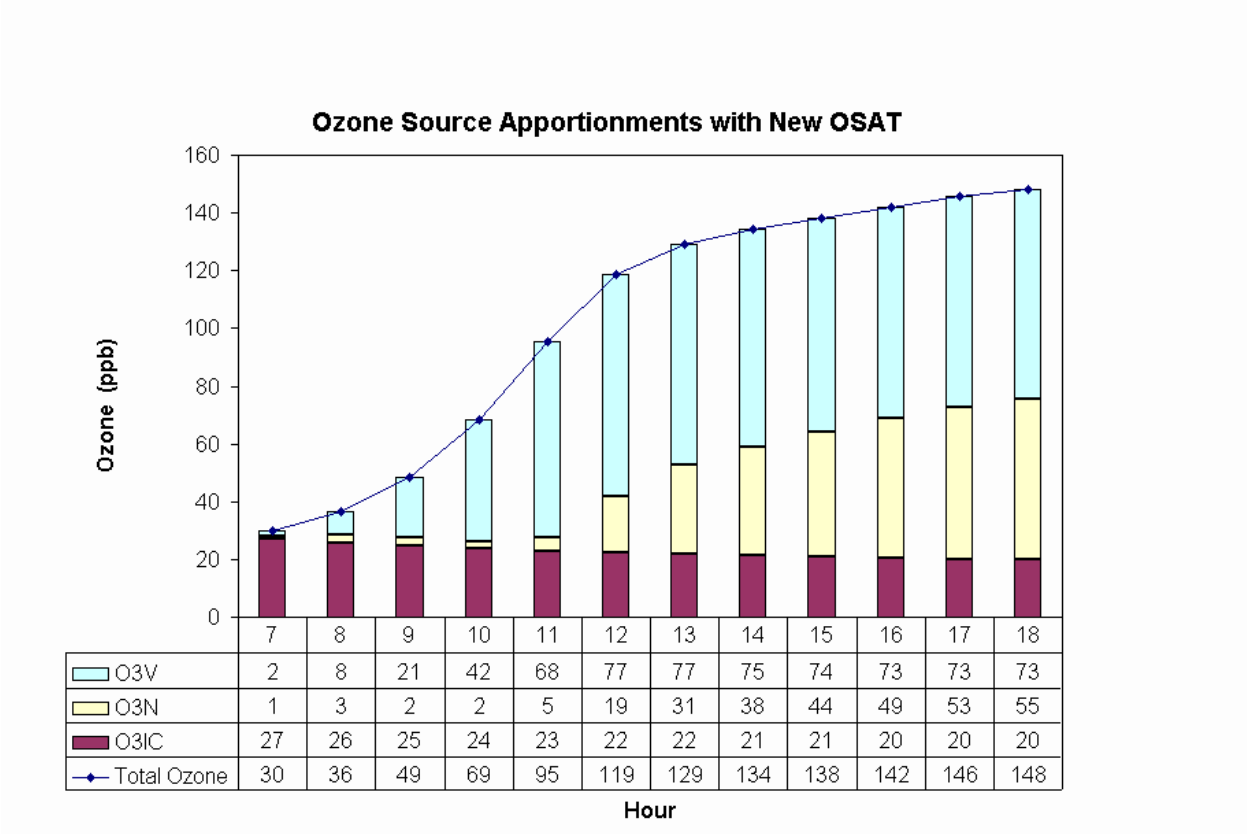

	7	8	9	10	11	12	13	14	15	16	17	18
O3V	2	8	21	42	68	77	77	75	74	73	73	73
O3N	1	3	2	2	5	19	31	38	44	49	53	55
O3IC	27	26	25	24	23	22	22	21	21	20	20	20
Total Ozone	30	36	49	69	95	119	129	134	138	142	146	148

Figure 6-4. Ozone time series for the box model test case with ozone apportioned to initial VOC, NOx and Ozone using the new OSAT algorithm.

Test of New OSAT with the Old Indicator Ratio

In the new OSAT, the scheme used to apportion ozone production between VOCs and NOx was changed from the (P_{H2O2}/P_{HNO3}) indicator ratio to equation 6-4. As just discussed, this update appeared to have little impact on the box model test results. To confirm this, the new OSAT was run with the old indicator ratio scheme. This comes down to adding ozone decay to the old OSAT. The apportionment of ozone to initial VOC, NOx and ozone using this hybrid OSAT algorithm is shown in Figure 6-5. Differences from the new OSAT result shown in Figure 6-4 are minor. The final ratio of VOC-limited to NOx-limited ozone is 75/53 compared to 73/55 in Figure 6-5. The transition between allocating ozone production predominantly from VOCs to NOx occurs between 11 and 12 with both schemes. The ratio of VOC-limited to NOx-limited ozone at hour 12 is 83/13 compared to 77/19.

The main difference between Figures 6-4 and 6-5 is that the new OSAT (equation 6-4) attributes a small amount of ozone production to NOx during the morning, whereas the (P_{H2O2}/P_{HNO3}) indicator attributes zero ozone production to NOx during the morning. The new OSAT result is unexpected given that in Figure 6-3 the DDM sensitivity to NOx is negative during the morning which would result in equation 6-4 attributing all ozone production to VOC. However, the new OSAT is not using the DDM sensitivities shown in Figure 6-4, but rather is calculating instantaneous sensitivities to VOC and NOx at each chemistry time-step with no memory of sensitivities from earlier time-steps. Close inspection of Figure 6-4 shows that the new OSAT builds a small amount of ozone attributed to NOx (3 ppb) between hours 7 and 8 but then does not attribute more ozone to NOx until midday. The 3 ppb ozone attributed to NOx between hours 7 and 8 is due to NO_2 (formed from ozone NO titration) photolysing to form ozone. In the early morning, the (P_{H2O2}/P_{HNO3}) indicator behaves more reasonably than equation 6-4 because it appropriately attributes zero ozone production to NOx during a period that clearly is VOC-limited.

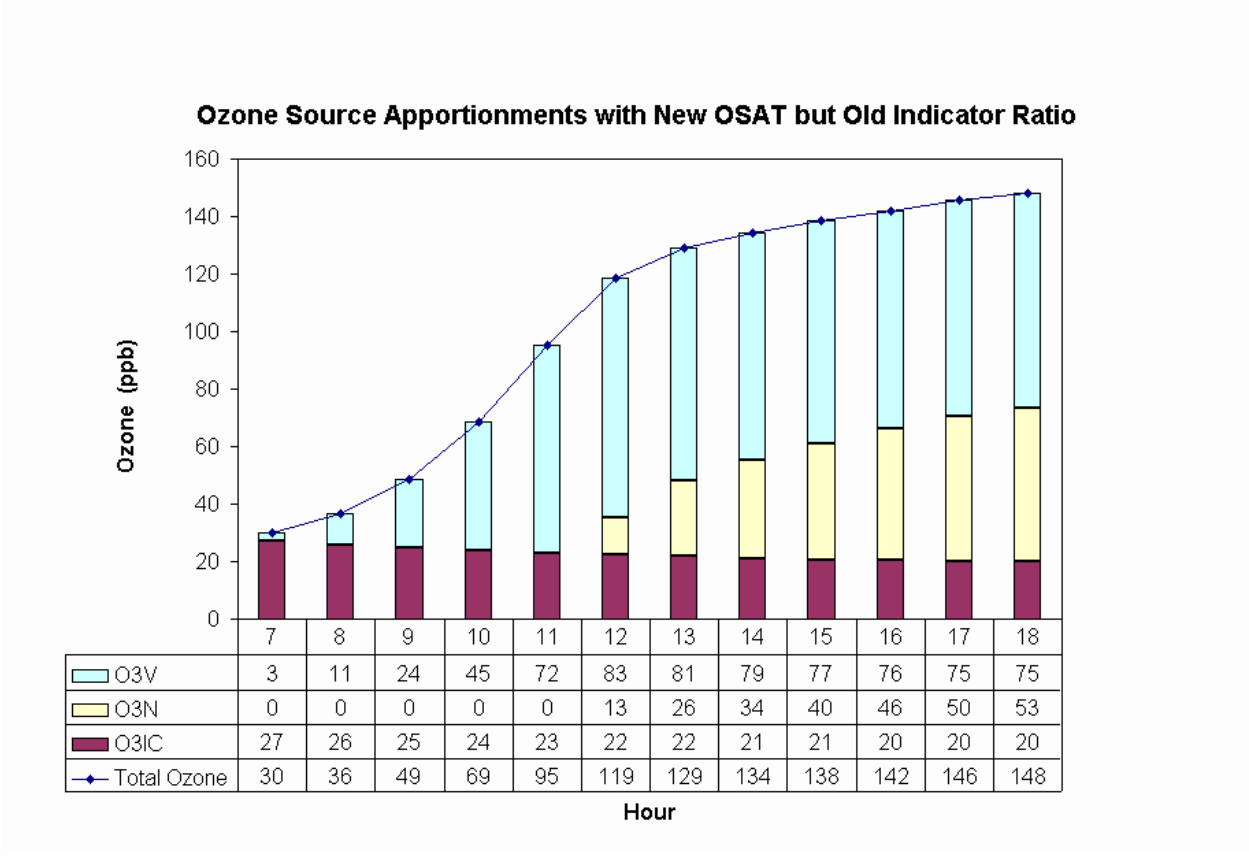

	7	8	9	10	11	12	13	14	15	16	17	18
O3V	3	11	24	45	72	83	81	79	77	76	75	75
O3N	0	0	0	0	0	13	26	34	40	46	50	53
O3IC	27	26	25	24	23	22	22	21	21	20	20	20
Total Ozone	30	36	49	69	95	119	129	134	138	142	146	148

Figure 6-5. Ozone time series for the box model test case with ozone apportioned to initial VOC, NOx and Ozone using the new OSAT algorithm but with the old (P_{H2O2}/P_{HNO3}) indicator ratio.

RESPONSES SURFACES FOR OZONE, OSAT AND DDM

The initial VOC and NOx levels in the box model run (described above) were varied to investigate the response of total ozone (i.e., and EKMA diagram), OSAT apportionments and DDM sensitivities. A matrix of 64 runs was completed with VOC and NOx levels independently scaled by factors of 1/8, 1/4, 3/8, 1/2, 5/8, 3/4, 7/8 and 1. The ozone response surface at hour 15 is shown in Figure 6-6. This figure shows the classic EKMA diagram response with VOC-limited condition on the left separated by a ridgeline of maximum ozone from the NOx-limited condition on the right. The highest ozone level occurred for the base case simulation (discussed above) with 2 ppmC VOC, 200 ppb NOx and a VOC/NOx ratio of 10.

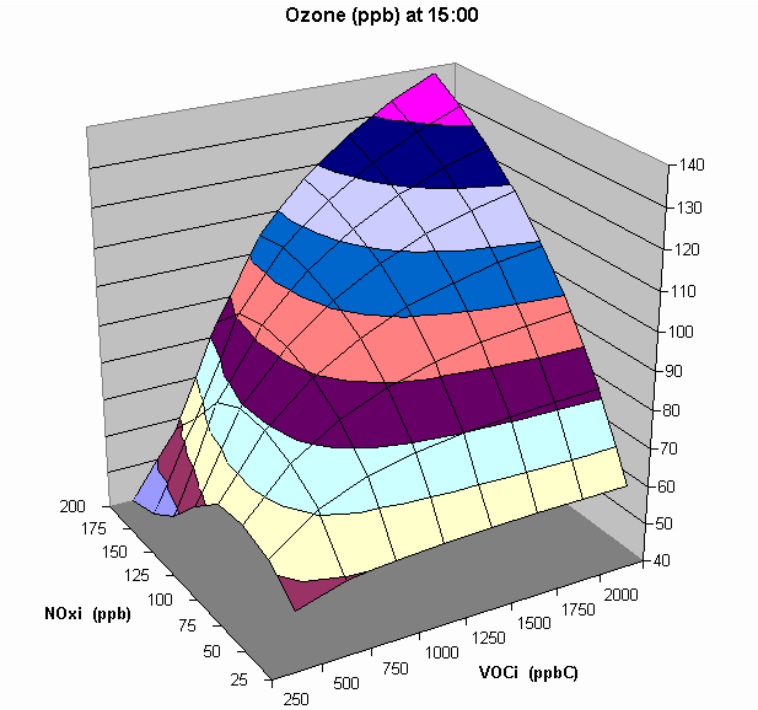

Figure 6-6. Response surface for ozone (ppb) at 15:00 to initial VOC and NOx

The response surfaces for DDM sensitivities and OSAT source apportionments are compared in Figure 6-7. All surfaces are for the same time and conditions as the ozone response surface in Figure 6-6. Sensitivities and source apportionments are shown for the initial VOC, initial NOx and initial ozone. As shown above, the first-order DDM sensitivities do not describe all of the ozone and the sum of the higher-order sensitivities is shown in Figure 6-8.

Comparing the OSAT and DDM response surfaces reveals the same features already seen above in the time series comparisons.

- Under strongly VOC-limited conditions the ozone sensitivity to NOx is strongly negative whereas the OSAT apportionment to NOx is small (new OSAT) or zero (old OSAT).

- Under strongly VOC-limited conditions the ozone sensitivity to VOC is maximized and is larger in magnitude than the old and new OSAT apportionments to VOC.

- Under NOx-limited conditions and near the ridgeline the ozone sensitivity to NOx appears similar to, but is slightly smaller than, the new OSAT apportionment to NOx (also shown in Figure 6-9a, discussed below).

- Under NOx-limited conditions and near the ridgeline the ozone sensitivity to VOC appears quite different from, and is smaller than, the new OSAT apportionment to NOx (also shown in Figure 6-9b, discussed below).

- The ozone sensitivity to initial ozone is different from the OSAT apportionment to initial ozone, regardless of whether ozone decay is accounted for in OSAT (i.e., old and new

OSAT). The largest difference is the strong positive sensitivity to initial ozone under strongly VOC-limited conditions where the magnitude of the sensitivity to initial ozone can exceed the intial ozone concentration (40 ppb).

- Accounting for ozone decay in new OSAT decreases the apportionment to initial ozone, decreases the apportionment to VOC and increases the apportionment to NOx (it was shown above that these changes are due to the ozone decay update).

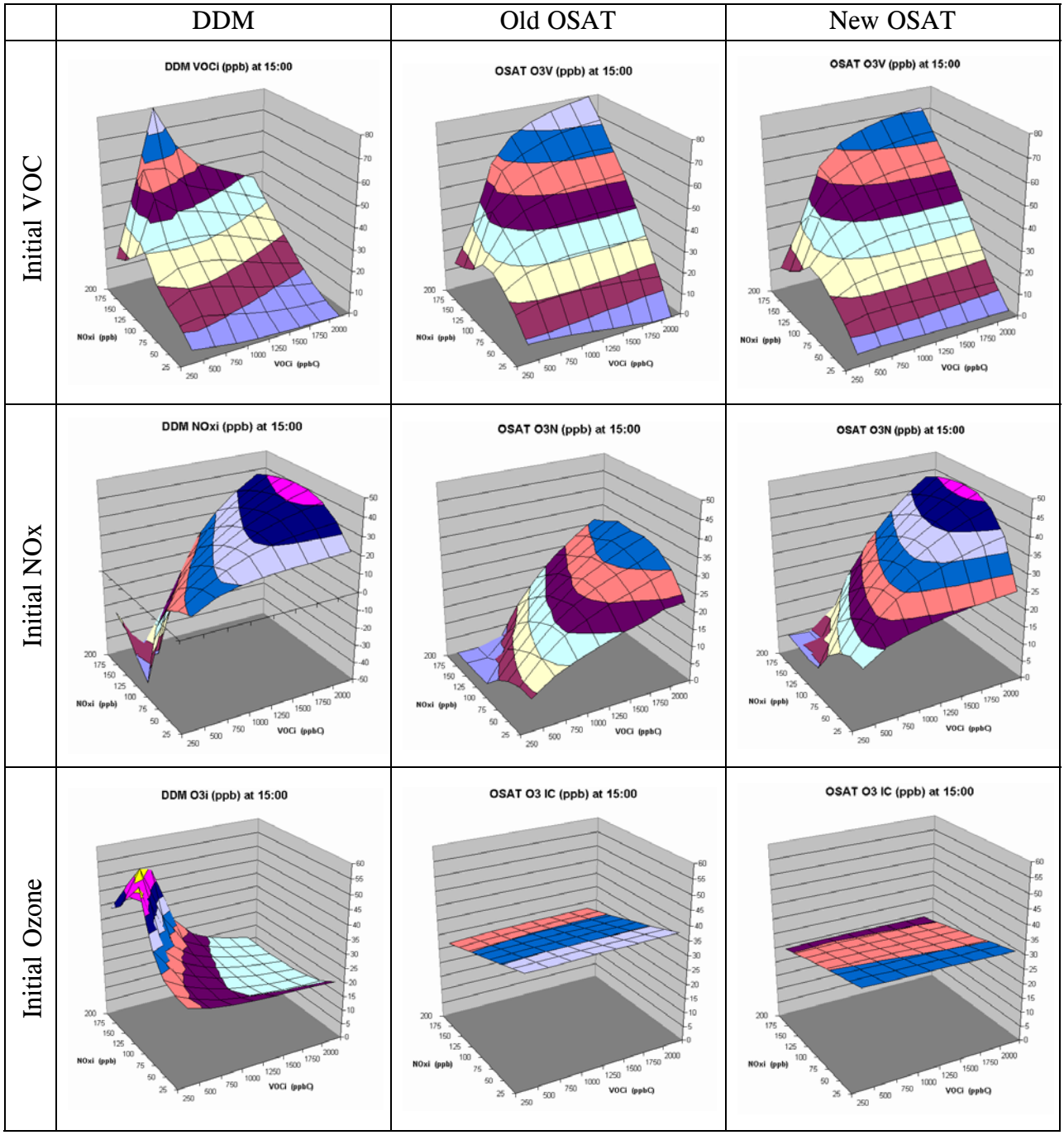

Figure 6-7. Response surfaces for ozone sensitivities/apportionments at 15:00 (ppb) to initial VOC and NOx for DDM, old OSAT and new OSAT.

The DDM sensitivities of O_3 to VOC and NOx shown in Figure 6-7 are the partial derivatives $\partial O_3/\partial VOC$ and $\partial O_3/\partial NOx$ of the ozone response surface shown in Figure 6-6. This provides a topological interpretation of the sensitivities as describing the shape of the ozone response surface.

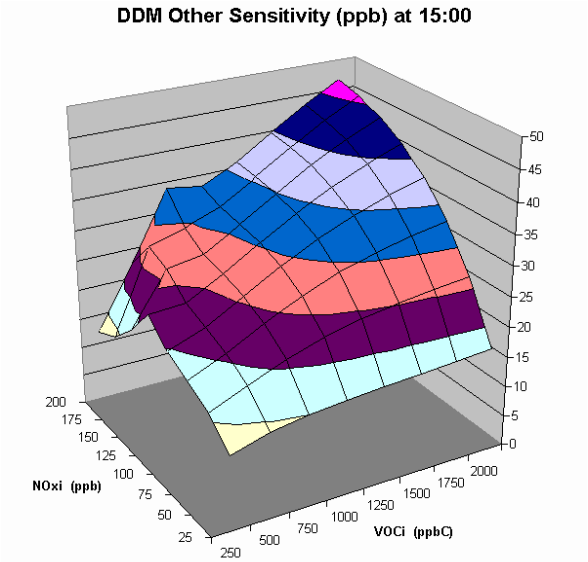

Figure 6-8. The DDM other sensitivity at 15:00 (ppb) as a function of initial VOC and NOx. Other sensitivity means the sum of higher-order ozone sensitivities.

The sensitivities/apportionments to VOC and NOx at hour 15 in the 64 box model runs are directly compared using scatter plots in Figure 6-9. The scatter plots show that OSAT apportionments to NOx are always larger than the sensitivity to NOx and that OSAT apportionments to VOC generally are larger than DDM sensitivities to VOC. The general tendency for OSAT apportionments to be larger than corresponding DDM sensitivities is because the contribution of higher-order sensitivities (Figure 6-8) is not accounted for in the comparison. The differences between OSAT apportionments and DDM sensitivities are greatest under strongly VOC-limited conditions, as discussed above.

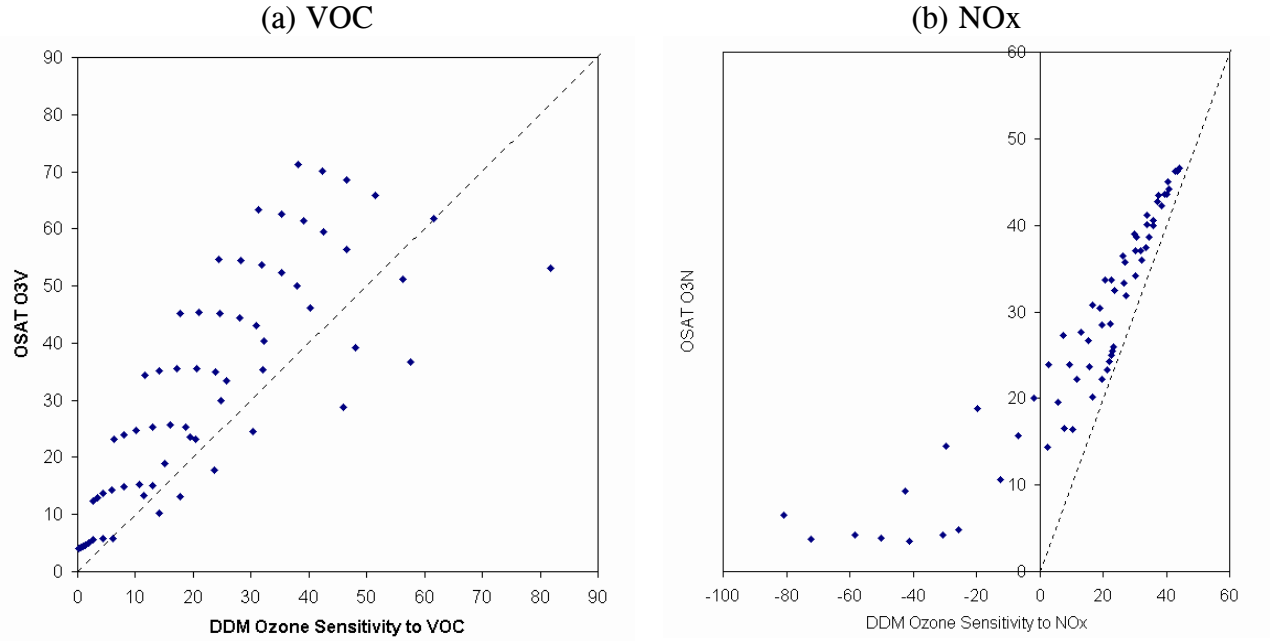

Figure 6-9. Comparison of new OSAT apportionments and DDM sensitivities of ozone to VOC and NOx in 64 box model scenarios with different levels of VOC and NOx.

ESTIMATING RESPONSE TO PRECURSOR REDUCTIONS WITH DDM AND OSAT

The ozone response surface shown in Figure 6-4 was calculated from a matrix of 64 box model runs that independently varied the initial VOC and NOx between 25% and 100% of the base level. These runs can be used like a base case and 63 control strategies to evaluate what happens when the base case apportionments/sensitivities are used to estimate the expected ozone level with reduced precursors. Equations 6-7 and 6-8 show how to estimate the ozone at hour 15 with different precursor levels using the OSAT and DDM results from the base case:

$$\text{New OSAT estimated ozone (ppb)} = 20.66 + 43.62\alpha + 74.08\beta \quad (6\text{-}7)$$

$$\text{DDM estimated ozone (ppb)} = 138.36 + 38.22\,(\alpha - 1) + 37.4\,(\beta - 1) \quad (6\text{-}8a)$$

$$= 62.74 + 38.22\,\alpha + 37.4\beta \quad (6\text{-}8b)$$

Where:

α = VOC scaling factor (base case = 1; zero out = 0)
β = NOx scaling factor (base case = 1; zero out = 0)

The coefficients in the OSAT equation are the base case source apportionments to initial ozone, O3V and O3N (respectively) as shown in Figure 6-4. The coefficients in the DDM equation 6-8a are the total ozone and the sensitivities to VOC and NOx (respectively) shown in Figure 6-3. Equation 6-8b rearranges terms in 6-8a to obtain the same form as equation 6-7 to allow direct comparisons of coefficients between OSAT and DDM. Both equations approximate the actual ozone response surface (Figure 6-6) as plane that passes through the

base case ozone level (the top right corner in Figure 6-6). The DDM equation describes a plane that is tangential to the ozone response surface at the base case point. The plane described by the OSAT equation does not have a similar topographic interpretation.

The OSAT and DDM estimated ozone levels for all 64 cases are compared to the actual ozone levels in Figure 6-10. The DDM sensitivity approach will estimate exactly the right ozone level for the limit of small precursor changes ($\alpha \rightarrow 1, \beta \rightarrow 1$) as can be seen by the convergence of points onto the 1:1 line at top right in the DDM plot. The DDM estimated ozone levels always tend to be larger than the actual result, so DDM tends to under-estimate the effect of reducing precursor levels. Linearly scaling the OSAT source apportionments can under or over-estimate ozone levels with reduced precursor levels. OSAT tends to over-estimate the effect of reducing precursors for moderate ozone changes (about 20 ppb ozone reduction) by about the same amount that DDM tends to under-estimate the same effect. OSAT does better than DDM in predicting the effects of large changes (more than 40 ppb ozone reduction)[1]. For OSAT, more points lie below than above the 1:1 line indicating an overall tendency for OSAT toward slightly over-predicting the effect of precursor reductions. Because OSAT tends to over-predict and DDM to under-predict the effect of precursor reductions, OSAT and DDM may appear to disagree quite strongly if they are compared directly against each other. Such disagreement will be largest for large precursor changes, but will not necessarily vanish for smaller changes since, for example, sensitivities and source apportionments may differ in sign. . Whether or not such differences are considered to be disagreement depends on whether source apportionment and source sensitivity are comparable concepts.

[1] Throughout the report, small medium and large perturbations are considered to be less than 20, 20 to 40 and greater than 40 percent changes in input emissions (or initial or boundary conditions), respectively.

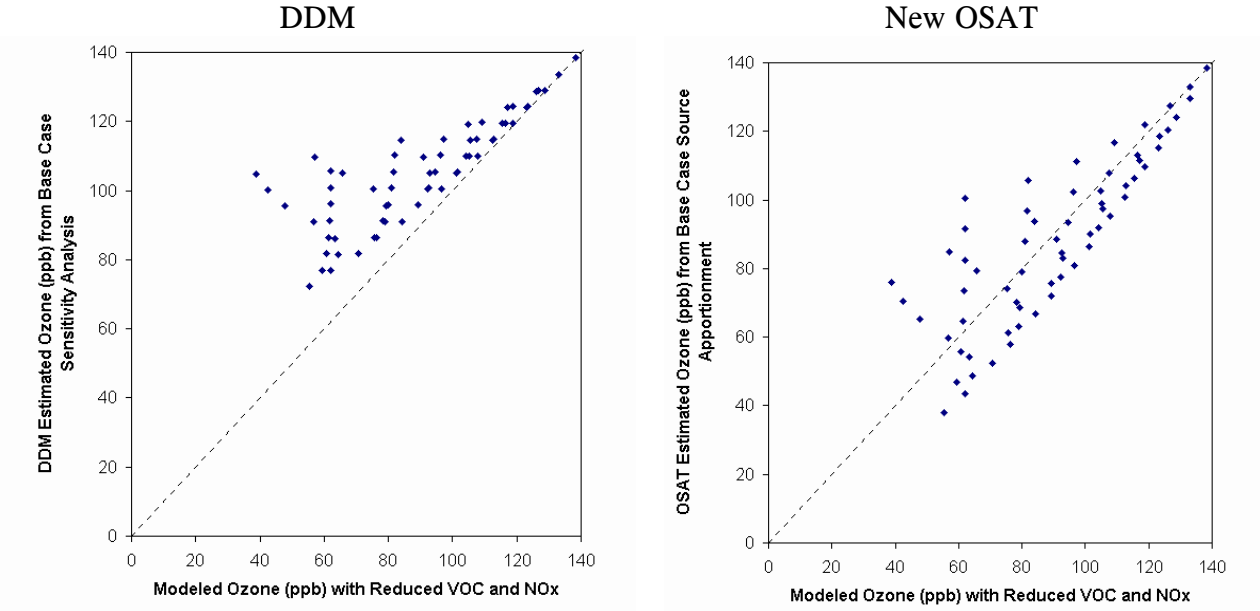

Figure 6-10. Comparison of ozone levels (ppb) estimated using DDM and OSAT to the actual modeled result of reducing precursor (VOC and/or NOx) levels.

SECOND ORDER SENSITIVITIES

The DDM has been implemented only for first-order sensitivities in CAMx, although the method is applicable to higher sensitivities (Dunker, 1986). Because higher-order sensitivities are non-trivial in the box model cases described above, we used the brute-force method to calculate the second-order sensitivities to NOx and VOC in the base case. This involved performing 6 box model runs with +/- 5% perturbations to NOx and VOC levels. The first order terms in equation 6-9a are unchanged from equation 6-8. Equation 6-9b rearranges terms in 6-9a to obtain similar form to equation 6-7 and allow direct comparisons of common coefficients between DDM and OSAT. The values of the linear coefficients in equation 6-9b differ from equation 6-8a. This does not mean that the first-order sensitivities were changed by calculating second-order sensitivities (they were not), but does suggest that interpreting DDM sensitivity coefficients in a manner similar to source apportionments (i.e., equations 6-8a and 6-9a) is altered by considering higher-order sensitivities.

$$\text{DDM estimated ozone (ppb)} = 138.36 + 38.22(\alpha-1) + 37.40(\beta-1) - 34(\alpha-1)^2 - 33(\beta-1)^2 + 55(\alpha-1)(\beta-1) \quad (6\text{-}9a)$$

$$= 50.74 + 51.22\alpha + 48.4\beta - 34\alpha^2 - 33\beta^2 + 55\alpha\beta \quad (6\text{-}9b)$$

As mentioned above, the first order sensitivities (equation 6-8a) define a plane that is tangential to the ozone response surface (Figure 6-6) at the base case. The first and second-order sensitivities (equation 6-9a) define a parabola that touches the ozone response surface at the base case, and this parabola is shown in Figure 6-11. Comparing Figure 6-11 to the actual ozone response surface (Figure 6-6) shows that second-order sensitivities can represent the shape of the EKMA diagram much better than first-order sensitivities (a plane). However,

even at second-order the sensitivities do not fully describe the occurrence of the NOx inhibition effect at low VOC/NOx ratios.

The homogeneous second-order coefficients (for α^2 and β^2 in equation 6-9b, which correspond to VOC^2 and NOx^2) are negative indicating a tendency for ozone to decrease with the square of either precursor. However ozone increases with increasing NOx or VOC (Figure 6-11), for α and β up to one, because the stronger effect of the first-order coefficients. This illustrates one difficulty in interpreting higher-order coefficients, namely a need to interpret higher-order coefficients together with lower-order coefficients. (To understand the effects of different sensitivities, as opposed to different coefficients, it is best to use eqn. 6-9a.)

The inhomogeneous second-order coefficient ($\alpha\beta$ in equation 6-9b, which corresponds to VOC• NOx) has the same sign as the first order sensitivities indicating a tendency for combined NOx and VOC to form ozone, consistent with the requirement for both NOx and VOC to be present to form ozone.

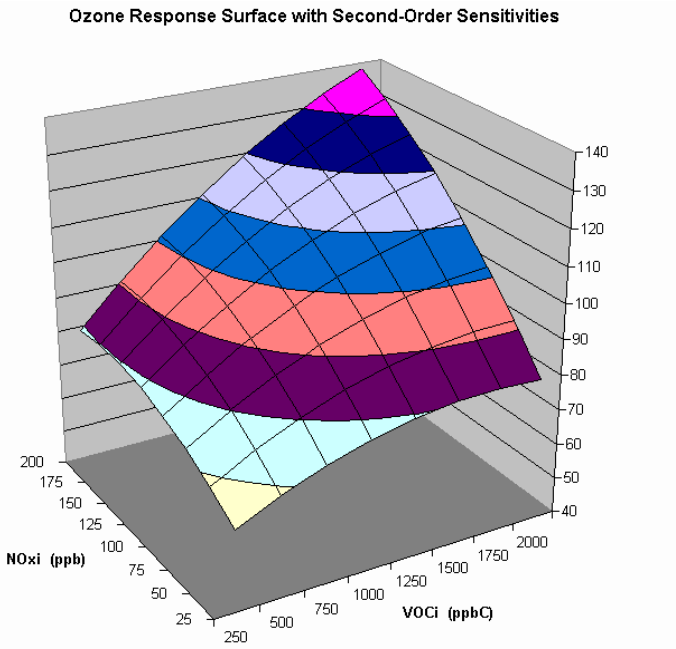

Figure 6-11. Ozone response surfaces calculated with first and second-order sensitivities.

Second-order sensitivities should be better able to describe the effects of precursor reductions than either first-order sensitivities or source apportionment. Figure 6-12 compares the ozone levels (ppb) estimated using equation 6-9 to the actual modeled result of reducing precursor (VOC and/or NOx) levels in the 64 box model cases. Figure 6-12 shows that second-order sensitivities work very well in predicting small to moderate ozone changes (up to about 50 ppb) and comparing Figure 6-12 to Figure 6-10 shows that second-order sensitivities perform better than both first-order sensitivities and source apportionment at all precursor reduction levels.

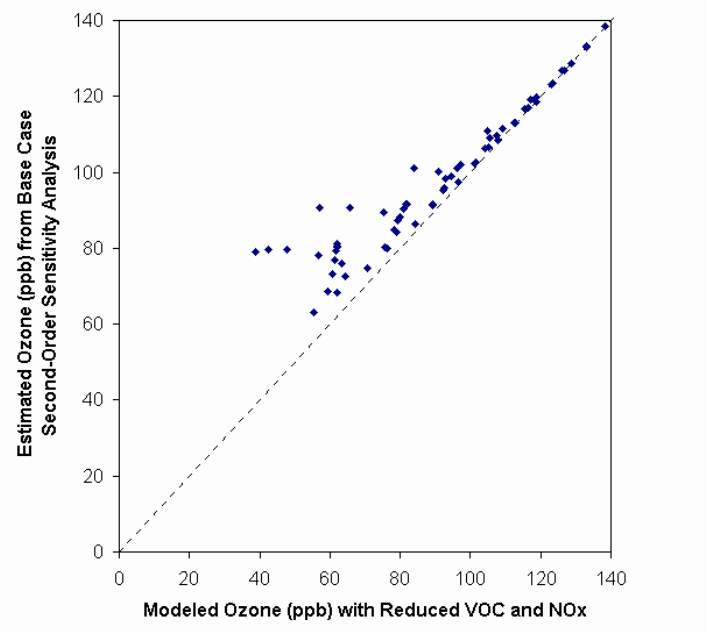

Figure 6-12. Comparison of ozone levels (ppb) estimated using second-order sensitivity analysis to the actual modeled result of reducing precursor (VOC and/or NOx) levels.

CONCLUSIONS

OSAT Updates

- Updating OSAT to account for chemical decay of ozone tracers is an important update. One consequence is that existing ozone apportionments are decayed more rapidly. A related consequence is that other apportionments must increase more rapidly to maintain consistency with the total ozone. This can change the relative amounts of ozone apportioned to VOC and NOx because ozone formation tends to be VOC-limited in the morning and NOx-limited in the afternoon.

- Replacing the (P_{H2O2}/P_{HNO3}) indicator ratio by a ratio of VOC to NOx sensitivities (equation 6-4) is not an important update and has some adverse effects. Both methods diagnose a virtually complete transition from VOC-limited to NOx-limited ozone formation at the same time. Because this transition takes place rapidly (at least under box model conditions), the ability of equation 6-4 to proportionally allocate ozone production to VOC and NOx has little advantage. The disadvantage of equation 6-4 is spurious allocation of some ozone production to NOx under early morning conditions.

- The reactivity weighting update for VOC-limited ozone (equation 6-6) was not tested by the box model scenarios.

- We will include the ozone decay and reactivity weighting updates in a future public release of the CAMx model. We do not plan to change the way ozone production is allocated between VOCs and NOx from the instantaneous (P_{H2O2}/P_{HNO3}) indicator ratio to the instantaneous ratio of VOC to NOx sensitivities used in this study.

Source Sensitivity and Source Apportionment

The box model tests described here are well-suited to understanding how source sensitivity is related to source apportionment because the simplified situation of a box model focuses attention on chemistry. The major difference between the grid model implementations of DDM and OSAT is in the chemistry. By definition, ozone sensitivity is the response of total ozone to changing a source of ozone, i.e., the local derivative. All the interactions among different chemical species, different emission sources, etc. are propagated through the model to determine the impact of a change in some input on ozone at a later time. Source apportionment should describe how the ozone that is present was formed. Ozone was formed in reactions that involved VOC and NOx precursors and the source apportionment should reflect how this ozone formation occurred. This implies the need for a memory of all the ozone formation events leading up to the current condition. To accurately retain this memory, source apportionments should behave like conserved properties.

Sensitivity has a rigorous mathematical definition but is more difficult to interpret physically. Source apportionment is a physical concept that does not always have a rigorous mathematical definition. In a linear system (e.g., a primary pollutant such as CO) source apportionment is the same thing as first-order sensitivity and the source apportionment is uniquely defined. The relationship between source apportionment and sensitivity is less clear for non-linear pollutants, such as ozone, where source apportionment is not uniquely defined.

- The box model comparisons demonstrate the conclusion that first-order sensitivity and source apportionment are different for ozone chemistry because the chemical equations are a non-linear system.

- When first-order sensitivities are attenuated under photochemically reactive conditions they are replaced by higher-order sensitivities. This is why first-order sensitivities typically sum to only about 2/3 of the total ozone in a grid model simulation (Dunker et al., 2002b).

- The rapid attenuation of first-order sensitivities under photochemically reactive conditions suggests limitations to the concept of source apportionment. A chemical interpretation of the rapid attenuation of the sensitivity to initial ozone is that “if the initial ozone were reduced, then the photochemical system would replace it rapidly.” The Lagrangian view of ozone transport is that if a background of X ppb is transported into an area, and the total leaving the area is (X + Y) ppb, then local emissions added Y ppb. The sensitivities are saying that if you reduce ozone transport (X), local ozone production (Y) will increase and partially compensate for the reduced transport. This fact should be recognized in ozone transport arguments and observation-based analyses that are used to support the development of ozone control strategies.

Comparing DDM and OSAT in CAMx

- Ozone source apportionments and source sensitivities should be related, but not identical. Dunker et al. (2002b) showed qualitative consistency in that DDM and OSAT consistently identify the same groups of ozone precursors as important, and identify similar areas of influence for groups of ozone precursors.

- Quantitative comparisons between OSAT and DDM are difficult because source apportionment and source sensitivity are not the same thing (discussed above). Nevertheless, useful insight can be gained from quantitative comparisons, e.g., identifying the need to account for ozone destruction in OSAT (Dunker et al., 2002b).

- DDM sensitivities accurately predict the effects of small to moderate[1] precursor changes.

- OSAT apportionments predict the effects of large precursor changes more accurately than first-order DDM sensitivities.

- DDM sensitivities tend to under-estimate the ozone decreases due to precursor reductions because the sum of the first-order sensitivities tends to be less than (typically about 2/3 of) the total ozone. There may be specific exceptions to this general trend.

- DDM tends to under-estimate the effect of precursor reductions because ozone production becomes more efficient (more ozone formed per precursor reacted) as precursors are reduced under most conditions. First-order sensitivities determine ozone production efficiency at the base case condition.

- OSAT apportionments may over or under-estimate the ozone decreases due to precursor reductions, but over-estimate more often than under-estimate.

- OSAT tends to over-estimate the effect of precursor reduction because ozone production becomes more efficient as precursors are reduced under most conditions. OSAT ozone production efficiencies are a weighted average over the conditions that prevailed as the base case ozone was formed.

- Some studies have addressed the difficulty in interpreting the magnitudes of DDM sensitivities because they do not add up to the total ozone by renormalizing the first order sensitivities (e.g, Zhang et al., 2002). This approach has several limitations:
    - Negative sensitivities make renormalization difficult. The negative values could be set to zero (e.g., Zhang et al., 2002) or the absolute value could be taken, but this eliminates or distorts information. Alternatively, the signed sensitivities could be multiplied by a scaling factor such that the sum of the scaled sensitivities equals the total ozone.

[1] Throughout the report, small medium and large perturbations are considered to be less than 20, 20 to 40 and greater than 40 percent changes in input emissions (or initial or boundary conditions), respectively.

- When the NOx sensitivities are negative, the remaining first order sensitivities can exceed the total ozone. Thus, the directional effect of renormalization may not be consistent, depending upon how the renormalization is performed.
- The advantage of rigorous mathematical definition is lost when sensitivities are renormalized.

Thus, we recommend against renormalizing sensitivities.

REFERENCES

Carter, W.P.L, G.S. Tonnesen, and G. Yarwood. 2002. "Investigation of VOC Reactivity Effects in Existing Regional Air Quality Models." Draft Report to American Chemistry Council for the NARSTO Reactivity Research Working Group. September.

Carter, W.P.L. 1994. Development of ozone reactivity scales for volatile organic compounds; *J. Air & Waste Manage. Assoc.* 1994, 44, 881-899.

Dunker, A.M., G. Yarwood, J. Ortmann, and G.M. Wilson. 2002a. The decoupled direct method for sensitivity analysis in a three-dimensional air quality model – Implementation, accuracy and efficiency. *Environ. Sci. and Tech.*, 36, 2965-2976.

Dunker, A.M., G. Yarwood, J. Ortmann, and G.M. Wilson. 2002b. Comparison of source apportionment and source sensitivity of ozone in a three-dimensional air quality model. *Environ. Sci. and Tech.*, 36, 2953-2964.

Dunker, A.M. 1986. The reduction and parameterization of chemical mechanisms for inclusion in atmospheric reaction-transport models. *Atmos. Environ.*, 20, 479-486.

Dunker, A.M. 1981. Efficient calculations of sensitivity coefficients for complex atmospheric models, *Atmos. Environ.* 15, 1155-1161.

Dunker, A.M. 1980. "The response of an atmospheric reaction-transport model to changes in input functions." *Atmos. Environ.* 14, 671-679.

ENVIRON. 2003. "Development of an Advanced Photochemical Model for Particulate Matter: PMCAMx." Prepared for Coordinating Research Council, Inc. CRC Project A-30. January.

ENVIRON. 2002a. "User's Guide to the Comprehensive Air Quality Model with Extensions, version 3.10" available from http://www.camx.com. April

ENVIRON. 2002b. " Development, Application, and Evaluation of an Advanced Photochemical Air Toxics Modeling System." Prepared for Coordinating Research Council, Inc. CRC Project A-42.September.

EPA. 1998. "Air Quality Modeling Technical Support Document for the NOx SIP Call." U.S. Environmental Protection Agency, Office of Air and Radiation, Research Triangle Park, North Carolina, September 23.

Imre, D.G.; Daum, P.H.; Kleinman, L.; Lee, Y-N.; Lee, J. H.; Nunnermacker, L.J.; Springston, S.R.; Newman, L.; Weinstein-Lloyd, J.; and Sillman, S. 1998. Characterization of the Nashville urban plume on July 3 and July 18, 1995. Part II. Processes, efficiencies, and VOC and NO_x limitation. Manuscript submitted to *J. Geophys. Res.*

Jeffries, H. E., and Tonnesen, S. 1994. Comparison of two photochemical reaction mechanisms using a mass balance and process analysis. *Atmospheric Environment* **28**:2991-3003.

OTAG. 2002. "Ozone Transport Assessment Group Technical Supporting Document." U.S. Environmental Protection Agency, Technology Transfer network (TTN), Research Triangle Park, North Carolina, August 28. http://www.epa.gov/ttn/naaqs/ozone/rto/otag/finalrpt/index.htm

OTAG. 1997. "Ozone Transport Assessment Group Modeling Protocol," U.S. Environmental Protection Agency, Office of Air Quality Planning and Standards, Research Triangle Park, North Carolina, February 29.

Sillman, S. 2000. The method of photochemical indicators as a basis for analyzing O3-NOx-hydrocarbon sensitivity, manuscript submitted to *Atmos. Environ.*

Sillman, S. 1995. The use of NO_Y, H_2O_2, and HNO_3 as indicators for ozone-NOx-hydrocarbon sensitivity in urban locations, *J. Geophys. Res.*, 100, 14175-14188

Tonnesen, G.S. 2001. Evaluation of the budgets of odd nitrogen compounds using Eulerian photochemical air quality models, Interim Report submitted to the American Chemistry Council, January.

Tonnesen, G.S. and R.L. Dennis. 2000a. Analysis of radical propagation efficiency to assess ozone sensitivity to hydrocarbons and NOx 1. Local indicators of instantaneous odd oxygen production sensitivity, *J. Geophys. Res.*, 105, 9213-9225.

Tonnesen, G.S. 1995. Development and application of a process analysis method for photochemical oxidant models, Ph.D. Dissertation in Environmental Engineering, University of North Carolina, Chapel Hill, NC, May, 1995.

Tonnesen, G.S. and H.E. Jeffries, 1994. Inhibition of odd oxygen production in the Carbon Bond Four and the Generic Reaction Set mechanisms, *Atmos. Environ.,* **28**, 1339-1349.

Zhang, Y., K. Vijayaraghavan, and C. Seigneur. 2002. "Evaluation of Probing Tools Implemented in CAMx." Prepared for Coordinating Research Council, Inc. CRC Project A-37-1. August.

Appendix A

Example Run Scripts for CAMx Probing Tools

This appendix contains run scripts for the following probing tools runs:

Base Case - Showing the base CAMx input files and the use of flexi-nesting to start the fine grid after 4 spin-up days.

OSAT (B1) - Showing how OSAT was configured, which was the same as for APCA (B5) configuration. Just the fine grid days are shown to save space.

OSAT (B2N) - Showing how DDM was configured for run B2N, which was similar to B2V. Just the fine grid days are shown to save space.

OSAT (B3) - Showing how DDM was configured for run B3. Just the fine grid days are shown to save space.

OSAT (B7) - Showing how DDM was configured for run B7. Just the fine grid days are shown to save space.

PA (B4) - Showing how PA was configured for run B4. The first coarse grid day and last fine grid days are shown because the receptor definitions change.

In addition, the source area maps are shown for OSAT runs B1 and DDM runs B2 and B3. The 17 source areas in the OSAT source map were re-assigned to 11 areas in DDM run B2 and 6 areas in DDM run B3.

The OSAT and DDM receptor definition file is shown. In order to get sensitivity information for layers aloft, several “wall-of-cells” receptor types were defined. All of the receptors are defined in coarse grid cells for CAMx version 3.1. Starting with CAMx version 4, the OSAT and DDM receptor file supports fine grid cell receptor definitions.

BASE CASE RUN

```
#!/bin/csh
#
set RUN     = "base "
#
# base case for the CRC Probing Tools project (A-37)
#
For efficiency, compile EXEC1 with 1 grid and EXEC2 with 2 grids
#
set EXEC1    = "../../src.v3.01/CAMx.otag1grd.1.linux"
set EXEC2    = "../../src.v3.01/CAMx.otag.1.linux"
#
set INPUT   = "../inputs"
set EMIS    = "../emiss"
set PTSRCE  = "../ptsrce"
set OUTPUT  = "../outputs/$RUN"
#
mkdir ./$RUN $OUTPUT
#
date
#
#  --- Start the first day with 1 grid
#
#  --- Create the input file (always called CAMx.in)
#
cat << ieof > CAMx.in
CAMx Version       |version3
Run Message        |CRC-A37 - July 07, 1995 - 2007 Base Case - $RUN
Root output name   |$OUTPUT/CAMx3.950707.07base.$RUN
Start yr/mo/dy/hr  |95 07 07    0.
End   yr/mo/dy/hr  |95 07 07 2400.
dtmx,dtin,dtem,dtou|0.25 1. 1. 1.
nx,ny,nz           |64  63  5
Coordinate ID      |LATLON
xorg,yorg,dx,dy    |-99. 26.  .5  .33333
time zone          |5
PiG parameters     |5000. 18.
Avg output species |17
                   |NO        NO2       O3        PAR       TOL       ETH
                   |OLE       PAN       ISOP      XYL       FORM      ALD2
                   |HNO3      NXOY      NTR       CO        H2O2
# nested grids     |0
SMOLAR,BOTT, PPM?  |BOTT
Chemistry solver   |CMC
Restart            |false
Chemistry          |true
Dry dep            |true
Wet dep            |true
PiG submodel       |false
Staggered winds    |false
Treat area emiss   |true
Treat point emiss  |true
1-day emiss inputs |true
3-D average file   |false
Probing Tool?      |false
Chemparam          |$INPUT/CAMx3.chemparm.3
Photolysis rates   |$INPUT/rate.ng.99jul95.ai.basD
Landuse            |$INPUT/surf.cc.commonfile.ai.basD
Height/pressure    |$INPUT/rams/hght.cc.07jul95.ne.rams1b
Wind               |$INPUT/rams/wind.cc.07jul95.ne.rams1b.CAMx2
Temperature        |$INPUT/rams/tmpr.cc.07jul95.ne.rams1b.CAMx2
Water vapor        |$INPUT/rams/wvap.cc.07jul95.ne.rams1b
Cloud cover        |$INPUT/clou.cc.07jul95.ld.basD
Rainfall           |$INPUT/anlrain.950707.out
Vertical diffsvty  |$INPUT/rams/vdif.cc.07jul95.wi.rams1bnew
Initial conditions |$INPUT/init.cc.07jul95.ld.basD
Boundary conditions|$INPUT/bndr.cc.07jul95.ld.basD.a0
Top concentration  |$INPUT/topc.ng.commonfile.ai.basD
Albedo/haze/ozone  |$INPUT/ahoz.cc.99jul95.ld.basD
Point emiss        |$PTSRCE/ptsrce.950707.07base.pig
```

```
Area emiss          |$EMIS/OTAG_36km/emiss.OTAG_36km.950707.07base.bin
ieof
#
#  --- Execute the model ---
#
/bin/time $EXEC1  |& tee ./$RUN/CAMx3.950707.07base.$RUN.stdout
date
#
# --- Run the next three days with 1 grid
#
foreach today (08 09 10 )
set yesterday = `echo $today | awk '{printf("%2.2d",$1-1)}'`
set todate = `echo $today | awk '{printf("%2.2djul95",$1)}'`
date
#
#  --- Create the input file (always called CAMx.in)
#
cat << ieof > CAMx.in
CAMx Version        |version3
Run Message         |CRC-A37 - July $today, 1995 - 2007 Base Case - $RUN
Root output name    |$OUTPUT/CAMx3.9507$today.07base.$RUN
Start yr/mo/dy/hr   |95 07 $today    0.
End   yr/mo/dy/hr   |95 07 $today 2400.
dtmx,dtin,dtem,dtou|0.25 1. 1. 1.
nx,ny,nz            |64  63  5
Coordinate ID       |LATLON
xorg,yorg,dx,dy     |-99. 26.  .5  .33333
time zone           |5
PiG parameters      |5000. 18.
Avg output species  |17
                    |NO        NO2       O3        PAR       TOL       ETH
                    |OLE       PAN       ISOP      XYL       FORM      ALD2
                    |HNO3      NXOY      NTR       CO        H2O2
# nested grids      |0
SMOLAR,BOTT, PPM?   |BOTT
Chemistry solver    |CMC
Restart             |true
Chemistry           |true
Dry dep             |true
Wet dep             |true
PiG submodel        |false
Staggered winds     |false
Treat area emiss    |true
Treat point emiss   |true
1-day emiss inputs  |true
3-D average file    |false
Probing Tool?       |false
Chemparam           |$INPUT/CAMx3.chemparm.3
Photolysis rates    |$INPUT/rate.ng.99jul95.ai.basD
Landuse             |$INPUT/surf.cc.commonfile.ai.basD
Height/pressure     |$INPUT/rams/hght.cc.$todate.ne.rams1b
Wind                |$INPUT/rams/wind.cc.$todate.ne.rams1b.CAMx2
Temperature         |$INPUT/rams/tmpr.cc.$todate.ne.rams1b.CAMx2
Water vapor         |$INPUT/rams/wvap.cc.$todate.ne.rams1b
Cloud cover         |$INPUT/clou.cc.$todate.ld.basD
Rainfall            |$INPUT/anlrain.9507$today.out
Vertical diffsvty   |$INPUT/rams/vdif.cc.$todate.wi.rams1bnew
Initial conditions  |
Boundary conditions|$INPUT/bndr.cc.$todate.ld.basD.a0
Top concentration   |$INPUT/topc.ng.commonfile.ai.basD
Albedo/haze/ozone   |$INPUT/ahoz.cc.99jul95.ld.basD
Point emiss         |$PTSRCE/ptsrce.9507$today.07base.pig
Area emiss          |$EMIS/OTAG_36km/emiss.OTAG_36km.9507$today.07base.bin
Coarse grid restart|$OUTPUT/CAMx3.9507$yesterday.07base.$RUN.inst.2
ieof
#
#  --- Execute the model ---
#
/bin/time $EXEC1  |& tee ./$RUN/CAMx3.9507$today.07base.$RUN.stdout
date
end
#
# --- Start the fine grid using flexi-nest restart
```

```
#
foreach today (11 )
set yesterday = `echo $today | awk '{printf("%2.2d",$1-1)}'`
set todate = `echo $today | awk '{printf("%2.2djul95",$1)}'`
date
#
#  --- Create the input file (always called CAMx.in)
#
cat << ieof > CAMx.in
CAMx Version       |version3
Run Message        |CRC-A37 - July $today, 1995 - 2007 Base Case - $RUN
Root output name   |$OUTPUT/CAMx3.9507$today.07base.$RUN
Start yr/mo/dy/hr  |95 07 $today    0.
End   yr/mo/dy/hr  |95 07 $today 2400.
dtmx,dtin,dtem,dtou|0.25 1. 1. 1.
nx,ny,nz           |64  63  5
Coordinate ID      |LATLON
xorg,yorg,dx,dy    |-99. 26.  .5  .33333
time zone          |5
PiG parameters     |5000. 18.
Avg output species |17
                   |NO        NO2       O3        PAR       TOL       ETH
                   |OLE       PAN       ISOP      XYL       FORM      ALD2
                   |HNO3      NXOY      NTR       CO        H2O2
# nested grids     |1
nest grid params   |15 59 19 54 7 3
SMOLAR,BOTT, PPM?  |BOTT
Chemistry solver   |CMC
Restart            |true
Chemistry          |true
Dry dep            |true
Wet dep            |true
PiG submodel       |false
Staggered winds    |false
Treat area emiss   |true
Treat point emiss  |true
1-day emiss inputs |true
3-D average file   |false
Probing Tool?      |false
Chemparam          |$INPUT/CAMx3.chemparm.3
Photolysis rates   |$INPUT/rate.ng.99jul95.ai.basD
Landuse            |$INPUT/surf.cc.commonfile.ai.basD
Height/pressure    |$INPUT/rams/hght.cc.$todate.ne.rams1b
Wind               |$INPUT/rams/wind.cc.$todate.ne.rams1b.CAMx2
Temperature        |$INPUT/rams/tmpr.cc.$todate.ne.rams1b.CAMx2
Water vapor        |$INPUT/rams/wvap.cc.$todate.ne.rams1b
Cloud cover        |$INPUT/clou.cc.$todate.ld.basD
Rainfall           |$INPUT/anlrain.9507$today.out
Vertical diffsvty  |$INPUT/rams/vdif.cc.$todate.wi.rams1bnew
Initial conditions |
Boundary conditions|$INPUT/bndr.cc.$todate.ld.basD.a0
Top concentration  |$INPUT/topc.ng.commonfile.ai.basD
Albedo/haze/ozone  |$INPUT/ahoz.cf.99jul95.ld.basD
Point emiss        |$PTSRCE/ptsrce.9507$today.07base.pig
Area emiss         |$EMIS/OTAG_36km/emiss.OTAG_36km.9507$today.07base.bin
Landuse         #2 |$INPUT/surf.ff.commonfile.ai.basD
Height/pressure #2 |$INPUT/rams/hght.ff.$todate.ne.rams1b
Wind            #2 |$INPUT/rams/wind.ff.$todate.ne.rams1b.CAMx2
Temperature     #2 |
Vertical diff   #2 |$INPUT/rams/vdif.ff.$todate.wi.rams1bnew
Area emiss      #2 |$EMIS/OTAG_12km/emiss.OTAG_12km.9507$today.07base.bin
Coarse grid restart|$OUTPUT/CAMx3.9507$yesterday.07base.$RUN.inst.2
Fine grid restart  |
ieof
#
#  --- Execute the model ---
#
/bin/time $EXEC2  |& tee ./$RUN/CAMx3.9507$today.07base.$RUN.stdout
date
end
#
# --- Run the remaining days with 2 grids
#
```

```
foreach today (12 13 14 15)
set yesterday = `echo $today | awk '{printf("%2.2d",$1-1)}'`
set todate = `echo $today | awk '{printf("%2.2djul95",$1)}'`
date
#
#  --- Create the input file (always called CAMx.in)
#
cat << ieof > CAMx.in
CAMx Version       |version3
Run Message        |CRC-A37 - July $today, 1995 - 2007 Base Case - $RUN
Root output name   |$OUTPUT/CAMx3.9507$today.07base.$RUN
Start yr/mo/dy/hr  |95 07 $today    0.
End   yr/mo/dy/hr  |95 07 $today 2400.
dtmx,dtin,dtem,dtou|0.25 1. 1. 1.
nx,ny,nz           |64  63  5
Coordinate ID      |LATLON
xorg,yorg,dx,dy    |-99. 26.  .5  .33333
time zone          |5
PiG parameters     |5000. 18.
Avg output species |17
                   |NO        NO2       O3        PAR       TOL       ETH
                   |OLE       PAN       ISOP      XYL       FORM      ALD2
                   |HNO3      NXOY      NTR       CO        H2O2
# nested grids     |1
nest grid params   |15 59 19 54 7 3
SMOLAR,BOTT, PPM?  |BOTT
Chemistry solver   |CMC
Restart            |true
Chemistry          |true
Dry dep            |true
Wet dep            |true
PiG submodel       |false
Staggered winds    |false
Treat area emiss   |true
Treat point emiss  |true
1-day emiss inputs |true
3-D average file   |false
Probing Tool?      |false
Chemparam          |$INPUT/CAMx3.chemparm.3
Photolysis rates   |$INPUT/rate.ng.99jul95.ai.basD
Landuse            |$INPUT/surf.cc.commonfile.ai.basD
Height/pressure    |$INPUT/rams/hght.cc.$todate.ne.rams1b
Wind               |$INPUT/rams/wind.cc.$todate.ne.rams1b.CAMx2
Temperature        |$INPUT/rams/tmpr.cc.$todate.ne.rams1b.CAMx2
Water vapor        |$INPUT/rams/wvap.cc.$todate.ne.rams1b
Cloud cover        |$INPUT/clou.cc.$todate.ld.basD
Rainfall           |$INPUT/anlrain.9507$today.out
Vertical diffsvty  |$INPUT/rams/vdif.cc.$todate.wi.rams1bnew
Initial conditions |
Boundary conditions|$INPUT/bndr.cc.$todate.ld.basD.a0
Top concentration  |$INPUT/topc.ng.commonfile.ai.basD
Albedo/haze/ozone  |$INPUT/ahoz.cf.99jul95.ld.basD
Point emiss        |$PTSRCE/ptsrce.9507$today.07base.pig
Area emiss         |$EMIS/OTAG_36km/emiss.OTAG_36km.9507$today.07base.bin
Landuse         #2 |$INPUT/surf.ff.commonfile.ai.basD
Height/pressure #2 |$INPUT/rams/hght.ff.$todate.ne.rams1b
Wind            #2 |$INPUT/rams/wind.ff.$todate.ne.rams1b.CAMx2
Temperature     #2 |
Vertical diff   #2 |$INPUT/rams/vdif.ff.$todate.wi.rams1bnew
Area emiss      #2 |$EMIS/OTAG_12km/emiss.OTAG_12km.9507$today.07base.bin
Coarse grid restart|$OUTPUT/CAMx3.9507$yesterday.07base.$RUN.inst.2
Fine grid restart  |$OUTPUT/CAMx3.9507$yesterday.07base.$RUN.finst.2
ieof
#
#  --- Execute the model ---
#
/bin/time $EXEC2  |& tee ./$RUN/CAMx3.9507$today.07base.$RUN.stdout
date
end
```

OSAT RUN B1

```
#!/bin/csh
#
set RUN     = "OSAT.B1 "
#
####
# OSAT with 17 source areas x 4 source categories.
# The 4 source categories are biogenic, onroad mobile, elevated
# anthropogenic (anthro) and other surface anthropogenic emissions.
####
#
set EXEC1   = "../../src.v3.d/CAMx.otag_1grid.280.linux"
set EXEC2   = "../../src.v3.d/CAMx.otag.280.linux"
set INPUT   = "../inputs"
set EMIS    = "../emiss"
set PTSRCE  = "../ptsrce"
set OUTPUT  = "../outputs/$RUN"
set PROBIN  = "../osat/inputs"
set PROBOUT = "../outputs/$RUN"
#
mkdir ./$RUN $OUTPUT $PROBOUT
#
#
# Days 7-11 omitted
#
# --- Run the remaining days with 2 grids
#
foreach today (12 13 14 15)
set yesterday = `echo $today | awk '{printf("%2.2d",$1-1)}'`
set todate = `echo $today | awk '{printf("%2.2djul95",$1)}'`
date
#
#  --- Create the input file (always called CAMx.in)
#
cat << ieof > CAMx.in
CAMx Version       |version3
Run Message        |CRC-A37 - July $today, 1995 - 2007 Base Case - $RUN
Root output name   |$OUTPUT/CAMx3.9507$today.07base.$RUN
Start yr/mo/dy/hr  |95 07 $today    0.
End   yr/mo/dy/hr  |95 07 $today 2400.
dtmx,dtin,dtem,dtou|0.25 1. 1. 1.
nx,ny,nz           |64  63  5
Coordinate ID      |LATLON
xorg,yorg,dx,dy    |-99. 26.  .5  .33333
time zone          |5
PiG parameters     |5000. 18.
Avg output species |17
                   |NO        NO2       O3        PAR       TOL       ETH
                   |OLE       PAN       ISOP      XYL       FORM      ALD2
                   |HNO3      NXOY      NTR       CO        H2O2
# nested grids     |1
nest grid params   |15 59 19 54 7 3
SMOLAR,BOTT, PPM?  |BOTT
Chemistry solver   |CMC
Restart            |true
Chemistry          |true
Dry dep            |true
Wet dep            |true
PiG submodel       |false
Staggered winds    |false
Treat area emiss   |true
Treat point emiss  |true
1-day emiss inputs |true
3-D average file   |false
Probing Tool?      |true
PT File Root       |$PROBOUT/CAMx3.9507$today.07base.$RUN
Technology type    |OSAT
PT Crs grid  output|true
PT Fin grid  output|true
Stratify Boundary  |false
# of Source Regions|17
```

```
# of Source Groups |4
Use leftover group |true
# timing releases  |0
Chemparam          |$INPUT/CAMx3.chemparm.3
Photolysis rates   |$INPUT/rate.ng.99jul95.ai.basD
Landuse            |$INPUT/surf.cc.commonfile.ai.basD
Height/pressure    |$INPUT/rams/hght.cc.$todate.ne.rams1b
Wind               |$INPUT/rams/wind.cc.$todate.ne.rams1b.CAMx2
Temperature        |$INPUT/rams/tmpr.cc.$todate.ne.rams1b.CAMx2
Water vapor        |$INPUT/rams/wvap.cc.$todate.ne.rams1b
Cloud cover        |$INPUT/clou.cc.$todate.ld.basD
Rainfall           |$INPUT/anlrain.9507$today.out
Vertical diffsvty  |$INPUT/rams/vdif.cc.$todate.wi.rams1bnew
Initial conditions |
Boundary conditions|$INPUT/bndr.cc.$todate.ld.basD.a0
Top concentration  |$INPUT/topc.ng.commonfile.ai.basD
Albedo/haze/ozone  |$INPUT/ahoz.cf.99jul95.ld.basD
Point emiss        |$PTSRCE/ptsrce.9507$today.07base.pig
Area emiss         |$EMIS/OTAG_36km/emiss.OTAG_36km.9507$today.07base.bin
Landuse         #2 |$INPUT/surf.ff.commonfile.ai.basD
Height/pressure #2 |$INPUT/rams/hght.ff.$todate.ne.rams1b
Wind            #2 |$INPUT/rams/wind.ff.$todate.ne.rams1b.CAMx2
Temperature     #2 |
Vertical diff   #2 |$INPUT/rams/vdif.ff.$todate.wi.rams1bnew
Area emiss      #2 |$EMIS/OTAG_12km/emiss.OTAG_12km.9507$today.07base.bin
Coarse grid restart|$OUTPUT/CAMx3.9507$yesterday.07base.$RUN.inst.2
Fine grid restart  |$OUTPUT/CAMx3.9507$yesterday.07base.$RUN.finst.2
Source area mapping|$PROBIN/source_map.crc.17area.osat
Receptor definition|$PROBIN/receptor.list
PT Cse grd restart |$OUTPUT/CAMx3.9507$yesterday.07base.$RUN.sa.inst.2
PT Fin grd restart |$OUTPUT/CAMx3.9507$yesterday.07base.$RUN.sa.finst.2
Area   Grp#1 Grd#1 |$EMIS/OTAG_36km/premerged/bio/bio2.cc.$todate-95.ne
Area   Grp#1 Grd#2 |$EMIS/OTAG_12km/premerged/bio/bio2.ff.$todate-95.ne
Point  Grp#1       |
Area   Grp#2 Grd#1 |$EMIS/OTAG_36km/premerged/motv/OTAG_36km.motv.9507$today.07base.bin
Area   Grp#2 Grd#2 |$EMIS/OTAG_12km/premerged/motv/OTAG_12km.motv.9507$today.07base.bin
Point  Grp#2       |
Area   Grp#3 Grd#1 |
Area   Grp#3 Grd#2 |
Point  Grp#3       |$PTSRCE/ptsrce.9507$today.07base.pig.copy
ieof
#
#  --- Execute the model ---
#
/bin/time $EXEC2 >& ./$RUN/CAMx3.9507$today.07base.$RUN.stdout
date
sleep 30
end
```

DDM RUN B2N

```
#!/bin/csh
#
set RUN     = "DDM.B2N"
#
####
# Run B2Na corrects error in location of Altoona receptor from B2N
#
# B2 split to B2N (NOx sensitivities) and B2V (VOC sensitivities)
# to fit within 1 GB of RAM
#
# DDM with 11 source areas x 3 source categories.
# The 3 source categories for biogenic, surface anthropogenic, and elevated.
# The source areas are 4, 5, 7, 8, 11, 12, 13, 14, 15, 16, and 17 as shown in Figure 1.
# NOTE that these are renumbered consecutively 1-11 within this run)
# Sensitivity to VOC and NOx from each source group.
####
#
# For efficiency, compile EXEC1 with 1 grid and EXEC2 with 2 grids
#
set EXEC1    = "../../src.v3.d/CAMx.otag_1grid.CO.825.linux"
set EXEC2    = "../../src.v3.d/CAMx.otag.CO.825.linux"
#
set INPUT   = "../inputs"
set EMIS    = "../emiss"
set PTSRCE  = "../ptsrce"
set OUTPUT  = "../outputs/$RUN"
set PROBIN  = "../ddm.inputs"
set PROBOUT = "../outputs/$RUN"
set PROBEMI = "../ddm.inputs/s_anthro"
#
mkdir ./$RUN $OUTPUT $PROBOUT
#
#
# Days 7-11 omitted
#
#
# --- Run the remaining days with 2 grids
#
foreach today (12 13 14 15)
set yesterday = `echo $today | awk '{printf("%2.2d",$1-1)}'`
set todate = `echo $today | awk '{printf("%2.2djul95",$1)}'`
date
#
#  --- Create the input file (always called CAMx.in)
#
cat << ieof > CAMx.in
CAMx Version       |version3
Run Message        |CRC-A37 - OTAG 2007 Base Case - $RUN
Root output name   |$OUTPUT/CAMx3.9507$today.07base.$RUN
Start yr/mo/dy/hr  |95 07 $today    0.
End   yr/mo/dy/hr  |95 07 $today 2400.
dtmx,dtin,dtem,dtou|0.25 1. 1. 1.
nx,ny,nz           |64  63  5
Coordinate ID      |LATLON
xorg,yorg,dx,dy    |-99. 26.  .5  .33333
time zone          |5
PiG parameters     |5000. 18.
Avg output species |17
                   |NO        NO2       O3        PAR       TOL       ETH
                   |OLE       PAN       ISOP      XYL       FORM      ALD2
                   |HNO3      NXOY      NTR       CO        H2O2
# nested grids     |1
nest grid params   |15 59 19 54 7 3
SMOLAR,BOTT, PPM?  |BOTT
Chemistry solver   |CMC
Restart            |true
Chemistry          |true
Dry dep            |true
Wet dep            |true
PiG submodel       |false
```

```
Staggered winds    |false
Treat area emiss   |true
Treat point emiss  |true
1-day emiss inputs |true
3-D average file   |false
Probing Tool?      |true
PT File Root       |$PROBOUT/CAMx3.9507$today.07base.$RUN
Technology type    |DDM
PT Crs grid output |true
PT Fin grid output |true
# IC Spec groups   | 0
# BC Spec groups   | 0
# Emis Spec groups | 1
Emis Species groups|NOX
# of source regions| 11
# of source groups | 3
Chemparam          |$INPUT/CAMx3.chemparm.3
Photolysis rates   |$INPUT/rate.ng.99jul95.ai.basD
Landuse            |$INPUT/surf.cc.commonfile.ai.basD
Height/pressure    |$INPUT/rams/hght.cc.$todate.ne.rams1b
Wind               |$INPUT/rams/wind.cc.$todate.ne.rams1b.CAMx2
Temperature        |$INPUT/rams/tmpr.cc.$todate.ne.rams1b.CAMx2
Water vapor        |$INPUT/rams/wvap.cc.$todate.ne.rams1b
Cloud cover        |$INPUT/clou.cc.$todate.ld.basD
Rainfall           |$INPUT/anlrain.9507$today.out
Vertical diffsvty  |$INPUT/rams/vdif.cc.$todate.wi.rams1bnew
Initial conditions |
Boundary conditions|$INPUT/bndr.cc.$todate.ld.basD.a0
Top concentration  |$INPUT/topc.ng.commonfile.ai.basD
Albedo/haze/ozone  |$INPUT/ahoz.cf.99jul95.ld.basD
Point emiss        |$PTSRCE/ptsrce.9507$today.07base.pig
Area emiss         |$EMIS/OTAG_36km/emiss.OTAG_36km.9507$today.07base.bin
Landuse         #2 |$INPUT/surf.ff.commonfile.ai.basD
Height/pressure #2 |$INPUT/rams/hght.ff.$todate.ne.rams1b
Wind            #2 |$INPUT/rams/wind.ff.$todate.ne.rams1b.CAMx2
Temperature     #2 |
Vertical diff   #2 |$INPUT/rams/vdif.ff.$todate.wi.rams1bnew
Area emiss      #2 |$EMIS/OTAG_12km/emiss.OTAG_12km.9507$today.07base.bin
Coarse grid restart|$OUTPUT/CAMx3.9507$yesterday.07base.$RUN.inst.2
Fine grid restart  |$OUTPUT/CAMx3.9507$yesterday.07base.$RUN.finst.2
Source area mapping|$PROBIN/source_map/source_map.crc.11area.ddm
Receptor file      |$PROBIN/receptor.list.a0
PT Cse grd restart |$OUTPUT/CAMx3.9507$yesterday.07base.$RUN.sa.inst.2
PT Fin grd restart |$OUTPUT/CAMx3.9507$yesterday.07base.$RUN.sa.finst.2
IC file name       |
BC file name       |
TC file name       |
Area   Grp#1 Grd#1 |$EMIS/OTAG_36km/premerged/bio/bio2.cc.$todate-95.ne
Area   Grp#1 Grd#2 |$EMIS/OTAG_12km/premerged/bio/bio2.ff.$todate-95.ne
Point  Grp#1       |
Area   Grp#2 Grd#1 |$PROBEMI/OTAG_36km/emiss.s_anthro.OTAG_36km.9507$today.07base.bin
Area   Grp#2 Grd#2 |$PROBEMI/OTAG_12km/emiss.s_anthro.OTAG_12km.9507$today.07base.bin
Point  Grp#2       |
Area   Grp#3 Grd#1 |
Area   Grp#3 Grd#2 |
Point  Grp#3       |$PTSRCE/ptsrce.9507$today.07base.pig.copy
ieof
#
#  --- Execute the model ---
#
/bin/time $EXEC2  >& ./$RUN/CAMx3.9507$today.07base.$RUN.stdout
date
end
```

DDM RUN B3

```
#!/bin/csh
#
set RUN     = "DDM.B3"
#
####
#
# DDM with 6 source areas x 3 source categories plus ICs and BCs.
# The 3 source categories for biogenic, surface anthropogenic, and elevated.
# The 6 source areas for B3 are 1, 2, 3, 6, 9, and 10 as shown in Figure 1
# (NOTE that these are renumbered consecutively 1-6 within this run)
# Sensitivity to ALL species combined from each source group.
####
#
For efficiency, compile EXEC1 with 1 grid and EXEC2 with 2 grids
#
set EXEC1    = "../../src.v3.d/CAMx.otag_1grid.CO.500.linux"
set EXEC2    = "../../src.v3.d/CAMx.otag.CO.500.linux"
#
set INPUT   = "../inputs"
set EMIS    = "../emiss"
set PTSRCE  = "../ptsrce"
set OUTPUT  = "../outputs/$RUN"
set PROBIN  = "../ddm.inputs"
set PROBOUT = "../outputs/$RUN"
set PROBEMI = "../ddm.inputs/s_anthro"
#
mkdir ./$RUN $OUTPUT $PROBOUT
#
#
# Days 7-11 omitted
#
foreach today (12 13 14 15)
set yesterday = `echo $today | awk '{printf("%2.2d",$1-1)}'`
set todate = `echo $today | awk '{printf("%2.2djul95",$1)}'`
date
#
#  --- Create the input file (always called CAMx.in)
#
cat << ieof > CAMx.in
CAMx Version       |version3
Run Message        |CRC-A37 - OTAG 2007 Base Case - $RUN
Root output name   |$OUTPUT/CAMx3.9507$today.07base.$RUN
Start yr/mo/dy/hr  |95 07 $today    0.
End   yr/mo/dy/hr  |95 07 $today 2400.
dtmx,dtin,dtem,dtou|0.25 1. 1. 1.
nx,ny,nz           |64  63  5
Coordinate ID      |LATLON
xorg,yorg,dx,dy    |-99. 26.  .5  .33333
time zone          |5
PiG parameters     |5000. 18.
Avg output species |17
                   |NO        NO2       O3        PAR       TOL       ETH
                   |OLE       PAN       ISOP      XYL       FORM      ALD2
                   |HNO3      NXOY      NTR       CO        H2O2
# nested grids     |1
nest grid params   |15 59 19 54 7 3
SMOLAR,BOTT, PPM?  |BOTT
Chemistry solver   |CMC
Restart            |true
Chemistry          |true
Dry dep            |true
Wet dep            |true
PiG submodel       |false
Staggered winds    |false
Treat area emiss   |true
Treat point emiss  |true
1-day emiss inputs |true
3-D average file   |false
Probing Tool?      |true
PT File Root       |$PROBOUT/CAMx3.9507$today.07base.$RUN
```

```
Technology type    |DDM
PT Crs grid output |true
PT Fin grid output |true
# IC Spec groups   | 1
IC Species groups  |ALL
# BC Spec groups   | 1
BC Species groups  |ALL
Stratify boundary? |false
# Emis Spec groups | 1
Emis Species groups|ALL
# of source regions| 6
# of source groups | 3
Chemparam          |$INPUT/CAMx3.chemparm.3
Photolysis rates   |$INPUT/rate.ng.99jul95.ai.basD
Landuse            |$INPUT/surf.cc.commonfile.ai.basD
Height/pressure    |$INPUT/rams/hght.cc.$todate.ne.rams1b
Wind               |$INPUT/rams/wind.cc.$todate.ne.rams1b.CAMx2
Temperature        |$INPUT/rams/tmpr.cc.$todate.ne.rams1b.CAMx2
Water vapor        |$INPUT/rams/wvap.cc.$todate.ne.rams1b
Cloud cover        |$INPUT/clou.cc.$todate.ld.basD
Rainfall           |$INPUT/anlrain.9507$today.out
Vertical diffsvty  |$INPUT/rams/vdif.cc.$todate.wi.rams1bnew
Initial conditions |
Boundary conditions|$INPUT/bndr.cc.$todate.ld.basD.a0
Top concentration  |$INPUT/topc.ng.commonfile.ai.basD
Albedo/haze/ozone  |$INPUT/ahoz.cf.99jul95.ld.basD
Point emiss        |$PTSRCE/ptsrce.9507$today.07base.pig
Area emiss         |$EMIS/OTAG_36km/emiss.OTAG_36km.9507$today.07base.bin
Landuse         #2 |$INPUT/surf.ff.commonfile.ai.basD
Height/pressure #2 |$INPUT/rams/hght.ff.$todate.ne.rams1b
Wind            #2 |$INPUT/rams/wind.ff.$todate.ne.rams1b.CAMx2
Temperature     #2 |
Vertical diff   #2 |$INPUT/rams/vdif.ff.$todate.wi.rams1bnew
Area emiss      #2 |$EMIS/OTAG_12km/emiss.OTAG_12km.9507$today.07base.bin
Coarse grid restart|$OUTPUT/CAMx3.9507$yesterday.07base.$RUN.inst.2
Fine grid restart  |$OUTPUT/CAMx3.9507$yesterday.07base.$RUN.finst.2
Source area mapping|$PROBIN/source_map/source_map.crc.6area.ddm
Receptor file      |$PROBIN/receptor.list.a0
PT Cse grd restart |$OUTPUT/CAMx3.9507$yesterday.07base.$RUN.sa.inst.2
PT Fin grd restart |$OUTPUT/CAMx3.9507$yesterday.07base.$RUN.sa.finst.2
IC file name       |
BC file name       |$INPUT/bndr.cc.$todate.ld.basD.a0.copy
TC file name       |$INPUT/topc.ng.commonfile.ai.basD.copy
Area   Grp#1 Grd#1 |$EMIS/OTAG_36km/premerged/bio/bio2.cc.$todate-95.ne
Area   Grp#1 Grd#2 |$EMIS/OTAG_12km/premerged/bio/bio2.ff.$todate-95.ne
Point  Grp#1       |
Area   Grp#2 Grd#1 |$PROBEMI/OTAG_36km/emiss.s_anthro.OTAG_36km.9507$today.07base.bin
Area   Grp#2 Grd#2 |$PROBEMI/OTAG_12km/emiss.s_anthro.OTAG_12km.9507$today.07base.bin
Point  Grp#2       |
Area   Grp#3 Grd#1 |
Area   Grp#3 Grd#2 |
Point  Grp#3       |$PTSRCE/ptsrce.9507$today.07base.pig.copy
ieof
#
#  --- Execute the model ---
#
/bin/time $EXEC2  >& ./$RUN/CAMx3.9507$today.07base.$RUN.stdout
date
end
```

DDM RUN B7

```
#!/bin/csh
#
set RUN     = "DDM.B7"
#
####
#
# DDM with 1 source area x 4 source categories.
# The 4 source categories are biogenic, onroad mobile, other surface
# anthropogenic (anthro) and elevated anthropogenic emissions.
# Sensitivity to VOC and NOx from each source group.
####
#
# For efficiency, compile EXEC1 with 1 grid and EXEC2 with 2 grids
#
set EXEC1    = "../../src.v3.d/CAMx.otag_1grid.CO.200.linux"
set EXEC2    = "../../src.v3.d/CAMx.otag.CO.200.linux"
#
set INPUT   = "../inputs"
set EMIS    = "../emiss"
set PTSRCE  = "../ptsrce"
set OUTPUT  = "../outputs/$RUN"
set PROBIN  = "../ddm.inputs"
set PROBOUT = "../outputs/$RUN"
set PROBEMI = "../ddm.inputs/o_anthro"
#
mkdir ./$RUN $OUTPUT $PROBOUT
#
#
# Days 7-11 omitted
#
#
# --- Run the remaining days with 2 grids
#
foreach today (12 13 14 15)
set yesterday = `echo $today | awk '{printf("%2.2d",$1-1)}'`
set todate = `echo $today | awk '{printf("%2.2djul95",$1)}'`
date
#
#  --- Create the input file (always called CAMx.in)
#
cat << ieof > CAMx.in
CAMx Version       |version3
Run Message        |CRC-A37 - OTAG 2007 Base Case - $RUN
Root output name   |$OUTPUT/CAMx3.9507$today.07base.$RUN
Start yr/mo/dy/hr  |95 07 $today    0.
End   yr/mo/dy/hr  |95 07 $today 2400.
dtmx,dtin,dtem,dtou|0.25 1. 1. 1.
nx,ny,nz           |64  63  5
Coordinate ID      |LATLON
xorg,yorg,dx,dy    |-99. 26.  .5  .33333
time zone          |5
PiG parameters     |5000. 18.
Avg output species |17
                   |NO        NO2       O3        PAR       TOL       ETH
                   |OLE       PAN       ISOP      XYL       FORM      ALD2
                   |HNO3      NXOY      NTR       CO        H2O2
# nested grids     |1
nest grid params   |15 59 19 54 7 3
SMOLAR,BOTT, PPM?  |BOTT
Chemistry solver   |CMC
Restart            |true
Chemistry          |true
Dry dep            |true
Wet dep            |true
PiG submodel       |false
Staggered winds    |false
Treat area emiss   |true
Treat point emiss  |true
1-day emiss inputs |true
3-D average file   |false
```

```
Probing Tool?      |true
PT File Root       |$PROBOUT/CAMx3.9507$today.07base.$RUN
Technology type    |DDM
PT Crs grid output |true
PT Fin grid output |true
# IC Spec groups   | 0
# BC Spec groups   | 0
# Emis Spec groups | 2
Emis Species groups|NOX       VOC
# of source regions| 1
# of source groups | 4
Chemparam          |$INPUT/CAMx3.chemparm.3
Photolysis rates   |$INPUT/rate.ng.99jul95.ai.basD
Landuse            |$INPUT/surf.cc.commonfile.ai.basD
Height/pressure    |$INPUT/rams/hght.cc.$todate.ne.rams1b
Wind               |$INPUT/rams/wind.cc.$todate.ne.rams1b.CAMx2
Temperature        |$INPUT/rams/tmpr.cc.$todate.ne.rams1b.CAMx2
Water vapor        |$INPUT/rams/wvap.cc.$todate.ne.rams1b
Cloud cover        |$INPUT/clou.cc.$todate.ld.basD
Rainfall           |$INPUT/anlrain.9507$today.out
Vertical diffsvty  |$INPUT/rams/vdif.cc.$todate.wi.rams1bnew
Initial conditions |
Boundary conditions|$INPUT/bndr.cc.$todate.ld.basD.a0
Top concentration  |$INPUT/topc.ng.commonfile.ai.basD
Albedo/haze/ozone  |$INPUT/ahoz.cf.99jul95.ld.basD
Point emiss        |$PTSRCE/ptsrce.9507$today.07base.pig
Area emiss         |$EMIS/OTAG_36km/emiss.OTAG_36km.9507$today.07base.bin
Landuse         #2 |$INPUT/surf.ff.commonfile.ai.basD
Height/pressure #2 |$INPUT/rams/hght.ff.$todate.ne.rams1b
Wind            #2 |$INPUT/rams/wind.ff.$todate.ne.rams1b.CAMx2
Temperature     #2 |
Vertical diff   #2 |$INPUT/rams/vdif.ff.$todate.wi.rams1bnew
Area emiss      #2 |$EMIS/OTAG_12km/emiss.OTAG_12km.9507$today.07base.bin
Coarse grid restart|$OUTPUT/CAMx3.9507$yesterday.07base.$RUN.inst.2
Fine grid restart  |$OUTPUT/CAMx3.9507$yesterday.07base.$RUN.finst.2
Source area mapping|$PROBIN/source_map/source_map.crc.1area.ddm
Receptor file      |$PROBIN/receptor.list.a0
PT Cse grd restart |$OUTPUT/CAMx3.9507$yesterday.07base.$RUN.sa.inst.2
PT Fin grd restart |$OUTPUT/CAMx3.9507$yesterday.07base.$RUN.sa.finst.2
IC file name       |
BC file name       |
TC file name       |
Area   Grp#1 Grd#1 |$EMIS/OTAG_36km/premerged/bio/bio2.cc.$todate-95.ne
Area   Grp#1 Grd#2 |$EMIS/OTAG_12km/premerged/bio/bio2.ff.$todate-95.ne
Point  Grp#1       |
Area   Grp#2 Grd#1 |$EMIS/OTAG_36km/premerged/motv/OTAG_36km.motv.9507$today.07base.bin
Area   Grp#2 Grd#2 |$EMIS/OTAG_12km/premerged/motv/OTAG_12km.motv.9507$today.07base.bin
Point  Grp#2       |
Area   Grp#3 Grd#1 |
Area   Grp#3 Grd#2 |
Point  Grp#3       |$PTSRCE/ptsrce.9507$today.07base.pig.copy
Area   Grp#4 Grd#1 |$PROBEMI/OTAG_36km/emiss.oanthro.OTAG_36km.9507$today.07base.bin
Area   Grp#4 Grd#2 |$PROBEMI/OTAG_12km/emiss.oanthro.OTAG_12km.9507$today.07base.bin
Point  Grp#4       |
ieof
#
#  --- Execute the model ---
#
/bin/time $EXEC2  >& ./$RUN/CAMx3.9507$today.07base.$RUN.stdout
date
end
```

PA RUN B4

```
#!/bin/csh
#
set RUN     = "PA.B4"
#
####
# Full process analysis (IPR, IRR, CPA) for 4 receptor areas
####
#
#For efficiency, compile EXEC1 with 1 grid and EXEC2 with 2 grids
#
set EXEC1    = "../../src.v3.d/CAMx.otag_1grid.35.linux"
set EXEC2    = "../../src.v3.d/CAMx.otag.35.linux"
#
set INPUT   = "../inputs"
set EMIS    = "../emiss"
set PTSRCE  = "../ptsrce"
set OUTPUT  = "../outputs/$RUN"
set PROBOUT = "../outputs/$RUN"
#
mkdir ./$RUN $OUTPUT $PROBOUT
#
date
#
#  --- Start the first day with 1 grid
#
#  --- Create the input file (always called CAMx.in)
#
cat << ieof > CAMx.in
CAMx Version       |version3
Run Message        |CRC-A37 - OTAG 2007 Base Case - $RUN
Root output name   |$OUTPUT/CAMx3.950707.07base.$RUN
Start yr/mo/dy/hr  |95 07 07    0.
End   yr/mo/dy/hr  |95 07 07 2400.
dtmx,dtin,dtem,dtou|0.25 1. 1. 1.
nx,ny,nz           |64  63  5
Coordinate ID      |LATLON
xorg,yorg,dx,dy    |-99. 26.  .5  .33333
time zone          |5
PiG parameters     |5000. 18.
Avg output species |17
                   |NO        NO2       O3        PAR       TOL       ETH
                   |OLE       PAN       ISOP      XYL       FORM      ALD2
                   |HNO3      NXOY      NTR       CO        H2O2
# nested grids     |0
SMOLAR,BOTT, PPM?  |BOTT
Chemistry solver   |CMC
Restart            |false
Chemistry          |true
Dry dep            |true
Wet dep            |true
PiG submodel       |false
Staggered winds    |false
Treat area emiss   |true
Treat point emiss  |true
1-day emiss inputs |true
3-D average file   |true
Probing Tool?      |true
PT File Root       |$PROBOUT/CAMx3.950707.07base.$RUN
Technology type    |IPR
# of PA domains    |4
Domain #1: Chicago |1
Beg/End index - X  |22 24
Beg/End index - Y  |47 49
Beg/End index - Z  |1  5
Domain #2: Atlanta |1
Beg/End index - X  |29 31
Beg/End index - Y  |23 25
Beg/End index - Z  |1  5
Domain #3: NewYork |1
Beg/End index - X  |50 52
```

```
Beg/End index - Y  |44 46
Beg/End index - Z  |1  5
Domain #4: Altoona |1
Beg/End index - X  |41 43
Beg/End index - Y  |43 45
Beg/End index - Z  |1  5
Chemparam          |$INPUT/CAMx3.chemparm.3
Photolysis rates   |$INPUT/rate.ng.99jul95.ai.basD
Landuse            |$INPUT/surf.cc.commonfile.ai.basD
Height/pressure    |$INPUT/rams/hght.cc.07jul95.ne.rams1b
Wind               |$INPUT/rams/wind.cc.07jul95.ne.rams1b.CAMx2
Temperature        |$INPUT/rams/tmpr.cc.07jul95.ne.rams1b.CAMx2
Water vapor        |$INPUT/rams/wvap.cc.07jul95.ne.rams1b
Cloud cover        |$INPUT/clou.cc.07jul95.ld.basD
Rainfall           |$INPUT/anlrain.950707.out
Vertical diffsvty  |$INPUT/rams/vdif.cc.07jul95.wi.rams1bnew
Initial conditions |$INPUT/init.cc.07jul95.ld.basD
Boundary conditions|$INPUT/bndr.cc.07jul95.ld.basD.a0
Top concentration  |$INPUT/topc.ng.commonfile.ai.basD
Albedo/haze/ozone  |$INPUT/ahoz.cc.99jul95.ld.basD
Point emiss        |$PTSRCE/ptsrce.950707.07base.pig
Area emiss         |$EMIS/OTAG_36km/emiss.OTAG_36km.950707.07base.bin
ieof
#
#  --- Execute the model ---
#
/bin/time $EXEC1  >& ./$RUN/CAMx3.950707.07base.$RUN.stdout
date
#
# Days 8-11 omitted
#
foreach today (12 13 14 15)
set yesterday = `echo $today | awk '{printf("%2.2d",$1-1)}'`
set todate = `echo $today | awk '{printf("%2.2djul95",$1)}'`
date
#
#  --- Create the input file (always called CAMx.in)
#
cat << ieof > CAMx.in
CAMx Version       |version3
Run Message        |CRC-A37 - OTAG 2007 Base Case - $RUN
Root output name   |$OUTPUT/CAMx3.9507$today.07base.$RUN
Start yr/mo/dy/hr  |95 07 $today    0.
End   yr/mo/dy/hr  |95 07 $today 2400.
dtmx,dtin,dtem,dtou|0.25 1. 1. 1.
nx,ny,nz           |64  63  5
Coordinate ID      |LATLON
xorg,yorg,dx,dy    |-99. 26.  .5  .33333
time zone          |5
PiG parameters     |5000. 18.
Avg output species |17
                   |NO        NO2       O3        PAR       TOL       ETH
                   |OLE       PAN       ISOP      XYL       FORM      ALD2
                   |HNO3      NXOY      NTR       CO        H2O2
# nested grids     |1
nest grid params   |15 59 19 54 7 3
SMOLAR,BOTT, PPM?  |BOTT
Chemistry solver   |CMC
Restart            |true
Chemistry          |true
Dry dep            |true
Wet dep            |true
PiG submodel       |false
Staggered winds    |false
Treat area emiss   |true
Treat point emiss  |true
1-day emiss inputs |true
3-D average file   |true
Probing Tool?      |true
PT File Root       |$PROBOUT/CAMx3.9507$today.07base.$RUN
Technology type    |IPR
# of PA domains    |4
Domain #1: Chicago |2
```

```
Beg/End index - X  |23 31
Beg/End index - Y  |86 94
Beg/End index - Z  |1  7
Domain #2: Atlanta |2
Beg/End index - X  |44 52
Beg/End index - Y  |14 22
Beg/End index - Z  |1  7
Domain #3: NewYork |2
Beg/End index - X  |107 115
Beg/End index - Y  |77  85
Beg/End index - Z  |1  7
Domain #4: Altoona |2
Beg/End index - X  |80 88
Beg/End index - Y  |74 82
Beg/End index - Z  |1  7
Chemparam          |$INPUT/CAMx3.chemparm.3
Photolysis rates   |$INPUT/rate.ng.99jul95.ai.basD
Landuse            |$INPUT/surf.cc.commonfile.ai.basD
Height/pressure    |$INPUT/rams/hght.cc.$todate.ne.rams1b
Wind               |$INPUT/rams/wind.cc.$todate.ne.rams1b.CAMx2
Temperature        |$INPUT/rams/tmpr.cc.$todate.ne.rams1b.CAMx2
Water vapor        |$INPUT/rams/wvap.cc.$todate.ne.rams1b
Cloud cover        |$INPUT/clou.cc.$todate.ld.basD
Rainfall           |$INPUT/anlrain.9507$today.out
Vertical diffsvty  |$INPUT/rams/vdif.cc.$todate.wi.rams1bnew
Initial conditions |
Boundary conditions|$INPUT/bndr.cc.$todate.ld.basD.a0
Top concentration  |$INPUT/topc.ng.commonfile.ai.basD
Albedo/haze/ozone  |$INPUT/ahoz.cf.99jul95.ld.basD
Point emiss        |$PTSRCE/ptsrce.9507$today.07base.pig
Area emiss         |$EMIS/OTAG_36km/emiss.OTAG_36km.9507$today.07base.bin
Landuse         #2 |$INPUT/surf.ff.commonfile.ai.basD
Height/pressure #2 |$INPUT/rams/hght.ff.$todate.ne.rams1b
Wind            #2 |$INPUT/rams/wind.ff.$todate.ne.rams1b.CAMx2
Temperature     #2 |
Vertical diff   #2 |$INPUT/rams/vdif.ff.$todate.wi.rams1bnew
Area emiss      #2 |$EMIS/OTAG_12km/emiss.OTAG_12km.9507$today.07base.bin
Coarse grid restart|$OUTPUT/CAMx3.9507$yesterday.07base.$RUN.inst.2
Fine grid restart  |$OUTPUT/CAMx3.9507$yesterday.07base.$RUN.finst.2
ieof
#
#  --- Execute the model ---
#
/bin/time $EXEC2  >& ./$RUN/CAMx3.9507$today.07base.$RUN.stdout
date
end
```

OSAT SOURCE AREA MAP

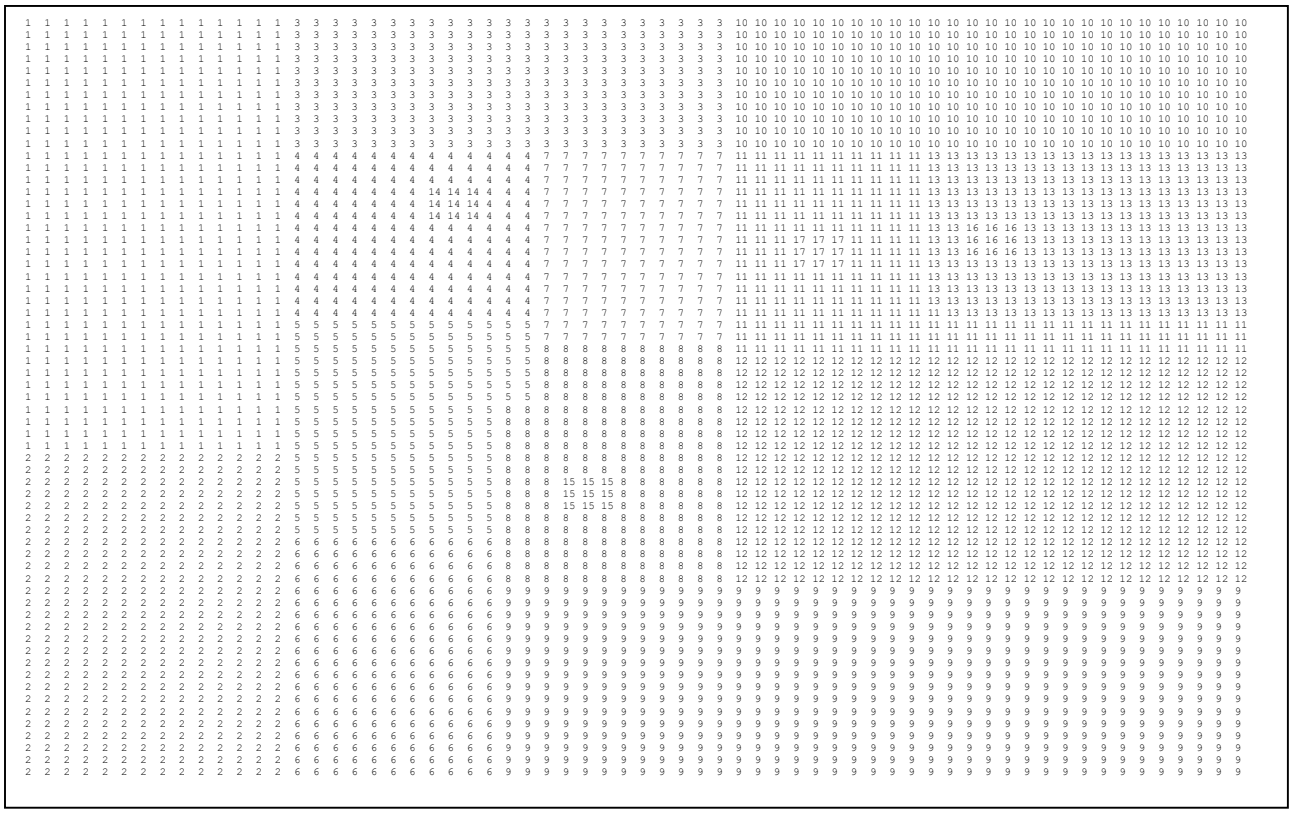

DDM SOURCE AREA MAP FOR RUN B2N

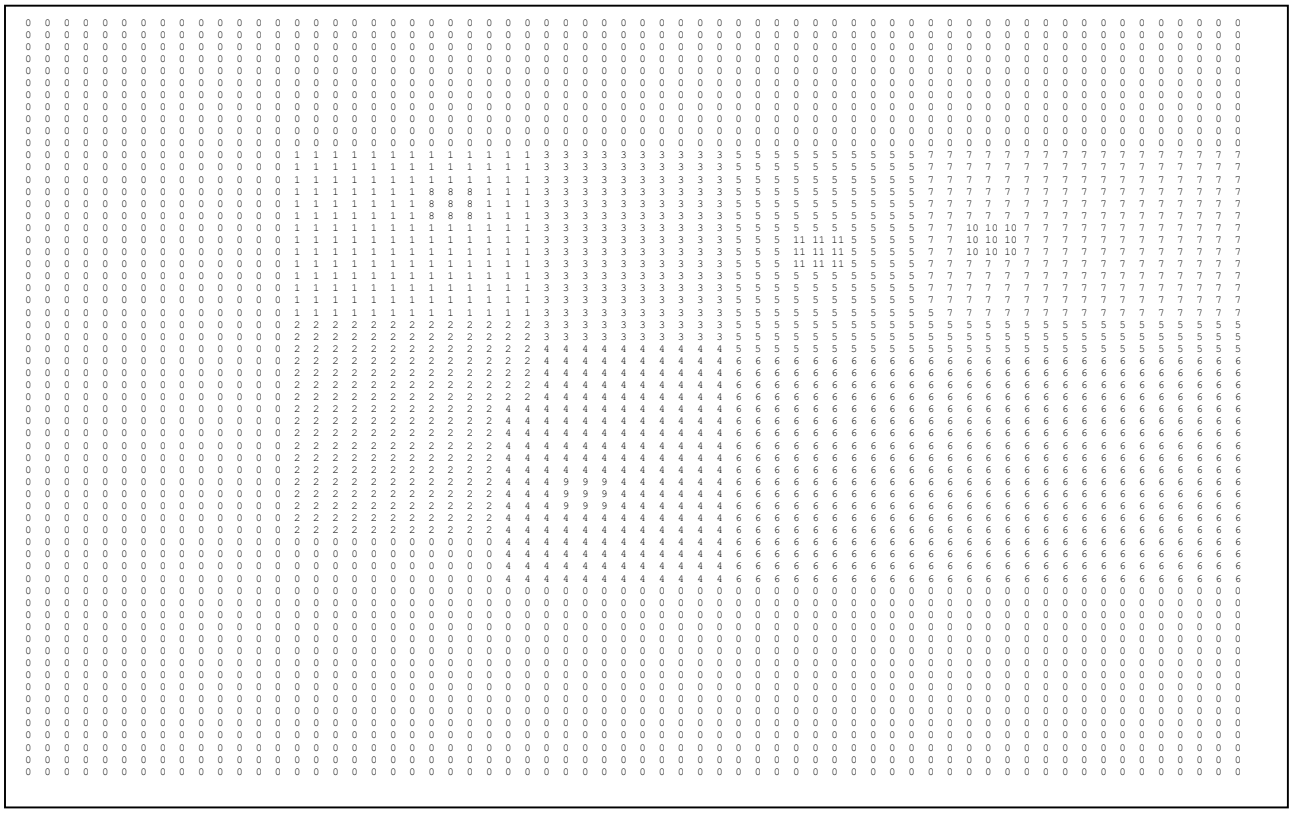

DDM SOURCE AREA MAP FOR RUN B3

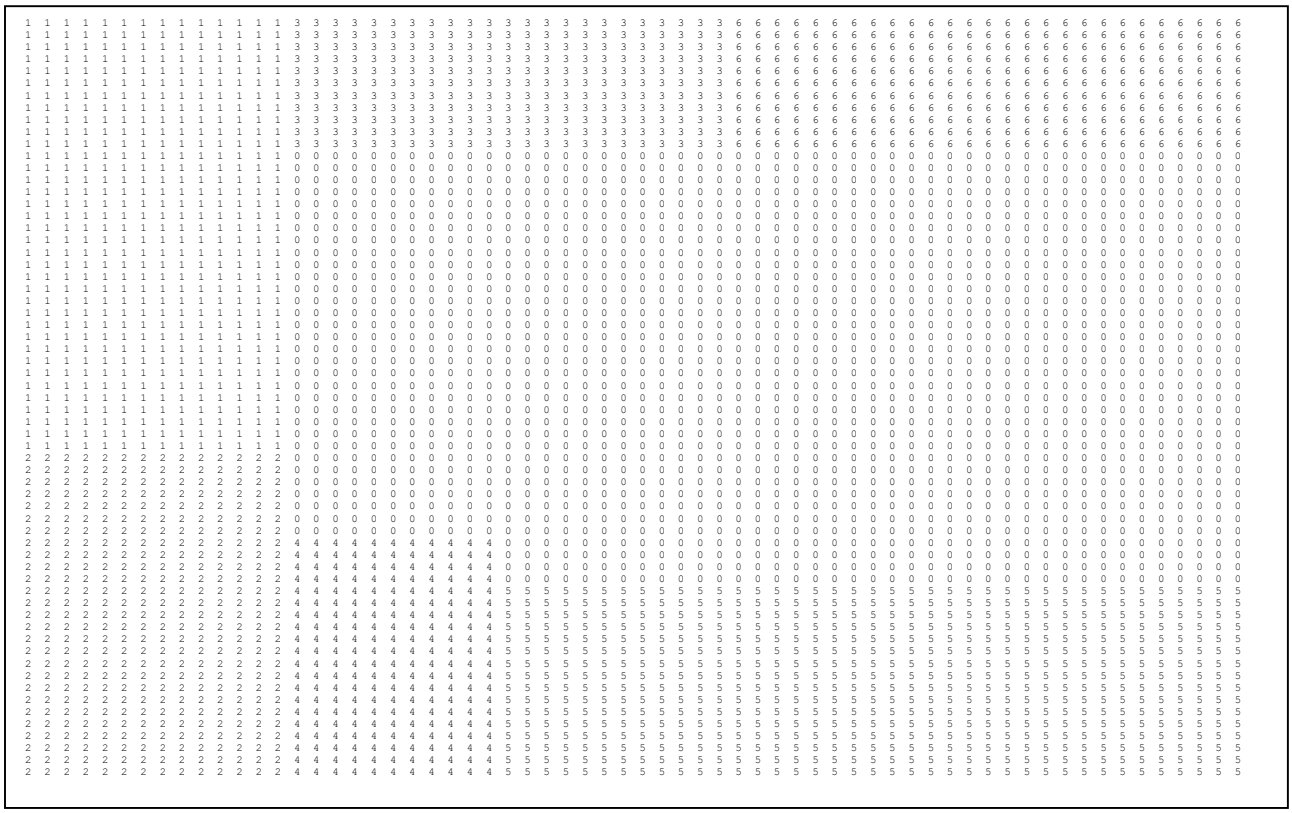

OSAT AND RECEPTOR DEFINITION FILE

```
SINGLE CELL         Chicago1    22          47
SINGLE CELL         Chicago2    23          47
SINGLE CELL         Chicago3    24          47
SINGLE CELL         Chicago4    22          48
SINGLE CELL         Chicago5    23          48
SINGLE CELL         Chicago6    24          48
SINGLE CELL         Chicago7    22          49
SINGLE CELL         Chicago8    23          49
SINGLE CELL         Chicago9    24          49
WALL OF CELLS       ChicagoL1   22          24
                                47          49
                                 1           1
WALL OF CELLS       ChicagoL2   22          24
                                47          49
                                 2           2
WALL OF CELLS       ChicagoL3   22          24
                                47          49
                                 3           3
WALL OF CELLS       ChicagoL4   22          24
                                47          49
                                 4           4
WALL OF CELLS       ChicagoL5   22          24
                                47          49
                                 5           5
SINGLE CELL         Atlanta1    29          23
SINGLE CELL         Atlanta2    30          23
SINGLE CELL         Atlanta3    31          23
SINGLE CELL         Atlanta4    29          24
SINGLE CELL         Atlanta5    30          24
SINGLE CELL         Atlanta6    31          24
SINGLE CELL         Atlanta7    29          25
SINGLE CELL         Atlanta8    30          25
SINGLE CELL         Atlanta9    31          25
WALL OF CELLS       AtlantaL1   29          31
                                23          25
                                 1           1
WALL OF CELLS       AtlantaL2   29          31
                                23          25
                                 2           2
WALL OF CELLS       AtlantaL3   29          31
                                23          25
                                 3           3
WALL OF CELLS       AtlantaL4   29          31
                                23          25
                                 4           4
WALL OF CELLS       AtlantaL5   29          31
                                23          25
                                 5           5
SINGLE CELL         NewYork1    50          44
SINGLE CELL         NewYork2    51          44
SINGLE CELL         NewYork3    52          44
SINGLE CELL         NewYork4    50          45
SINGLE CELL         NewYork5    51          45
SINGLE CELL         NewYork6    52          45
SINGLE CELL         NewYork7    50          46
SINGLE CELL         NewYork8    51          46
```

SINGLE CELL	NewYork9	52	46
WALL OF CELLS	NewYorkL1	50	52
		44	46
		1	1
WALL OF CELLS	NewYorkL2	50	52
		44	46
		2	2
WALL OF CELLS	NewYorkL3	50	52
		44	46
		3	3
WALL OF CELLS	NewYorkL4	50	52
		44	46
		4	4
WALL OF CELLS	NewYorkL5	50	52
		44	46
		5	5
SINGLE CELL	Altoona1	41	43
SINGLE CELL	Altoona2	42	43
SINGLE CELL	Altoona3	43	43
SINGLE CELL	Altoona4	41	44
SINGLE CELL	Altoona5	42	44
SINGLE CELL	Altoona6	43	44
SINGLE CELL	Altoona7	41	45
SINGLE CELL	Altoona8	42	45
SINGLE CELL	Altoona9	43	45
WALL OF CELLS	AltoonaL1	41	43
		43	45
		1	1
WALL OF CELLS	AltoonaL2	41	43
		43	45
		2	2
WALL OF CELLS	AltoonaL3	41	43
		43	45
		3	3
WALL OF CELLS	AltoonaL4	41	43
		43	45
		4	4
WALL OF CELLS	AltoonaL5	41	43
		43	45
		5	5